Terms and Conditions of Use of Digitised Theses from Trinity College Library Dublin

Copyright statement

All material supplied by Trinity College Library is protected by copyright (under the Copyright and Related Rights Act, 2000 as amended) and other relevant Intellectual Property Rights. By accessing and using a Digitised Thesis from Trinity College Library you acknowledge that all Intellectual Property Rights in any Works supplied are the sole and exclusive property of the copyright and/or other IPR holder. Specific copyright holders may not be explicitly identified. Use of materials from other sources within a thesis should not be construed as a claim over them.

A non-exclusive, non-transferable licence is hereby granted to those using or reproducing, in whole or in part, the material for valid purposes, providing the copyright owners are acknowledged using the normal conventions. Where specific permission to use material is required, this is identified and such permission must be sought from the copyright holder or agency cited.

Liability statement

By using a Digitised Thesis, I accept that Trinity College Dublin bears no legal responsibility for the accuracy, legality or comprehensiveness of materials contained within the thesis, and that Trinity College Dublin accepts no liability for indirect, consequential, or incidental, damages or losses arising from use of the thesis for whatever reason. Information located in a thesis may be subject to specific use constraints, details of which may not be explicitly described. It is the responsibility of potential and actual users to be aware of such constraints and to abide by them. By making use of material from a digitised thesis, you accept these copyright and disclaimer provisions. Where it is brought to the attention of Trinity College Library that there may be a breach of copyright or other restraint, it is the policy to withdraw or take down access to a thesis while the issue is being resolved.

Access Agreement

By using a Digitised Thesis from Trinity College Library you are bound by the following Terms & Conditions. Please read them carefully.

I have read and I understand the following statement: All material supplied via a Digitised Thesis from Trinity College Library is protected by copyright and other intellectual property rights, and duplication or sale of all or part of any of a thesis is not permitted, except that material may be duplicated by you for your research use or for educational purposes in electronic or print form providing the copyright owners are acknowledged using the normal conventions. You must obtain permission for any other use. Electronic or print copies may not be offered, whether for sale or otherwise to anyone. This copy has been supplied on the understanding that it is copyright material and that no quotation from the thesis may be published without proper acknowledgement.

Characterisation of County Clare's Wave Energy Resource and Factors Affecting SOWC Wave Energy Converter Design

By

David Carr, B.A., B.A.I., PG Dip. Stat.

A Thesis submitted for the Degree of Doctor of Philosophy in Engineering to the University of Dublin, Trinity College

Supervisors: Dr. Aonghus McNabola & Dr. Laurence Gill

Department of Civil, Structural and Environmental Engineering,
University of Dublin,
Trinity College,
Dublin.

DECLARATION

I DAVID CARR declare that this thesis has not been submitted as an exercise for a degree at this or any other university and it is entirely my own work.

I agree to deposit this thesis in the University's open access institutional repository or allow the library to do so on my behalf, subject to Irish Copyright Legislation and Trinity College Library conditions of use and acknowledgement.

DAVID CARR
2014

ABSTRACT

Aim. There were two aims: (i) To characterise the wave climate for a domain off the coast of County Clare adjacent to Loop Head which is an area of interest for ocean energy development in Ireland. (ii) To use the findings from a wave climate modelling study conducted to achieve the first aim, and build upon an earlier TCD study to investigate design parameters which may influence the survivability and feasibility of potential subterranean oscillating water columns (SOWCs) installed at Loop Head.

Method. To achieve the first aim, a 3rd generation spectral wave model for a domain off the coast of County Clare adjacent to Loop Head was developed, calibrated and validated using DHI's MIKE 21 spectral wave modelling software along with sea state, met-ocean and bathymetric data from a range of sources. To achieve the second aim, factors affecting SOWC wave energy converter design were investigated and used to determine bounds for chamber design. A numerical hydrodynamic model of a SOWC wave energy converter was developed with a boundary element method code, WAMIT. The model was benchmarked by comparing its performance with those of similar small scale tank tests. The effects of altering two design parameters (chamber width and front wall thickness) which have implications for SOWC survivability in extreme sea states as well as SOWC performance were evaluated at two potential sites: Arch point and the tip of Loop Head. The upper limit for mean annual power and capture width ratio were used as performance indicators. The research programme was informed by a selective literature review and a preliminary site viability study and survey.

Results. A 3rd generation spectral wave model for a domain off the coast of County Clare adjacent to Loop Head was developed which yielded information on a range of indices including annual mean wave power, exploitable wave power, maximum wave height, percentage occurrence of a range of sea states and wave directionality at off-shore, near-shore, and on-shore locations. For these regions, results were presented using several graphical methods including bar charts, time series graphs, scatter plots and wave roses. Percentage occurrence of each sea state was presented using scatter diagrams. Output from this spectral wave model facilitated an

assessment of performance for each SOWC chamber design at Arch point and the tip of Loop Head. The tip of Loop Head possessed higher mean annual and exploitable wave power values compared with Arch Point. However both exhibited similar values for the most commonly occurring range of energy periods for all depth contours. This information is central to the design and efficiency of a given SOWC wave energy converter. Regarding the second aim of this research programme, numerical modelling of numerous SOWC chamber designs showed that within established SOWC chamber design bounds, the highest level of absorbed power was achieved when exposed to the annual wave conditions at the tip of Loop Head. This was based on an 11 m wide chamber with a front wall thickness of 4.8 m. Increasing front wall thickness and reducing chamber width beyond such values were associated with comparative losses in SOWC annual power production at Arch Point and the tip of Loop Head .However, the literature review indicated that these SOWC chamber modifications would be associated with increased survivability of SOWCs exposed to extreme sea states.

Conclusions. The spectral wave model developed in this research programme will be useful for future wave energy research on the west coast of Ireland. Results from this model indicate that the domain off County Clare possesses an exploitable resource with promising levels of energy for potential wave energy projects. They also show that the near-shore and on-shore environment in this domain maintains good levels of power with relative filtering of extreme waves. Both Arch Point and the Tip of Loop Head possess favourable annual mean wave power values relative to established European wave energy test sites. With respect to the second aim, this thesis provides useful information on SOWC design features that may help guide prospective developers towards possible solutions to the inherent challenges of SOWC refinement and installation highlighted in this thesis. The optimal design for SOWCs involves balancing parameter values that favour performance with those that favour survivability.

TABLE OF CONTENTS

LIST OF FIGURES

LIST OF TABLES

ACKNOWLEDGEMENTS

Thanks to my supervisors, Dr. Aonghus McNabola and Dr. Laurence Gill for the opportunity to conduct postgraduate research in an area in which I hope to develop my future career, and for their support throughout this project. Also, I would like to thank Prof. Kingston for his encouragement and sharing his time. They have each been a great source of inspiration.

Many people in the field of marine renewables and engineering have provided me with expert advice and contributed data sets that facilitated this research. My thanks go to Henrik Koefoed Hansen from the Danish Hydraulics Institute, George Lane from Sewave Ltd., Paddy McConnell from Boliden Tara Mines, Michael McCarthy from Priority Drilling, Brian Holmes, Gareth Thomas, and Brendan Cahill from the Hydraulics Maritime Research Centre, Sean O'Callaghan, Kevin Tarrant and William Dick from Trinity College, Alan Henry, Trevor Whittaker and Matt Folley from Queen's University Belfast, Sarah Gallagher and Roxana Tiron from University College Dublin. Also I have been lucky enough to discuss my research regularly with colleagues from the International Network for Off-shore Renewable Energies (INORE), particularly Borja, Imanol and Davide. Thanks to Paul McMahon and his family for kindly lending their power boat for the site survey, as well as Damien and Pat for their help with logistics. Thanks to David Mullaney from Cisco Systems and Gerry O'Brien from TCD's School of Computer Science who kindly helped set up a high performance computer cluster to run computationally intensive simulations.

A special mention has to go to 193 Pearse Street, Andrew, Seanie, Ted, Aisling, John, Mairead, Mary and Francesco. I would also like to extend my thanks to fellow postgraduate students and staff of the Department of Engineering who have made the past years a valuable learning experience. A big thanks must go to my friends who supported me through this journey. My Mum, Dad and Sister have been exceptionally supportive throughout this experience and I cannot thank them enough for their advice throughout my years of education. To all, I am very grateful. Finally, I would like to dedicate this work to my grandparents Ted, Muriel, Bunny and Joan who opened my eyes to how much the world can change in a lifetime, and how it's possible to make a positive difference.

Chapter 1
INTRODUCTION

1.1 INTRODUCTION

The source of our energy supply, now and in the future, is a central concern for society. World-wide demand for electricity is expected to rise by 40% within the next 20 years (BP, 2010; IEA, 2009). Since 2001, Ireland has been approximately 90% dependent on imported fossil fuels. A report on Ireland's energy security published by Sustainable Energy Authority of Ireland (2011) highlighted that Ireland's energy security is declining due to the diminishing supplies of oil and gas in the EU and OECD. In line with this, the cost of importing fuels is set to rise continually into the future. Although the recent developments in fracking technology and shale gas presents an opportunity for Ireland to become less dependent on importing fossil fuels, there are serious concerns that the exploitation of this resource could cause widespread pollution and other environmental issues on many levels (Hewitt, 2012; Jones et al., 2013; Walter, 2010).

There is also recognition that CO_2 emissions from fossil fuels contribute to climate change. The fifth report by the Intergovernmental Panel on Climate Change (IPCC), published in 2013 has raised the probability that most global warming is manmade to 95%, from 90% in its previous report in 2007 (IPCC, 2013). The report is based on contributions from over 900 scientists, which links the increasing global temperatures to unprecedented rises in the concentration of CO_2 in the atmosphere. CO_2 levels have risen from 280 parts per million (ppm) in pre-industrial times, to 400 ppm as of May 2013 (Dossey, 2013).

To combat this, international policy measures including the Kyoto Protocol have been put in place with an aim of moving towards a low carbon economy. As part of the Kyoto Protocol, Ireland agreed by 2020 to reduce greenhouse gas emissions by 20% compared to 2005 levels (European Commission, 2008). Linked with this agreement, Ireland has set a target that 33% of its electricity will be generated from renewable resources by 2020 (Dept. of Communications, Marine and Natural Resources, 2007).

The sources of renewable energy planned to contribute to this target are wind, hydropower, biomass, solar, geothermal, tidal and wave. Each of these resources, along with their technical barriers and 2020 targets, are discussed in relation to Ireland by Rourke et al. (2009). This comprehensive review paper indicates that the greatest levels of available renewable energy in Ireland are associated with wind and wave. Given the maturity of the wind industry in comparison to the emerging ocean energy industry, on shore wind is set to be the predominant source of renewable energy used to reach the 33% electricity targets. To support this plan, dynamic power generation is required, which employs smart electrical grids to appropriately balance this intermittent energy source with reliable energy sources provided by hydropower, biomass and fossil fuel plants. This process is known as load balancing and is essential for a stable and reliable supply of electricity to meet demand. To balance sudden and unexpected drops associated with electricity generation via wind, operating reserve is needed. This is the generating capacity available to an electrical grid operator within a short interval of time to meet demand in case there is a disruption in the supply. Higher risks of sudden unexpected drops in the electrical network increases the necessary operating reserve, which often requires further electricity generation via fossil fuels. Hence, the uncontrollable nature of wind power negatively impacts their effectiveness in reducing the requirement for thermal plants (Fusco et al., 2010). This can affect the environmental benefits that wind power sources intend to bring (ABB, 2012).

Although wave energy is still at a nascent stage, research on the pattern of power production of combinations of co-located wind and wave technologies, based on real power productions, has shown that joint production provides more stable power outputs than wind technologies working individually. Studies based on Ireland

(Fusco et al., 2010), Denmark (Soerensen, 2005) and California (Stoutenburg et al., 2010) along with a European research effort (Cradden et al., 2011) describe the advantages of supplementing wind energy with wave energy to improve the reliability and decrease the variability of power production.

Unlike many countries that are implementing wind power to meet their renewable targets, Ireland possesses an enviable wave resource as shown in Figure 1.1. A recent study on the wave climate off the west coast of Ireland has shown the average annual wave energy to be approximately 71 kW/m at the 100m depth contour (M. Curé, 2011).

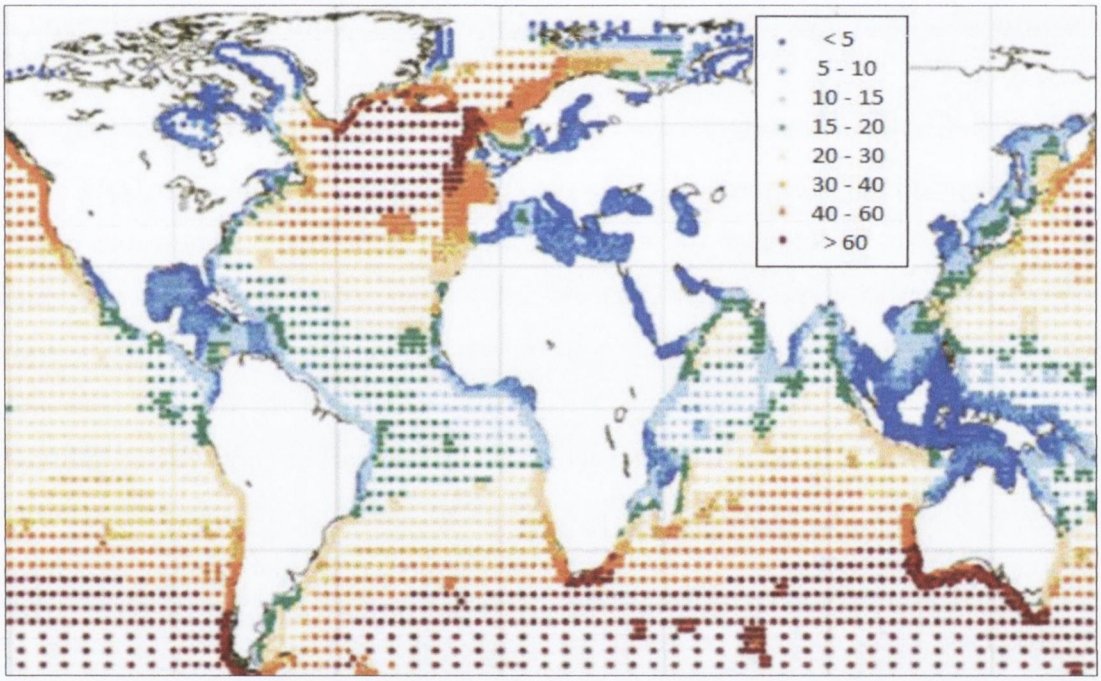

Figure 1.1 Global mean annual wave power estimates (kW/m) obtained from the WAM archive of the ECMWF calibrated and corrected with Fugro OCEANOR against a global buoy and Topex satellite altimeter data base. Source:(Cruz, 2008)

Fusco et al. (2010) showed how the West and South coast generally experience large swell waves which have little correlation with the local wind conditions and also possess less variability. Hence, the two resources can appear different at times and the integration of wave with wind facilitates a more reliable, less variable and more predictable electrical power production. Although the two resources complement each other and Ireland benefits from a particularly abundant wave energy resource, an economic means to extract this resource has yet to be proven.

1.2 Ocean Wave Energy

At present the wave energy industry is at a pre-commercial stage. It is the harsh environment and extreme sea states associated with locations that possess favourable wave energy levels which present a challenge to successful development of a wave energy converter. The cost of over-engineering designs to survive exceptional storms can lead to excessive capital costs. Additionally, uncertainties related to the survivability of wave energy conversion technologies can reduce investor confidence. This directly affects the financial support available to confidently progress the wave energy converter through a structured technology readiness level development plan which outputs a marketable wave energy converter (Nielsen and Holmes, 2010). Nevertheless, ambitions to develop wave energy remain, both internationally and in Ireland.

At the International Conference on Ocean Energy (ICOE) 2012 held in Dublin, Dr. Eddie O'Connor, co-founder and chief executive of Mainstream Renewable Power, founder of Airtricity and former chief executive officer of Bord na Móna presented his vision for the wave energy industry in Ireland. He emphasised that 'It is Ireland's greatest carbon free renewable energy resource, which could deliver a sizeable enterprise sector in the process of achieving a low-carbon economy. Although commercialisation of this technology is a challenge, we must envisage our ambition for many years in the future as well as taking the preparatory steps now to achieve this ambition'.

Dr.O'Connor also drew parallels with the wind industry. During the start of the wind industry's development curve, a number of wind turbine concepts evolved to a leading design. Subsequently, advancements in each element of wind turbine technology relating to materials, control, power take off, construction etc. led to a more reliable cost effective technology. This process was aided by the creation of standardised methods for project development. The wave power industry is now following in these footsteps.

Many governments around the world, including Ireland, have been drawing up policies for development for wave power amongst other renewable energies. With appropriate support from the Government and governing bodies and action by the

industry, power utilities and regulators, an annual output from wave energy sources in Ireland between 20 TWh (lower estimate) and 120 TWh (higher estimate) could be expected by 2050 (Sustainable Energy Authority of Ireland, 2010). Although investment in the wave industry is still uncertain, the Marine Renewables Industry Association (MRIA) stated that by 2030 a fully developed island of Ireland ocean energy sector, providing for home and global markets, could produce a total Net Present Value (NPV) of around €9 billion and many thousands of jobs. To help move these aspirations towards reality, further commitment by involved parties would be required.

There are different philosophies and design strategies for future wave energy conversion technologies. One Irish marine energy developer prioritises the requirements, favourable qualities and limitations for a Wave Energy Converter (WEC) and its deployment site, as follows:
'Survival is paramount. Full marine insurance is a prerequisite typically based on the 100-year extreme seas and for the anticipated life of the project. Any device should be capable of an operational lifetime of 20+ years. Maintenance costs should be minimised. Economics dictate that electrical power output be as great as practicable. Regarding site selection, deep waters possesses higher wave energy. As with any natural resource, economics tend to favour the richest and most accessible locations. With wave energy levels of circa 40 kW/m, installed capacities of at least 1MW would be justified: anything less implies heavier unit costs for deployment, moorings, grid connection and servicing.'

The latter point is in line with a recent paper outlining maximum power capacities of leading wave energy conversion technologies (Babarit and Hals, 2011). This paper also estimated that the upper limit of wave power absorption for a single off-shore heaving WEC is circa 1MW with a capture width of 30-50 m when exposed to annual average resource of 20-30 kW/m. As the eventual national targets for wave energy production are in the region of 20 to 120 TWh, it can be seen that numerous WECs would be required. The necessary scale of WEC installation, along with a range of other factors, influences decisions regarding the sites for their location.

1.2.1 Wave Energy Sites

There are three domains associated with wave energy conversion, off-shore, near-shore and on-shore, shown in Figure 1.2.

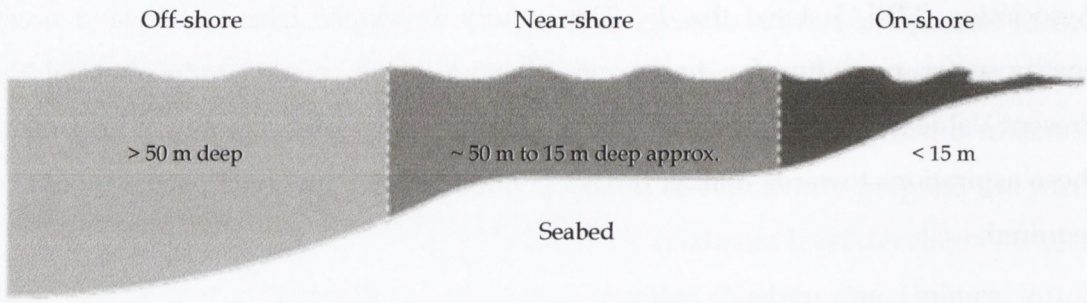

Figure 1.2 Cross sectional view of off-shore, near-shore and on-shore domain with approximate depth ranges based on wave conditions off the West Coast of Ireland.

There are advantages and disadvantages associated with each of these sites, as follows. To achieve national targets for wave energy, WECs deployed in large arrays are required (Sustainable Energy Ireland Authority of Ireland, 2010). Considering the scale and space requirements of these arrays, it is evident that these wave farms need to be predominantly located at near-shore and off-shore locations rather than on-shore. Off-shore sites would particularly allow for large farm sizes and the placement of several farms in close proximity. Thus in this respect, off-shore sites would be most advantageous. Also the highest wave energy values are recorded for off-shore sites (McCullen, 2005). A disadvantage associated with off-shore sites, is the potential for extreme sea states to damage the WEC installations. Also their distance from shore directly increases costs for installation of infrastructure and issues related to access and maintenance.

With respect to near-shore sites, their proximity to land affords lower costs for these aspects and they may be more sheltered from extreme waves. However, near-shore arrays may need to be of a smaller scale than those off-shore and may be visible from land, and thus subject to planning and consent problems due to visual impact.
With respect to the on-shore domain, the level of wave power reduces as water depth decreases, which reduces the economic attractiveness of such sites. However, the loss of power is relatively small up to a water depth of approximately 10 - 15m (Folley and Whittaker, 2009). Therefore, if it is possible to identify shoreline locations that possess a minimum water depth of 10-15m with a favourable wave energy

resource, it increases the viability of the site. Additionally, in this depth range, the reduction in wave power levels is due in part to filtering of extreme sea states, which could improve the survivability of devices at this location. Furthermore, it is of note that the energies associated with extreme sea states in off-shore sites are not exploitable, as in these conditions WECs are shifted into a protective non-operational mode (Smith et al., 2012). Thus the actual difference between the useable energy of open seas versus deep-water shoreline sites is not as great as it can first appear. The quantification of the exploitable resource at shoreline sites is central to the feasibility of a shoreline location.

Overlooking planning permissions and consenting, the next issue concerns cost effective construction of a suitable means to extract wave energy at shoreline sites. Previous shoreline projects have shown in-situ shoreline construction to be difficult and expensive (Heath, 2003; Neumann et al., 2007). This has been due to the construction of a typically concrete structure in a volatile shoreline environment coupled with the strong structural requirements to withstand violent waves (WaveNet, 2003). At the time of these constructions, the lack of commonly accepted approaches to estimate the impact loads on these structures caused by breaking waves increased uncertainty with respect to economic and safe design. Since then European and US efforts have delivered standards (Oumeraci et al., 1999; U.S. Army Corps of Engineers, 2002) that provide more widely accepted approaches for achieving this. Overall, in the context of construction costs, the opinion shared by shoreline wave energy converter evaluation reports encourages a concept shift in construction techniques (The Carbon Trust, 2005; WaveNet, 2003).

Regarding the performance of shoreline wave energy conversion, it will be seen in later sections that it is important to design the wave energy converter based on the wave climate at the deployment site. In previous shoreline wave energy converter projects, it has been challenging to accurately characterise wave conditions at coastal locations. Issues with respect to inaccurate seabed mapping and wave climate predictions at shoreline locations can cause suboptimal WEC design and performance (Wavegen, 2003). Few wave measurement buoys have been deployed at coastal sites of interest for a sufficient period of time to accurately characterise the wave climate. Regarding numerical wave climate modelling, the challenge stems

from the complex near-shore and coastal processes (depth induced friction, depth induced breaking, triad interaction etc.) that prove difficult to model without the necessary resources. If it is possible to reduce the uncertainty at coastal areas with water depths greater than 10 - 15 m, this could facilitate the development of appropriate WEC design at these potentially viable shoreline locations.
Finally, it should be acknowledged that many favourable shoreline sites are located in areas of natural beauty, where such wave energy conversion structures would be strongly opposed on environmental and tourist trade grounds. Such important political and social factors may limit the potential for extracting ocean wave energy by appending structures on to coastlines.

1.3 RATIONALE

Of all the various advantages and disadvantages of the different locations for WECs described above, the factor which is most influencing the direction of current development is the potential for installing WEC arrays on a large scale, in off-shore and near-shore sites; particularly off-shore, given the expansiveness of this domain. However, there are reasons for continuing to explore the energy production of all marine domains, including on-shore sites.

Earlier in this chapter, the concept of combining wind and wave power was discussed. It is possible that renewable energy projects may entail both wind and wave farms in a given region, supported by development of various types of infrastructure, such as electrical grid power take-off systems, resources to facilitate access and maintenance, personnel supports etc. In order to maximise use of such infrastructure, it would be beneficial to tap into all opportunities for energy production within the area concerned. Furthermore, bringing as many different installations as reasonably possible into one system may potentially improve the continuity of even power supply. Therefore where there are regions off the west coast of Ireland which have become designated for developing marine energy, it would be useful to explore all aspects of the wave resource adjacent to them with a view to possibly developing other installations that could be channelled through shared infrastructure.

It is of note that there are areas off Killard Point and Spanish Point, Loop Head, Co. Clare which are being investigated for installation of WEC farms, in both off-shore and near-shore domains. This is linked with the WestWave project (Slevin et al., 2011) which is a pre-commercial wave energy project being developed by ESB in partnership with a number of wave energy companies. At the outset of this thesis, the wave resource off the surrounding areas had undergone basic wave climate analysis. This was compiled as part of the 'Accessible Wave Energy Resource Atlas for Ireland (McCullen, 2005)'. However, the level of detail in this is relatively limited. Therefore there was reason to further investigate the wave climate in this area. Earlier in this chapter the drawbacks associated with shoreline WECs thus far were outlined. However, if adaptations were made to overcome these disadvantages, shoreline installations may yet be feasible particularly in a marine domain adjacent to planned WEC development. It is in that context that the subterranean oscillating water column (SOWC) wave energy converter was considered as the research subject for this thesis.

1.4 THE SUBTERRANEAN OSCILLATING WATER COLUMN WAVE ENERGY CONVERTER

A SOWC wave energy converter is a version of an oscillating water column (OWC) wave energy converter, which is constructed within a cliff. For details of its operation, see Section 2.3.2. A SOWC and its power conversion processes are presented diagrammatically in Figure 1.3 below.

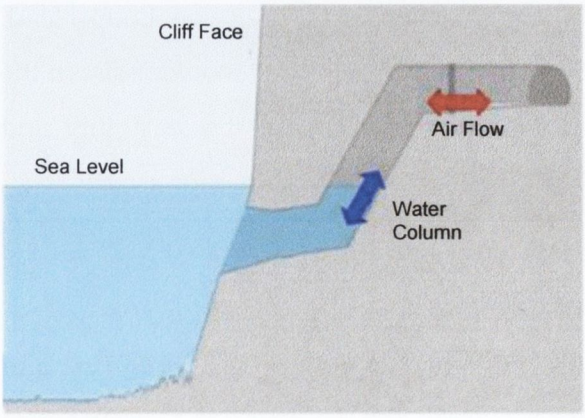

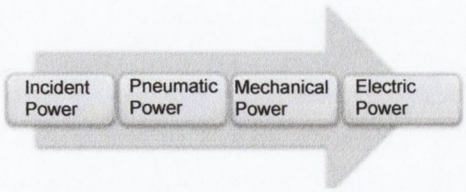

1. Ocean waves impinge upon the OWC chamber;
2. This causes the water column within the chamber to oscillate which compresses & expands the inner air mass;
3. This induces alternating air flow within the chamber.
4. The bi-directional air flow actuates a turbine linked to an electric generator.

Figure 1.3 The SOWC wave energy converter (left) and power conversion process (right).

As the SOWC is concealed within a cliff it may be more visually acceptable than other shoreline devices. Also this concept can afford access to water that is relatively deep, in comparison to other shoreline technologies. This in turn allows access to a greater wave energy resource with the associated potential of greater energy production than that achieved by other shoreline devices in shallower positions. Furthermore, there are possibilities that its construction costs may be lower and its survivability greater compared to some other WEC installations. Also the development of sophisticated 3rd generation spectral wave models coupled with high performance computing has significantly increased the level of accuracy that can be achieved in near-shore and coastal wave energy resource assessments, thus facilitating investigation into the feasibility and design of shoreline devices.

Previous investigative work has been carried out on the feasibility and performance of SOWC wave energy converters in Ireland, headed by the Trinity College Dublin School of Business Studies, funded by the Marine Institute (Marine Institute, 2000). This research showed that the use of established tunnelling methods could be applied to construct SOWC chambers within ocean facing cliffs. The technique was explored in relation to a potential site at Loop Head, Co. Clare. The findings of this research showed that the approach held promise (HMRC, 1997). The outcomes were presented in two Colloquia held in Dublin (TCD, 1996; 1997) which were published in summary form by the Marine Institute (Marine Institute, 2000). It was noted above, that an area of interest for marine energy is located at Loop Head, Co. Clare and that further mapping of wave energy resources in adjacent areas may be useful. It is also noted that the site identified by Trinity's earlier study on SOWCs was Loop Head, which is also adjacent to this area. Therefore the mapping exercise would assist in the process of building on the Trinity study to further investigate the feasibility and design of SOWC installations at Loop Head.

1.5 Research Aims and Objectives

The research programme described in this thesis had two main aims. The first aim was to characterise the wave climate for a domain off the coast of County Clare adjacent to Loop Head, as this is an area of interest for ocean energy development in Ireland. The second aim was to use the findings from a wave climate modelling study conducted to achieve the first aim and build upon an earlier TCD (Marine

Institute, 2000) study to investigate design parameters which may influence the survivability and feasibility of potential SOWCs installed at Loop Head.

The first aim of characterising the wave climate for a domain off the coast of County Clare adjacent to Loop Head entailed the following specific objectives.

- To develop and calibrate a 3rd generation spectral wave model for on-shore, near-shore and off-shore domains off Loop Head
- To assess wave power levels off the County Clare coast from off-shore to near-shore and on-shore domains (for the purpose of this thesis, this area is referred to as the 'Clare Domain')
- To determine the wave climate characteristics in regions adjacent to Arch Point and Loop Head extending from depths of approximately 80 m to the cliff base
- To establish the percentage of occurrence of each sea state at locations in the off-shore, near-shore and on-shore areas of the Clare Domain
- To establish the percentage of occurrence of each sea state at specific SOWC sites (Arch Point and the tip of Loop Head).

The second aim of using the findings from a wave climate modelling study conducted to achieve the first aim and build upon an earlier TCD study (Marine Institute, 2000) to investigate design parameters which may influence the survivability and feasibility of potential SOWCs installed at Loop Head was achieved by pursuing the following objectives:

- To investigate factors affecting subterranean oscillating water column (SOWC) wave energy converter to determine bounds for chamber design.
- To develop a numerical hydrodynamic model of a SOWC wave energy converter
- To validate this model by benchmarking it against tank testing data
- To validate this model by benchmarking it against a hydrodynamic model of the full scale Pico OWC (Brito-Melo et al., 1999)
- To use a hydrodynamic model to identify trends in efficiency associated with changes in SOWC design parameters which may be necessary to promote the survivability of these WECs in their potential locations at Arch Point and the tip of Loop Head.

1.6 THESIS PLAN

In this thesis, relevant literature on wave energy converters, wave climate modeling and hydrodynamic modeling will be reviewed in Chapter 2. The research programme described in later chapters was conducted at Loop Head. To check that this location was appropriate for wave energy project development, a preliminary site viability study and survey were conducted. These will be presented in Chapter 3. In Chapter 4 the spectral wave modelling methodology used in this research programme will be described. This will be followed in Chapter 5 with the results of the spectral wave modelling which indicates characteristics of the wave energy resource at Loop Head. This chapter is particularly relevant to the first aim of the research programme: to characterise the wave climate for a domain off the coast of County Clare adjacent to Loop Head.

The design of SOWC wave energy converters, and factors affecting SOWC chamber design, will be considered in Chapter 6. This will be followed in Chapter 7 with a description of the numerical modeling and hydrodynamic analysis procedures used to assess SOWC design performance at particular sites around Loop Head. This chapter is particularly relevant to the second aim of the research programme to use the findings from a wave climate modelling study conducted to achieve the first aim and build upon an earlier TCD study (Marine Institute, 2000) to investigate design parameters which may influence the survivability and feasibility of potential SOWCs installed at Loop Head. In Chapter 8 the results of the research programme will be discussed with reference to its overall aims and objectives. Limitations of findings will also be critically appraised in this closing chapter before considering future research priorities in this field.

Chapter 2
LITERATURE REVIEW

In this chapter literature relevant to the aims and objectives of the research programme described later in this thesis will be reviewed. This programme aimed to (i) characterise the wave climate for a domain off the coast of County Clare adjacent to Loop Head and (ii) use the findings from a wave climate modelling study conducted to achieve the first aim and build upon an earlier TCD (Marine Institute, 2000) study to investigate design parameters which may influence the survivability and feasibility of potential SOWCs installed at Loop Head. The literature review in this chapter will be prefaced by a discussion of factors influencing the feasibility of WECs and best practice standards in this area. Reasons for selecting the type of methodology employed to investigate potential deployment sites, their wave climate, and the interaction of the wave climate with SOWC chamber designs will also be outlined. More focused reviews of literature on certain topics specifically related to either the first aim or the second aim of the overall research programme described in this thesis, will be presented in Chapters 4 and 6 respectively.

2.1 EXTERNAL INFLUENCES ON THE FEASIBILITY OF WAVE ENERGY CONVERTERS

Various government initiatives, academic groups and commercial enterprises potentially support the development of wave energy technology and hence affect the feasibility of further research. The need to develop energy sources to replace fossil fuels and to address rising atmospheric CO_2 levels and climate change are now prominent issues for heads of government across the world. Hence significant effort is devoted to seeking alternative energy systems. Initiatives to support this are being

developed at many levels by government agencies, academic groups and commercial enterprise. Furthermore government, academic and business interests are linking to form international structures, bodies and consortiums aiming to improve the efficiency of research and development in this area. Full exploration of all these developments is beyond the scope of this thesis. However, some international and national agencies and academic groups will be discussed that are relevant to developments in Ireland.

2.1.1 Development of Wave Energy in Ireland

As mentioned in Chapter 1, Ireland has developed its own policy in line with International and European frameworks. As part of the Kyoto Protocol, Ireland agreed by 2020 to reduce greenhouse gas emissions by 20% compared to 2005 levels (European Commission, 2008).The policy of the Irish government is discussed in the government White Paper (2007) outlining the Energy Policy Framework 2007-2020. This covers all areas related to energy and incorporates policy on sustainable and wave energy. It refers to other government policies and reports such as the All Island Energy Framework (2004), National Climate Strategy (2006), Planning and Development Act (2006) and National Development Plan (NDP) 2007-2013), which support the development of sustainable technologies. In 2014, the Minister for Communications, Energy and Natural Resources, Mr. Pat Rabbitte launched the Off-shore Renewable Energy Development Plan (2014) which provides the updated framework for the the sustainable development of Ireland's off-shore renewable energy resources. Irish government agencies that support wave energy include Sustainable Energy Authority of Ireland (SEAI) and the Marine Institute. One of the roles of these agencies is to channel government funding into third level research projects and their collaboration with private companies (Ocean Energy Developments in Ireland, SEI and Marine Institute, 2008).

In 2009, the Marine Renewables Industry Association (MRIA) was established which represents all of the main interests related to wave and tidal energy on the island of Ireland. Members of the MRIA include utilities, such as ESB international and Bord Gais Eireann, site developers, firms engaged in device development and manufacture, consultants, R & D business, supply chain activities and academic

researchers. The MRIA provides a forum to identify the needs for wave energy to progress and to support these in various ways (Coyle, 2012). The current view of the MRIA is that Ireland has an unprecedented opportunity to build a position of strength as a supply chain to the world-wide ocean energy industry. However, the Irish Government needs to give the private sector the confidence to invest in ocean energy. This can be achieved through (i) the provision of an allocation of ocean energy Renewable Energy Feed-In Tariff (REFIT) to incentivise early investment, (ii) clear consenting process administered by a single body, (iii) capital grants regime which addresses the needs of device developers and (iv) clear route to grid access (MRIA, 2013). This is required if wave energy is to contribute to Ireland's renewable energy targets. At present, it is uncertain how much wave energy will contribute to Ireland's target of 33% of its electricity generated via renewable resources by 2020 (Dept. of Communications, Marine and Natural Resources, 2007). However, the considerable opportunities for the industry have been presented in the Ocean Energy Roadmap to 2050 (Sustainable Energy Authority of Ireland, 2010). This indicates that with appropriate support from the Government and governing bodies and action by the industry, power utilities and regulators, an annual output from wave energy sources between 20 TWh (lower estimate) and 120 TWh (higher estimate) could be expected by 2050. Referring to the same document, An Taoiseach, Enda Kenny, expressed his belief that the ocean energy industry has the potential to create up to 70,000 jobs with a cumulative economic benefit approaching €120 billion by 2050 (Mayo Today, 2012). Recent government support includes a €15 million investment in ocean energy with the construction of a state of the art lab for marine renewables, titled the Beaufort Lab, in Co. Cork (The Journal, 2012).

Regarding the support of wave energy converter concepts at developmental stage, the Marine Renewable Infrastructure Network (MARINET) offers the opportunity of free-of-charge- access to R&D facilities. It is an €11m European initiative, open to all ocean energy researchers in Europe, which is funded through the EU's Seventh Framework Programme (FP7). This initiative was established in 2011 with an aim to accelerate the commercialisation of marine renewable energy (Healy, 2012).

Overall it can be seen that there are complex systems of international and European organisations, government initiatives, agencies and advisory bodies, academic

interest groups, and commercial companies all involved in an increasingly interconnected manner in order to support the development of wave energy. This increases the opportunity for the development of feasible wave energy converters. However, points made by the MRIA suggest that further governmental support is required to achieve commercially viable deployment of full scale WECs on Ireland's coast.

2.2 Standards and Codes of Best Practice

Considerable work has been carried out over the last decade on the development of guidelines and codes of best practice. Particularly important to the progress of the wave industry has been the creation of standardised methods for project development. In addition to detailing testing and analysis protocols, these standards aim to provide developers and investors with key milestones that show and quantify device progression. This has culminated in the 2013 publication of International Standards for marine energy conversion systems by the established International Electrotechnical Commission (IEC).

The IEC is one of the oldest standards making bodies in existence and facilitates access to the electricity market via its renowned standardisation approach for testing and certification. In 2007 it established the Technical Committee, TC114, to prepare international standards for marine energy conversion systems. This signifies the growth of the industry as it follows in the footsteps of the wind energy industry which established its IEC Technical Committee, TC 88, in 2006 to provide uniform information exchange for monitoring and control of wind power. The intended users of such standards include project developers, device developers, utility investors, policy-makers, planners and consultants involved in producing resource data. Their interests will include return on investment, performance of the device, the reliability and predictability of power supply, usage of seascape, optimisation of resource, and production of a compatible, readable data format etc. In Ireland, the Electrotechnical Council of Ireland (ETCI) has set up a technical committee known as TC18 which links with the TC114.

The basis for the 2013 IEC standards were laid by existing standardisation documents produced by the International Energy Agency-Ocean Energy Systems (IEA-OES)

Annexes, the Equimar initiative, the European Marine Energy Centre (EMEC) guidelines, the Hydraulics and Maritime Research Centre (HMRC), the UK Department of Trade and Industry (DTI), Det Norske Veritas (DNV) and Germanischer Lloyd (GL). Notable documents consulted during this research programme were:

- Equimar Deliverable D2.2 Wave and Tidal Resource Characterisation (Venugopal, Davey, Helen Smith, et al., 2011)
- Equimar Deliverable D2.3 Numerical Models (Venugopal et al., 2010)
- Equimar Deliverable D2.4Wave Model Intercomparison (Venugopal, Davey, Smith, et al., 2011)
- Equimar Deliverable D2.6 Extremes and Long Term Extrapolation (Prevosto, 2011)
- Equimar Deliverable D2.7 Protocols for wave and tidal resource assessment (Davey et al., 2010)
- Equimar Deliverable D7.2.1 Procedures for Economic Evaluation (Ingram et al., 2011)
- EMEC - Assessment of Performance of Wave Energy Conversion Systems (Pitt, 2009)
- Ocean Energy: Development and Evaluation Protocol (Holmes, 2003).
- Annex II Task 2.1 Guidelines for the Development & Testing of Wave Energy Systems (Nielsen and Holmes, 2010);
- Off-shore Service Specification DNV-OSS-312: Certification of Tidal and Wave Energy Converters (Det Norske Veritas, 2008)
- Guidelines on design and operation of wave energy converters: A guide to assessment and application of engineering standards and recommended practices for wave energy conversion devices' (Carbon Trust, 2005).

For further information on the use of such standards as applied to wave energy resource assessment, see Chapter 4.

Other progress in the use of standards comes with the development of the Technology Readiness Levels (TRLs) framework. This has been adopted by Ireland's Electricity Supply Board (ESB), and directly correlates with five stages of WEC development outlined in the Development and Evaluation Protocol produced by the

Hydraulics Maritime Research Centre (Holmes, 2003). A summary of the relationship between the 9 TRLs and 5 stages of development for a wave energy converter is presented in Table 2.1 below with the associated functional and lifecycle aims.

Table 2.1 Technology readiness levels (TRLs) adopted by ESB to promote WEC development WEC concept to commercialisation. Source: (Fitzgerald and Bolund, 2012)

Stage	TRL	Functional Readiness	Lifecycle Readiness	Scale
1 Concept Validation	1	Basic principles observed and reported	Potential uses of technology identified	n/a
	2	Technology concept formulated.	Market and purpose of technology identified	>1:100
	3	Analytical and experimental critical function and/or characteristic proof-of concept.	Initial capital cost and power production estimates / targets established	>1:25
2 Design Validation	4	Technology component and/or basic technology subsystem validation in a laboratory environment.	Preliminary Lifecycle design	>1:15
3 Systems Validation	5	Technology component and/or basic technology subsystem validation in a relevant environment.	Supply-chain Mobilisation	>1:4
	6	Technology system model or prototype demonstration in a relevant environment.	Customer interaction	>1:4
4 Device Validation	7	Technology system prototype demonstration in an operational environment.	Ocean Operational Readiness	1:2
	8	Actual Product completed and qualified through test and demonstration.	Actual Marine Operations completed and qualified through test and demonstration.	1:1
5 Economics Validation	9	Operational performance and reliability of an array demonstrated	Fully de-risked business plan for utility scale deployment of arrays	1:1

To give an indication of the level of advancement associated with each stage, TRLs 1 to 9 will be briefly described. The primary objectives for TRLs 1-3 are: (1) concept verification with monochromatic waves of small amplitude; (2) investigation into performance and responses with simplified power take off and (3) device optimisation, optimising wave energy converter design for site specific wave climates.

An excerpt from the stage development summary table given in 'Annex II, Guidelines for the Development and Testing of Wave Energy Systems' is presented in Table 2.2. It presents the objectives and investigations associated with TRL 1-3 along with recommendations for the numerical modelling programme.

Table 2.2 Stage development summary table: TRL objectives and associated recommendations for numerical modelling programme. Source: (Holmes and Nielsen, 2010)

	Stage 1: Concept Validation		
Development Protocol	TRL 1: Confirmation of Operation	TRL 2: Performance Convergence	TRL 3: Device Optimisation
Objective/ Investigations	Operation Verification Design Variables Physical Process Validate/Calibrate Maths Model Damping Effect	Real Generic Seas Design Variables Damping PTO Natural Period Power Absorption Wave to Device response	Wave Energy Converter Geometry Components Configurations Power Take Off Characteristics Design Engineering
Maths Methods (Computer)	Hydrodynamic, numerical frequency domain to solve the model undamped linear equations of motion.		Finite waves Applied Damping Mult. Freq. Inputs

It can be seen that the row titled *maths methods* recommends that a numerical frequency domain model be implemented to solve the linear equation of motion for the undamped and damped system. This section of the *Guidelines for the Development and Testing of Wave Energy Systems* relates to aspects of the present research programme and is addressed in Chapter 7 on hydrodynamic analysis. Costing estimates for TRL 1-3 range from €25,000 to €75,000. This accounts for tank testing WEC models at small scale, 1:25-100.

TRL 4 relates to final wave energy converter design with accurate power take off (PTO) and control strategy. The recommended scale for a physical modelling programme is approximately 1: 10-25. Recommendations for the accompanying numerical model include a time domain response model comprising control strategy. Costing estimates for TRL 4 test programme range from €50,000 to €250,000. TRLs 5-6 relate to a testing schedule that demonstrates all wave energy converter subsystems, incorporating a fully operational PTO that enables demonstration of the energy conversion process from wave to wire. The scale associated with physical testing is approximately 1:4. The estimated cost of this testing programme is

€1,000,000 to €2,500,000. TRL 7-8 relate to a solo machine pilot plant validation at sea in a scale approaching 1:1, full size. To progress to TRL 9, the device as a whole must be proven fit for purpose and be connected to the grid. TRL 7-8 is considered pre-commercial, with a testing programme costing €10m to €20m. TRL 9 is the final stage, relating to arrays of proven wave energy converters, providing electricity to the grid. The cost and model scale associated with each stage of development are summarised in Figure 2.1 below.

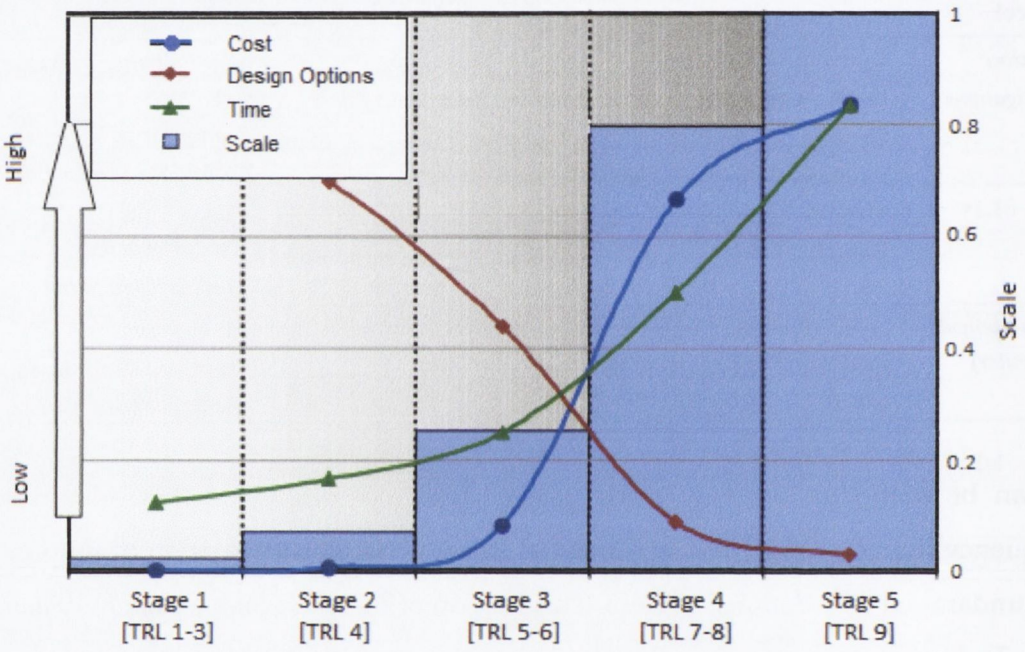

Figure 2.1 Cost, design options, time and scale associated with each stage of development, from TRL 1 to 9. Source: (Holmes and Nielsen, 2010)

It can be seen that the cost increases significantly from TRL 4 onwards as larger scale models are required to meet the objectives of TRLs 5-9. The red line represents the level of WEC design options altered at each stage of development. During the initial stages of development, many design alterations may be made to optimise the design. Numerical modelling can form an important part of this work as it permits many design alterations in comparison to physical models. While optimising the WEC structure, a simplified power take off may be employed. However once the core WEC design is established, investigations shift to the behaviour of more realistic power take off mechanisms which require a larger model scale. This relates to TRL 4 onwards, and it can be seen in Figure 2.1 that scale increases accordingly. Relative time required to complete each stage is plotted as a green line. Although many issues

may affect the time taken for each stage, the green line provides a generalisation that more time is required at higher TRLs.

This research programme did not have access to physical tank testing facilities. However, hydrodynamic analysis of SOWC chamber designs was carried out using the boundary element method (BEM) code, WAMIT. It will be seen in Chapter 7 on hydrodynamic analysis that this facilitated analysis of numerous SOWC chamber designs in the presence of waves. Using this method, it was possible to assess the effects alterations in chamber design had on the hydrodynamic behaviour of the water column, including identification of the natural period. Dampings were applied to represent the power take off. Using this numerical modelling technique, investigations relating to parts of TRL 1-3 were carried out.

2.3 WAVE ENERGY CONVERTERS

There is an extensive range of wave energy converter technologies and it is not appropriate to consider each in this selective literature review. A review of the principle technologies as well as a history of wave energy conversion can be found in Falcao (2010) 'Wave Energy Utilisation: A review of technologies'. In this review, detailed information on each technology can be obtained from the accompanying references.

Regarding the OWC principle, the first known existence of practical wave energy conversion was from a device constructed around 1910 at Royan near Bordeaux in France (Falnes, 2000). Here, Mr. Bochaux-Praceique supplied his house with 1 kW of light and power from a turbine, driven by air which was pumped by the oscillations of sea water in a vertical bore hole in a cliff'. This represents the first reported OWC-type WEC in practical use and comprised the complete power conversion chain from wave-to-wire. However, it is predominantly since the mid 1970s that research and development on wave energy has been carried out. Demonstration of the initial wave energy converters began in the mid 1980s. Various full and part scale OWC prototypes were tested at sea, particularly in the last decade. Literature detailing these developments includes 'Wave Energy Conversion' by Brooke (2003) and 'Ocean Wave Energy: Current Status and Future Perspectives' by Cruz. et al (2008).

Currently, the wave energy industry is at the pre-commercial stage, with a number of different technologies evolving to face the challenges presented by the harsh marine environment.

2.3.1 WEC Classification

The different types of wave energy converter are classified according to the direction of the wave in relation to the device, and their method of energy extraction. With respect to the directional characteristic, there are:

- Point absorbers. These float and absorb energy in all directions through movement at or near the water surface.
- Terminators. These have a principal axis parallel to the incident wave crest, upon which the wave terminates.
- Attenuators. These are floating devices with elements perpendicular to the wave direction that can be constrained to produce energy.

With respect to the energy extraction characteristic, there are:

- Oscillating water columns (OWCs). These are partially submerged hollow structures enclosing a column of air above a column of water. Waves cause the water column to rise and fall, alternately pressurising the column of air. The energy is extracted from the air column via a turbine.
- Overtopping devices. Water is captured from the waves, stored above sea level and released to produce energy.
- Wave activated bodies. The motion of different parts of the device relative to each other activates a hydraulic system, often to compress oil which then drives a generator.

This variety of working principles induces different characteristic capture width ratios. Capture width ratio is defined as the power absorbed with respect to the incident wave power available to the wave energy converter. The capture width ratio for three notable devices outlined in a recent numerical benchmarking study (Babarit et al., 2012) are presented in Table 2.3

Table 2.3 Range of capture width ratios for three WECs. Source: (Babarit et al., 2012)

WEC Concept	Range of Capture Width Ratio
Floating oscillating water column	38 % - 50%
Floating three body oscillating flap	7 % - 20 %
Bottom fixed oscillating flap	52 % - 72%

2.3.2 The OWC Wave Energy Converter

Among the variety of wave energy conversion principles and associated technologies that have reached the pre-commercial stage of development, OWCs have attracted significant attention. The OWC wave energy converter can be classified as a terminator device. This denotes an absolute reactional reference frame, meaning that the reactional forces required to extract energy from the waves are provided by the fixed OWC structure. A terminator WEC has its principal axis parallel to the incident wave crest and terminates the wave. The energy extracted from the system comes from the heaving motion of the water column within the chamber. The primary energy conversion component is the pressurised air chamber, which is referenced to the atmospheric air pressure via a turbine and power take off. The turbine exerts a damping force on the oscillating air flow which facilitates the energy extraction. A generator is then employed to convert the mechanical energy from the turbine to usable electrical energy. This description is in line with the WEC classification template developed by Equimar (Myers et al., 2010). Figure 2.2 presents a cross sectional view of the conventional OWC caisson positioned at coastal location.

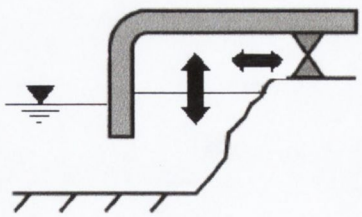

Figure 2.2 Device classification. Source: (Myers et al., 2010)

The Oscillating Water Column (OWC) wave energy converter can be considered as a number of sequential subsystems which link together to output electrical power. Each subsystem relates to an energy conversion process which is required to transform the incident wave energy to electrical energy. There are three dominant energy conversion processes which take place within the OWC system.

Initially, the hydrodynamic power of the impinging wave field is converted into aerodynamic power via the pressurisation and depressurisation of air within the OWC chamber. Secondly, the inhaling and exhaling airflow is transformed to mechanical power by means of an air turbine. The rotating drive shaft of the turbine is coupled with a generator to convert the mechanical power to electric power. This is the third energy conversion process. The electric power is then delivered to the grid, which is considered as a separate external system with which the OWC wave energy converter interacts. The governing subsystems in the OWC wave energy converter are the OWC chamber, turbine and generator. The relationship between these governing subsystems is illustrated in Figure 2.3 below.

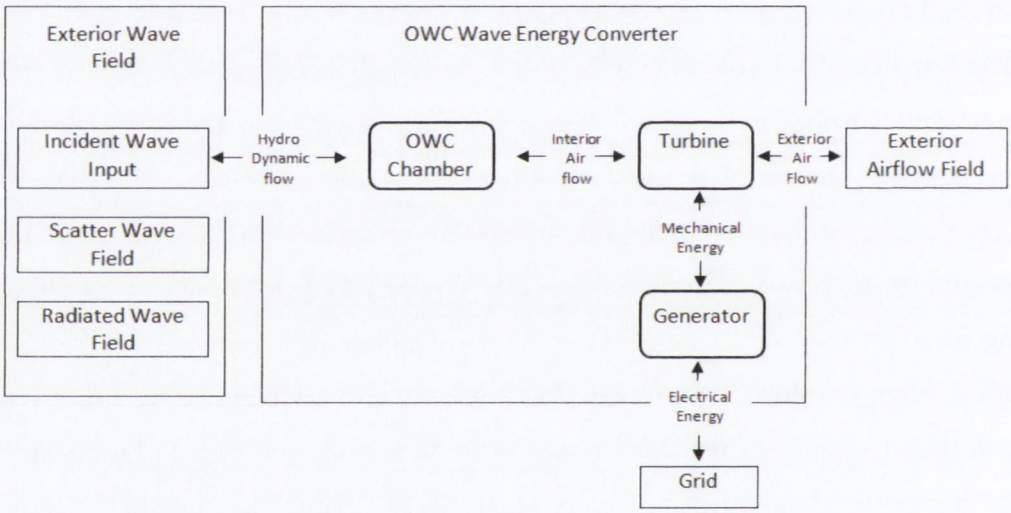

Figure 2.3 Relationship between subsystems in an OWC wave energy converter

The overall efficiency of an OWC plant is given by the product of the three governing subsystem efficiencies:

$$\eta = \eta_{owc}\eta_t\eta_e \tag{2.1}$$

where η_{owc} is the efficiency of the OWC, η_t is the turbine efficiency and η_e is the electrical generator efficiency. The objective is to arrive at a configuration that can provide a high overall efficiency spanning the predicted range of input conditions. To achieve this, an optimal arrangement and sizing of the OWC chamber, turbine and generator is required.

In terms of annual energy output, the results need to be presented in the form of average electrical power generated over the range of wave conditions at the OWC WEC site. This is because high efficiency of one component in the chain at one operating condition is likely to be misleading and insufficient to characterise performance. To maximise average electrical power output, the output from each subsystem must be optimised to suit the input requirements of the succeeding subsystem. Therefore, to design an OWC wave energy converter correctly, a theoretical understanding of each subsystem is essential. However depending on the level of theoretical assumptions, the way in which the subsystems operate in theory and reality can vary significantly depending on the wave conditions.

One of the advantages of OWCs is that they are considered robust as they have few mechanical moving parts. Additionally, these moving parts do not interact with the impinging waves, as the power take-off is located at a distance from the free surface. OWCs can be installed at off-shore, near-shore and shoreline locations which each have their characteristic advantages and disadvantages. Full-sized OWC prototypes have been built in Norway (Toftestallen, 1985), Japan (Sakata, 1990), India (Vizhinjam, 1990), Portugal (Pico, Azores, 1999), and the UK (the LIMPET plant in Islay island, Scotland, 2000). The largest of all, a near-shore bottom-standing plant named OSPREY, was destroyed by the sea in 1996 shortly after having been towed and sunk into place near the Scottish coast. Most notably, the first OWC wave power plant consisting of 16 OWC chambers was recently built in Spain (Mutriku, 2010). The cost of the project was shared with the development of the breakwater in which the OWCs were built. In all of these cases, the structures are fixed (bottom-standing or built on a rocky sloping wall) and the main piece of equipment is the Wells air turbine driving an electrical generator. All of the structures are made of concrete, except the OSPREY.

It is primarily the initial construction capital cost of the chamber that has compromised the commercial feasibility of shoreline OWCs (Thorpe, 2001; Falcao, 2003). The initial capital cost of constructing concrete shoreline OWCs is too high, in comparison to the revenue returned by the power they generate. The Carbon Trust carried out an evaluation of OWC wave energy converters in line with the Marine Energy Challenge (2005) which estimated 27 €c/kWh for a 500kW shoreline OWC

with 10% project rate of return. This is an optimistic value compared to that given in a more recent report entitled 'Results of the Marine Energy Challenge: Cost Competitiveness and growth of wave and tidal energy (2006)'. According to this report the cost is 17 - 63 €c/kWh for small wave farms, with central estimates in the sub-range of 31 – 36 €c/kWh. Furthermore, arrays of wave energy converters have the intrinsic benefit of economies of scale. It is also argued in this report that a 50% reduction in civil costs would be required to reach an economic rate of 18 €c/kWh. A reduction of this magnitude would require OWC costs to be shared with related infrastructural projects (such as the previously mentioned breakwater at Mutriku) or a radical change of concept.

2.3.3 The SOWC Wave Energy Converter

One possible change of concept in relation to OWCs is to locate them inside natural existing shore-line features, i.e. cliffs and to use a different construction method utilising tunnelling. This type of OWC is known a Subterranean OWC (SOWC). As mentioned above, the cost of constructing traditional concrete shore-line OWCs is considered to be too high. As the drilling technology which could be used to create SOWCs is well established and at an advanced stage, this approach could possibly reduce the initial construction cost significantly. There is the possibility therefore that this modification could increase the feasibility of installing future OWC devices. Additionally, this construction technique facilitates a means of extracting wave energy at deep water coastal locations with annual average power estimates comparable with near-shore locations. The basic design of the SOWC, excluding the power take off, is presented in Figure 2.4.

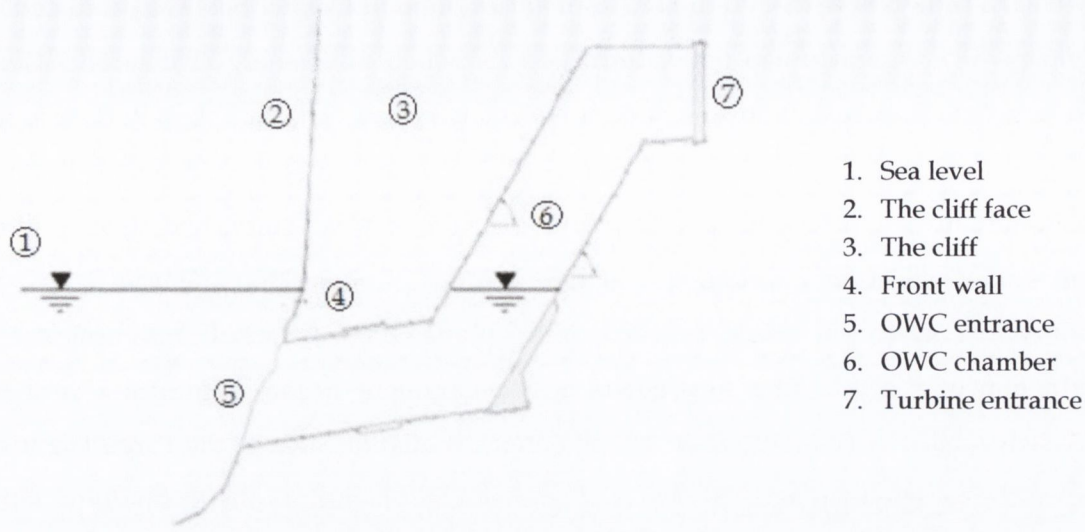

Figure 2.4 The SOWC wave energy converter (cross sectional view)

Previous investigative work has been carried out into the feasibility and performance of subterranean OWC systems in Ireland headed by the TCD School of Business Studies, funded by the Marine Institute (Marine Institute, 2000). This research showed that the use of advanced Scandinavian underground space technology could be applied to making OWC chambers from the cliffs themselves by drilling from the cliff top and blasting rock from the underwater cliff face and behind it, out into the sea. The findings of this research were presented in two Colloquia held in Dublin (TCD, 1996; 1997) which were published in summary form by the Marine Institute (Marine Institute, 2000).

Another attempt to develop subterranean OWC technology funded by the UK government occurred at a worked-out copper mine in Cornwall. Here copper seams had been mined out to the faces of seashore cliffs, leaving potentially ready-made OWC chambers. The experiment, however, was only partly successful mainly because the mouth of the cave selected for testing was not constantly fully submerged throughout the lunar tidal cycle. Also too much wave energy reaching the cliff was reflected before the swell entered the chamber (DTI, 2004).

The most advanced work carried out on the concept of subterranean OWCs to date was by the company Sewave Ltd. This company emerged from collaboration between the electric utility, SEV, based in the Faroe Islands and the company,

Wavegen (now known as Voith-Hydro) that developed LIMPET. Sewave produced a report which demonstrated the viability of a tunnelled wave energy converter based on the OWC principle. It outlined how to develop a demonstration plant in the Faroe Islands and establish the information needed for optimisation and detailed design. Although this report is not in the public domain, it was established that system performance has been investigated via a programme of physical model tests to assess hydrodynamic to pneumatic power capture (Lane, 2009; Personal communication with Sewave, 2010). This facilitated the development of an optimum chamber geometry and PTO configuration for potential installation sites in the Faroe Islands. Sewave also demonstrated the potential commercial viability of the technology with reference to technology improvements, economies of scale, growing demand for wave power, and the future price of electricity. Additionally, Sewave Ltd. has identified the west coasts of Norway and Ireland as areas where their technology could potentially be implemented. In 2005, Sewave Ltd. conducted a TWEC site feasibility study on the Irish coastline. It established that there is 77 km of Irish coastline potentially suitable for the implementation of a tunnelled chamber. The report, on which this result is based, is classified (Sewave, 2011, personnel communication).

2.4 Influence of Location on Feasibility

As has been seen, there are many options for a potential wave energy project developer to consider, including the fact that there is a wide range of different wave energy converter designs. Different designs are suited to different marine locations. These locations include the off-shore domain, the near-shore domain and the on-shore domain. There are pros and cons associated with each. These have been discussed in Chapter 1 but are re-capped as follows:

To reach national targets for wave energy, WECs deployed in large arrays, analogous to wind farms would be needed. Wave farms are likely to be deployed in long arrays at right angles to the dominant wave direction. The total size of the array will depend on the space required by each unit on its moorings, its capture width and its installed capacity. In light of the scale and space requirements of these arrays, it is apparent that these wave farms need to be predominantly located at near-shore and off-shore locations. Off-shore sites would also allow for the placement of several farms in close proximity. Furthermore the highest wave energy values are recorded off-shore.

However a disadvantage associated with off-shore sites, is the potential for extreme sea states to damage the WEC installations. Also the remoteness of the site can lead to higher costs for access and maintenance.

In near-shore sites the sizes of WEC arrays are more limited in comparison to those located off-shore, but advantages include being more accessible and somewhat sheltered from extreme waves. However, near-shore sites can be visible from the land and may occupy areas otherwise used for leisure sailing, fishing etc. This could cause difficulties regarding acceptability to the public and the tourism industry, and therefore could be associated with more planning and consent problems due to visual impact in scenic locations etc.

With respect to the on-shore domain, wave power reduces as water depth decreases, primarily due to depth induced wave breaking, depth induced friction, triad interaction and refraction. This has a significant effect on the economic attractiveness of a shoreline site. However, research has shown that that for the majority of sea states (i.e. less than 100 kW/m), the loss of wave power is relatively small up to a water depth of approximately 10 - 15 m (Folley and Whittaker, 2009). Therefore, if it is possible to identify shoreline locations that possess a minimum water depth of 10 - 15 m with a favourable wave energy resource, it increases the viability of the site. The quantification of the exploitable resource at shoreline sites is central to the feasibility of a shoreline location. Also as mentioned above, construction costs, the smallness of scale of possible installations, public acceptance and consent issues have militated against deployment of shore-line WECs. However, there may be some potential advantages for shore-line WECs, as discussed in Chapter 1. To recap, examples of such reasons include the following:

1) An appropriate shore-line WEC may facilitate assessment of wave integrated with wind, without the associated cost, risk, etc. associated with near-shore and off-shore deployment.
2) Also at areas of interest to marine renewables, studies have shown that the integration of different wave energy converters promotes a more stable electrical output (Chozas et al., 2012). The evolution of the wave energy industry may lead to deployment of feasible WECs with particular technologies suited to the off-shore, near-shore and shore-line domain, as

depicted by Figure 2.5. With the advancement of near-shore and off-shore technologies, the SOWC WEC offers itself as a means to supplement their power production. If the electrical grid and infrastructure is in place at a certain location, the power production from as many sources as possible produces a more even power output.

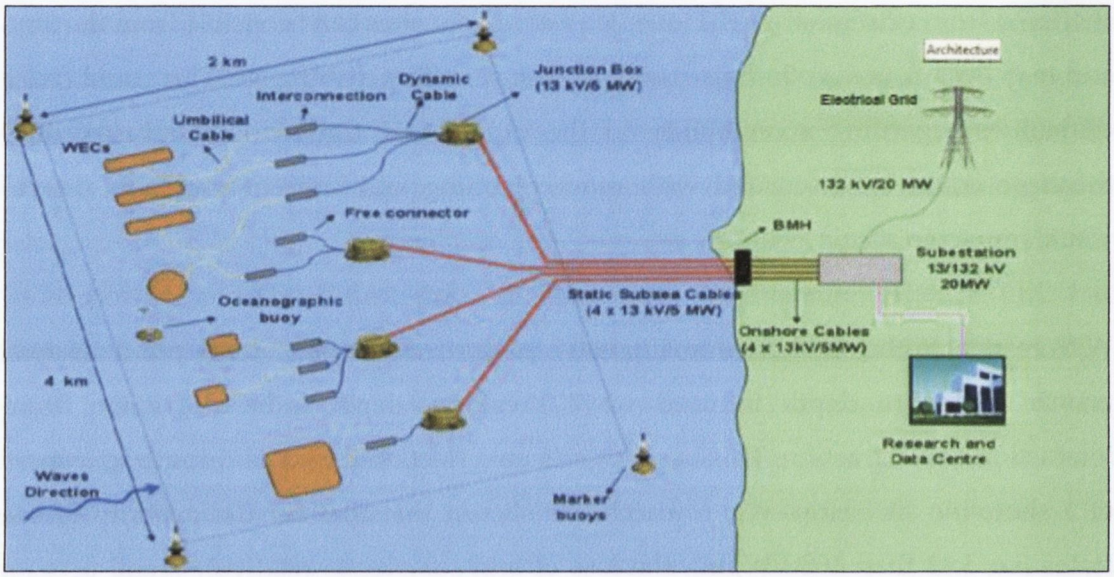

Figure 2.5 Off-shore, near-shore and on-shore domains with grid connection point.

In summary, these points have relevance to the two main aims of this thesis. They indicate the possible value in estimating the level of potential wave energy in a near-shore domain in an area designated for ocean energy deployment. This links to the first aim of the project which was to characterise the wave climate for a domain off the coast of County Clare adjacent to Loop Head. Also as discussed above, with respect to possible deployment of a shoreline WEC, SOWCs may have advantages over traditionally constructed shoreline OWCs if they are found to offer comparative benefits in cost, survivability and environmental acceptance. Therefore while reservations have developed about the commercial deployment of shoreline WECs, including OWCs, it is reasonable to investigate the feasibility of deploying SOWCs in this domain. This links to the second aim of this project which was to use the findings from a wave climate modelling study conducted to achieve the first aim and build upon an earlier TCD (Marine Institute, 2000) study to investigate design parameters which may influence the survivability and feasibility of potential SOWCs installed at Loop Head.

2.5 WAVE ENERGY RESOURCE CHARACTERISATION

To support and improve the development of wave energy converters, it is important to characterise the physical conditions at potential deployment sites. An understanding of the wave climate based on a number of years of measurements facilitates every stage of the WEC development process from concept to commercialisation. Some of the key benefits associated with WEC design include optimisation with respect to power generation and WEC design regarding survivability. Then at all levels of development, wave energy resource characterisation assists predictions for power generation. Regarding full scale commercial deployment, characterisation of the wave energy resource is essential to estimating predictability of electricity generation and income. This benefits investors in terms of return on investment. Additionally, long term statistical wave data may be used to predict number of days suitable for maintenance per year, i.e. weather windows.

To characterise the resource at a given location, long term measurements for a range of parameters are required. If the wave measurements are limited to a relatively short length of time, the level of confidence that can be placed in results is reduced. This is due to aleotory uncertainty which is associated with the variability of the wave climate from year to year. It stems from the fact that the period chosen for analysis may not be fully representative of the long-term prevailing wave climate. This is described by Figure 2.6, which shows the average wave power at Wavehub from 1960 to 2000.

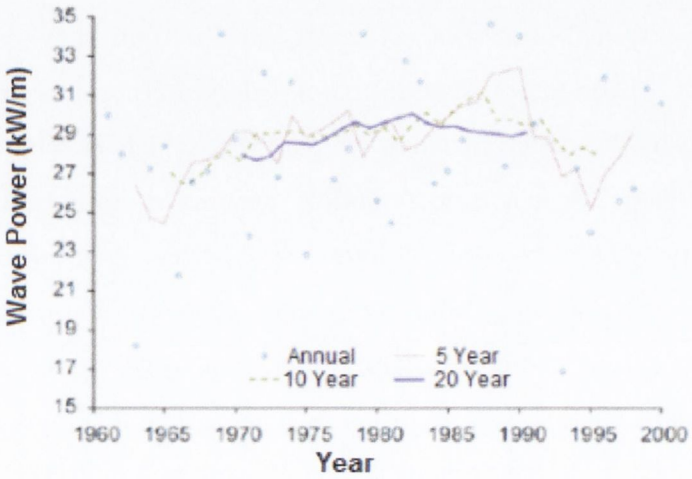

Figure 2.6 Variation in wave power at the WaveHub site 1960-2000. Source: (Folley et al., 2012)

Looking at Figure 2.6, it can be seen that the average wave power value based on 1 year of records is more variable than the average wave power based on a 20 year record. Similarly it can be seen that a 5 year record provides a variable average in comparison to a 10 year average. In line with this, the IEC standards recommend measurements spanning 10 years when carrying out a wave energy resource assessment.

This leads to the requirement for wave climate modelling, particularly for the near-shore and on-shore domain. Few wave measurement buoys have been deployed at wave energy test sites for 10 years. However, Global and European wave models such as those developed by European Centre for Medium-Range Weather Forecasts (ECMWF), Oceanweather Inc. (OWI), Danish Hydraulics Institute (DHI) and National Centres for Environmental Prediction (NCEP) (Kållberg et al., 2005), have been used to run hindcast models for extended periods of time. In most cases, these have been validated using networks of off-shore wave measurement buoys and satellite altimeters. Therefore, long term measurements exist at certain points within the aforementioned European and Global models. However, these points are off-shore, often far from the wave energy test site which requires resource characterisation. Thus, a means is required to transform validated long term wave measurements at off-shore locations to the area of interest.

The IEC standards have identified the 3rd generation spectral wave model as the recommended means to achieve this (Folley et al., 2013). In comparison to the 1st and 2nd generation spectral models, the 3rd generation spectral model provides a full description of the physical processes governing wave evolution (Venugopal, Davey, Smith, et al., 2011). 1st generation spectral models do not account for nonlinear wave interactions between the different wave frequencies, which is seen as a limitation (Bouws et al., 1998). 2nd generation models possess a limitation based on its parameterised approximations used to model the nonlinear spectral interactions. The 3rd generation spectral wave model overcomes these shortcomings. Numerous studies comparing output from 3rd generation spectral wave models with physically measured wave data have shown high levels of accuracy (Gallagher, Tiron, et al., 2013; Lawrence et al., 2009; Venugopal, Davey, Smith, et al., 2011). It simulates the growth, decay and transformation of wind-generated waves and swell in off-shore,

near-shore and coastal areas, accounting for the following: non-linear wave-wave interaction, dissipation due to white capping, dissipation due to bottom friction, wave growth by action of wind, dissipation due to bottom friction, dissipation due to depth-induced wave breaking, refaction and shoaling due to depth variations and the effect of time-varying water depth caused by the tide. The local bathymetry and coastal topography are taken in to account with the discretisation of the governing equation in geographical and spectral spectral space.

Based on this, the Equimar (Venugopal, Davey, Smith, et al., 2011) and IEC standards (Folley et al., 2012) have endorsed 3rd generation spectral wave models and their related data bases as the most suitable tools to study the long term wave conditions in areas of potential interest to marine renewables. This method was employed to characterise County Clare's wave energy resource. Chapter 4 Spectral Wave Model and Chapter 5 Wave Energy Resource Characterisation describes the process required to transform validated boundary data to a given location, validate measurements at the area of interest and use these measurements to characterise the wave resource. The following section provides the theory behind 3rd generation spectral wave modelling.

2.5.1 Spectral Wave Modelling

Komen et al., (1994) identify the question that lead to the evolution of the equation on which 3rd generation spectral models are based. If one knows the sea state at a given moment, how can the general laws of physics be used to compute the sea state at a later time? The answer to this is the action balance equation. This is the governing equation for a 3rd generation spectral wave model and is described by Equation 2.2.

$$\frac{\partial N}{\partial t} + \nabla \cdot (\vec{v}N) = \frac{S}{\sigma} \tag{2.2}$$

Where $N(\vec{x}, \sigma, \theta, t)$ is the action density, t is the time, σ is angular frequency and $\vec{x} = (x, y)$ is the Cartesian co-ordinates, $\vec{v} = (c_x, c_y, c_\sigma, c_\theta)$ is the propogation velocity of a wave group in the four dimensional phase space $\vec{x}$, σ, θ and S is the source term for the energy balance equation. ∇ is the four dimensional differential operator in the x, σ, θ space.

The boundary data used in the spectral wave model described in Chapter 4 was action density. Boundary conditions in the form of energy density $E(\sigma, \theta)$ are also viable. This is related to action density via Equation 2.3 below.

$$N = \frac{E}{\sigma} \tag{2.3}$$

Where σ is given by Equation 2.4.

$$\sigma = \sqrt{gktanh(kd)} = \omega - \vec{k} \cdot \vec{U} \tag{2.4}$$

Where g is the acceleration due to gravity, k is the wave number, d is water depth, ω is absolute angular frequency, $\vec{k}$ is the wave number vector and $\vec{U}$ is the current velocity vector.

Reverting to the action balance equation, off-shore and near-shore processes are accounted for via the source function S, described by Equation 2.5.

$$S_{tot} = S_{in} + S_{nl} + S_{ds} + S_{bot} + S_{surf} \tag{2.5}$$

Where S_{in} represents the generation of energy by wind, S_{nl} is the wave energy transfer due to non-linear wave-wave interaction, S_{ds} is the dissipation of wave energy due to whitecapping, S_{bot} is the dissipation due to bottom friction and S_{surf} is the dissipation of wave energy due to depth-induced wave breaking. S_{nl}, S_{ds} are off-shore processes and $S_{ds}, S_{bot}, S_{surf}$ are near-shore processes.

Detailed descriptions of each source term are presented in scientific documentation manual for MIKE 21 Spectral wave (DHI Software, 2011). These are accompanied by definitions of the output terms employed in Chapter 4 Spectral Wave Model and Chapter 5 Wave Energy Resource Characterisation. Key terms are significant wave height H_s, energy period T_e and omnidirectional wave power P_{wave} described by Equations 2.6, 2.7 and 2.8 respectively.

$$H_s = \sqrt{m_o} \tag{2.6}$$

$$T_e = \sqrt{2}H \tag{2.7}$$

$$P_{wave} = \rho g \int S(f) c_g(f) df \tag{2.8}$$

Where $m_0 = \int S(f)df$, H is the monochromatic wave height, ρ is the density of sea water, c_g is the wave group velocity and f is the frequency. Most notably, $S(f)$ is the wave spectrum. Wave spectra are central to characterising the resource at a given location. Standard spectra appropriate for certain sites are described in the next section.

2.5.2 Wave Spectra

Due to the stochastic process that is central to the complex form of ocean waves, it can be difficult to estimate the available wave energy at a certain location at a given point in time. Seminal oceanographic research implemented the concept of the wave spectrum (Rice, 1944) to estimate the available wave energy in a particular sea state. This has become a standard approach for characterising the wave energy resource which lends itself to estimating the power absorption by wave energy converters. In the present research programme, this technique was used to calculate the wave energy relating to sea states associated with the scatter diagram for locations of interest. In turn, this information was used to calculate the SOWC's upper limit for power absorption, described in Chapter 7.

The change in sea surface elevation due to waves of differing dimensions can be represented as an infinite series of sine and cosine functions of different wave dimensions. Then, as wave length and wave frequency are related through the dispersion relation, the sea surface can be denoted as an infinite sum of sine and cosine functions of different frequencies. A measured wave record represented as its sine and cosine components is presented in Figure 2.7. It can be seen that the irregular wave time series record is expressed via Fourier series analysis as a sum of a number of regular wave components, each with its own frequency and amplitude.

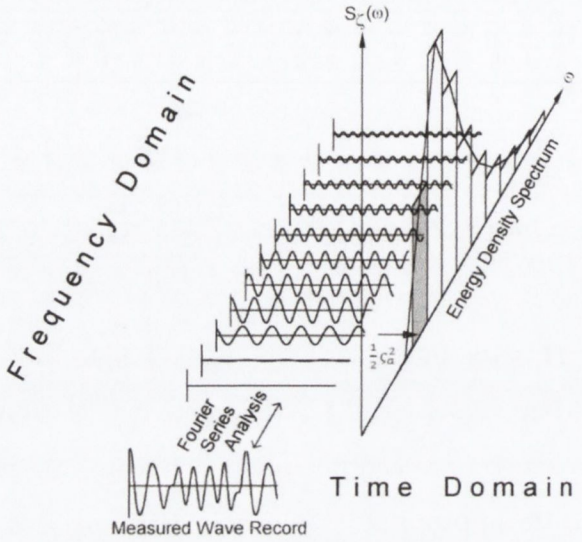

Figure 2.7 Wave record analysis. Source: (Journée and Massie, 2001)

The energy density spectrum $S_\varsigma(\omega)$ can be determined using Equation 2.9, which applies $\frac{1}{2}\varsigma_{a_n}^2$ to each regular wave component associated with the measured wave record, where ς_a is the wave amplitude.

$$S_\varsigma(\omega) \cdot \Delta\omega = \sum_{\omega_n}^{\omega_n+\Delta\omega} \frac{1}{2}\varsigma_{a_n}^2(\omega) \tag{2.9}$$

The energy density spectrum for the aforementioned wave record is presented on the right hand side of Figure 2.7. At certain points in the present research programme, wave spectra have been calculated using frequency *f*, as well as angular frequency ω. The wave spectrum in terms of frequency $S_\varsigma(f)$ can be determined using the relation between f and ω the frequencies $f = \omega/2\pi$.

From the spectrum $S_\varsigma(f)$, the total energy per unit area of sea surface can be calculated using Equation 2.10.

$$E = \rho g \int S(f)\, df \tag{2.10}$$

Wave spectra were computed in the present research programme using the fast Fourier transform (FFT), developed by Cooley and Tukey (1965). It will be seen that

the energy density spectrum is not always regular. Irregular seas induce broad spectra that show several peaks. The peaks may be separated or amalgamated into a broad curve with humps. In contrast, swell waves, which possess a more sinusoidal shape than other wave types, generally give a narrow spectrum. This signifies that the energy is focused in a narrow range of frequencies around a peak value. An example of a spectrum calculated by applying the FFT to a wave record is presented in Figure 2.8. It shows many peaks, signifying that the energy is spread over a range of frequencies.

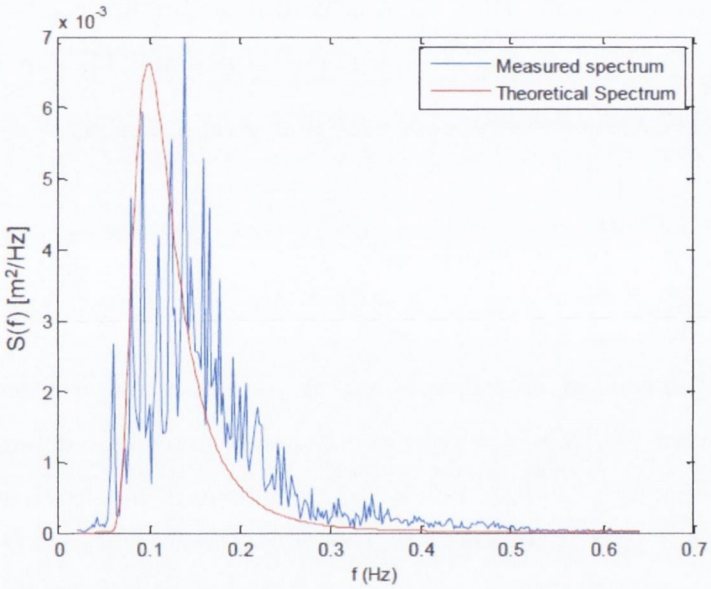

Figure 2.8 Measured spectrum and fitted theoretical spectrum.

In order to compute the measured wave spectrum, high temporal resolution wave records detailing surface elevation are required. For the Loop Head region, wave records of this type were a limited resource in the present research programme. In line with this, appropriate models of the spectrum were investigated. A number of model forms for wave spectra have been developed. These are known as standard wave spectra. Essentially, they are mathematical formulations used to obtain an estimate of the entire spectrum using limited parameters such as significant wave height and wave period. An example of mathematical formulation used to estimate the wave spectrum is denoted by the red line in Figure 2.8. It was plotted using values for significant wave height and peak period.

Examples of standard wave spectra are Bretschneider, JONSWAP, and the TMA spectrum. These have been derived as part of international efforts to accurately

characterise irregular wave conditions in a concise manner. Each named standard spectrum was developed to approximate the actual wave spectrum based on assumptions relating to the location to which it is to be applied. A brief description of the aforementioned standard spectra follows.

The Bretschneider Spectrum was accepted by the 2nd International Ship Structures Congress in 1967 and the 12th International Towing Tank Conference in 1969 as a standard for sea keeping calculations and model experiments (Journée and Massie, 2001). It is particularly suited for open seas and is commonly employed in ocean energy studies. Its mathematical formulation (Equation 2.11) can be described in terms of significant wave height H_s, peak frequency *fp*, and frequency *f*.

$$S(f) = \frac{5}{16}\frac{H_s^2}{f_p}\left(\frac{f_p}{f}\right)^5 \exp\left[-1.25\left(\frac{f_p}{f}\right)^4\right] \tag{2.11}$$

The JONSWAP spectrum was developed as part of a major international effort, known as the Joint North Sea Wave Project, which investigated fetch limited wave evolution (Hasselmann, K. et al., 1976). The basic form of the spectrum is in terms of the peak frequency, as shown in Equation 2.12.

$$S(f) = \frac{\alpha g^2}{(2\pi)^4 f^5}\exp\left[-1.25\left(\frac{f_p}{f}\right)^4\right]\cdot\gamma^{\exp\left[\frac{-(f-f_p)^2}{2\sigma^2 f_p^2}\right]} \tag{2.12}$$

The key element of this standard spectrum is the peak enhancement factor, γ, which allows the spectrum to be tailored to typical wave conditions at a particular region. If the characteristic wave conditions are associated with a wind sea, γ is set to 1. With γ equal to 1, the spectrum approximates the Bretschneider spectrum. However, if the wave conditions at the location of interest are associated with long swell waves, γ is set to 7. This induces an increased spectral peak making it sharper than the Bretschneider. For sites on the west of Europe directly facing the Atlantic ocean, γ is typically set to 3.3 (Babarit, 2011). Thus, for the Loop Head region, γ is set to 3.3.

The TMA spectrum was developed to account for water depth and is described in the Guide to Wave Analysis and Forecasting published by the World Meteorological

Organisation (Bouws et al., 1998). This guide details that in situations with moderate variations in the wave field, the frequency of the waves seems to have a universal spectral shape in shallow water in the same sense as it seems to have in deep water. This assumption prompted Bouws et al. (1985) to propose a universal shape of the spectrum in shallow water that is very similar to the JONSWAP spectrum in deep water. It differs in that the f^{-5} tail is replaced with a transformational constant k^{-3}. The TMA spectrum was developed using measurements made at coastal sites during three separate field experiments (Texel, Marsen and Arsloe). The TMA mathematical formulation can be considered as an extension to the JONSWAP spectrum which facilities the inclusion of water depth at location of interest. This can be seen in Equation 2.13.

$$S(f) = \frac{\alpha g^2}{(2\pi)^4 f^5} \exp\left[-1.25\left(\frac{f_p}{f}\right)^4\right] \cdot \gamma^{\exp\left[\frac{-(f-f_p)^2}{2\sigma^2 f_p^2}\right]} \cdot \phi \tag{2.13}$$

As with the JONSWAP spectrum, the peak enhancement factor γ, is employed to tailor the spectrum to a wind and/or swell sea. The term ϕ is a function of frequency, f, and depth, d. Specifically, ϕ is described by Equation 2.14.

$$\phi = \frac{|k(f,d)|^{-3}\frac{\partial k(f,d)}{\partial f}}{|k(f,\infty)|^{-3}\frac{\partial k(f,\infty)}{\partial f}} \tag{2.14}$$

As water depth increases towards deep water, the TMA spectrum approximates the JONSWAP spectrum with the same peak enhancement factor. As depth reduces, the spectral peak reduces. Using the above Equations 2.11, 2.12 and 2.13, the Bretschneider spectrum, JONSWAP spectrum and TMA spectrum were plotted for the statistically most common sea state in the area under study in this research programme, Co. Clare. This sea state comprises a significant wave height of 1.5 m and energy period equal to 8, based on hourly wave data over four years. The plots for each spectrum are presented in Figure 2.9.

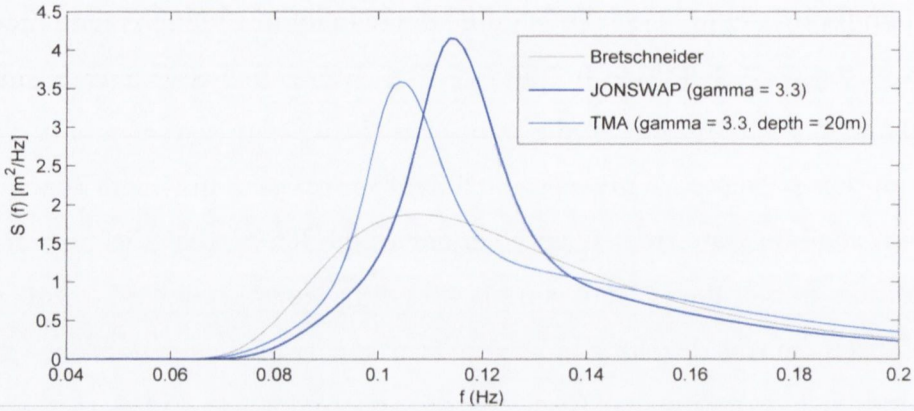

Figure 2.9 Bretschneider spectrum, Jonswap spectrum (γ = 3.3) and TMA spectrum (γ = 3.3, depth = 20m) for the most common sea state at Arch Point, Co. Clare; H_s = 1.5, Te = 8_s.

From Figure 2.9, it can be seen that the curves for each standard spectrum exhibit their characteristic shape that was previously described when outlining their associated mathematical formulation. The JONSWAP spectrum with γ set to 3.3, displays an increased spectral peak inducing a narrower spectrum than the Bretschneider spectrum. The TMA spectrum, with γ set to 3.3, and depth equal to 20 m exhibits a lower spectral peak as expected. The selection of an appropriate standard spectrum to characterise the site is important as it directly influences estimates on wave energy available to the wave energy converter and predictions on wave power absorption.

2.6 HYDRODYNAMIC MODELLING

In line with aforementioned standards and best codes of practice, modelling of WECs is essential to their development from concept to full scale. Modelling may be categorised as physical or mathematical/numerical. Physical modelling concerns scaled WEC designs, whereby the selection of scale size is dependent on the objectives of the study. Regarding wave and structure interaction, generally there are three kinds of forces of comparable importance. These are associated with inertia, gravitation and viscosity. When designing a scale model, it is desirable to retain the same balance between inertial, gravitational and viscous effects as that of the full scale phenomenon (Payne, 2008). In relation to fixed OWCs, an additional factor must be must be considered. This is the aerodynamic behaviour above the water column. Both inertia and pressure act as restoring forces in the heaving motion of the water column. These are generally incompatible scaling criteria which presents a challenge for experimental studies on OWCs. To address this, previous studies have

designed scaled models with different scales above and below the water line. The horizontal section of the chamber remains the same but the chamber height is increased (Murphy, 2012). As the hydrodynamic and pneumatic flows require different model scales, this makes mathematical and numerical modelling a particularly valuable tool in the development of OWCs (Cruz, 2008).

In mathematical and numerical modelling, equations are formulated which govern the operation of the OWC wave energy converter and can be used to estimate absorbed power and power output. Mathematical methods vary from different analytical approaches to a range of numerical techniques. Depending on the objectives of the study, a variety of combinations of mathematical and modelling techniques may be employed. Models may be based on linear wave theory or may take account of more realistic and complex non-linear wave forms. At shoreline locations, the incident wave field is likely to be non-linear where near-shore and shoreline processes affect the wave regime. In deeper waters outside the wave breaking limit for a given wave height, non-linear effects are reduced and may approach a weakly non-linear environment. Despite this environment, most of the modelling of OWCs accounting for a power take off has assumed that linear wave theory is valid (Cruz, 2008). A brief chronological review of mathematical formulations developed for the OWC wave energy converter follows.

The first mathematical description of an OWC described the behaviour of a wave oscillating within two closely spaced vertical walls (Newman, 1974). Evans later extended Newman's work and envisaged the OWC free surface as a weightless plate connected to a mechanical spring damper system (Evans, 1978a). This is known as the rigid piston-type model. In the context of this paper, the term piston mode was coined, relating to the heave motion of the water column. Subsequently, Falcão & Sarmento introduced the theory of periodic surface pressure and its application to an OWC wave energy extraction (Falcão and Sarmento, 1980). Evans then generalised findings from this paper and introduced the concept of an oscillating pressure patch on the water surface, equivalent to the interior water surface of the OWC (Evans, 1982). This is known as the pressure distribution model. The aforementioned seminal studies provided the initial understanding of wave making theory and energy absorption in the context of OWCs. Regarding optimisation of the OWC wave energy

converter design, Reitan (1991) described the relationship between capture width of the OWC and wave frequency which allowed different chamber designs to be compared. An advancement in the accurate representation of the OWC system was detailed in Evans and Porter (1995). This study outlined a mathematical model for the determination of the hydrodynamic coefficients of an OWC with a bi-directional Wells turbine. The method was based on an idealised two-dimensional representation of a shore-mounted OWC with finite submergence of the OWC inlet, as shown in Figure 2.10. It can be seen that the inlet depth, chamber breadth and water depth are denoted as a, b and h respectively. The turbine was represented as a further mass-dash-pot supplemented to the model developed by Evans (1982).

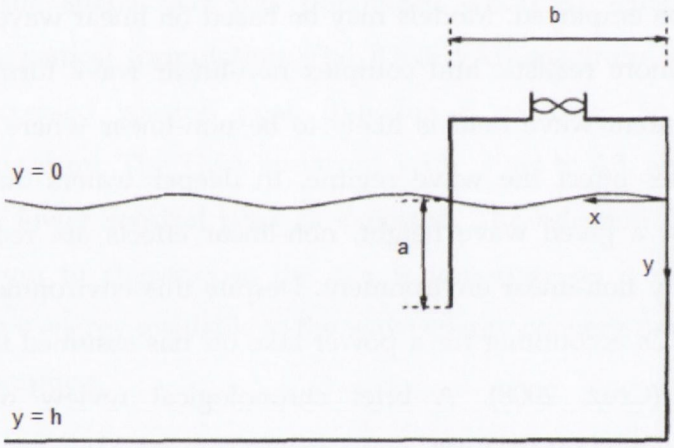

Figure 2.10 Definition sketch of the OWC system. Source: (Evans and Porter, 1995)

The model consisted of a two-dimensional vertical thin plate of arbitrary distance from the plane wall with a uniform pressure applied to the free surface between the plate and the wall. To estimate the hydrodynamic properties associated with the chamber design, the radiation problem and scattering problem were considered in the absence of uniform pressure. Evans and Porter then extended these ideas from the aforementioned study to three dimensions (Evans and Porter, 1997). This paper confirmed that the method can be used with confidence to explore the effect chamber design has on hydrodynamic behaviour of the water column. Central to this model is the decomposition of the hydrodynamic problem into the diffraction problem and radiation problem. This formulation provides the basis for commercial and scientific radiation-diffraction codes that have been developed for analysing hydrodynamic interactions with between structures and ocean waves. Prominent hydrodynamic

codes that have been used for the analysis of shoreline OWC wave energy converters are WAMIT (Lee et al., 1996) and AQUADYN (Brito-Melo et al., 1999). These facilitate hydrodynamic analysis of different chamber designs. It will be seen in Chapter 7 that WAMIT was used to analyse SOWC chamber geometries.

2.6.1 Hydrodynamic Theory

The aforementioned hydrodynamic codes provide a powerful tool for the analysis of structures in the presence of ocean waves. This section details the theory on which they are based along with accepted methods for describing the hydrodynamic behaviour of a fixed OWC wave energy converter.

Linear potential flow theory is assumed. The motion of the fluid is assumed to be inviscid and irrotational. The fundamental behaviour of the free surface waves are governed by inertial and gravitational forces. A velocity potential ϕ can be used to describe the fluid velocity component in a point in the fluid in any chosen direction, also known as the fluid velocity vector. Considering a fixed Cartesian coordinate system, the fluid velocity vector can be denoted as $V(x, y, z, t) = (u, v, w)$ at time t the location $x = (x, y, z)$. Since the flow is assumed irrotational, the velocity vector adheres to Equation 2.15. Helmholtz first familiarised this expression in 1895 (Milne-Thomson, 1968).

$$\nabla \times v = 0 \tag{2.15}$$

The fluid velocity vector can then be described by Equation 2.16, where ∇ signifies the gradient of the velocity potential.

$$v = \nabla\phi \equiv i\frac{\partial\phi}{\partial x} + j\frac{\partial\phi}{\partial y} + k\frac{\partial\phi}{\partial z} \tag{2.16}$$

The vectors along the x, y and z axis are denoted by i, j and k respectively. The motion of the fluid obeys the continuity equation which relies on the fundamental conservation of mass. This equation was first demonstrated by Euler in 1755 (Euler, 1755). An adaptation of this equation is presented in Equation 2.17, where ρ is the fluid density and t is time.

$$\frac{\partial \rho}{\partial t} + \nabla \cdot (\rho v) = 0 \tag{2.17}$$

As the fluid is assumed to be incompressible and of constant density, Equation 2.17 can be simplified to Equation 2.18.

$$\nabla \cdot v = 0 \; or \; \frac{\partial u}{\partial x} + \frac{\partial v}{\partial y} + \frac{\partial w}{\partial z} = 0 \tag{2.18}$$

Combining Equation 2.16 and 2.18 shows that the velocity potential has to satisfy the Laplace equation (Laplace, 1782).

$$\nabla^2 \phi = \frac{\partial^2 \phi}{\partial x^2} + \frac{\partial^2 \phi}{\partial y^2} + \frac{\partial^2 \phi}{\partial z^2} = 0 \tag{2.19}$$

where $\phi = Re\{\phi(x, y, z)e^{-i\omega t}\}$. The concept of the velocity potential simplifies the analysis of irrotational flow. It shows that the fluid velocity component in a point in the fluid consists of the solution of the Laplace equation with relevant boundary conditions on the fluid.

The boundary conditions that follow consider a fixed OWC wave energy converter in finite depth with an applied pressure acting on the interior free surface of the chamber. The boundary conditions on the fluid in finite depth, $z = -h$, is given by:

$$\frac{\partial \phi}{\partial z} = 0 \tag{2.20}$$

The boundary condition on the wetted surface of the fixed OWC structure is:

$$\frac{\partial \phi}{\partial n} = 0 \tag{2.21}$$

Where n is the free surface elevation. The boundary condition on the interior free surface within the chamber assumes that motion takes place in the heave and pitch mode. This can also be known as the piston mode and the first sloshing mode.

The velocity potential of the incident wave is given by Equation 2.22.

$$\phi_I = \frac{igA}{\omega}\frac{\cosh[k(z+h)]}{coshkh} e^{(-ikxcos\beta - ikysin\beta)} \tag{2.22}$$

Where A is the wave amplitude, β is the wave angle and k is the wave number defined by the dispersion relation:

$$\frac{\omega^2}{g} = ktanhkh \tag{2.23}$$

A key advantage of linear wave theory is the possibility to decompose the velocity potential ϕ into the radiation and diffraction components:

$$\phi = \phi_D + \phi_R \tag{2.24}$$

The calculation of these components is known as the diffraction problem and the radiation problem. Separating the overall hydrodynamic problem in to these two sub-problems is common practice in the hydrodynamic analysis of structures using linear wave theory and has been customary in the off-shore and maritime industry for many years. The diffraction problem is solved by decomposing it further, as described by Equation 2.25.

$$\phi_D = \phi_I + \phi_S \tag{2.25}$$

Where ϕ_I is the velocity potential which defines the incident wave system, as described by Equation 2.22, and ϕ_S is the velocity potential which represents the scattered disturbance of the incident wave field due to the presence of the OWC structure in the hydrodynamic domain. It is the superposition of these two velocity potentials that represent the diffracted wave field. WAMIT solves the diffraction problem by satisfying the boundary condition of zero normal velocity on the interior free surface within the chamber. The boundary condition is applied to the submerged section of the chamber.

To describe the radiation problem, it is appropriate to outline its application to a simple floating body prior to describing it for a fixed OWC wave energy converter. In this case, the radiation problem is solved by applying a force to the floating body in an undisturbed fluid. The force applied to the floating body causes the body to oscillate in the otherwise calm water. This forced motion of the floating body causes it to oscillate and generate outgoing waves. As there are no incident waves, the only waves considered in the radiation problem are those radiated from the oscillating body. These waves are known as the radiated wave field and can be observed when throwing a stone in to still water. The forced motion of the floating body results in oscillating fluid pressures on the body surface. Integration of these fluid pressure forces over the body surface allows the key hydrodynamic forces to be calculated. Chief hydrodynamic forces derived from this process are the added mass and radiation damping terms, which are central to determining the response amplitude operator for the body. These hydrodynamic forces may be calculated for any of the six modes of motion associated with the floating body: surge, sway, heave, roll, pitch and yaw. The radiation potential may be described by Equation 2.26 where j corresponds to the mode of the velocity potential.

$$\phi_R = i\omega \sum_{j=1}^{N} \xi_j \phi_j \tag{2.26}$$

Where ξ_j denotes the complex amplitude of the body motion for the specified body motion. For a fixed OWC, solving the radiation problem is analogous to that for a floating body, although there are the following adaptations. As the structure is fixed, the six modes of motion associated with a floating body are disregarded. However, the water column within the chamber operates predominantly in heave and pitch, also known as the piston mode and first sloshing mode (Sykes, 2012). Hence, the water column possesses two principal modes, heave and pitch. With WAMIT, it is possible to extend the mathematical formulation for a floating body to an OWC by accounting for these two modes of motion associated with the OWC. Instead of the external force being applied to the floating body, it is applied to the water column within the chamber. Consequently, the oscillation of the water column within the chamber generates outgoing waves, radiating from the fixed OWC structure. As power generation from an OWC is predominantly due to the heave motion of the

water column, it is this piston mode that is of primary interest to this study. The piston mode of the water column is denoted by the subscript 7 as it can be seen as an additional mode to the aforementioned 6 modes associated with a floating body. To calculate the hydrodynamic forces associated with this mode, the following boundary condition is applied:

$$\frac{\partial \phi_7}{\partial n} = n_7 \tag{2.27}$$

where ϕ_7 and n_7 is the velocity potential and elevation of the free surface of the water column respectively.

2.6.1.1 Hydrodynamic Properties

The calculation of the velocity potentials enables the calculation of the pressure on the interior surface of the water column. From this, forces and moments may be calculated via integration. The excitation force on the water column may be expressed as:

$$F_e = -\rho \iint_S i\omega(\phi_I + \phi_S) n_7 dS \tag{2.28}$$

where S denotes the interior free surface within the chamber. The added mass relating to the heave motion of the water column M_a is calculated using Equation 2.13.

$$M_a = \rho \iint_S Re\phi_7 n_7 dS \tag{2.29}$$

The damping B is calculated using Equation 2.30.

$$B = -\rho\omega \iint_S Im\phi_7 n_7 dS \tag{2.30}$$

WAMIT employs the Green function to solve the above integrals, as described in manual. These parameters may be non-dimensionalised using the density of the fluid ρ and a length scale L, as shown in the Equation 2.31 and 2.32 below.

$$\overline{M_a} = \frac{M_a}{\rho L^{\kappa}} \tag{2.31}$$

$$\bar{B} = \frac{B}{\rho L^{\kappa} \omega} \tag{2.32}$$

Where κ is a designated value dependent on the mode of motion under investigation. It will be seen that the non-dimensionalised form was adopted for the benchmarking study on the hydrodynamic model set-up described in Chapter 7, Section 7.6. The above parameters are central to the equation of motion for the SOWC system analysed in Chapter 7 and provide the basis for Section 7.3 Model Formulation.

2.6.2 Frequency Domain

It will be seen that the model is formulated in the frequency domain. One advantage of modelling using linear wave theory and analysis in the frequency domain is that this method is well established and has been utilised extensively in the analysis of wave energy converters, including shoreline OWCs (Brito-Melo et al., 1999; Wavegen, 2002a). It facilitates an investigation of the fundamental workings of the system. In terms of chamber geometry optimisation, modelling in the frequency domain lends itself to principle system investigation more so than the time domain. The associated linear equation of motion limits the number of variables affecting hydrodynamic performance, which allows direct relationships to be inferred between chamber design and hydrodynamic behaviour.

This approach also has limitations. As it relies on mathematical assumptions and approximations which simplify the wave structure interaction, it is understood that the behaviour of an actual OWC system deviates from the numerical model in non-linear conditions. Specifically, in the case of energetic sea conditions and shallow waters there can be discrepancy between a full scale OWC operation and corresponding frequency domain model predictions. This is due to the exclusion of important effects including, but not restricted to: hydrodynamic loss effects; air

compressibility or losses at the power take off which may affect the pneumatic damping characteristic and non-linear wave effects.

More sophisticated modelling strategies which facilitate the inclusion of non-linearities provide more realistic values for actual power output. Specifically, modelling strategies that are carried out in the time domain and spectral domain cater for non-linear effects associated with OWCs, such as drag effects linked to vortex shedding within the chamber. Additionally, the time domain facilitates the inclusion of control strategies and certain power take off systems.

Given the different attributes of the different models, they tend to have different uses. In general, numerical modelling implementing linear wave theory is associated with the initial stages of wave energy converter design as it facilitates an investigation of the fundamental workings of the system and comparison of different designs. For estimates of actual power output, use of non-linear time domain models affords more accuracy. The application of time domain modelling often assumes that the hydrodynamic problem has been resolved, that the OWC has been constructed and control strategies are now the element under investigation (Cruz, 2008).

With respect to this project, international guidelines (Annex II, Guidelines for the Development and Testing of Wave Energy Systems, Nielsen & Holmes, 2010) propose that model formulation in the frequency domain is appropriate for the early stages of WEC design, corresponding to TRL 1-3 (as previously shown in Table 2.2). The primary objectives for TRL 1-3 outlined in Table in Table 2.2 link with the aims of the present research programme.

2.7 SUMMARY

In this chapter it was noted that the research programme described in this thesis aimed to (i) characterise the wave climate for a domain off the coast of County Clare adjacent to Loop Head, as this is an area of interest for ocean energy development in Ireland, and (ii) use the findings from a wave climate modelling study conducted to achieve the first aim and build upon an earlier TCD (Marine Institute, 2000) study to investigate design parameters which may influence the survivability and feasibility of potential SOWCs installed at Loop Head. Guidelines and codes of best practice

which specify key milestones in WEC development have been published. For SOWC wave energy converters at their present stage of development in Ireland, guidelines indicate that numerical modelling is appropriate, and so this approach was taken in the current research programme. In particular it was noted that international guidelines propose that model formulation in the frequency domain is appropriate for the early stages of WEC design. Literature on WECs, particularly OWCs and SOWCs, wave climate modeling and hydrodynamic modeling was considered. Reasons for selecting the type of methodology employed to investigate potential deployment sites, their wave climate, and the interaction of wave climate with SOWC chamber designs was outlined. More focused reviews of literature on topics specifically related to either the first aim or the second aim of the overall research programme described in this thesis, will be presented in Chapters 4 and 6 respectively. The research programme described in later chapters was conducted at Loop Head, Co. Clare. To check that this location was appropriate for wave energy project development, a preliminary site viability study and survey were conducted. These are described in the next chapter.

Chapter 3
SITE VIABILITY STUDY AND SURVEY

A site viability study and survey are described in this chapter. These were conducted at the start of the research programme to check and re-confirm that the locations selected for investigation were appropriate for further study in relation to the rationale for this project and their potential for wave energy project development. Two locations were selected and each was linked to one of the two main project aims. The location associated with the first aim (which was to characterise the wave climate for a domain off the coast of County Clare adjacent to Loop Head, as this is an area of interest for ocean energy development in Ireland) will be referred to as the Clare domain. The Clare domain is presented in Figure 3.1. It is an off-shore, near-shore and on-shore domain adjacent to Loop Head and County Clare Coast. The location associated with the second aim (which was to use the findings from a wave climate modelling study conducted to achieve the first aim and build upon an earlier TCD (Marine Institute, 2000) study to investigate design parameters which may influence the survivability and feasibility of potential SOWCs installed at Loop Head) is the coastline at the tip and northern shore of Loop Head peninsula. As described in Chapter 1, the rationale for this research programme rested in part upon the chosen locations having proximity to other areas of interest for marine energy. Therefore the above sites were reviewed with respect to this characteristic. Also, according to current recommendations for wave energy project development, potential sites should be explored in relation to specific selection criteria. Therefore, the above sites were reviewed in relation to both proximity to other areas of interest for marine energy, and specific site selection criteria. A review of site selection guidelines, previous studies and a site survey contributed to this process, all of which are

described in this chapter. In addition, this chapter describes the process of selecting two specific points along the Loop Head coast line for modelling potential SOWC installations.

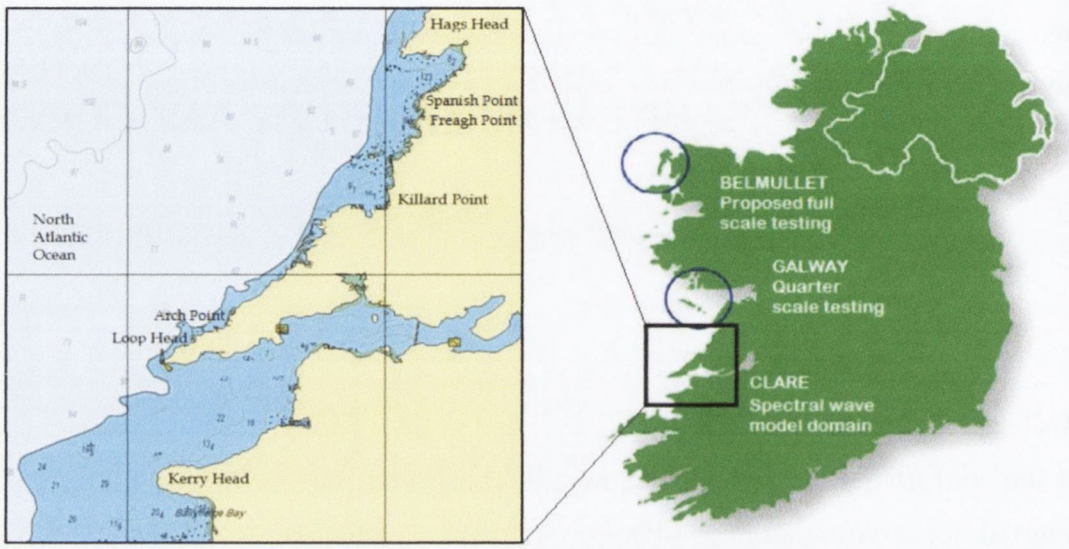

Figure 3.1 Clare Domain, relative to the Atlantic Marine Energy Test Site (AMETS) off Belmullet and the quarter scale testing facility in Galway Bay. Source: (UKHO, 2008; Marine Institute, 2010)

3.1 Proximity to Other Areas of Interest for Marine Energy

In 2008, the 'Wave Energy Connection Project' was published by the Marine Institute and ESB (Marine Institute and ESB, 2008). It reported on a survey of near-shore and off-shore sites adjacent to the west coast of Ireland which held potential for WEC deployment. The seven most promising sites were investigated in relation to a range of issues, including wave resource, infrastructure, and environmental and social concerns. The site selected for the Atlantic Marine Energy Test Site (AMETS) was off Bellmullet, Co. Mayo. However a site off Goleen bay, approximately 15 km north of Loop Head, was placed highly in the ranking system. This indicated that the area of Loop Head was adjacent to an area of interest for marine energy. Confirmation of the region's importance soon followed. In 2010 the Marine Renewables Industry Association endorsed the potential of a number of locations, including the area between Loop Head and Hags Head (MRIA 2010), shown in Figure 3.1. Also in the report 'Supply Chain Study for Westwave' (Slevin et al 2011) an area off Killard was one of three areas prioritised for development of the Westwave project. This area lies off the Clare coast, to the north of Loop Head. Figure 3.2 shows these three prioritised areas.

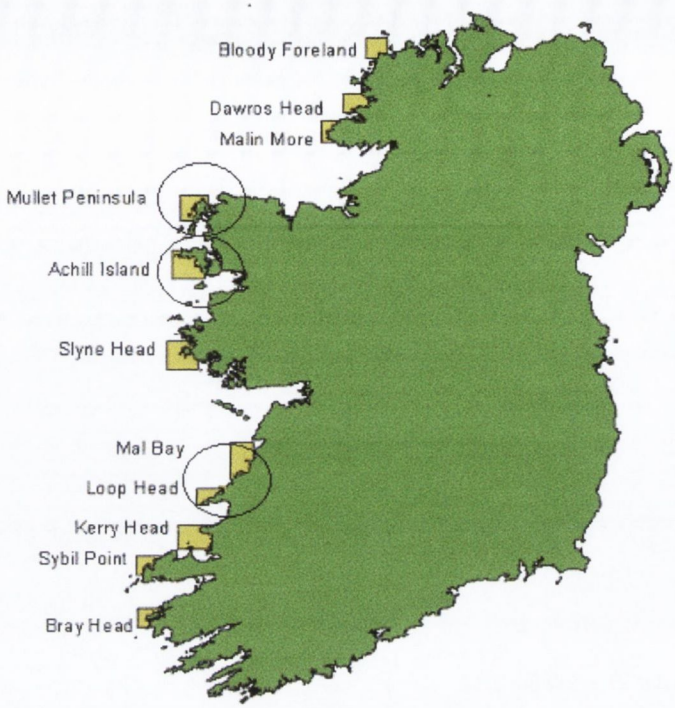

Figure 3.2. Areas of interest to marine renewables in Ireland. Source:(Slevin et al., 2011)

The WestWave project recently received €19.8 million in EU funding with an aim of developing the first wave energy farm (SEAI, 2013). Four wave energy conversion technologies have been considered for deployment at this farm: Oyster 800 (Aquamarine Power Ltd.), OE buoy (Ocean Energy Ltd.), Wavebob (Wavebob Ltd.) and Pelamis (Pelamis Wave Power Ltd.). Oyster 800 is a near-shore technology while the rest are off-shore devices. With respect to Technology Readiness Levels (TRLs), these projects are at an advanced stage of development. In addition, an Australian company, Carnegie, have secured a foreshore licence for the area between Freagh Point and Spanish point (see Figure 3.1) off the count Clare coast (Fievez & Brien, 2011).

In summary, it can be confirmed that the Clare Domain and Loop Head cliff bases have proximity to other areas of interest for marine energy. Given the above developments it is likely that there would be a concentration of infrastructure that would support wave energy in the region of Loop Head and the Clare coast.

3.2 SITE SELECTION CRITERIA

3.2.1 Site Selection criteria for Wave Energy Converters

The European project, Waveplam, has developed methodology and recommendations for site selection which outline the factors that should be considered and the corresponding importance of each. These reports are: 'D3.1 Methodology for site selection (Zubiate et al. 2009)' , 'Methodology for site selection for wave energy projects (Zubiate et al., 2009)' and 'Wave Energy : A guide for investors and policy makers (Waveplam, 2009)'. The stages of the methodology outlined in the aforementioned reports are presented below with their main objectives.

Stage 1: Defining characteristics of the project

- Defining an interest area for further study

Stage 2: Preliminary Assessment

- Gathering information on the relevant subjects
- Carrying out a detailed resource assessment

Stage 3: Collation of information

- Use of Geographical Information System (GIS) tool to present collated information.

Waveplam stages 1 and 2 were used as guidance regarding the site selection review in this study and also for the further information to be obtained in the course of the feasibility investigation. The areas which Waveplam recommend for consideration in stages 1 and 2, for WEC projects in off-shore, near-shore or on-shore domains are as follows:

- Wave Energy Resource
- Seabed Bathymetry
- Tidal Range
- Grid Accessibility
- Environmental and Planning issues
- Interaction with other Human Activities.

Another influential report regarding site selection is 'Options for the Development of Wave Energy in Ireland, SEI (2002)'. It makes recommendations similar to those of Waveplam.

3.2.2 Site Selection criteria for OWC Wave Energy Converters

The OWC wave energy converter evaluation report produced by the Carbon Trust (2005) focuses on site selection criteria for OWCs. In this report rankings were used to prepare an evaluation matrix that showed both the best areas to develop for shoreline OWCs and the potential resource for a given location. A range of 0 to 4, with 0 being worst and 4 being best, was used for each ranked variable. Factors were derived for each variable to allow different importance to be ascribed to each aspect of the overall suitability of OWC deployment. The themes ranked were as follows: Wave Energy Resource; The Average Sea-bed Slope (Bathymetry); Tidal Range; Electrical Grid Connection; Cost of construction; Overall capital cost. With the exception of the cost rankings which are outside the scope of this study, these themes are discussed as follows.

3.2.2.1 Wave Energy Resource

Wave power at a site location is central to the decision of whether a site is feasible or not. Wave power is conventionally rated in terms of the energy flux crossing an imaginary line (the 'wave front', or a contour of stated depth) and has been recorded at many locations around Ireland (Options for the Development of Wave Energy in Ireland, 2002). The unit for measuring the wave energy resource is the average kilowatt per meter wave front (kW/m). The Carbon Trust ranking method for wave energy resource is shown in Table 3.1 below. Due to its significance, wave energy is given a higher weighted value over other factors.

Table 3.1 Wave energy resource ranking scheme. Source: (The Carbon Trust, 2005)

Mean Annual Wave Power	Ranking Points
< 5 kW/m	0
5 - 10 kW/m	1
10 -15 kW/m	2
15 - 25 kW/m	3
> 25 kW/m	4

3.2.2.2 Average Sea-Bed Slope

The seabed profile affects the available energy at inshore locations significantly. A steep sloped seabed retains more of the wave's energy compared with a shallow sloping seabed. This is due to mechanisms such as seabed friction and wave breaking. The slope represented as a ratio can be used to rank sites in order of steepness, as shown in Table 3.2.

Table 3.2 Average sea-bed slope ranking scheme. Source: (The Carbon Trust, 2005)

Sea-bed Slope	Ranking Points
> 1 : 500	0
1: 100 - 500	1
1: 50 - 100	2
1: 1 - 50	3
1: 0 - 1	4

3.2.2.3 Tidal Range

The trough level of the highest wave anticipated must be significantly above an OWC chamber mouth to prevent any debris created by construction being returned by wave action. This may lead to further accretion and blocking of the chamber entrance. Also there must be enough water depth to ensure that at the lowest tides the SOWC chamber mouth remains submerged. Having the inlet of the OWC at the right water depth improves the performance of the device. A narrow tidal range allows this depth to be approximately maintained for more of the time than if the sea level varies with the tides a great deal. Therefore a narrow tidal range is preferable for SOWC installation sites. The ranking scheme is shown in Table 3.3.

Table 3.3 Tidal range ranking scheme. Source: (The Carbon Trust, 2005)

Tidal Range	Ranking Points
> 6 m	0
4 - 6 m	1
2 - 4 m	2
1 - 2 m	3
0 - 1 m	4

3.2.2.4 Grid Accessibility

A critical consideration in harnessing wave power is the connection to the electricity grid. While pilot projects can be connected to the 10/20 kV systems, the deployment of early commercial phases of wave energy systems will require connection at least to

the nearest 38 kV substation. The Carbon Trust indicates that for full size large wave farms, connection to 132 kV stations is required. The nearest equivalents in the Irish transmission system are the 110 kV substations. The ranking scheme is shown in Table 3.4.

Table 3.4 Grid access ranking scheme. Source: (The Carbon Trust, 2005)

Grid Accessibility	Ranking Points
> 50 km	1
31 - 50 km	2
11 - 30 km	3
< 10 km	4

3.2.3 Site Selection criteria for SOWC Wave Energy Converters

There are few publicly available guidelines describing selection criteria which are specific to SOWCs. In addition to criteria identified in the Carbon Trust's OWC Wave Energy Converter Evaluation Report (2005) and SEI's Options for the Development of Wave Energy in Ireland (2002), the geology of the site location and the cliff height are important with respect to drilling and construction cost (2nd Dublin Colloquium, 1996). Also water depth at the cliff base is a factor to consider.

3.2.3.1 Geology

With respect to the SOWC chamber construction techniques the composition of the rock at each potential site is an important factor. The geology of the site can have an influence on the ease of construction and on the cost. It has been stated that quartzite is one of the preferred types of rock for SOWC construction (Holland, 1996). A ranking scheme similar to those outlined above could be adapted to this parameter, considering the various types of rock and the ease of construction associated with them.

3.2.3.2 Cliff Height

Cliff height affects the ease of construction and cost of SOWC installation. A higher cliff implies more drilling from the surface to reach the cliff base chamber. This potentially results in a higher overall cost for SOWC installation. However, the height of the cliff does also need to be sufficient to allow the turbine to be placed above the reach of extreme seas.

3.2.3.3 Water Depth at Cliff Base

For a number of reasons outlined in Section 2.4 Influence of Location on Feasibility, Section 6.3 Wave Climate and Section 6.7 Constructoin and Design, adequate water depth at the cliff base is required. Based on these sections, the depth should be at least 15 m.

To summarise, an ideal site for subterranean OWC implementation has a high wave energy resource, a steep sloped sea-bed and a small tidal range in a location with convenient access to the electricity grid. Regarding ease of construction and project cost, a cliff comprising homogenous rock is favoured. Cliff height, water depth and other factors as recommended by Waveplam also require consideration. Certain factors are more influential than others in relation to site selection. Particularly important factors are wave energy resource and bathymetry.

3.3 Review of Locations of Interest

The Clare domain and locations on Loop Head peninsula were reviewed in relation to the aforementioned site selection criteria.

3.3.1 Previous Site Selection Study of Clare Domain

The findings of a site evaluation study described earlier (Marine Institute and ESB, 2008) for coastal and near-shore areas adjacent to and overlapping with this area were reviewed. Information from the Wave Energy Connection Project carried out by the Marine Institute and ESB (2008) is used to rank the suitability of Co. Clare as a location for SOWC installation.

3.3.2 Previous Site Selection study of Cliff Sites

A previous study on potential SOWC sites which was carried out by Trinity College Dublin in 1997 provides detailed information on specific cliff sites (Holland, 1997). Information from this study was sourced from Dublin University Sub-Aqua Club and the Environmental Sciences Unit, Trinity College Dublin (TCD, 1997). They provided bathymetry information for 21 sites along with the depth of water at the cliff base at chart datum. The sites were located along the West Coast of Ireland, from Co. Kerry to Co. Donegal. These are presented in Table 3.5.

Table 3.5. List of 21 sites investigated for SOWC installation . Source: (TCD, 1997)

Balteen	Kerry Head	Deelick Point
Killurly	Malin Head	Spanish Point
Castle Point	Tullaghan	Duggerna
Carrigfadda	Dooega	Loop Head
Downpatrick Head	Benwee	Darbys Hole
Lackmeeltaun South	Lackmeeltaun North	Erris Head
Rossan Point	Doonan	Annagh Head

Additionally, a report concerning the geology of potential sites was provided by TCD Geology department. With respect to the implementation of SOWCs, a select list of seven sites on the west coast of Ireland with suitable rock characteristics was prepared in 1996 by TCD Geology Department (TCD, 1996). The geology at Loop Head was reported as compatible with SOWC installation.

Following the collection of this data, the 2nd Dublin Colloquium regarding Rock Engineering for Ocean Wave Energy (1997) took place. An evaluation method centred on the opinions of each expert attending the Colloquium. In relation to bathymetry, Galway was discarded due to shallow waters and island sites were excluded due to remoteness. From a geological point of view, sites in Donegal, Loop Head and the Burren were preferred (Holland, 1997).

3.3.3 Site Visit and Marine Survey

Additional information was required to supplement that provided by previous studies: (i) Depth measurements at the base of cliff sites around Loop Head and (ii) photographs of the geological formation of potential SOWC sites. As part of this, a site visit was carried out at Loop Head. Prior to the site visit, a meeting was held with staff at the Geological Survey of Ireland Offices in order to obtain further advice on carrying out a small scale bathymetric survey of the area. To carry out the survey, a powerboat, global positioning system and echo sounder were sourced. These are presented Figure 3.3 below.

Figure 3.3. Equipment used to survey coastal bathymetry: Power boat (left), GPS and echo sounder (right)

The survey began on the north coast of Loop Head peninsula, continued southwest to the tip of Loop Head and finished on the south coast of Loop Head. The survey spanned 5.2 km of coastline. The survey was conducted in a 4.5 m Humber rigid inflatable boat (RIB) with a 50 horsepower Suzuki outboard engine with the assistance of a qualified powerboat driver. The RIB was launched at Kilbaha public slipway on the south coast of Loop head. Figure 3.3 shows the cliffs at Loop Head as seen from the RIB during the survey. Using a hand held GPS (Garmin GPS map 60CSx) to identify precise longitude and latitude co-ordinates, the depth of the seabed was measured with a pair of hand held echo sounders (hondex PS-7FL) at intervals ranging from 50-200 m. The GPS identified locations with a margin of error of +/-5 m. To record the depth at each location the pair of echo sounders were held at distance of about 0.3 m apart and angled until both gave similar readings. This procedure insured that depth recordings were taken vertically. The depths at each of the co-ordinates were recorded in a database during the survey. The locations at which these depth readings were taken are shown in Figure 3.4.

Figure 3.4. Overhead view of Loop Head with locations of depth readings (left) and photograph of geological formation of cliff site (right)

The survey was conducted on a day when the wind was light (5-10 km/hr) and the sea-swell was less than 1 m. These conditions allowed for accurate recordings of locations and depths to be made. However, as a record of the tidal level during each measurement was not made, a potential error of +/- 2 m exists when relating the depths to chart datum. The predominant findings pertain to the depth at the cliff base at a number of locations. The greatest coastal depths were recorded at the tip of Loop Head with depths ranging from 17m to 20 m. Therefore this was selected as a specific site of interest when characterising the wave energy resource using a spectral wave model. Additionally, photographs of the geological formation of cliff sites, including the tip of Loop Head, facilitated investigations into their suitability with respect to SOWC chamber construction (See Section 6.5 Geology).

3.3.4 Review of Site Selection Criteria

The Clare domain and the cliff base along the coast of Loop Head base were reviewed in relation to themes recommended by Waveplam (2009) and the Carbon Trust report (2005). The ranking points for each domain are presented in Table 3.6 below.

Table 3.6 Ranking points for Clare Domain and the tip of Loop Head

Ranking Parameter	Clare Domain	Loop Head, Cliff Base
Wave Energy Resource	4	3
Bathymetry	3	3
Grid Accessibility	3	2
Tidal Range	3	2

Details underpinning each ranking score are presented in the following sections. For each parameter the source of data is presented along with important points relating to the Clare Domain and the tip of Loop Head. In addition, the Loop Head cliff base was reviewed in relation to site selection criteria specific to SOWCs.

3.3.4.1 Wave Energy Resource

For both the Clare domain and the Loop Head cliff base the main sources of data were the Accessible Wave Energy Resource Atlas: Ireland, Marine Institute and ESB (2005) and the Wave Energy Connection Project, Marine Institute and ESB, (2008). These sources indicated that there was an acceptable level of wave energy at the locations in question with an annual average value of approximately 30 kW/m. This is sufficient to warrant further exploration for wave energy extraction. However, the level of wave resource information was too basic for use by a potential WEC developer or for the 2nd aim of this thesis which was to use the findings from a wave climate modelling study and build upon an earlier TCD (Marine Institute, 2000) study to investigate design parameters which may influence the survivability and feasibility of potential SOWCs installed at Loop Head. It was therefore necessary to characterise the resource with more detail and accuracy. A means of achieving this for the location in question was essential for the project to proceed. Access to the information necessary for developing a 3rd generation spectral wave model was required. The following data had to be available: bathymetric data possessing suitable resolution, off-shore boundary data, metocean data and local measurements for model calibration and validation. The Clare domain is one of a limited number of sites along the Irish west coast which has had a Wave Rider Buoy in situ for a considerable length of time. The quality and quantity of resource data provided by such buoys are imperative for the successful calibration of a wave climate model. It

will be seen in Chapter 5 that the calibrated wave climate model confirms annual average wave power values greater than 30 kW/m.

3.3.4.2 Bathymetry

For both the Clare domain and the Loop Head cliff base the main sources of data were admiralty charts, fair sheet data, GSI, Infomar and the site survey. The admiralty charts provided information at a sufficient level of detail. These had been obtained some time ago by basic methods. The site visit provided confirmation that the potential cliff sites possessed 15 m water depth, which is the minimum water depth required to accommodate the SOWC concept.

3.3.4.3 Grid Accessibility

For both the Clare domain and the Loop Head cliff base the main source of data was the Wave Energy Connection Project, Marine Institute and ESB (2008). This report indicated that Loop Head is within range of the Money Point power station. There is a 38 kV substation in the vicinity of Kilkee and a 110 kV substation in the vicinity of Kilrush as shown in Figure 3.5.

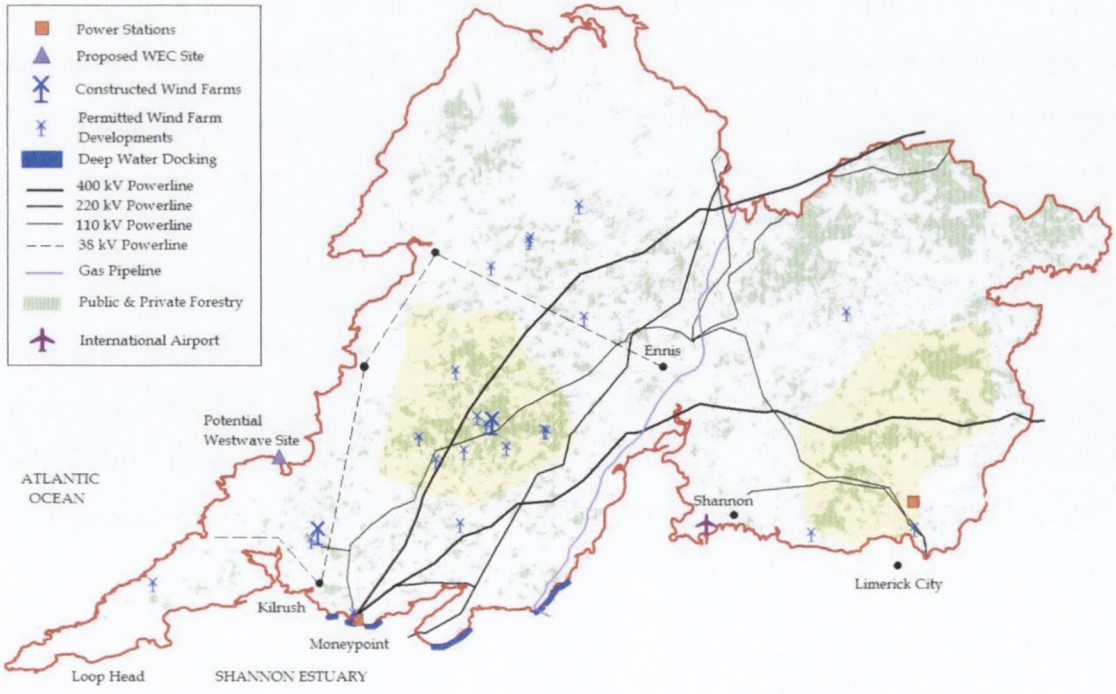

Figure 3.5. County Clare's electrical grid and energy infrastructure. Source: (Clare County Council, 2012)

3.3.4.4 Environmental and Planning Issues

For both the Clare domain and the Loop Head cliff base the main sources of data were the Wave Energy Connection Project, Marine Institute and ESB, (2008), the National Parks and Wild Life Service (2013), Google Earth, and the Geological Survey of Ireland (2005). The Clare County Council development plan encourages support for renewable energy enterprises, in balance with other environmental needs. The coastal domains in question and most of Loop Head's northern coast are not designated as conservation or natural heritage sites under the national parks and wild life service. There are some circumscribed areas around the tip of Loop Head and to the south of the peninsula, which are designated as natural heritage sites or conservation areas, under the National Parks and Wild Life Service. However this is not the case for the most of the northern coast of Loop Head. The presence of such areas does not imply a blanket ban on planning applications. Applications are dealt with on a case by case basis. As SOWC devices would be hidden within cliff bases they should not impact on the appearance of the natural habitat.

3.3.4.5 Cliff Characteristics

The site visit allowed close up inspection of a range of cliff bases at Loop Head. Loop Head has steep cliffs. In some locations along the headland, the cliff face descends straight down into deep water, greater than 15 m. This characteristic reduces the decline in wave power due to shoreline processes, which induces a more favourable wave climate for wave energy extraction.

3.3.4.6 Geology

The main source of information about the geology of the Loop Head site was that obtained from the initial study carried out by Holland (1997). It designated Loop head as suitable for SOWC installation. Further information obtained during the course of this study led to some qualification of this view (See Section 6.5 Geology).

3.3.4.7 Summary

The wave energy resource for the two locations under review (the Clare domain and the Loop Head cliff base) appeared high and sufficient to warrant further study. Of key importance was the availability of adequate wave buoy data so that a 3rd

generation spectral wave model could be developed. This was essential for the project to proceed. Another key element was the bathymetric data, which was also available in sufficient detail and appeared compatible with potential SOWC installation. According to the Waveplam recommendations, out of all the factors listed, wave energy resource and bathymetry have the greatest weighting in determining site suitability.

With respect to infrastructure, there appeared to be some appropriate supports in the surrounding areas. With respect to the physical environment, cliffs with an appropriate height and water depth at their base for potential SOWC installation were present. At the time of this initial review, the available information indicated the geology of the cliffs was appropriate. There was the potential for some questions regarding planning and human activities due to conservation and scenic areas at the tip of Loop Head. This did not constitute an automatic barrier to further exploration of the area as a whole. A main section of Loop Head coast line being considered was not in a conservation area. As many variables are involved in site selection, no one site is likely to be optimal in all respects. Regarding the four Carbon Trust rankings used, scores were at or above the midpoint of the scale, and wave energy resource, the most important factor, received a maximum score.

3.4 Specific Sites for Resource Characterisation

In light of the above, the next step was to select specific locations at Loop Head to focus on when developing a 3rd generation spectral wave model for the region. The site survey and other information sources mentioned previously assisted in this process. An essential feature for such sites was sufficient unobstructed water depth of 15 m at the cliff base. This narrowed the options to some degree.

A site on the northwest side of the tip of Loop Head had an appropriate cliff configuration. It also appeared to have the highest level of potential wave energy for the region. A relative disadvantage was proximity to a conservation area. Arch Point was another site. It is an area on the northwest coast of Loop Head approximately 10 km from the tip. It is the point along this coast which is closest to the wave rider buoy which was being used to validate the wave climate model. Hence there was the best available accuracy in results extracted from the wave climate model at this site.

Furthermore it is not within or near to a conservation area. However the level of wave energy, while adequate for the purposes of this study, was not as high as that at the tip of Loop Head.

Thus different sites had different profiles of different advantages and disadvantages. In order to incorporate a range of features which might prove relevant to this study, both of these sites were chosen for the modelling of a potential SOWC installation.

3.5 CONCLUSION

A site viability study and survey were described in this chapter. These were conducted to check and re-confirm that the locations selected for investigation were appropriate for further study in relation to the rationale for this project and their potential for wave energy project development. Two locations were the Clare domain and the Loop Head cliff base. Each was linked to one of the two main project aims. The Clare domain was selected to achieve the first aim of the research programme, which was to characterise the wave climate for a domain off the coast of County Clare adjacent to Loop Head, as this is an area of interest for ocean energy development in Ireland. The Loop Head domain was selected to achieve the second aim of the research programme which was to assess the feasibility of installing a SOWC at Loop Head. The above sites were found to be close to other areas of interest for marine energy, and to meet a number of specific site selection criteria. It is of note that this thesis entailed minimal outlay of resources. If preliminary feasibility of WEC deployment were to be demonstrated, and if financial investment were to be considered, then strategic environmental assessment, environmental impact assessment, foreshore licence for site investigation, foreshore lease, planning permission statement and grid connection offer would be required. However, for the purposes of this study, this review provided sufficient information to indicate that further exploration was warranted for the Clare domain and the Loop Head cliff base.

Having established the appropriateness of the Loop Head site for WEC development, the next step in the research programme was the development of a spectral wave model for the Loop Head region. This process is described in the next chapter.

Chapter 4
SPECTRAL WAVE MODEL

This chapter will focus on the development, calibration and validation of a 3rd generation spectral wave model for the Loop Head region. It will be seen that this model facilitates the first aim of the research programme which was to characterise the wave climate for a domain off the coast of County Clare adjacent to Loop Head, as this is an area of interest for ocean energy development in Ireland. The selection of this site has been described in Chapter 3. The data sources used to develop the spectral wave model for the Loop Head region will be described with reference to established modelling standards and stages of modelling. The calibration process will be outlined along with the validation of the spectral wave model at locations where concurrent wave data is available. The validation of the spectral wave model at locations near potential SOWC wave energy converter sites allows a level of confidence to be placed in wave energy resource estimates and wave direction. Specifically, scatter diagrams based on data from the spectral wave model detail the annual percentage occurrence of each sea state at locations of interest. This facilitates calculations of the upper limit for power output by SOWC wave converter designs described in the Chapter 6.

4.1 INTRODUCTION

As the wave energy industry advances, and initiatives such as the Westwave project progress (Burca, 2011), there is a need to model the resource at locations of interest in greater detail. For the west coast of Ireland, there are established wave climate models with varying levels of accuracy, based on numerical grids with different resolutions. These include European Centre for Medium-Range Weather Forecasts

(ECMWF)'s operational global model (Cruz, 2008), NOAA's Wavewatch III north Atlantic model (Tolman, 2002a) and the Marine Institute's SWAN model (McCullen, 2005) with resolutions of 0.5 degrees, 0.25 degrees and 0.025 degrees respectively. Although these can be used for site reconnaissance to identify preferable areas for wave energy utilisation, their levels of accuracy are inadequate as the objective shifts to project feasibility assessment and wave energy converter design.

Therefore, to assess the feasibility and energy potential of a SOWC at Loop Head, Co. Clare, it was necessary to investigate the wave climate using a 3rd generation spectral wave model with a higher degree of accuracy than those previously mentioned. As outlined in Chapter 3, the Loop Head area is one of Ireland's prime locations for the exploitation of wave energy, with a steep seabed gradient inducing a favourable resource relatively close to shore.

The objectives for this section of research were as follows:

- To develop and calibrate a 3rd generation spectral wave model for on-shore, near-shore and off-shore domains off Loop Head
- To assess wave power levels off the County Clare coast from off-shore to near-shore and on-shore domains (for the purpose of this thesis, this is referred to as the 'Clare Domain')
- To determine the wave climate characteristics in regions adjacent to Arch Point and Loop Head extending from depths of approximately 80 m to the cliff base
- To establish the percentage occurrence of each sea state at locations in the off-shore, near-shore and on-shore areas of the Clare Domain
- To establish the percentage occurrence of each sea state at specific SOWC sites (Arch Point and the tip of Loop Head).

4.2 Modelling Methodology

4.2.1 Standards for Resource Assessment

As mentioned in Chapter 2, standards have been drawn up which guide all aspects of wave energy development (see Section 2.2). Detailed guidelines for assessing wave energy resources are included within these. They are tailored to the stage of progress,

level of analysis and outputs related to resource assessment. Those with particular relevance to this topic include:

- International Electrotechnical Commission (IEC) standards for the assessment and characterisation of wave energy resources (2013)
- DTI MRDF - Preliminary Wave Energy Device Performance Protocol (Smith and Taylor, 2007)
- DECC/EMEC - Assessment of Performance of Wave Energy Conversion Systems (Pitt, 2009)
- EquiMar – Protocols for the Equitable Assessment of Marine Energy Converters, Resource Assessment Protocol (Venugopal et al., 2011)

A further notable document by the World Meteorological Organisation (Bouws et al., 1998) provides background reading on a number of key topics addressed in the above mentioned standards.

The protocols address different aspects of resource assessment. The documents produced by DTI and EMEC focus their attention on the resource assessment's requirements to complement device testing. EquiMar's protocol details a wider view of resource assessment, outlining recommendations and requirements from early stage assessment to project development to wave energy converter operation. The three chief stages of resource assessment are Site Reconnaissance, Project Development and Operation which are outlined in Table 4.1 below along with associated levels of analysis and outputs.

Table 4.1. Stages of Resource Assessment. Source: (Ingram et al., 2011)

Level (Shoreline Extent)	Level of Analysis/Objectives	Outputs
Site Reconnaissance (>300km)	Resource Characterisation Establish first order resource characteristics Identified areas of interest which warrant further, more detailed investigation	Estimate of Annual Resource Seasonal Variability Inter-annual Variability Uncertainties
Project Development (20 to 500km)	Establish detailed site characteristics for specific project planning and prediction	Quantification of site specific resource Detailed sea state for engineering design Spectra and Spectral Shapes (Bandwidth & Multi-modality) Directionality- Mean Direction Summary Statistics
Operation (< 25km)	Monitoring resource and benchmarking energy production	Quantification of Resource for benchmarking purposes Output prediction: Real time modelling/measurement Forecasting: Real time modelling/measurement required

Site Reconnaissance: In this stage suitable geographical areas for wave energy converter deployment are identified. In general, this stage relies on existing data such as wave atlases based on global wave models and historical measurement programmes. Outputs from this process include an estimate of the annual and seasonal resource with extensive coverage of the coastline. For Ireland, a significant tool to aid this stage's level of assessment is the Accessible Wave Energy Resource Atlas: Ireland (McCullen, 2005). This work, initiated by ESBi, SEAI and the Marine Institute, has investigated the theoretical, technical, practicable and accessible wave energy resource for the Irish Coastline using a course grid wave analysis model. This provided annual and seasonal mean wave energy resource estimates for a number of locations around the Irish coast. The site reconnaissance stage was covered in Chapter 3 Site Selection, when Loop Head. Co. Clare was identified as preferable location for a SOWC wave energy converter.

Project Development: In this stage the aim is to provide a detailed assessment of a particular site to characterise the wave energy resource. The listed protocols for this stage recommend a sophisticated 3rd generation spectral wave climate modelling tool such as TOMAWAC (Venugopal, Davey, Smith, et al., 2011), SWAN (SWAN team, 2006) or MIKE 21 SW (DHI Software, 2011) to transfer wave climate model statistics from global wave climate model grid points, such as those available from the Wavewatch iii model, to the location of a desired wave energy converter (WEC) site. It is required that the 3rd generation wave climate model be calibrated and validated using wave data records from a measurement buoy located as close to the WEC site as possible. The outputs from this high resolution wave climate model include a comprehensive characterisation of the sea states at the site as well as high level summary parameters.

It is this stage of resource assessment that has been carried out in the present project as part of the investigation of the energy potential of a Subterranean OWC at Loop Head, Co. Clare. It will be seen that MIKE 21 Spectral Wave was the 3rd generation spectral wave climate modelling tool used in this study. An in-depth description of the wave climate modelling methodology, data requirements, outputs and analysis are presented in the following sections of this chapter.

Operation: In this stage, operational assessment is conducted following the installation of the wave energy converter at the site. The objective for this stage is that the resource is measured synchronously with the wave energy converter output. This is done for benchmarking purposes and to facilitate short-term forecasting of the predicted energy potential impinging upon the wave energy converter. This can be used for electricity production and management purposes. Operational assessment is not relevant to the present study. Accordingly, model requirements and standards for this stage are not applied to this study's methodology.

Figure 4.1 shows, in the project development stage, the methodology adopted in this study to characterise County Clare's wave energy resource.

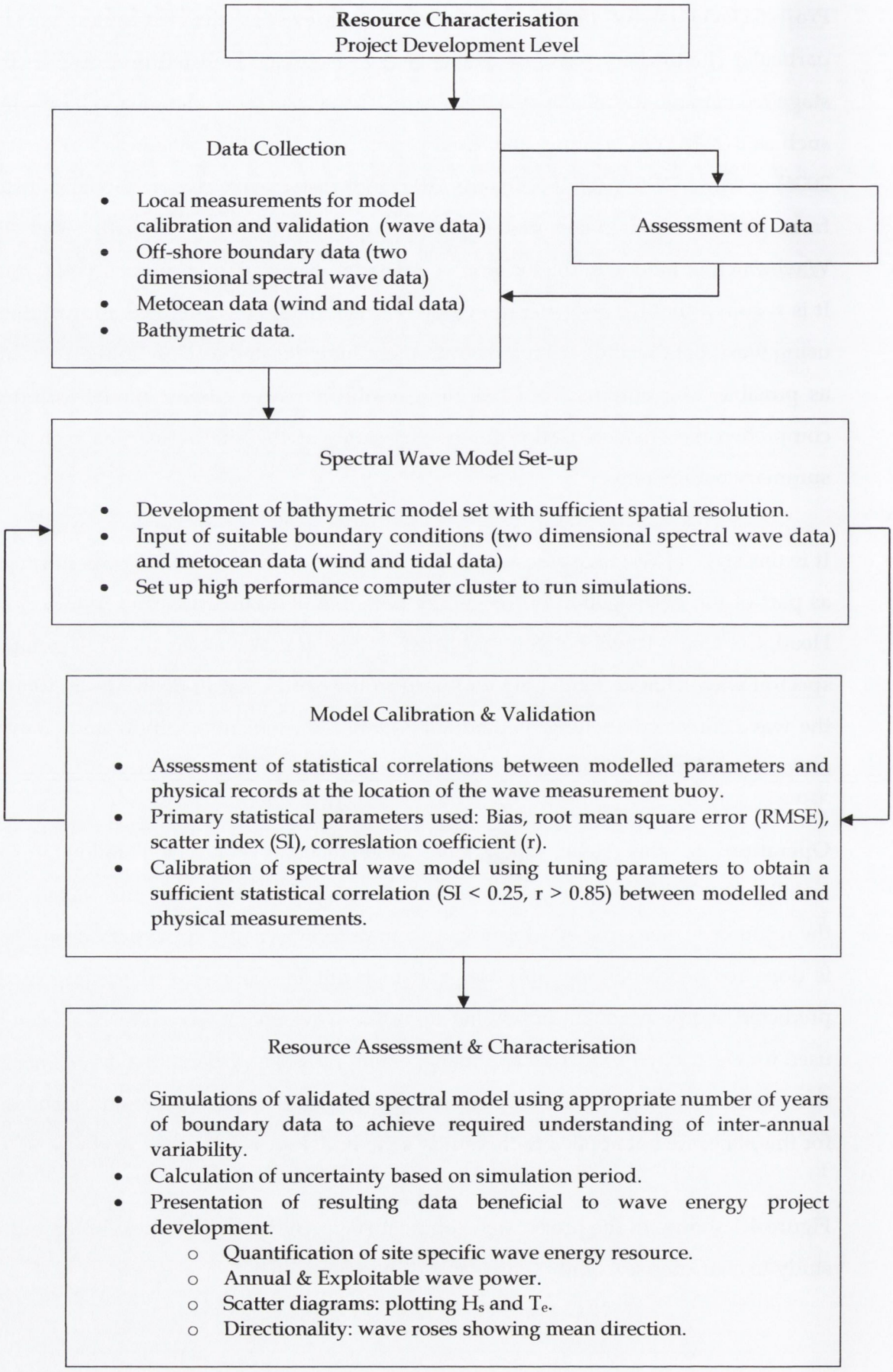

Figure 4.1 Methodology for resource assessment: Project development level

4.3 DATA COLLECTION

The model input data must characterise the complex ocean environment to a certain degree of accuracy to enable realistic simulation by the 3rd generation spectral model. As outlined in the data collection box in Figure 4.1, there are four dominant data components recommended for the development of a spectral wave model. These are (i) local measurements for model calibration and validation, (ii) off-shore boundary conditions, (iii) metocean conditions, and (iv) bathymetric data. For each of these components, the data and sources of data can vary considerably in quality, directly impacting on the accuracy of the resource assessment. Recent evidence suggests that given identical grid domain and input parameters, the majority of near-shore 3rd generation spectral models produce very comparable results (Venugopal, Davey, Smith, et al., 2011). Hence, it is predominantly poor quality data that lead to inaccurate model outputs. By the same token, it is important to assess the quality of each dataset considered for the model. In the subsequent sections, a description of the data sourced for this study is presented along with the protocol requirements, an assessment of the sourced data and its use in the model.

4.3.1 Local Wave Measurements

Primary wave data in the Loop Head area were available from a nondirectional Datawell Waverider wave measurement buoy owned by ESBi. The buoy was located off Achill Point, Loop Head (52°39'N, 9°47'W) and was deployed as part of a study on sea and swell spectra carried out by the Hydraulic Maritime Research Centre (HMRC), Irish Hydrodata (IHD), NUI Maynooth and Met Eireann (Holmes 2009; B Holmes & Barrett, 2007). SEAI funded the study and deployment of the waverider buoy and with a grant of €47, 395 (SEAI, 2005). Figure 4.2 displays a chart showing its position in relation to other wave measurement buoys deployed off the west coast of Ireland.

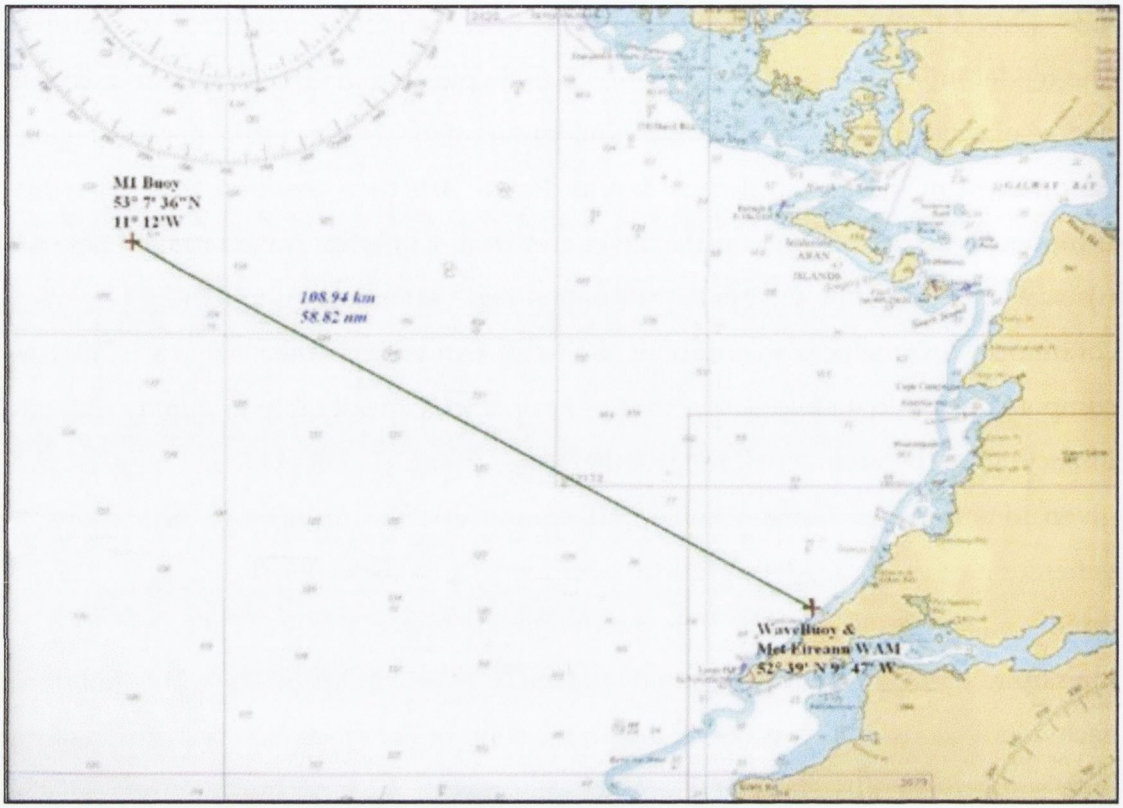

Figure 4.2 Wave measurement buoys off County Clare providing data to this study: Waverider buoy (Arch Point, Loop Head) and M1 Buoy. Source: (Holmes and Barrett, 2007)

The datawell waverider buoy deployed at Arch point measured data by means of an accelerometer. This measures acceleration in the vertical direction, which is then double integrated to obtain the surface elevation of the sea state. The data management system on board the buoy employed a sampling frequency of 2.56 Hz with the raw elevation data file consisting of 3072 points which resulted in a portion of 20 minute time series data. Wave parameters characterising the sea state were deduced from a spectrum generated from the 20 minute portions of time series surface elevation measurements. This was logged approximately hourly. However, when surface elevation surpassed a certain threshold, the frequency at which the buoy recorded measurements increased. Thus, during storm seas, wave measurements were recorded more frequently than hourly (Holmes, 2009). This issue was important to note during the spectral wave model calibration process, when comparisons were made between waverider buoy data and model data at corresponding time intervals. Data from the spectral wave model was recorded once every hour. Therefore, multiple readings per hour from the waverider buoy caused timing mismatches when comparing both data sets. To solve this, timestamps for measured and modelled data were manually checked and synchronised.

Wave records from this buoy cover the period December 2003 to June 2004. The buoy was lost in July 2004 and a second wave rider was deployed from September 2004 to June 2005. For this study, a data set spanning January to June 2004 was available along with one other month, January 2005. Both buoys were positioned at the same depth of approximately 55 m. Parameters deduced from the waverider buoy records were significant wave height, energy period, average wave height, average period, maximum wave height and period corresponding to maximum wave height. Plots of significant wave height, H_s , and energy period, T, are presented in Figure 4.3.

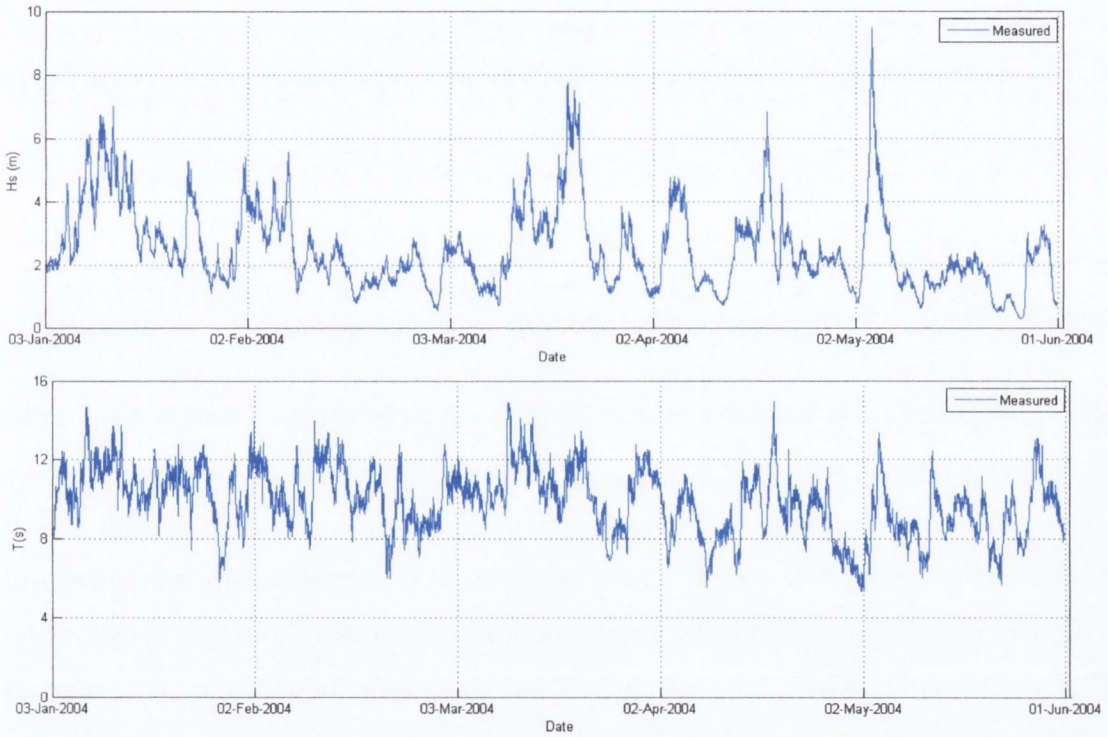

Figure 4.3. Time series records measured by waverider buoy located at Arch Point, Loop Head. Time Span: January to June 2004. Top: H_s (m), Bottom: T (s)

In addition to the data set spanning January to June 2004, data from January 2005 were sought as they covered two exceptionally stormy periods which took place in a relatively short time frame. Numerically modelling wave climates during stormy periods can prove more challenging than modelling less energetic sea states due to the high levels of non-linearity associated with stormy conditions. Thus, the January 2005 data set lent itself to the model validation process, allowing a comparison to be made between the data set and the numerical model for this meteorologically significant month. The two significant storms developed on the 12th and 18th of January, as depicted in the red circles in Figure 4.4.

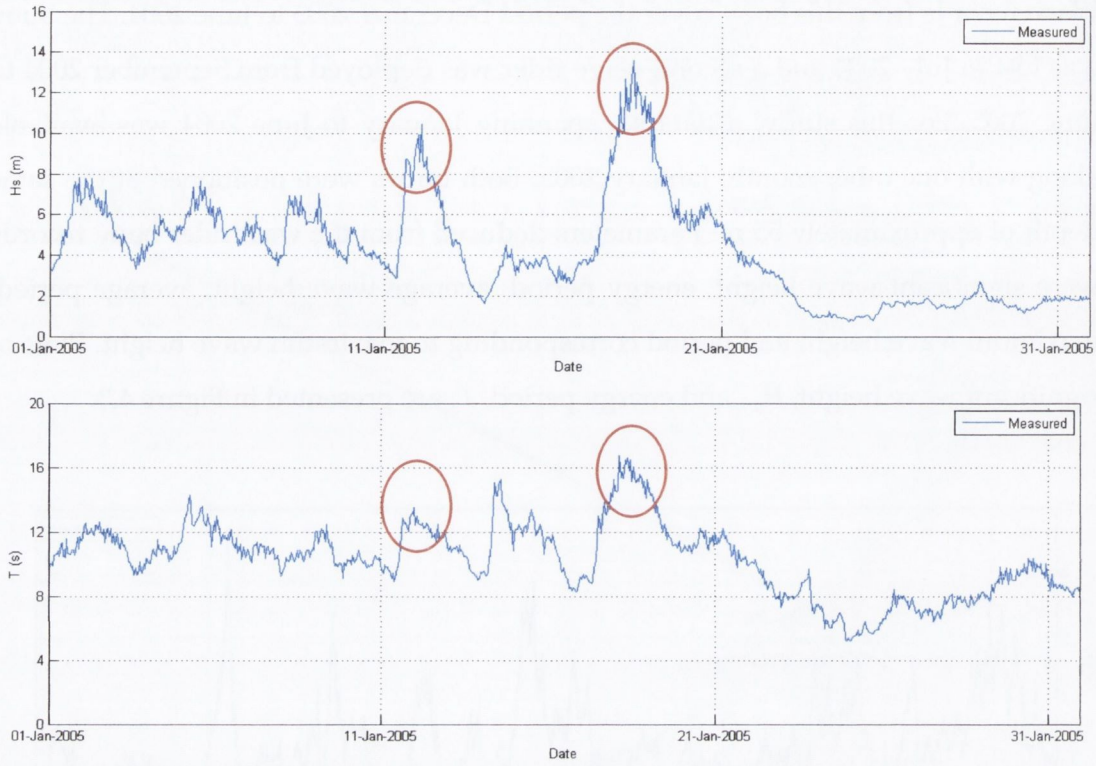

Figure 4.4 Time series records measured by waverider buoy located at Arch Point, Loop Head. Time Span: January 2005. Top: H_s (m), Bottom: T (s)

Regarding Figure 4.4, it should be noted that the two dimensional time series graphs of H_s and T only show a slice of the full picture in terms of wave energy within the presented sea states. Figure 4.5 displays a three dimensional spectrograph which plots wave period and date in the horizontal axes and spectral density on the vertical axis. The two peaks in Figure 4.5 represent spectral densities during storms on the 12th and 18th of January. As described in Chapter 2, in the literature review, spectral density is dependent on wave height and frequency and relates to the energy density within the sea state.

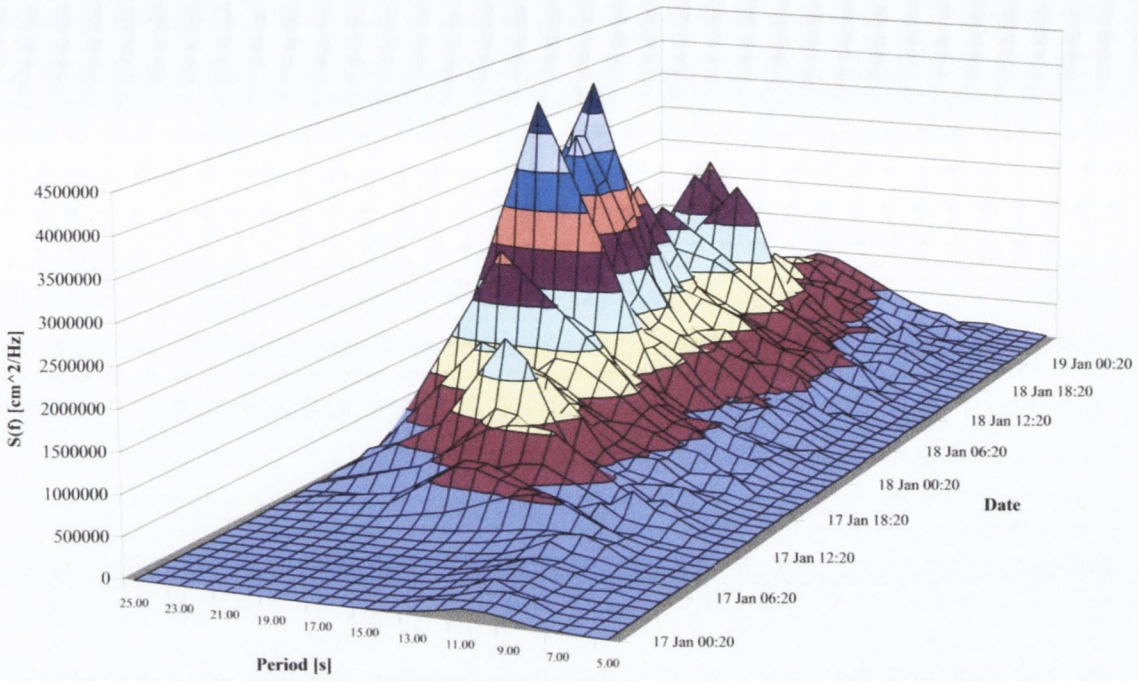

Figure 4.5 Storm Spectograph based on data recorded by waverider buoy located at Arch Point. Time Span: 17th - 19th January 2005.

The information on spectral density that can be drawn from these local measurements is important with respect to predicted performance of wave energy converters. However, for calibration and validation of the spectral wave model, specifically the time series data sets were used.

The selection of further data sets required for the development of a validated spectral wave model is outlined in subsequent sections. The viability of off-shore boundary data and metocean data were dependent on whether their time spans overlapped with that of the local measurements. As local wave measurements are essential to the calibration and validation of a wave climate model, the prerequisite for all other data sets was that they had to overlap with the following dates:

- January - June 2004
- January 2005

4.3.2 Off-shore Boundary Conditions

Detailed off-shore boundary conditions are critical to the accuracy of a wave climate model. In line with this, numerous sources of off-shore wave data were considered

and assessed for this wave energy resource characterisation study. The assessment of data sets was conducted to ensure that an acceptable level of confidence could be placed in the accuracy of the outputs from the model. The aforementioned standards, Equimar - Protocols for the Equitable Assessment of Marine Energy Converters, Resource Assessment Protocol were utilised in the assessment process.

As stated by these standards, there are two categories of potential wave data that can be input at the model boundaries: (i) measured data and (ii) output from other wave models. Each possesses positive and negative attributes.

Physically measured data recorded by Acoustic Doppler Profilers (ADP), wave measurement buoys, satellite or radar delivers the most accurate description of the sea state. As well as measuring the surface elevation directly, these sources generally provide data at a higher temporal resolution than wave models. However for localised wave climate models, data of this type are generally limited to one or two specific locations within the model domain due to the financial implications associated with a large network of measurement instruments.

Output from global and regional wave models is more widely available, both in terms of location and historical records. Although these data do not encompass the real-time temporal accuracy of physically measured data, they do provide comparable data at grid points across the globe. For resource assessments at the project development stage, the boundary conditions must be defined by frequency-directional spectra with a minimum temporal resolution of 3 hours (Venugopal, Davey, Helen Smith, et al., 2011). Non-directional wave data in the form of time series records of wave motion do not allow a sufficient level of accuracy to be achieved within the model.

A primary reason for this is that for a 3rd generation spectral wave model to achieve its potential as an accurate means of characterising the wave energy resource, two-dimensional spectral data are obligatory at the off-shore model boundaries. This form of data details the composition of the sea state in terms of wind waves and swell waves along with their associated wave height, period and direction. It describes the mean surface elevation variance and presents it as a function of frequency and

propagation direction as shown in Figure 4.6. In this example, the radial lines in the polar plot depict the directional resolution of the model. The concentric circles are plotted at 0.1 Hz intervals, where the innermost circle corresponds to 0.1 Hz and the outmost circle corresponds to 0.4 Hz. The colour bar outlines the range of wave energy density for spectra. Red indicates high energy density while blue indicates low energy density.

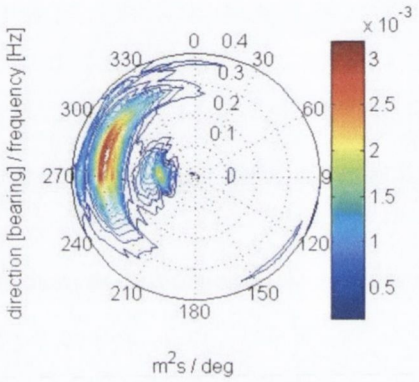

Figure 4.6 Example of two-dimensional directional spectra wave data

In Figure 4.6 it can be seen that the red area lies by the concentric band which denotes a wave frequency of 0.3 Hz. Directional information can be deduced from the position of the coloured areas within the polar plot. 0°, 90°, 180° and 270° represents north, east, south and west respectively. The area of high energy density which lies between 270 and 300 indicates that the predominant wave direction ranges from West to North West. Swell waves can also be distinguished in this case, due to an area of relatively high energy density possessing a characteristic low frequency of 0.1 Hz. The yellow area on the 0.1 Hz band is concentrated around 270° denoting a Westerly direction.

Two dimensional directional spectral data may be sourced from both wave models and wave measurement buoys that measure directionality as well as wave heights and period.

4.3.2.1 Physical Wave Measurements

For wave measurement buoys, which are inherently single point measuring systems, a number of techniques have been developed to generate accurate 2D directional spectral records using recorded buoy displacements in three directions. The most

commonly used techniques are direct Fourier transform method (DFTM), extended maximum likelihood method (EMLM), Bayesian direct method (BDM), iterated maximum likelihood method (IMLM) and extended maximum entropy method (EMEP) (Steele et al., 1992). These methods focus on extracting directional data from sea states based on the buoy's measurement of its heave acceleration, hull azimuth, pitch and roll. The instrumentation required to record wave directionality is not possessed by all wave measurement buoys. This is the case for the limited number of buoys that have been deployed in the Loop Head region. Thus, data records were limited to one dimensional spectra and time series data which were unsuitable to apply as boundary conditions. Furthermore, records from only two buoys were available to this study which was insufficient spatial coverage to accurately develop a spectral wave model. This includes the waverider buoy described in Section 4.3.1. The other wave measurement buoy was deployed as part of the Irish Marine Weather Buoy Network and is known as the M1 buoy. It was in operation from November 2000 to July 2007. Its location was 53°7'36''N, 11°12'W, approximately 110 km from Loop Head, as shown in Figure 4.2. Data records from this wave measurement buoy are freely available from Met Eireann and the Marine Institute. Time series data were sourced for a number of parameters including wind speed, wind direction, significant wave height, wave period, max wave height and max wave period.

Although these data were not suitable for developing a spectral wave model, it was valuable information in terms of providing physical time series wave measurements to compare against data sets sourced from global and regional models. This permitted an assessment of global and regional model data and allowed the quality of the model's data to be quantified.

4.3.2.2 Global and Regional Models

In contrast to wave measurement buoys, two dimensional spectral data are a standard output from most global and regional wave models. Since the 1980s, a number of meteorological centres and research groups have developed various global and regional wave models. In brief, these wave models simulate the growth, decay and propagation of ocean waves based on input winds over the area in question. Historical wind records have permitted the simulation of long-term hindcasts, providing a longer temporal range of wave records compared to wave

measurement buoys. Furthermore, their spatial coverage provides potential boundary data sets for substantially more locations in a given model domain.
It is for these reasons that global and regional models have been the source of two dimensional spectral data for several notable European wave resource assessment studies including high resolution metocean modelling at European Marine Energy Centre's (UK) marine energy test sites (Lawrence et al., 2009), a fifteen year model based on wave climatology of Belmullet, Ireland for SEAI (Curé, 2011), a near-shore wave energy atlas for Portugal (Pontes et al., 2005), and a detailed investigation of the near-shore wave climate and the near-shore wave energy resource on the west coast of Ireland (Gallagher et al., 2013).

When employing data from a wave model as boundary data, aforementioned resource assessment standards (Venugopal et al., 2010) recommend that the source of data be validated against physical wave measurements at a location in the model domain. As data from wave models are secondary data, this caveat is necessary for the level of uncertainty in the model to be quantified. For this study, data from the M1 buoy were used to assess secondary data from wave models.
Accordingly, potential boundary data sets had to overlap the time period for which the M1 buoy was deployed, November 2000 to July 2007. This was in addition to the prerequisite for all data sets, that the time span must correspond with the dates associated with the local measurements required for model calibration (January - June 2004; January 2005).

In line with these criteria, the following global and regional models were investigated: European Centre for Medium-Range Weather Forecasts (ECMWF)'s Interim, era 15, Era 40 and operational models (Persson and Grazzini, 2011); National Centres for Environmental Prediction (NCEP) Reanalysis 1 and Reanalysis 2; The National Oceanic and Atmospheric Administration's (NOAA) Wave Watch iii global wave model (Tolman, 2002b); Oceanweather Inc's (OWI) hindcast model, known as GROWFAB (Grow Fine North Atlantic Basin) (Swail et al., 2000); and the Danish Hydraulic Institute's (DHI) United Kingdom and North Sea (UKNS) model (Beg, 2013).

To select the most appropriate spectral boundary data for the Loop Head model, each model was assessed. The assessment was based on (i) spatial resolution (ii) temporal resolution (iii) quantified level of accuracy (iv) number of data output points in Loop Head region (iv) public availability and (v) time span of available data. Table 4.2 below, presents a summary outlining each model's coverage, spatial resolution and temporal resolution.

Table 4.2 Summary of Global and Regional Models

Model	Coverage	Spatial Resolution (degs)	Temporal Resolution
ECMWF Interim	Global	Range: 1.5° to 0.75°	6 hours
ECMWF Era 15	Global	1.5°	6 hours
ECMWF Era 40	Global	Range: 2.5° to 1.125°	6 hours
ECMWF Operational	Global	Range: 0.2° to 0.1°	6 hours
NCEP Reanalysis 1	Global	2.5°	6 hours
NCEP Reanalysis 2	Global	2.5°	6 hours
NOAA's WW iii	Global	0.5°	6 hours
Oceanweather Inc. North Atlantic Model	Regional	0.5°	3 hours
UKNS	Regional	Flexible Mesh (~0.1°)	1 hour

ECMWF's complement of wave climate models is well established internationally. The ECMWF is an independent intergovernmental organisation supported by 34 States (European states being Austria, Belgium, Denmark, Finland, France, Germany, Greece, Iceland, Ireland, Italy, Luxembourg, the Netherlands, Portugal, Slovenia, Spain, Sweden, Switzerland, Turkey and United Kingdom). A study in 2007 which compared the accuracy of a number of global wave climate models showed that data sets from ECMWF's operational wave model possessed the best accuracy of all global models. This was based on its scatter index for significant wave height, comparing model data and physically measured data at a number of corresponding locations. Over a 5 year time span, 2002 to 2007, the average scatter index was 0.17 (Cruz, 2008).

The scatter index is a non-dimensional measure of the root mean square error used for assessing the correlation between modelled wave parameters and physical records. A scatter index below 0.2 indicates a high level of model accuracy (Reguero, 2012). In terms of quantified model accuracy, the model most suitable for supplying spectral boundary data for this study was ECMWF's operational model. However, data from this source was unattainable for this study due to limited financial resources.

NCEP's reanalysis 2 possesses a slightly higher average scatter index of 0.19. This was based on the same 2007 study which quantified ECMWF's model accuracy. However, the NCEP data were on a relatively coarse grid of 2.5° degrees. This denotes a distance of approximately 270 km between points at which spectral data are available. Consequently, there was one solitary point off Loop Head's coast at which spectral data were available.

NOAA's WaveWatch III (WW3) global model has a spatial resolution of 0.5 degrees. A recent model validation study presented two dimensional polychromatic charts signifying the scatter index value for different areas across the globe (Chawla et al., 2008). The scatter index for significant wave height in the east Atlantic domain was approximately 0.18. Spectral data were sought from this model. However, the archived spectral data sets for the Loop Head region were limited in their temporal range and did not extend back to the time period corresponding to the local wave measurement. Therefore, boundary data sets from this model were not applicable as they did not overlap with local measurements required for model validation.

Oceanweather Inc.'s hindcast model for the north Atlantic was investigated as it holds archived spectral data extracted from three locations near Loop Head. A section of the north Atlantic model domain is shown in Figure 4.7 below. Points at which spectral data have been extracted from the model and archived are signified with a black astrix, ✳.

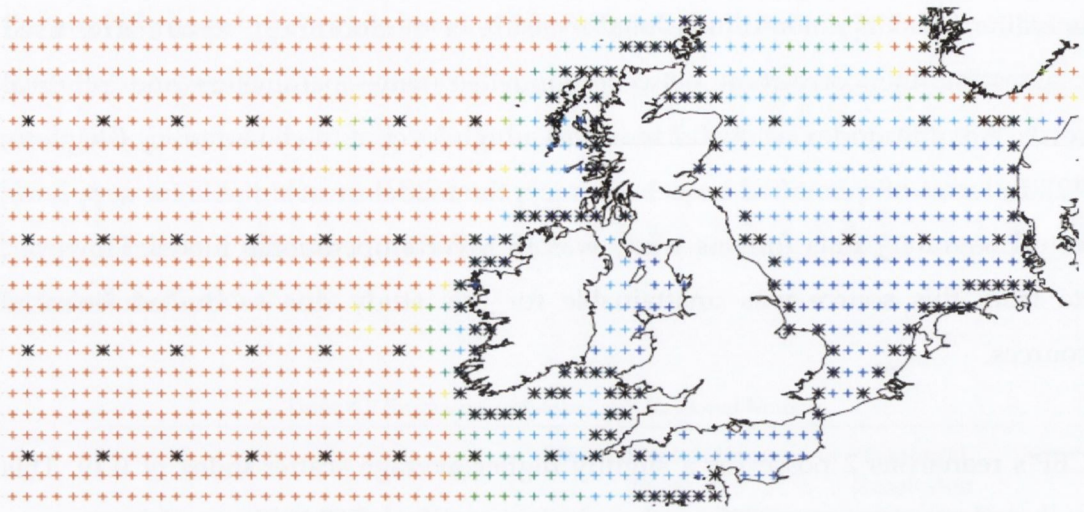

Figure 4.7 Section of Oceanweather's North Atlantic Hindcast model domain. Points at which spectral data has been extracted from the model are signified with a black astrix, ✳.

The quantified accuracy of this model is similar to both ECMWF and NCEP's models, with a mean scatter index of 0.18. This was based on the model's hindcast data on significant wave height compared with in situ buoy and platform measurements over the time period spanning 1978 - 2005 (Harris et al., 2006). Spectral data from Oceanweather Inc.'s archives may be purchased, with cost dependent on number of points ✳ and time span of data set. Due to limited resources, this source of data was not used.

The final model investigated as a potential source for spectral boundary data was DHI's United Kingdom and North Sea (UKNS) model. This regional model was explored as its spatial and temporal resolution surpassed all previously mentioned models. Correspondingly, there were a considerable number of points in the Loop Head area for which spectral data was available. The model domain can be seen in Figure 4.8 below. This regional model exhibits a flexible mesh, meaning that the spatial resolution is variable. The mesh size is refined at certain parts of the domain and coarser in deep water locations. Off the west coast of Ireland, the spatial resolution is approximately 10 km.

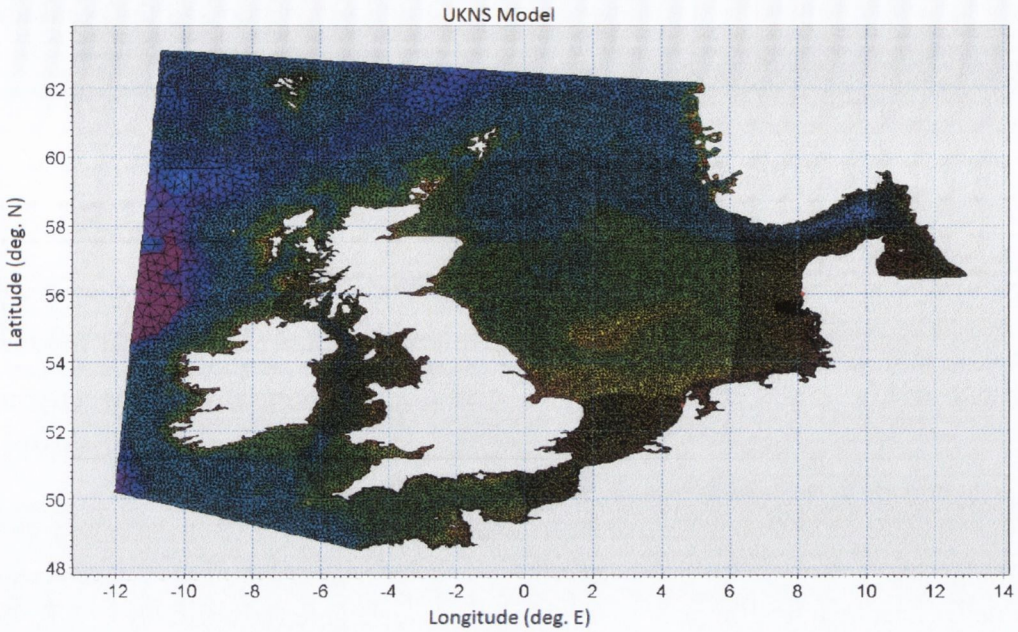

Figure 4.8 United Kingdom and North Sea Model Domain

This is a recently developed model and as such, documentation on the accuracy of this model is limited. A publicly available study detailing the accuracy of the model was carried out in 2011 (Akin, 2011). This report revealed an average scatter index of 0.19 for significant wave height. In contrast to the extensive studies applied to previously mentioned models, the scatter index was based on model data versus physically measured data from a solitary point in the North Sea. Consequently, this reduced the confidence that could be placed in data output from this model at locations off Ireland's west coast. Thus, an assessment of the UKNS model's accuracy at a location off the west coast of Ireland was essential. This is described in the following section.

4.3.3 UKNS Model Assessment

To assess the quality of data from the UKNS model at a location off the west coast of Ireland, physical measurements from the M1 buoy were utilised. Time series data were extracted from the UKNS model at the M1 buoy location (53°7'36''N, 11°12'W), shown in Figure 4.2 (Loop Head chart). This data set consisted of hourly data on significant wave height and zero crossing period, spanning 4 years from January 2004 to January 2008. The temporal resolution and selected parameters corresponded to physical measurements available from the M1 buoy. The 4 year time span was

comparable to that applied in the aforementioned study which assessed the accuracy of the ECMWF and NCWP models (Cruz 2008).

For each parameter, UKNS model data were compared against M1 buoy records at equivalent one hour time steps. To quantify the agreement between numerically modelled data and physical measured data, standardised statistical parameters were employed as per Equimar's protocol detailing the application of numerical models (Venugopal et al., 2010). This facilitates a quantitative comparison between the accuracy of the UKNS model and previously mentioned wave models (ECMWF's operational model, NOAA's WaveWatch III (WW3) global model, etc.).

Additionally, graphical techniques were utilised to investigate the accuracy of UKNS model data at different sea states. This complement of analysis techniques was carried out with an aim to assess whether or not the UKNS model was a suitable source of boundary data.

4.3.3.1 Assessment via Statistical Parameters

To obtain a quantitative and objective indication of how well UKNS model data compared with physically measured data from a point off the west coast of Ireland, industry standard statistical parameters were calculated. These are known as *quality indices* and have been implemented for comparing physical measurements, *me*, with numerically modelled data, *mo*. The primary quality indices are bias, root mean square error (RMSE), scatter index (SI) and correlation coefficient (r) (Ris et al., 1999). These are calculated as follows:

$$bias = \frac{1}{N}\sum_{i=1}^{N}(mo_i - me_i) \tag{4.1}$$

$$RMSE = \sqrt{\frac{1}{N}\sum_{i=1}^{N}(mo_i - me_i)^2} \tag{4.2}$$

$$SI = \frac{RMSE}{\overline{me}} \tag{4.3}$$

$$r = \frac{\sum_{i=1}^{N}(me_i - \overline{me})(mo_i - \overline{mo})}{\sqrt{\sum_{i=1}^{N}(me_i - \overline{me})^2 \sum_{i=1}^{N}(mo_i - \overline{mo})^2}} \quad (4.4)$$

Bias is the mean difference between modelled, *mo*, and measured, *me*, data, given by Equation 4.1. This is specified in the units associated with the parameter being assessed and can be positive or negative. Root mean square error (RMSE), Equation 4.2, is another measure of discrepancy between modelled and measured data. The scatter index (SI), Equation 4.3, is a non-dimensional measure of the root mean square error relative to the measured data, *me*. Low values of SI indicate that data sets are well matched, with values below 0.25 considered as appropriate diagnostic values for this parameter (Reguero, 2012). The correlation coefficient, also known as Pearson's product-moment correlation coefficient, is given by Equation 4.4. This non-dimensional parameter quantifies the covariance between modelled and measured data. A value of 1 indicates perfect correlation while 0 implies that there is no linear relationship between the two data sets. Values above 0.85 denote a sufficient agreement between modelled and measured data (Lawrence et al., 2009).

Quality indices calculated for significant wave height, H_s, and zero crossing period, T_{02}, are presented in Table 4.3. As previously mentioned, these are based on concurrent measurements at hourly intervals spanning 4 years, which amounts to 35064 values in each data set.

Table 4.3 Quality Indices for H_s (m) and T_{02} (s). UKNS model vs. Met Eirean's M1 buoy

	n	**RMSE**	**bias**	**S.I.**	**r**
H_s (m)	35064	0.624	-0.473	0.205	0.975
T_{02} (s)	35064	0.842	-0.272	0.119	0.914

From Table 4.3, it can be seen that both parameters meet the relative criteria for scatter index and correlation coefficient. Both parameters exhibit a scatter index less than 0.25 and a correlation coefficient greater than 0.85. As previously stated, this indicates sufficient agreement between modelled and measured data. Furthermore, the values for scatter index are comparable with those calculated for the previously

mentioned UKNS model assessment study for the North Sea (Akin, 2011). These are presented in Table 4.4.

Table 4.4 Scatter Index for H_s(m) and T_{02} (s) at M1 buoy location and FIN01 Station

	M1 Buoy - Atlantic Ocean 53°7'36''N, -11°12'E	**FIN01 Station - North Sea** 54°2'9''N, 6°36'48''E
	S.I.	**S.I.**
H_s (m)	0.205	0.22
T_{02} (s)	0.119	0.19

This shows performance consistency at two disparate locations in the UKNS model domain. In addition, recalling scatter index values stated for the aforementioned wave models considered in this study, UKNS model exhibits comparable accuracy. With respect to significant wave height, ECMWF's operational wave model, NCEP's reanalysis 2, NOAA's WaveWatch III global model and Ocean weather Inc.'s hindcast model for the North Atlantic possess an average scatter index of 0.17, 0.19, 0.18 and 0.18 respectively. Thus, the recently developed UKNS model's scatter index for significant wave height denotes a respectable level of agreement with physically measured values. In summary, the above quality indices provide statistical evidence that the UKNS model is a suitable source of boundary data for spectral wave models developed for the west coast of Ireland.

However, as quality indices are averaged measures based on a certain time span, these single value statistical parameters may not be representative of the data quality during rare events. Therefore, graphical techniques were utilised to examine the accuracy of UKNS model data for different sea states.

4.3.3.2 Assessment via Graphical Techniques

Five graphical techniques were employed to investigate the quality of data extracted from the UKNS model. These investigated the correlation between UKNS model data and physically measured data sourced from the M1 buoy. The five graphical techniques used were time series comparisons, scatter plots, quantile-quantile plots, frequency distribution plots and residual plots.

Time series comparisons of wave parameters provide a visual insight into data agreement facilitating comparisons at significant events, such as storms. However,

extensive data sets entail difficulties with respect to clear presentation of data. In line with this, time series plots comparing UKNS model and M1 buoy data were curtailed and display only a portion of the data set's temporal profile. All subsequent data analysis methods present results based on a four year time span, 2004 - 2008.

Scatter diagrams present the value of the numerically modelled parameter against physical measurements of the parameter for all common available time steps. These were used to qualitatively demonstrate the degree of correlation between UKNS model data and M1 buoy data. Residual plots presented the $parameter_{model}$ - $parameter_{measured}$ against the measured parameter value and allowed detection of specific trends, if any. Frequency distribution plots facilitate an investigation into data set agreement for each sea state. QQ plots (Quantile-Quantile plots) provided a graphical technique for determining if the two data sets came from populations with a common distribution. These graphs were plotted for significant wave height and zero crossing period.

4.3.3.3 Significant Wave Height

A time series comparison for significant wave height, Hs (m), is presented in Figure 4.9 below. This figure displays the temporal profile for a period spanning 3rd January 2004 to 31st March 2005. This time period was selected as it exhibits a full year of seasonal trends, allowing comparisons to be made for a large variety of sea states. Each individual graph plots the physically measured H_s (blue) against numerically modelled H_s (red) at corresponding hourly intervals. To clearly represent data, the time series graphs have been segmented into 5 month periods.

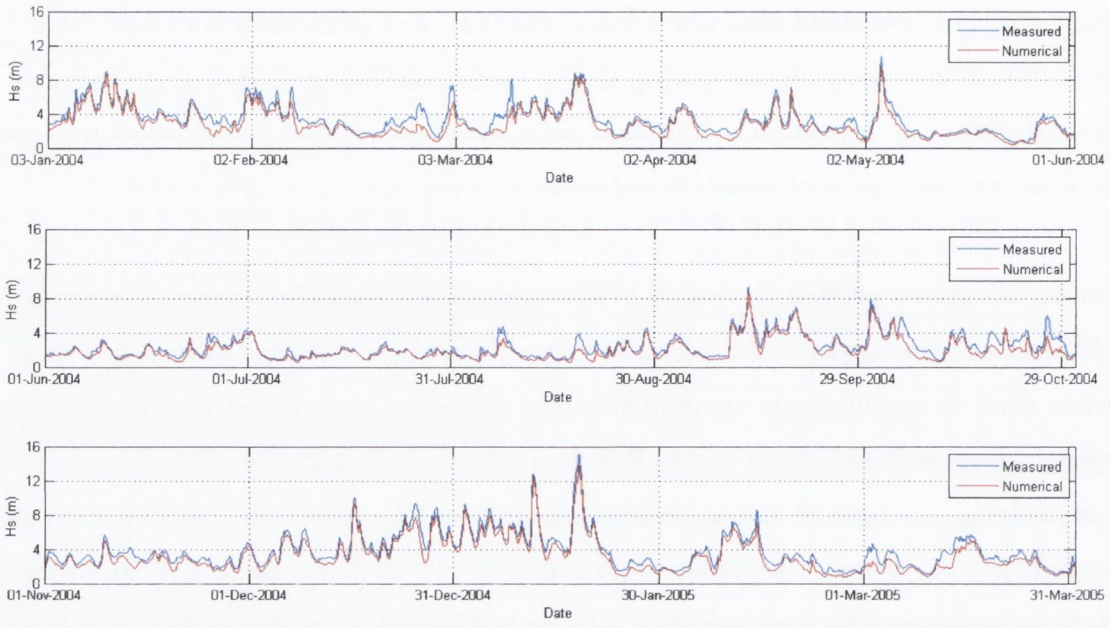

Figure 4.9 Time series comparison: H_s (m) from UKNS model against H_s (m) measured by Met Eirean's M1 buoy. Location: 53.1266°N, 11.2000°W. Time span: January 2004 to March 2005

It can be seen from Figure 4.9 that the UKNS model slightly underestimates the significant wave height, more specifically at the higher sea states. It should be noted that the M1 buoy calculated significant wave height as four times the root mean square (RMS) value of the wave. The heave sensor recorded this for 17.5 minutes and then calculated an average which was recorded hourly. The range of the heave sensor was 0-25 m and its accuracy has been documented on the Marine Institute website as ± 2 - 5 % (Heave Sensor, 2013). However, even with this potential error in the physical measurements, the temporal profile shows that the UKNS underestimates by more than 5% at a number of occasions. A scatter diagram plotting numerical H_s (m) against measured H_s (m) and a plot of residuals, in Figure 4.10 (a) and (b), supports the inference that the UKNS model underestimates the significant wave height. The scatter plot's data points are slightly skewed below the 45 degree line which represents perfect correlation. In line with this, the residual plot which graphs [Numerical H_s (m) - Measured H_s (m)] vs. Measured H_s (m) exhibits a trend denoting increasing error as wave height increases.

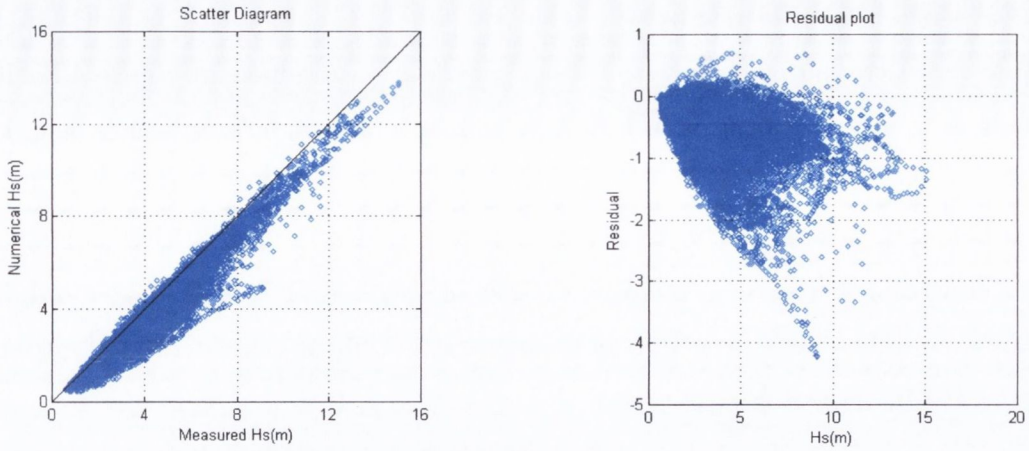

(a) (b)

Figure 4.10 Evaluation plots: H_s (m) from UKNS model vs. H_s (m) measured by Met Eirean's M1 buoy. Location: 53.1266°N, 11.2000°W. Time span: January 2004 – June 2008. (a) Scatter diagram, b) Residual plot: [Numerical H_s (m) - Measured H_s (m)] vs. Measured H_s (m)

The frequency distribution plot presented in Figure 4.11(a) compares the percentage occurrence of each significant wave height physically measured and numerically modelled. The blue histogram represents that measured by the M1 buoy while the red line denotes that recorded by the UKNS model. Corresponding to Figure 4.9 and Figure 4.10, a trend can be seen in Figure 4.11(a) that indicates the UKNS model underestimates significant wave height. The same is evident in the quantile-quantile plot in Figure 4.11 (b).

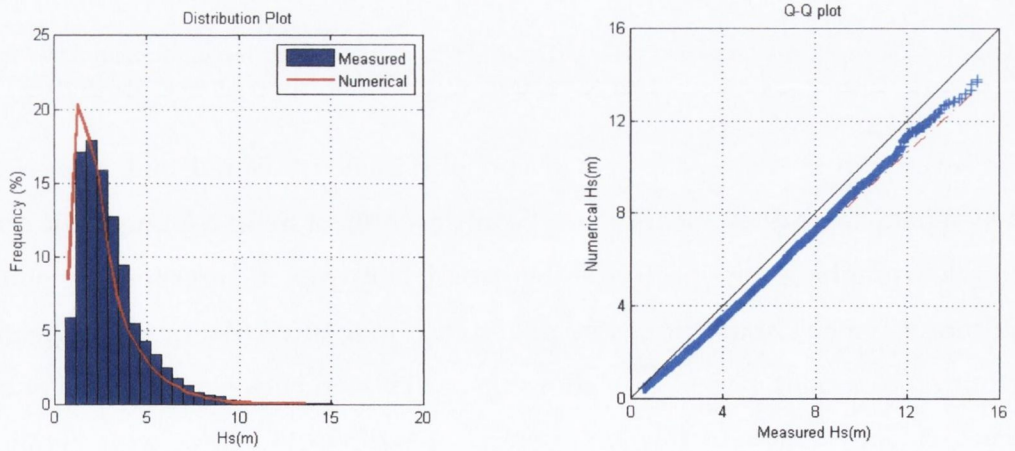

(a) (b)

Figure 4.11 Evaluation plots: H_s (m) from UKNS model vs. H_s (m) measured by Met Eirean's M1 buoy. Location: 53.1266°N, 11.2000°W. Time span: January 2004 – June 2008. (a) Frequency distribution comparison, (b) Quantile-Quantile plot

4.3.3.4 Zero Crossing Period

A time series comparison for zero crossing period is presented in Figure 4.12. It is plotted for the same time period as that displayed for significant wave height in Figure 4.9 (3rd January 2004 to 31st March 2005). Similarly to the plots for significant wave height, times series graphs are presented for fifteen months as it facilitates a visual comparison over a wide range of seasonal sea states. Physically measured zero crossing period is indicated by a blue line and UKNS numerical model output is represented by the red line.

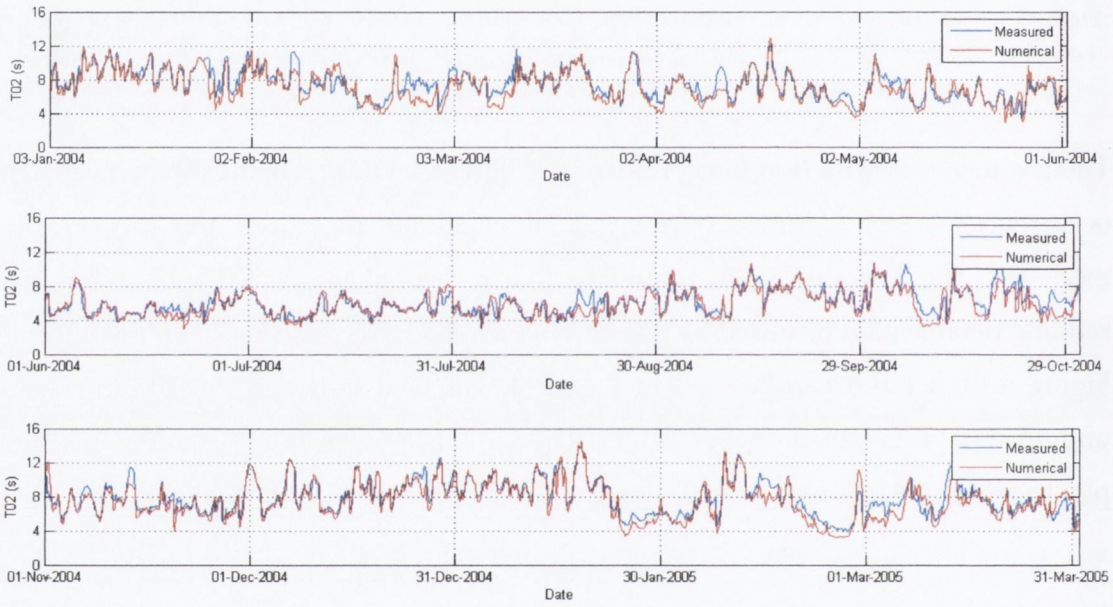

Figure 4.12 Time Series Comparison: T_{02} (m) from UKNS model against T_{02} (m) measured by Met Eirean's M1 buoy. Location: 53.1266°N, 11.2000°W. Time span: January 2004 to March 2005

When investigating discrepancies between physically measured and numerically modelled data, there does not appear to be any prominent trend relating to the errors when solely graphing zero mean crossing period. However, if corresponding plots of significant wave height are presented above each individual five month segmented graph of zero crossing period, a relationship can be seen between the errors of both parameters. An example of this is presented in Figure 4.13 below, with significant errors highlighted using dashed boxes.

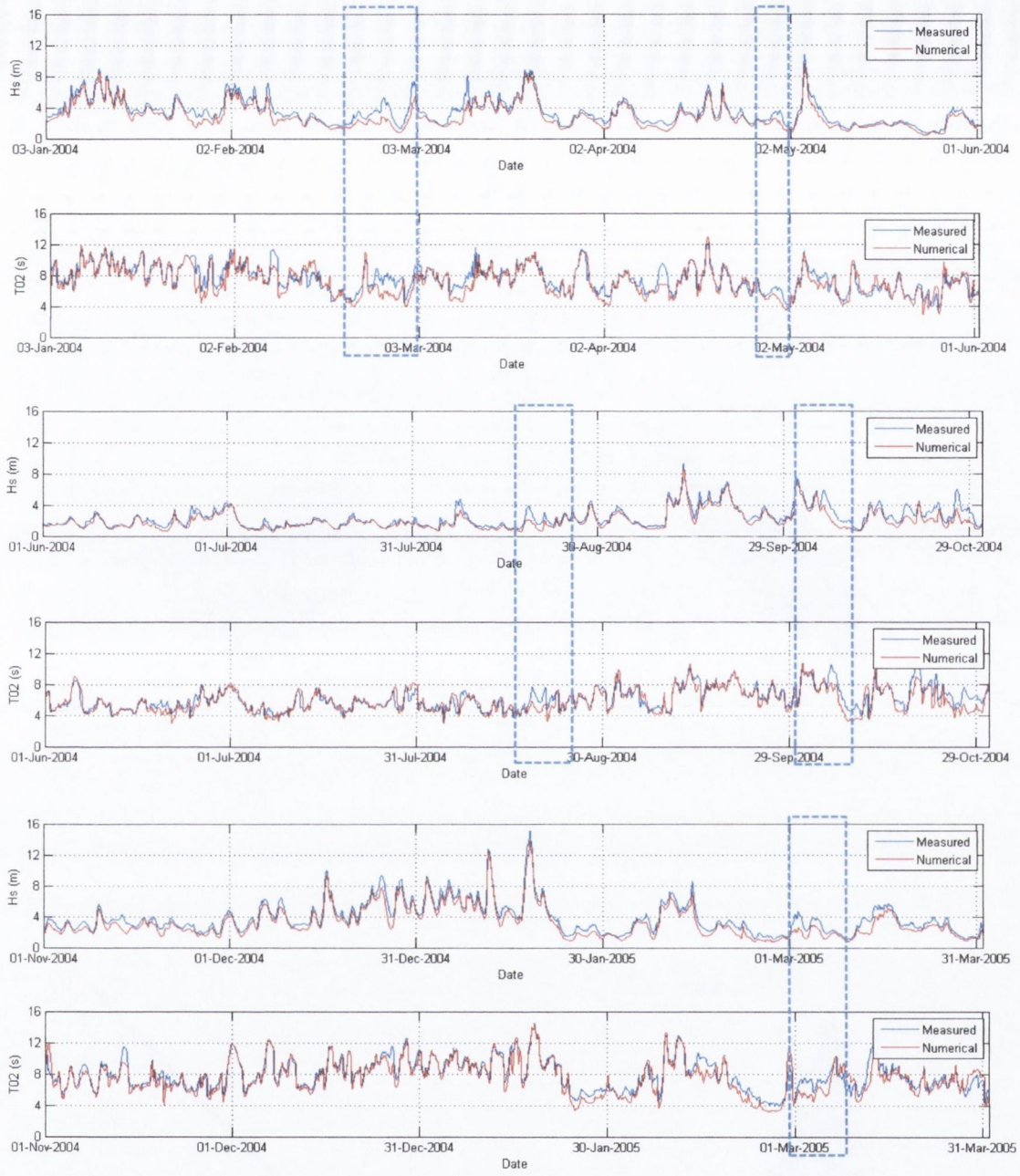

Figure 4.13 Time series comparison. Relationship between H_s and T_{02} errors. Location: 53.1266°N, 11.2000°W. Time span: January 2004 to March 2005

Over the fifteen month period it can be seen that discrepancies occur in both data sets on a number of occasions. It should be noted that zero mean crossing period is a measure of the mean time between wave cycles and is obtained from the sea surface elevation record. Hence, this parameter is affected by the wind, sea and swell waves. From corresponding wind records measured by the M1 buoy, it is interesting to note that discrepancies occur during periods of high and variable wind speed. A spectral wave model comparison study on Figueria da Foz, Portugal showed the influence of wind to contribute to discrepancies in zero mean crossing period (Venugopal, Davey,

Helen Smith, et al., 2011). However, further investigation into the precise combination of reasons causing these rare inaccuracies was halted as the number of prominent discrepancies was sufficiently low to substantiate the UKNS model as source for boundary data. Further graphical representations comparing physically measured and numerically modelled zero mean crossing period supports this decision (Figure 4.14 and Figure 4.15).

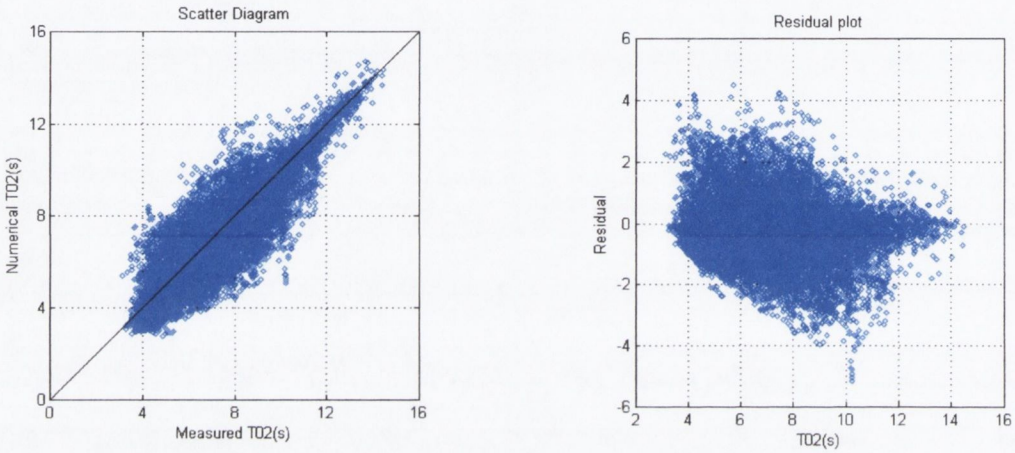

(a) (b)

Figure 4.14 Evaluation plots: T_{02} (s) from UKNS model vs. T_{02} (s) measured by Met Eirean's M1 buoy. Location: 53.1266°N, 11.2000°W. Time span: January 2004 - June 2008. (a) Scatter diagram, (b) Residual plot: [Numerical T_{02} (s) - Measured T_{02} (s)] vs. Measured T_{02} (s).

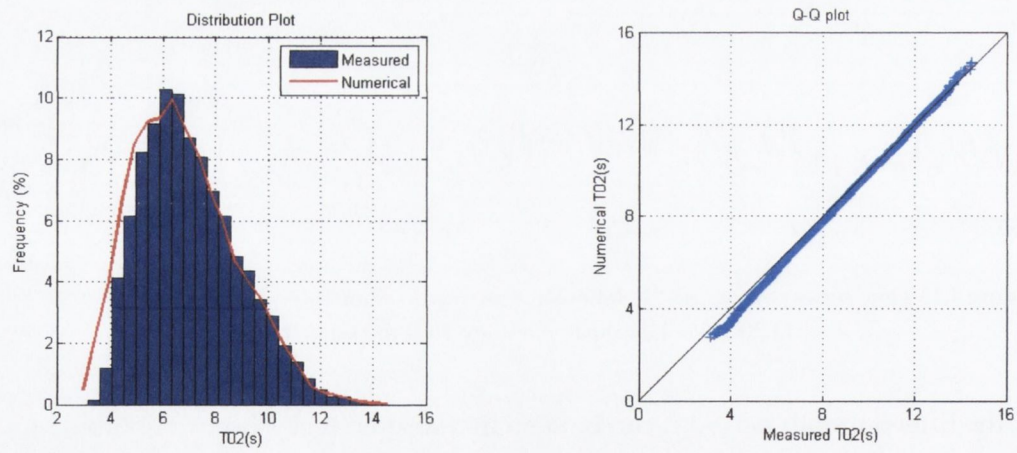

(a) (b)

Figure 4.15 Evaluation plots: T_{02} (s) from UKNS model vs. T_{02} (s) measured by Met Eirean's M1 buoy. Location: 53.1266°N, 11.2000°W. Time span: January 2004 - June 2008. (a) Frequency distribution comparison, (b) Quantile-Quantile plot.

In summary, based on the model assessment factors outlined at the start of this section; (i) spatial resolution (ii) temporal resolution (iii) quantified level of accuracy (iv) number of data output points in Loop Head region (iv) public availability and (v)

time span of available data; the UKNS model was selected as a suitable source of boundary data for areas off the West coast of Ireland. Although slight errors between modelled and measured data were identified, the standard statistical parameters, SI and r which quantified the level of agreement, were within appropriate bounds outlined the study 'High-resolution metocean modelling at the European Marine Energy Centre's test site (Lawrence et al., 2009)' - specifically, SI < 0.25 and r > 0.85. Additionally, the UKNS model's superiority in relation to temporal and spatial resolution permitted hourly two dimensional spectral wave data to be sourced for 30 points around the Loop Head model domain. These points lay on three ocean boundaries surrounding the area of interest: Western boundary (52.15°N, 11.2°W to 53.40°N, 11.2°W) Southern boundary (52.15°N, 11.2°W to 52.15°N, 10.48°W) and Northern boundary (53.40°N, 11.2°W to 53.40°N, 10.20°W). This directly affected the required model coverage and therefore, the extent of bathymetric data necessary to adequately span the model domain.

4.3.4 MetOcean Data

Following a comprehensive assessment of the UKNS model, metocean data were also obtained from this source. This comprised hourly time series data for wind and change in water level due to tide.

4.3.4.1 Wind Data

Similar to the UKNS model assessment for wave data, wind data were extracted from the model at the M1 buoy location and compared against concurrent physically measured wind records. The M1 buoy measured wind speed via an anemometer which logged the average wind speed every hour. Its accuracy has been documented on the Marine Institute website as ± 5 % (Marine Institute, 2013).

To quantify the level of accuracy associated with UKNS model wind data off the west coast of Ireland, quality indices were calculated. Bias, RMSE, Scatter Index and correlation coefficient are presented in Table 4.5.

Table 4.5 Quality Indices for v (m/s) UKNS model vs. Met Eirean's M1 buoy

	n	RMSE	bias	S.I.	r
v (m/s)	35064	1.662	-1.037	0.191	0.951

Results are based on hourly data spanning 4 years, which is equivalent to that for H_s and T_{02}. In accordance with the same standard criteria as those applied to wave data, in Section 4.3.2, the scatter index must be below 0.25 and correlation coefficient above 0.85. Values for these parameters in Table 4.5 meet these criteria.

Temporal profiles for physically measured and numerically modelled wind data spanning January to June 2004 are presented in Figure 4.16 (top). Similar to H_s and T_{02}, the UKNS model slightly underestimates wind speed. Corresponding time series graphs for H_s and T_{02} are presented below wind speed to show the reoccurring trend of underestimated parameter values. Prominent discrepancies are highlighted using dashed boxes. Notwithstanding these discrepancies, the full data set exhibits an acceptable level of agreement to justify the UKNS model as a suitable source for wind data.

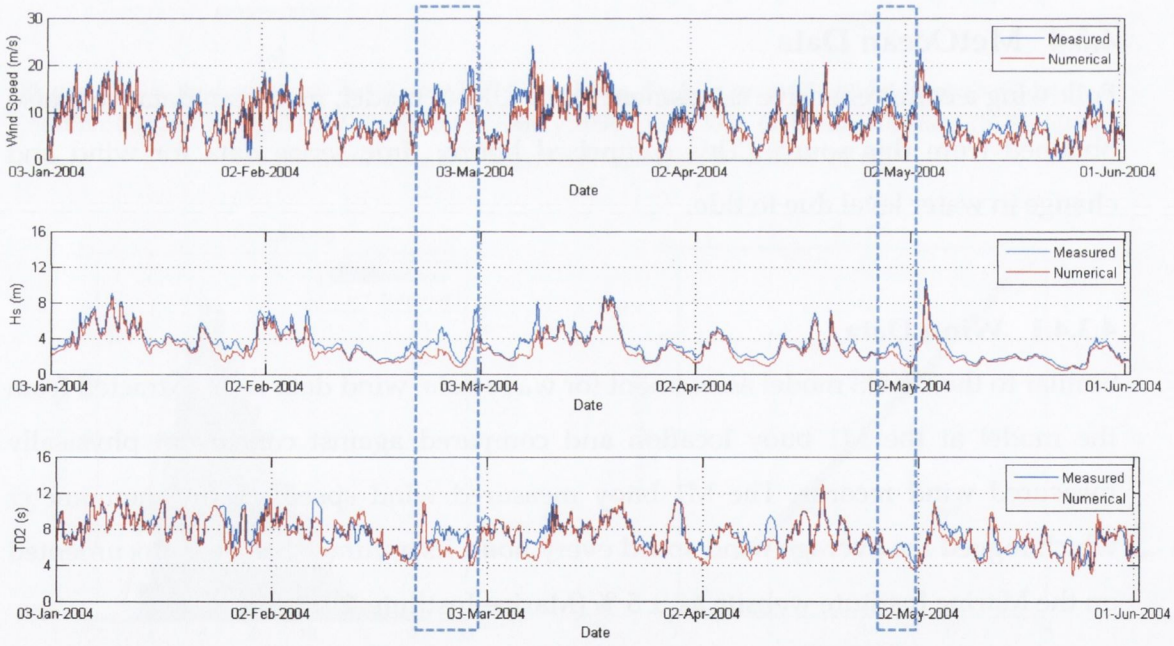

Figure 4.16 Time Series Comparison: Top: v (m/s) , Middle: H_s (m), Bottom: T_{02} (s). UKNS model against v (m/s) measured by Met Eireann's M1 buoy. Location: 53.1266°N, 11.2000°W. Time span: January - June 2004.

Further graphical representations comparing physically measured and numerically modelled wind speed demonstrate a suitable level of agreement (Figure 4.17 and Figure 4.18). The Scatter Diagram in Figure 4.17 (a) exhibits a concentration of points on the 45 angle line which represents perfect agreement. However, the UKNS

model's partial underestimation of wind is evident in the residual plot, frequency distribution and quantile-quantile plot displayed in Figure 4.17 (b), Figure 4.18 (a) and Figure 4.18 (b) respectively.

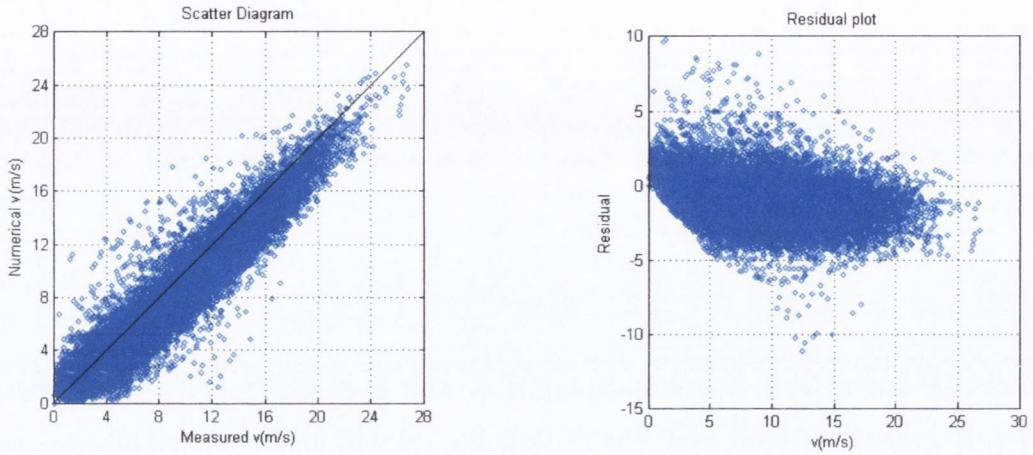

(a) (b)

Figure 4.17 Evaluation plots: v (m/s) from UKNS model vs. v (m/s) measured by Met Eirean's M1 buoy. Location: 53.1266°N, 11.2000°W. Time span: January 2004 - June 2008. (a) Scatter diagram, (b) Residual plot: [Numerical v (m/s) - Measured v (m/s)] vs. Measured v (m/s).

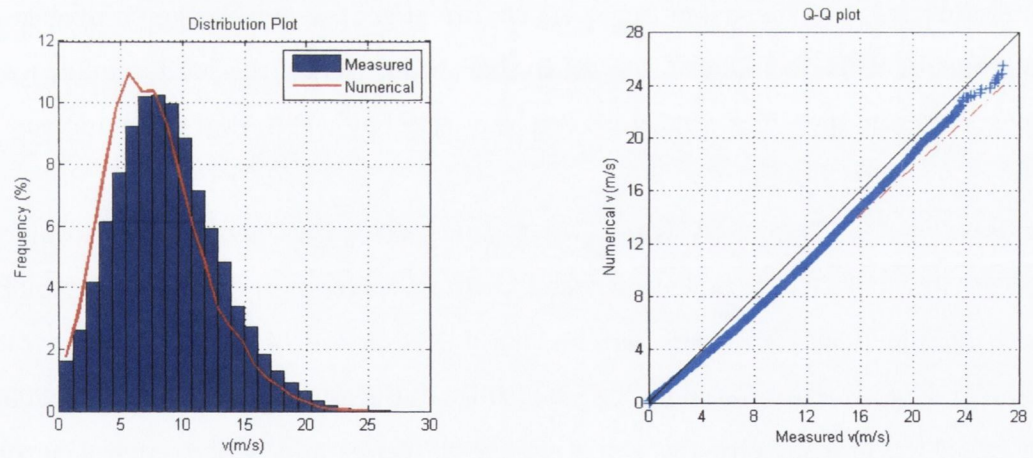

(a) (b)

Figure 4.18 Evaluation plots: v (m/s) from UKNS model vs. v (m/s) measured by Met Eirean's M1 buoy. Location: 53.1266°N, 11.2000°W. Time span: January 2004 - June 2008.
(a) Frequency distribution comparison, (b) Quantile-Quantile plot.

4.3.4.2 Tidal Range Data

Information on water level fluctuations over the model domain due to tide was sourced from the UKNS model. This was an important parameter to take into account considering that the wave energy converter under investigation was a shoreline device. A portion of the time series data set is shown Figure 4.19.

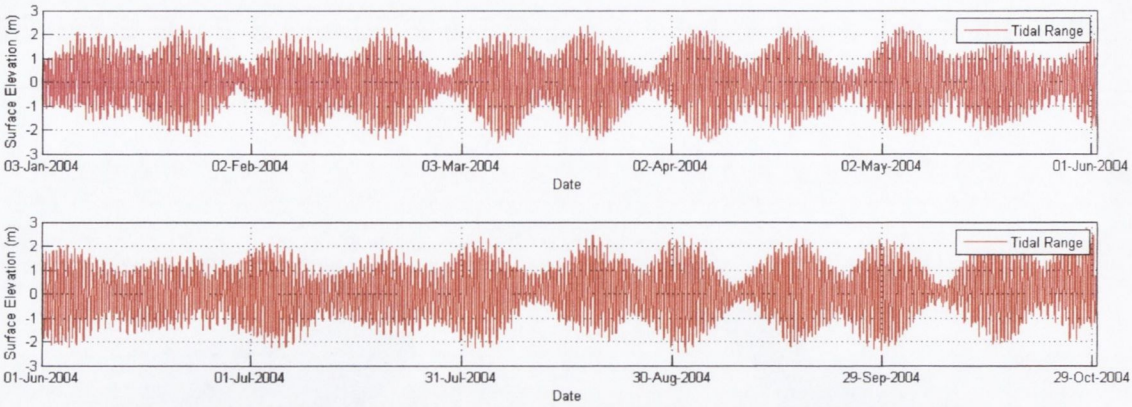

Figure 4.19 Water level fluctuations due to tide. Location: 53.1266°N, 11.2000°W. Time span: January 2004 - October 2004.

Changes in water depth at the location of a near-shore or shoreline wave energy converter can have a significant effect on the wave conditions to which it is exposed. An alteration in water level can reposition the point at which near-shore processes affect the impinging waves. The primary near-shore processes taken into account by the spectral wave model used in this study were depth induced friction, depth induced breaking and triad interaction, which were previously described in Chapter 2, Literature review. These non-linear effects can affect the percentage occurrence of each sea state at the location of interest in this study. Hence, the predominant wave energy converter operating conditions can be affected by water level fluctuations.

Additionally, the change in water level can specifically alter the performance characteristics of a fixed oscillating water column wave energy converter. Notable effects include a wavering shift in the natural response of the oscillating water column and exposure of the chamber inlet orifice to the atmosphere (Wavegen, 2002). Both affect the efficiency of the wave energy converter and hence, energy output. These are discussed in Chapter 6, SOWC Wave Energy Converter Design.

In light of the above, it was important to validate tidal data sourced from the UKNS model with concurrent data from the area of interest, Loop Head. Hourly time series data on water level fluctuations from the UKNS model were compared against corresponding measured data sourced from a tidal gauge at Carrigaholt, Co. Clare (Figure 4.20).

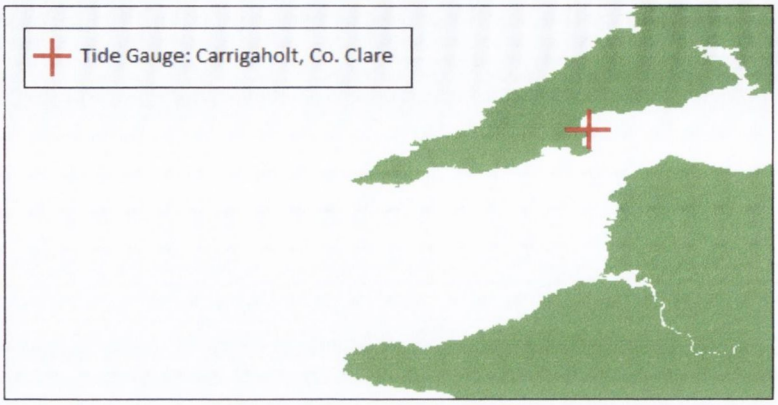

Figure 4.20 Location of tidal data source: Carrigaholt, Co. Clare

Temporal profiles for tidal range records from UKNS model and tidal gauge readings at Carrigaholt, Co. Clare are presented in Figure 4.21.

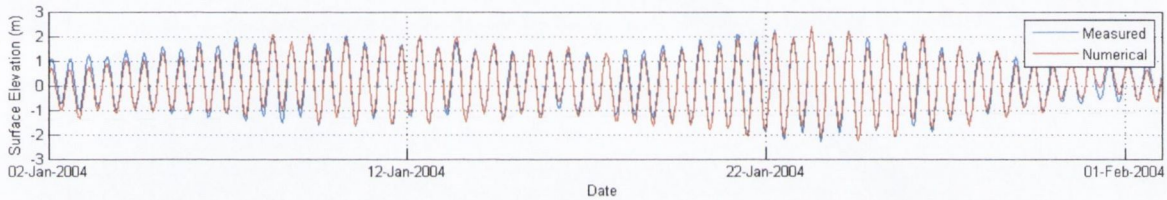

Figure 4.21 Time Series Comparison: Tidal Range (m) from UKNS model against Tidal Range (m) measured by Tide Gauge. Location: Carrigaholt, Co. Clare. Time span: January - February 2004

This time period demonstrates a strong agreement between both data sets. However, discrepancies in the order of 0.1 to 0.4 m were detected at points in the full data set. This can be seen in the temporal profile of both data sets when spanning a longer period of time, January to June 2004 (Figure 4.22).

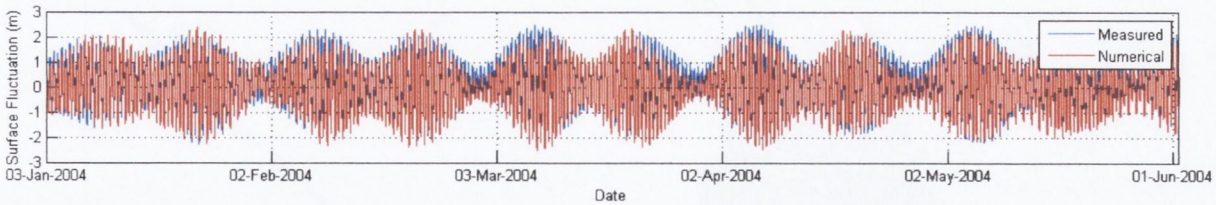

Figure 4.22 Time Series Comparison: Tidal Range (m) from UKNS model against Tidal Range (m) measured by Tide Gauge. Location: Carrigaholt, Co. Clare. Time span: January 2004 - June 2008

To quantify the level of accuracy and hence the validity of UKNS model tidal data, the correlation coefficient is the most appropriate statistical parameter to state. As the tidal range data set varies around a mean value of zero, the scatter index was affected since its denominator is an average of all measured values. Thus a denominator of

approximately zero proves the scatter index inapplicable. Table 4.6 presents all other primary quality indices bar scatter index.

Table 4.6 Quality Indices for tidal range (m) UKNS model vs. Carrigaholt Tidal Gauge

	n	RMSE	bias	r
Tidal Range (m)	6356	0.227	-0.953	0.986

A correlation coefficient of 0.986 provides evidence of the strong agreement between both data sets. This is supported by standard evaluation plots in Figure 4.23 and Figure 4.24.

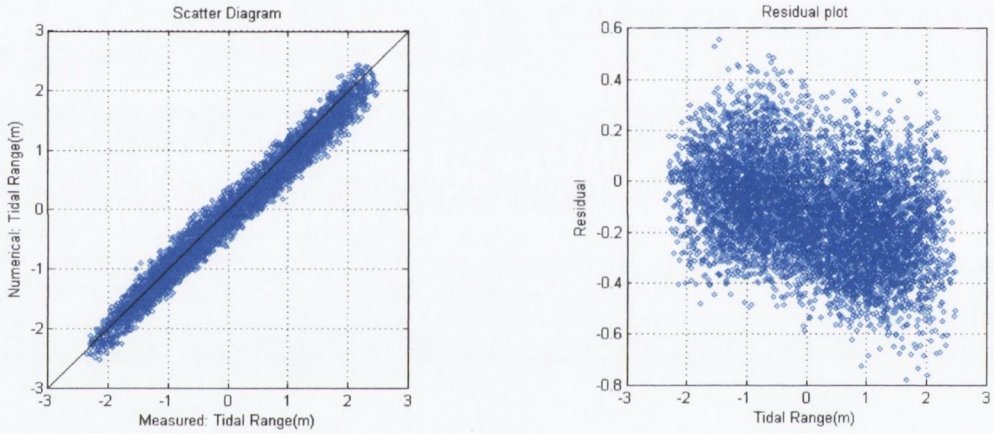

(a) (b)

Figure 4.23 Evaluation plots: Tidal Range (m) from UKNS model vs. Tidal Range (m) measured by Carrigaholt Tidal Gauge. Time span: January - September 2004. (a) Scatter diagram, (b) Residual plot

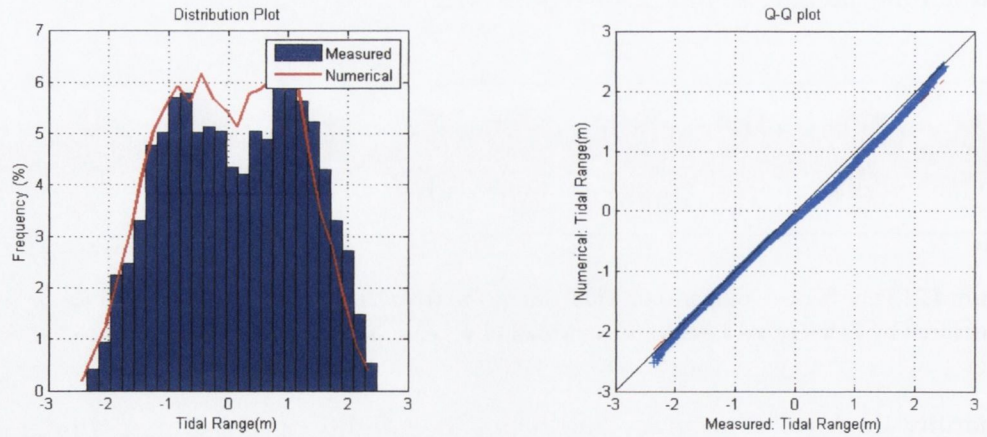

(a) (b)

Figure 4.24 Evaluation plots: Tidal Range (m) from UKNS model vs. Tidal Range (m) measured by Carrigaholt Tidal Gauge Time span: January - September 2004 (a) Frequency distribution comparison, (b) Quantile-quantile plot

4.4 BATHYMETRIC DATA

In order to precisely characterise the wave energy resource at a coastal location, an accurate bathymetry is of fundamental importance. At off-shore deep water locations, relatively low resolution bathymetric data is permitted as the depth is too great for the seabed to affect the wave characteristics. The specific depth in meters corresponding to the term deep water is dependent on the wave propagating over the seabed. Deep water is defined as a depth greater than half a wavelength (Tucker & Pitt, 2001). At depths greater than half a wavelength, the bathymetry is of minor importance and results of deep water wave climate models maintain a good level of accuracy at deep water locations. Conversely in the near-shore and shoreline domain, wave phenomena such as shoaling, refraction, triad interaction and depth induced wave breaking are directly influenced by the bathymetry.

Thus the resolution of depth points must be sufficiently high to ensure appropriate seabed features are resolved. Although the IEC Standards have not been officially published, the project team has reached a point where it can be shared with the wave energy community to obtain feedback for further improvement. The bathymetric resolution recommendations outlined in this pending report are presented in Table 4.7.

Table 4.7 Recommended resolutions of bathymetric data

	Reconnaissance	Feasibility	Design
Recommended maximum percentage difference in water depth between adjacent bathymetric points in water depths less than 200 m	10%	5%	2%
Recommended maximum horizontal spacing of bathymetric data in water depths less than 200 m	500 m	100 m	25 m
Recommended maximum horizontal spacing of bathymetric data in water depths less than 20 m	100 m	50 m	10 m

For this study, a range of bathymetric and topographical sources were utilised to create a digital seabed elevation model extending from the off-shore boundary, where suitable boundary conditions were available, to the region of interest, Loop Head, Co. Clare. In accordance with Section 4.3.2 Off-shore boundary conditions, the most suitable data available to this study were available at three ocean boundaries

surrounding Loop Head: Western boundary (52.15°N, 11.2°W to 53.40°N, 11.2°W) Southern boundary (52.15°N, 11.2°W to 52.15°N, 10.48°W) and Northern boundary (53.40°N, 11.2°W to 53.40°N, 10.20°W). As a result it was obligatory to extend the model domain to these bounds, as shown in Figure 4.25 below.

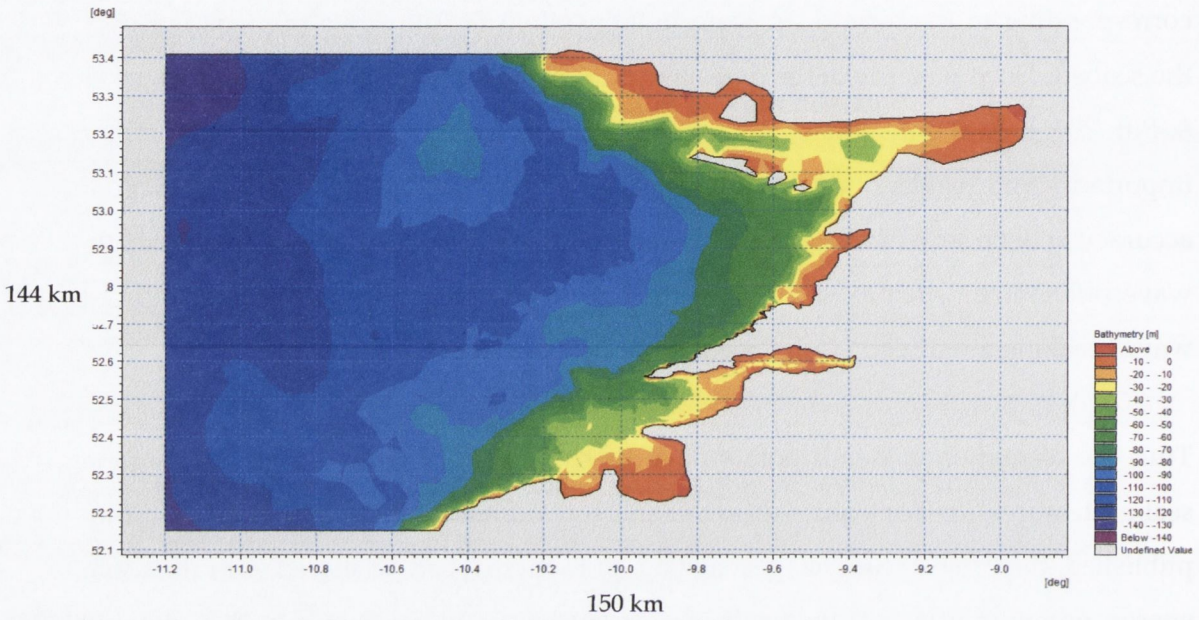

Figure 4.25 Spectral wave model domain (144 km x 150 km)

Although the model domain appears extensive, previous research has established that, given high quality boundary conditions, the third generation Mike 21 Spectral Wave model can accurately transfer wave conditions approximately 150 km from off-shore boundaries to the region of interest with minimal losses of spectral information (DHISoftware, 2011). This was the case for a prominent resource characterisation study carried out on the Orkney Islands which are located off the northern coast of Scotland (Lawrence et al., 2009). The aim of the study was to establish a long term high resolution wave hindcast model for the derivation of prevailing and extreme wave conditions at the European Marine Energy Centre (EMEC). This hosts the world's leading multi-berth, purpose built, open sea test facility for wave energy converters, which is located Billia Croo, positioned off the western coast of the Orkney Islands. The model domain implemented in this study is shown in Figure 4.26. The area of interest was Billia Croo test site, denoted by a red cross.

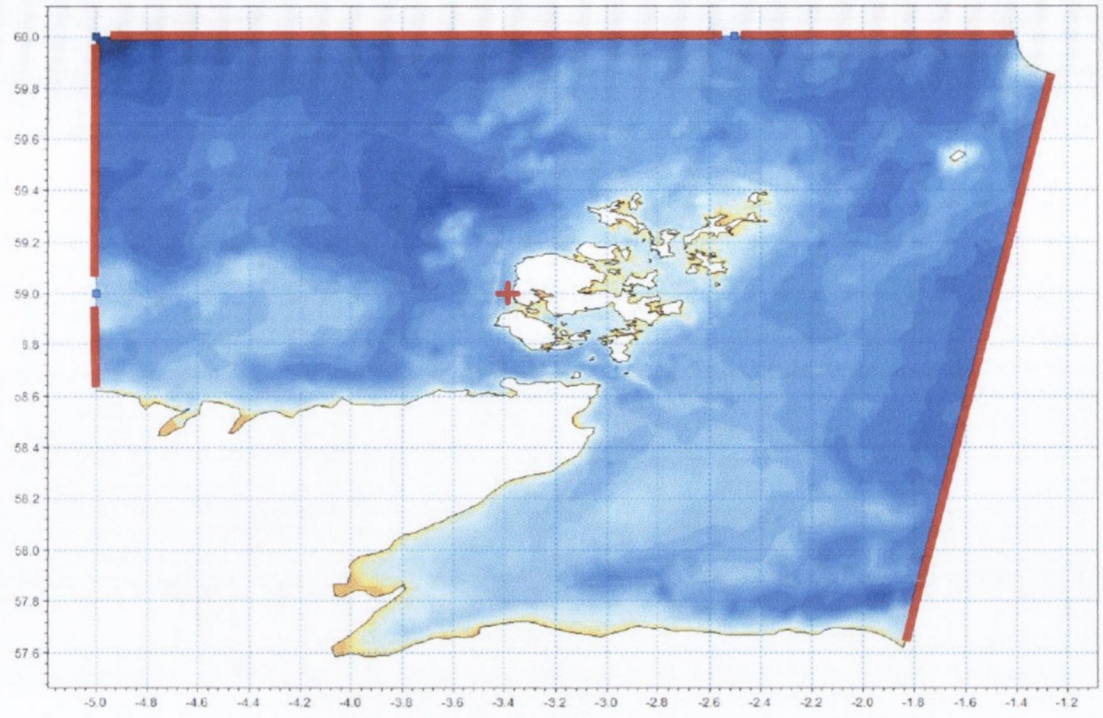

Figure 4.26 Model domain for EMEC wave energy resource characterisation study. EMEC wave test site at Billia Croo is denoted by a red cross.

Two dimensional directional spectral wave data, sourced from Oceanweather Inc, were applied at model boundaries. Wave records from a directional waverider buoy located at Billia Croo test site were utilised in the validation process. Regardless of the relatively large model domain, a high degree of accuracy was achieved, as shown in Figure 4.27.

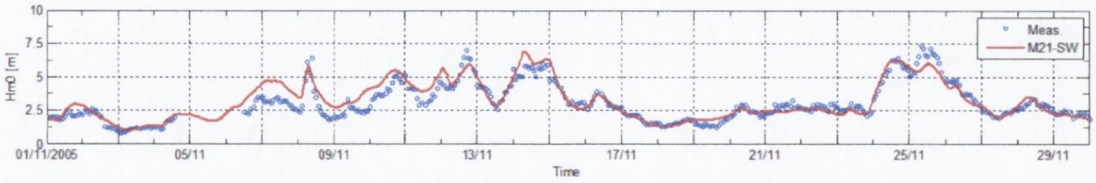

Figure 4.27 Time series comparison: H_s (m) from Mike 21 SW model against H_s (m) measured by waverider buoy. Location: Billia Croo test site. Time period: November 2005. Source: (Lawrence et al., 2009).

Quantifying the accuracy for this model, the scatter index for significant wave height was 0.18. This provided sufficient evidence that Mike 21 Spectral Wave model can achieve the required level of accuracy when adopting a large model domain with coverage of approximately 150 km squared.

For deep water off-shore locations, the use of relatively low resolution data was permitted in the scope of the present study but as the required data resolution increased approaching the site of interest, appropriate high resolution data became imperative. Figure 4.28 displays point depths as brown diamonds in the model domain. An increase in the resolution of bathymetric data can be observed, moving from off-shore to the area of interest, Loop Head.

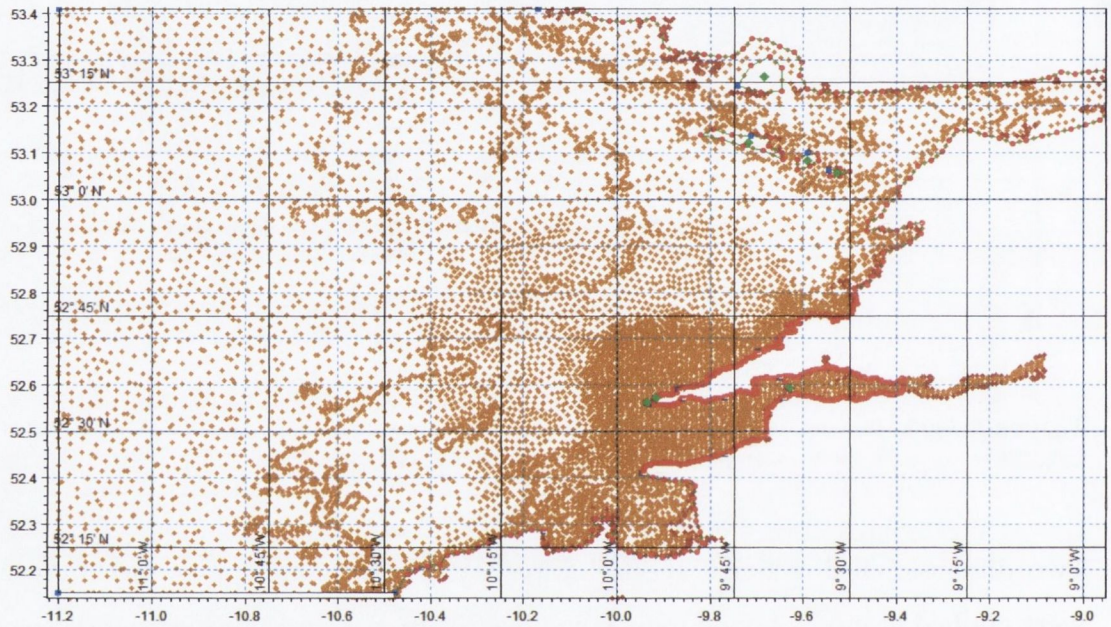

Figure 4.28 Resolution of bathymetric data in seabed model developed for this study

The off-shore topographical data was sourced from admiralty charts and input to the model in its digital form. The delineation of prominent bathymetric contour lines was the most vital feature of these data. This was accomplished by georeferencing admiralty chart images and superimposing them onto the model domain.

To correctly project the image onto the gridded model domain, image rectification was necessary. Rectification is the process of transforming data from one grid system to another grid system using an nth order polynomial (DHI Software, 2011). This practice was obligatory as the required admiralty chart images did not appropriately align with Mike 21's specific map projection. An image rectifying software package (Image Rectifier ®) was used to suitably rectify the admiralty chart images. A number of known longitudes and latitudes on the admiralty chart were assigned as ground control points (GCPs). This allowed the map to be appropriately distorted longitudinally and latitudinally to match the projection system used in Mike 21. An

example of a regular admiralty chart image and a suitably rectified image are shown in Figure 4.29.

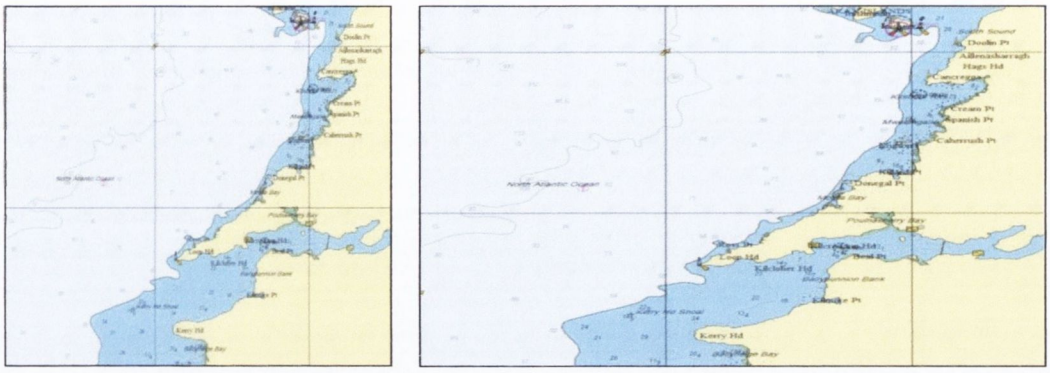

(a) (b)

Figure 4.29 Admiralty chart (a); Rectified admiralty chart (b)

Subsequently, the image was projected onto the two dimensional bathymetric model of Loop Head in order to input prominent bathymetric contours. Figure 4.30 (a) and (b) show sections of the bathymetric model under development, with input depths denoted by brown diamonds.

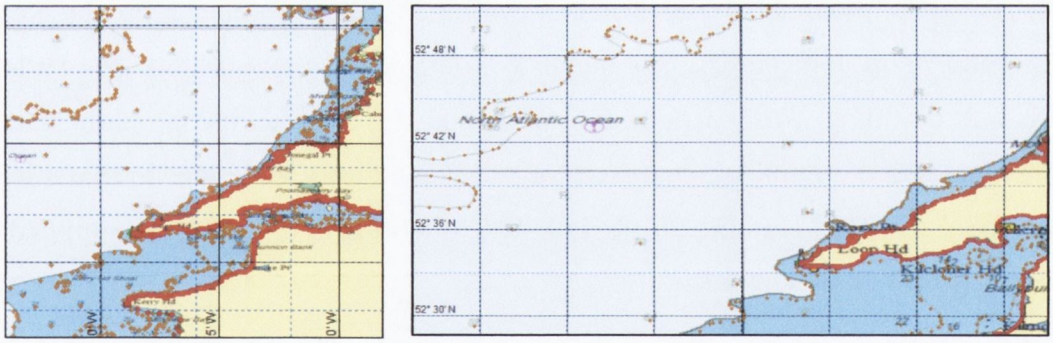

(a) (b)

Figure 4.30 Admiralty charts projected onto Mike 21 bathymetric model.
Admiralty chart (a); Rectified admiralty chart (b)

A number of admiralty charts for the west coast of Ireland were utilised in this way to achieve the recommended resolution for off-shore regions with depths less than 200m, as outlined in Table 4.7. Successively, an emphasis was placed on sourcing all available bathymetric data sets for the Loop Head area. The objective of this was to develop a mosaic of data sets with sufficient resolution to maintain accurate wave climate simulation in the near-shore and shoreline domain to the required standard. The region for which data sets were sought is illustrated as densely populated brown diamonds around Loop Head in Figure 4.28. The data files acquired to attain this

resolution are outlined in the Table 4.8 below, along with their source, date and method of acquisition and resolution.

Table 4.8 Bathymetric data sets

File Name	Source	Date/Method of Acquisition	Resolution
189m_Grid.xyz	UK Hydrographic Office	1842-56: leadline	189 m x 189 m
Shannon_5m_UTM.29	Geological Survey of Ireland/Marine Institute	2004: Multibeam Echosounder	5 m x 5 m
Chart_Contours.xyz	Admiralty Charts	1846-56: leadline	-
UKHO_Fair_Sheet.xyz	UK Hydrographic Office	1842-46: leadline	-
2011_Survey.xyz	Author	2011: Singlebeam EchoSounder	150 m x 150 m approx.

It can be seen from Table 4.8 that the bathymetric data available for the Loop Head area was of varying quality. Until recently, the majority of large scale bathymetric surveys were initiated by the British government and conducted by the Royal Admiralty in the 19th century. The method of data acquisition was the use of a lead line and de-tiding was carried out following the survey, using mathematical techniques based on time of measurement and tide tables. Corrections to charts were introduced in 1832 (Taunton, 2010). Thus it was assumed, de-tiding was applied to the surveys listed in Table 4.8.

Conversely, the recent surveys initiated by Geological Survey of Ireland and the Marine Institute have mapped the seabed using vessels with multibeam echo sounders, as part Ireland's Infomar (INtegrated Mapping FOr the sustainable development of Ireland's MArine Resource) program. In contrast to measuring depths using a lead line, multibeam technology employs hundreds of very narrow adjacent beams arranged in a swath which record high resolution bathymetric data as the data acquisition vessel moves over the seabed. De-tiding data recorded as part of the Infomar program was achieved using a high spec global position system (GPS), which referenced the depths to chart datum as the survey was carried out.

Graphical representations of a portion bathymetric data utilised in this study are shown in Figure 4.31 - Figure 4.34.

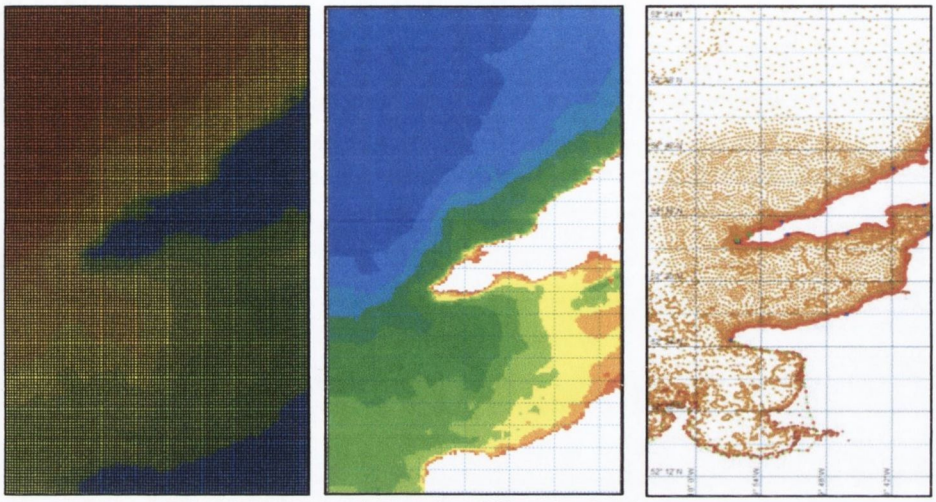

Figure 4.31 UK Hydrographic Office digitised admiralty charts

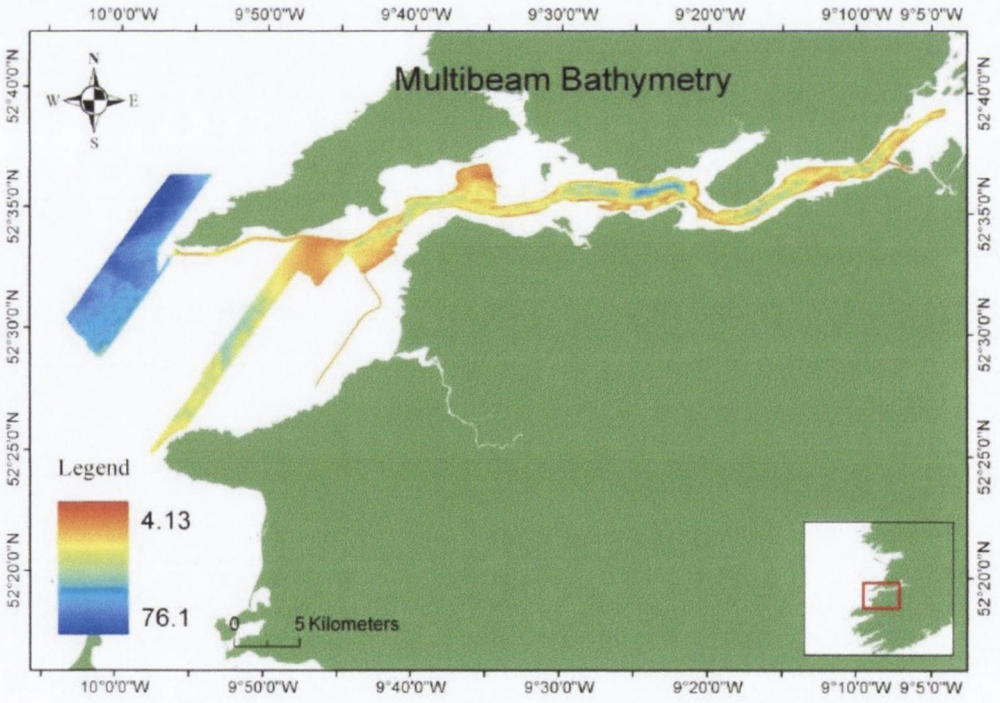

Figure 4.32 Geological Survey of Ireland/Marine Institute/Infomar digitised data

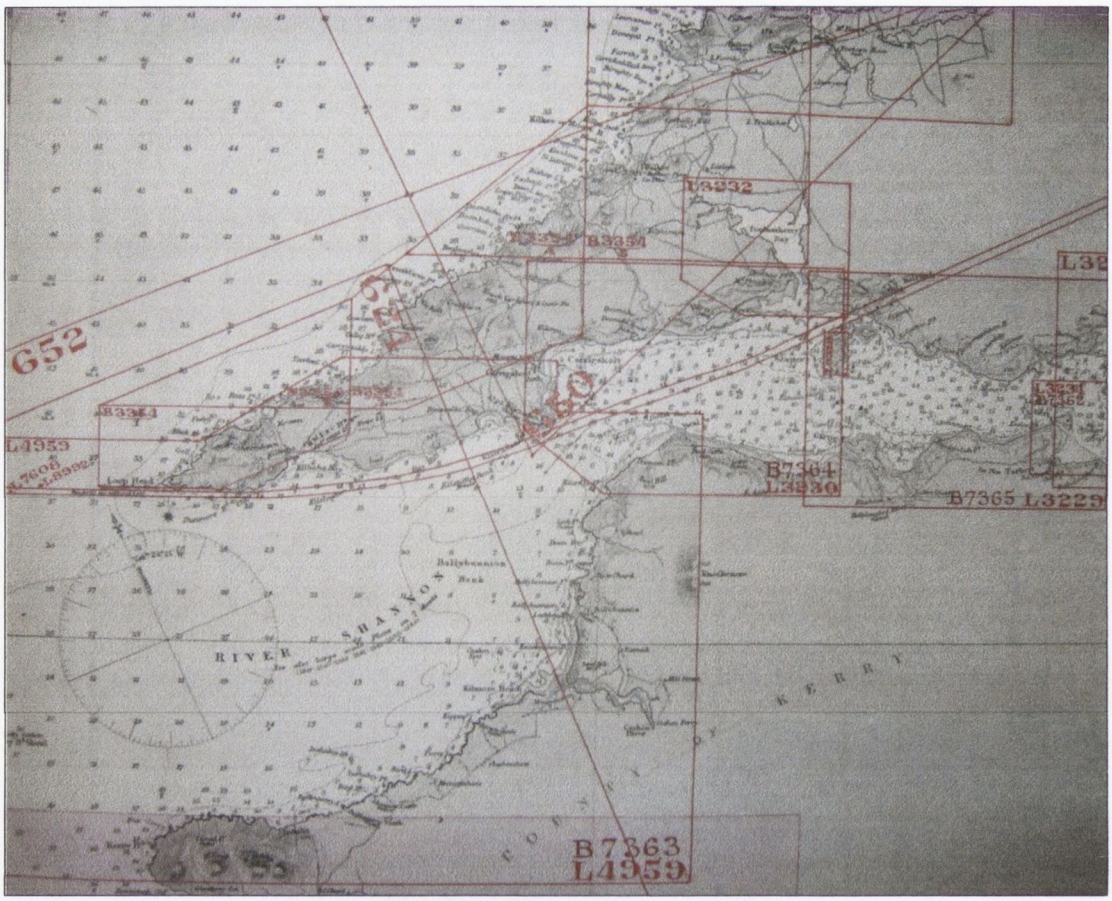

Figure 4.33 UKHO Bathymetric Survey Index

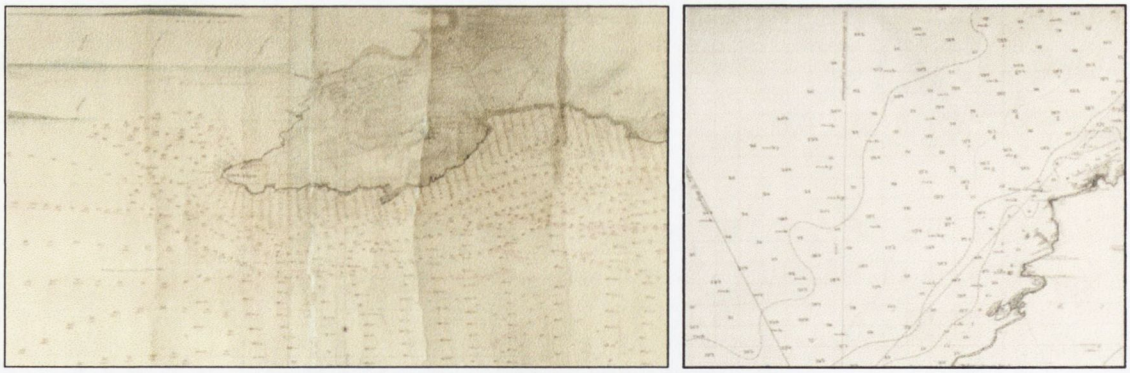

Figure 4.34 UK Hydrographic Office fair sheet data

The data were ranked based on their quality and priority given to the highest ranked datasets during the meshing of the digitised bathymetric model. This was done by assigning each data set a priority level within the bathymetric model prior to mesh generation.

The ranking system used was adopted from Sustainable Energy Authority of Ireland's Wave Climatology Study of Belmullet, Ireland as part of the development

of the Atlantic Marine Energy Test Site (AMETS) (M. Curé, 2011). From highest to lowest priority, the criteria to assess quality was (1) Most recent data, since methods of de-tiding the data have advanced in recent years (2) Multibeam and LIDAR data (3) Spot depths from echo sounders on board vessels (4) Digitised Admiralty Charts (5) Other.

This system led to the following quality ranking: (i) Shannon_5m_UTM.29 (ii) 2011_Survey.xyz (iii) 189m_Grid.xyz (iv) Chart_Contours.xy (v) UKHO_Fair_Sheet.xyz.

4.5 Spectral Wave Model Set Up

4.5.1 Spatial Resolution

The model domain is presented in Figure 4.28. The 2D model of the region was constructed using the aforementioned data sets. First, admiralty chart data was input using the previously described image rectification method. Predominant depth contours leading from off-shore to on-shore were refined. This provided coarse resolution bathymetric data for the complete model domain. Subsequently, digitised admiralty chart data for the County Clare domain (Figure 4.31) was incorporated to the model, increasing the bathymetric resolution for the region to 189 m x 189 m. 5 m resolution data, sourced from the GSI, was input for the area shown in Figure 4.32 and compared with surrounding bathymetric data. A reasonable level of agreement of +/- 1.5 m was found. To reach the required resolution of depth points for the near-shore and on-shore domain around Loop Head and Arch Point, fair sheet data was employed (Figure 4.34). These measurements were converted from fathoms to meters and input around the coast. The full set of data incorporated to the model domain is presented in Figure 4.28 where depth points are denoted as brown dots. The next step comprised the development of a flexible mesh with a focus on the County Clare region. The final computational mesh for the main area of interest is shown in Figure 4.35 below.

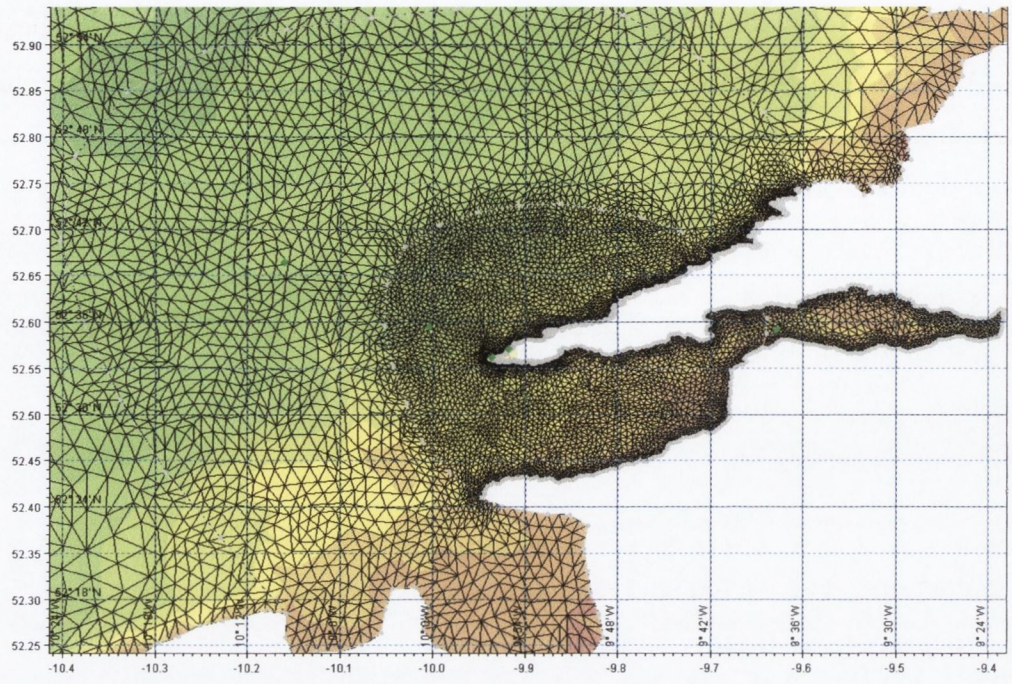

Figure 4.35 Flexible mesh for County Clare domain with increased resolution around Loop Head peninsula, Arch Point and near-shore/coastal areas

Using a smooth meshing technique, the resolution of the grid was increased around Loop Head peninsula. Specifically, the County Clare domain was divided into a number of zones: outer domain, Loop Head domain, Arch Point domain and near-shore/coastal domain. In each domain, the mesh resolution was controlled by assigning an appropriate node density based on the location and water depth. At near-shore and coastal locations within the Loop Head and Arch Point domain, the resolution was increased, as shown by the dark region surrounding the coast. As the wave energy resource at near-shore and coastal regions is strongly influenced by the effects of the seabed, a high resolution mesh at these locations is a primary requirement. The resolution of the mesh in this domain was approximately 50 m. The limitation with mesh size relates to computational expense. As with many computational methods, simulation time increases with increased mesh size.

4.5.2 Boundary Conditions

Based on the assessment of a number of options, spectral data sourced from the UKNS model was employed at each ocean boundary. This source provided hourly two-dimensional spectral wave data input at 30 points at model boundaries. For this study, 4 years of this high spatial and temporal resolution data was available. This

describes the frequency and direction of the sea state with a higher level of accuracy than many of the other options available for a longer period of time. As the simulation proceeds, the boundary data is propagated through the model domain.

4.5.3 Metocean Data

The boundary conditions were supplemented with metocean data input at hourly intervals corresponding to the two-dimensional spectral wave data. This comprised hourly time series data for wind and change in water level due to tide, as previously described. Using the coupled air-sea interaction formulation and background Charnock parameter, the inclusion of this metocean data increases the accuracy of the model. This will be seen in model validation. The coupled air-sea interaction formulation was applied according to Komen et al. (1994). This formulation means the momentum transfer from the wind to the waves or drag depends on both the wind and waves. The applied background roughness Charnock parameter was set to 0.01, as recommended by DHI's MIKE 21 Spectral Wave Model User Guide (2012).

4.5.4 Settings

The MIKE 21 Spectral Wave model simulates the growth, decay and transformation of wind generated sea and swells. Regarding model formulation, the fully spectral formulation was used. This is based on the wave action conservation equation where the directional frequency wave action spectrum is the dependant variable. Regarding the spectral discretization, the wave spectrum grid uses 25 frequencies on a logarithmic scale with a frequency factor of 1.15 and 24 directions. The frequencies range from 0.03 Hz to 0.5 Hz. The time step is defined by the numerical model itself and is equal to 75 s. Quadruplet-wave interaction is included as is white capping. For the latter, two dissipation coefficients are employed, Cdis and δdis. These are set to 2 and 0.5 respectively. Wave breaking is also included in the spectral wave model with the formulation based on Battjes and Jensen (1978) with χ set to 0.8. Regarding representation of the land boundary, communications with the developers of MIKE 21 SW confirmed that a standard land boundary should be used rather than a reflective boundary for cliff sites (Kofoed-Hansen, 2011). This facilitates more realistic power values as well as percentage occurrence of each sea state compared with a reflective boundary. In addition, bottom friction is included in the wave model using

the Nikuradse roughness coefficient, kN, of 0.01 m. This parameter is estimated by $k_N = 2d_{50}$ where d50 is the median grain size. This setup is based on theoretical knowledge of the scenario being modelled and stated coefficients may be refined during the calibration process. These settings coupled with the aforementioned data sets and bathymetric model were used in the calibration and validation process.

4.6 MODEL CALIBRATION AND VALIDATION

Calibration and validation were performed against the local measurements for Loop Head, described in Section 4.3.1. As the local measurements available to this study were time series data for significant wave height and energy period at hourly intervals, equivalent parameters were extracted from the spectral wave model domain at the exact location of the waverider buoy. The location of the wave rider buoy was west of Arch Point, 52.65°N, 9.7833°W, as shown in Figure 4.2. This provided a means to compare the simulated results with those recorded physically. The same quantitative and graphical techniques used to assess boundary data, were used to validate the spectral wave model.

4.6.1 Assessment via Statistical Parameters

Quality indices calculated for significant wave height and energy period are presented in Table 4.9 below.

Table 4.9 Quality Indices for H_s (m) and T_e (s). MIKE 21 SW vs. waverider buoy

	n	RMSE	bias	S.I.	r
H_s (m)	3641	0.413	-0.012	0.164	0.96
T_e (s)	3641	1.034	-0.322	0.105	0.861

Both parameters exhibit a scatter index less than 0.25 and a correlation coefficient greater than 0.85. The predominant means to achieve this accuracy was increasing the resolution of the mesh for the Loop Head region. The model formulation and settings were those previously described. A larger data set for comparison is favourable as it facilitates a comparison for a wider range of sea states. However, it will be seen when plotting the time series comparison that highly energetic, moderate and calm conditions are present within the data set.

4.6.2 Assessment via Graphical Techniques

4.6.2.1 Significant Wave Height

A time series comparison for significant wave height is presented in Figure 4.36 below. This figure displays the temporal profile for a period spanning 3rd January to 1st June 2004.

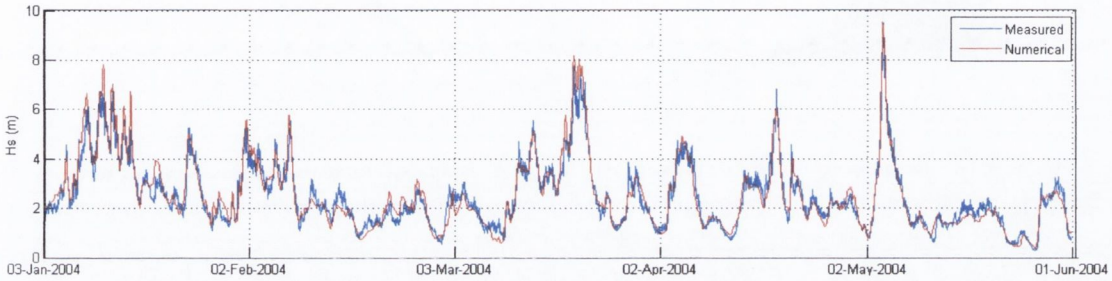

Figure 4.36 Time Series Comparison: MIKE 21 SW against H_s (m) measured by wave rider buoy. Location: 52.65°N, 9.7833°W. Time span: January - June 2004.

Overall it can be seen that there is a high level of agreement between both data sets. The corresponding scatter diagram, residuals, frequency distribution and quantile-quantile plots presented in Figures 4.37 and 4.38 confirm the high level of agreement.

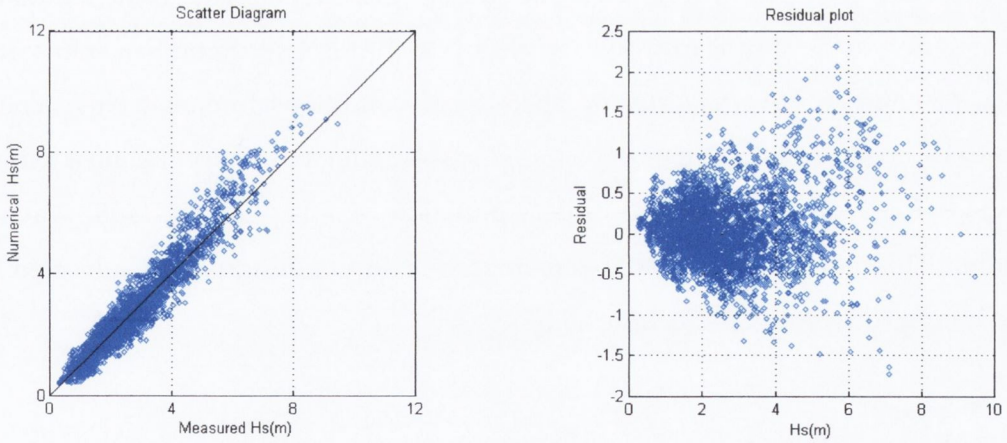

(a) (b)

Figure 4.37 Evaluation plots: H_s (m) from MIKE 21 SW vs. H_s (m) measured by waverider buoy. Location: 52.65°N, 9.7833°W. Time span: January - June 2004. (a) Scatter diagram, (b) Residual plot: [Numerical H_s (m) - Measured H_s (m)] vs. Measured H_s (m).

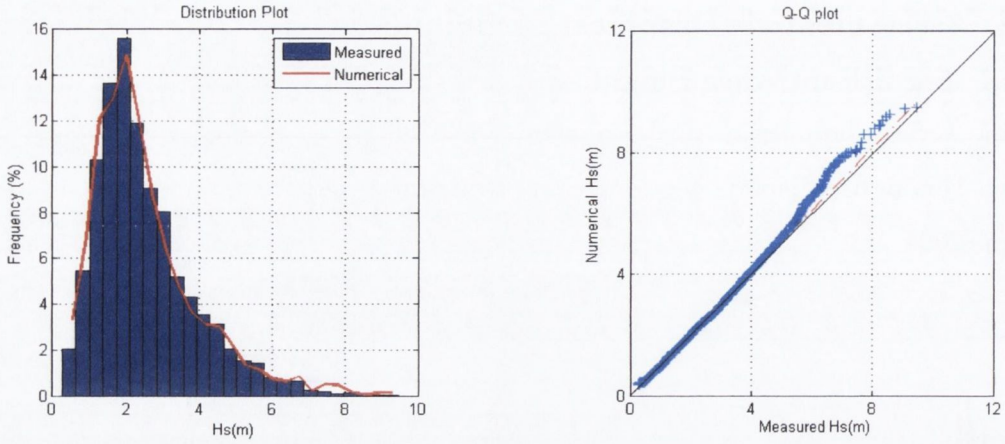

(a) (b)

Figure 3.38 Evaluation plots: H_s (m) from MIKE 21 SW vs. H_s (m) measured by waverider buoy. Location: 52.65°N, 9.7833°W. Time span: January - June 2004. (a) Frequency distribution comparison, (b) Quantile-Quantile plot.

Each of the above graphs identifies that a higher level of agreement between modelled and measured data is found for significant wave heights between 0 and 5 m. As the wave climate becomes increasingly non-linear, the accuracy of the spectral wave model reduces. Considering Figure 3.38 (b), the quantile-quantile graph highlights a reduction in model accurancy for sea states possessing a significant wave height greater than approximately 5 m. With respect to the use of the wave climate model to aid power predictions for wave energy converters, the accurate simulation of sea states with a significant wave height up to 5 m is important. Sea states up to this point comprise the majority of operational conditions for most wave energy converters. Regarding the use of the wave climate model to identify the most extreme sea states for a given region, accurate simulation of exceptionally large waves is desirable. This allows estimates to be made for maximum design loads subjected to a wave energy converter (See Section 6.3.6).

4.6.2.2 Energy Period

A time series comparison for energy period corresponding to the time span for significant wave height is presented in Figure 4.39.

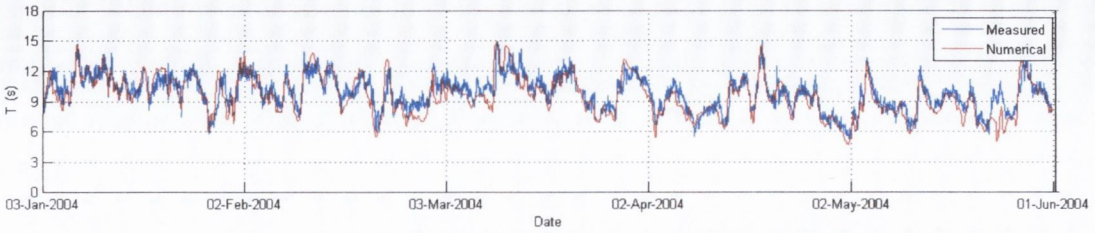

Figure 4.39 Time Series Comparison: MIKE 21 SW against T_e (s) measured by wave rider buoy. Location: 52.65°N, 9.7833°W. Time span: January – June 2004.

A similar level of agreement to that for significant wave height is exhibited. However, when consulting the scatter diagram, residuals, frequency distribution and quantile-quantile plots presented in Figures 4.40 and 4.41, discrepancies can be observed.

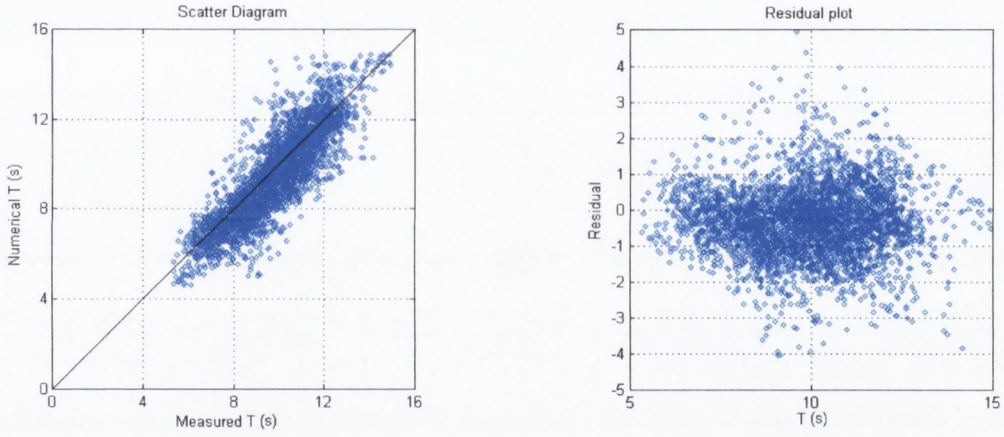

(a) (b)

Figure 4.40 Evaluation plots: T_e (s) from MIKE 21 SW vs. T_e (s) measured by waverider buoy. Location: 52.65°N, 9.7833°W. Time span: January – June 2004. (a) Scatter diagram, (b) Residual plot: [Numerical T_e (s) – Measured T_e (s)] vs. Measured T_e (s).

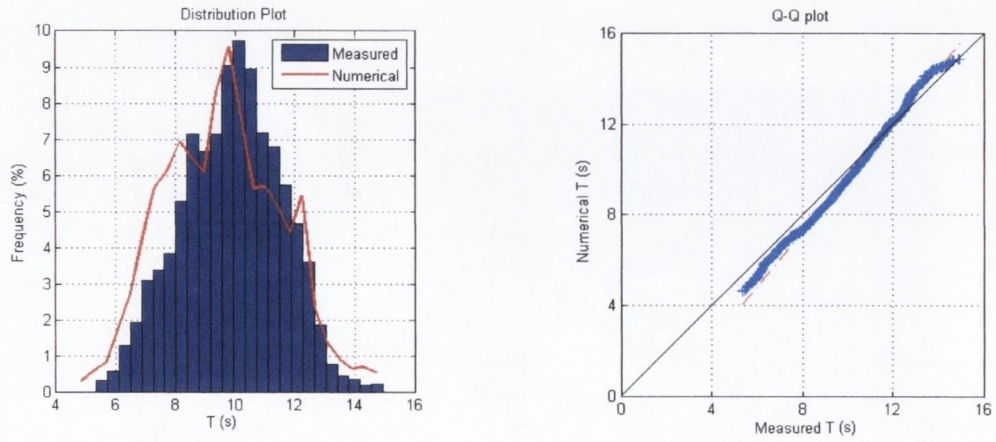

(a) (b)

Figure 4.41 Evaluation plots: T_e (s) from MIKE 21 SW vs. T_e (s) measured by waverider buoy. Location: 52.65°N, 9.7833°W. Time span: January – June 2004. (a) Frequency distribution comparison, (b) Quantile-Quantile plot.

Looking at Figure 4.41 (a), it can be seen that an inconsistency exists between modelled and measured data for low, medium and high period values. However, this discrepancy was deemed sufficiently small to continue with this model set-up. This comprised a fine resolution grid around the Loop Head peninsula with a further increase in mesh size beyond the 25 m depth contour.

It is important to note that the above process validates the model up to location of the wave rider buoy. The uncertainty associated with results extracted between the wave rider buoy and the coast increases with distance and reducing water depth. To assess model accuracy at a shallower water depth closer to the coast, a further data set was sourced.

4.7 Spectral Wave Model Comparison Study

A research group at University College Dublin recently carried out a wave energy resource assessment on Killard Point (Gallagher, Tiron, et al., 2013). As identified in Chapter 3, this is an area of interest to marine renewables. The area was modelled using a spectral wave model known as WaveWatch III (WWIII). Spectral wave data and wind data provided by the ECMWF were employed at model boundaries. Using a long-term reanalysis data set, ERA-INTERIM, a 10 year simulation (2002 - 2012) was run using Ireland's Centre for High-End Computing (ICHEC). The model was validated against a wave rider buoy off Killard Point in 2011.

Killard Point is located within the model domain developed for this study, as shown in Figure 4.42 below.

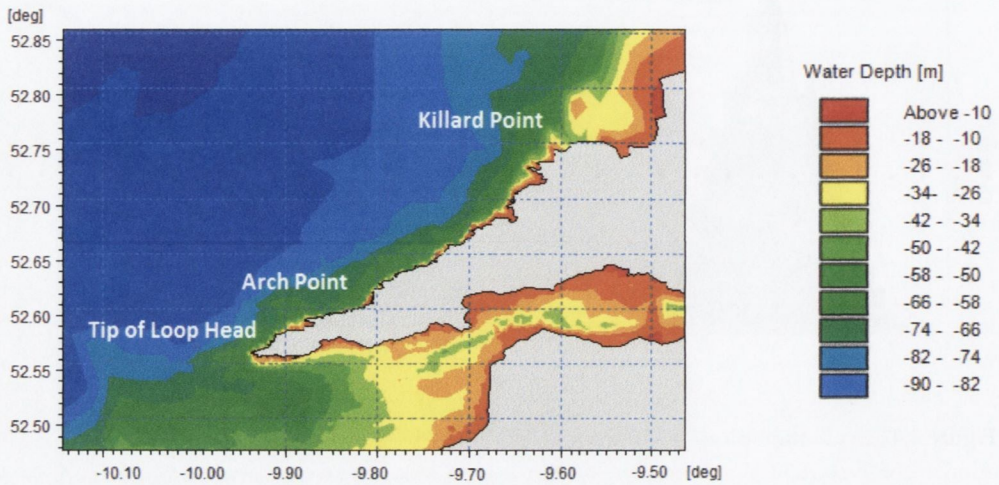

Figure 4.42 Location of Killard Point in relation to the wave rider buoy located off Arch Point

As the 10 year hindcast study extends back to 2002, the time period overlaps with the time period for this study. This facilitated a comparison study at Killard Point using data presented in Gallagher, Tiron, et al. (2013). Data was extracted from both the MIKE21SW model and WWIII model at 52.766°N, 9.579°W. This is located at the 20 m depth contour.

4.7.1 Assessment via Statistical Parameters

Quality indices calculated for significant wave height and energy period are presented in Table 4.10 below. Results are based on data extracted every hour from January 2004 to January 2006.

Table 4.10 Quality Indices for H_s (m) and T_e (s). MIKE 21 SW vs. WW3

	n	RMSE	bias	S.I.	r
H_s (m)	18221	0.387	-0.152	0.198	0.97
T_e (s)	18221	0.940	-0.010	0.105	0.928

Both parameters meet the relative criteria for scatter index (< 0.25) and correlation coefficient (> 0.85). The level of agreement between data sets increases the confidence that may be placed in the MIKE 21 SW model accuracy at the 20 m depth contour.

4.7.2 Assessment via Graphical Techniques

4.7.2.1 Significant Wave Height

A time series comparison for significant wave height is presented in Figure 4.43 below. This figure displays the temporal profile for a period spanning 3rd January to 1st June 2004.

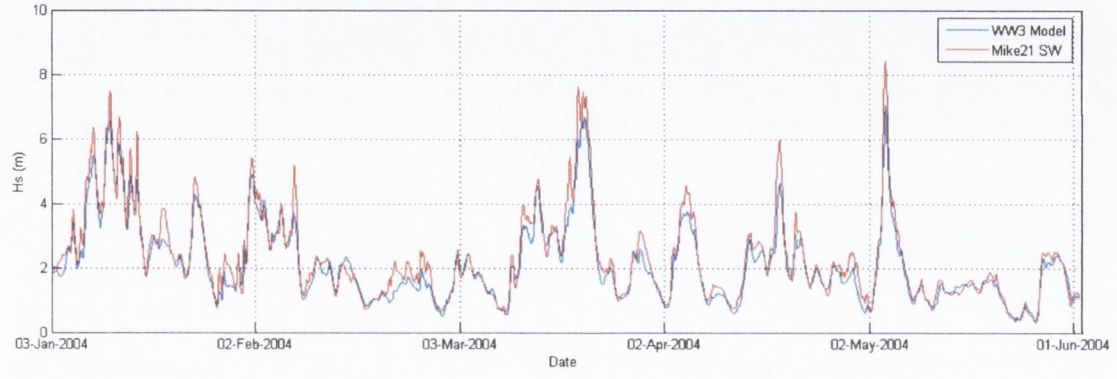

Figure 4.43 Time Series Comparison: H_s (m) from MIKE 21 SW against H_s (m) from WWIII. Location: 52.766°N, 9.579°W. Time span: January – June 2004.

It can be seen that a trend exists between the MIKE 21 SW model in comparison to WWIII. MIKE 21 SW consistently predicts a slightly higher significant wave height compared with WWIII. This is also highlighted in Figures 4.44 and 4.45 shown below. It is most easily identified in Figure 4.44 (a) and Figure 4.45 (b) where both data sets are skewed above the diagonal line which represents perfect correlation.

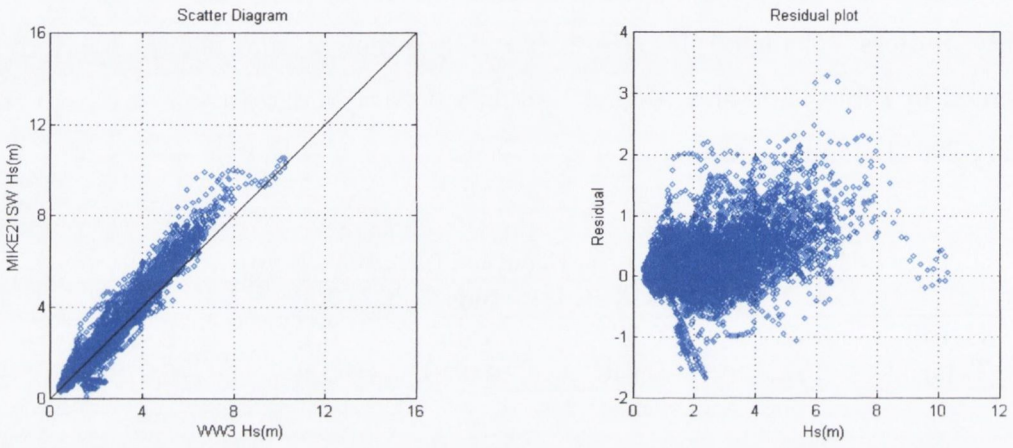

(a) (b)

Figure 4.44 Evaluation plots: H_s (m) from MIKE 21 SW vs. H_s (m) from WW3 model. Location: 52.766°N, 9.579°W. Time span: Jan 2004 – Jan 2006. (a) Scatter diagram, (b) Residual plot

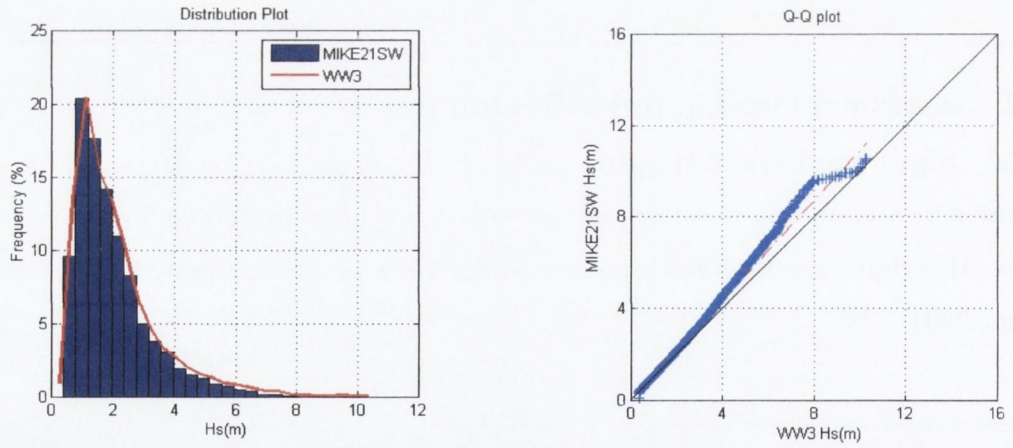

(a) (b)

Figure 4.45 Evaluation plots: H_s (m) from MIKE21SW vs. H_s (m) from WW3 model. Location: 52.766°N, 9.579°W. Time span: Jan 2004 – Jan 2006. (a) Frequency distribution comparison, (b) Quantile-Quantile plot.

4.7.2.2 Energy Period

A time series comparison for energy period corresponding to the time span for significant wave height is presented in Figure 4.46 below. This is accompanied by the corresponding scatter diagram, residual plot, frequency distribution and quantile-

quantile plot presented in Figures 4.47 and 4.48. In comparison to graphs plotted for significant wave height, no specific trend can be identified between the data sets.

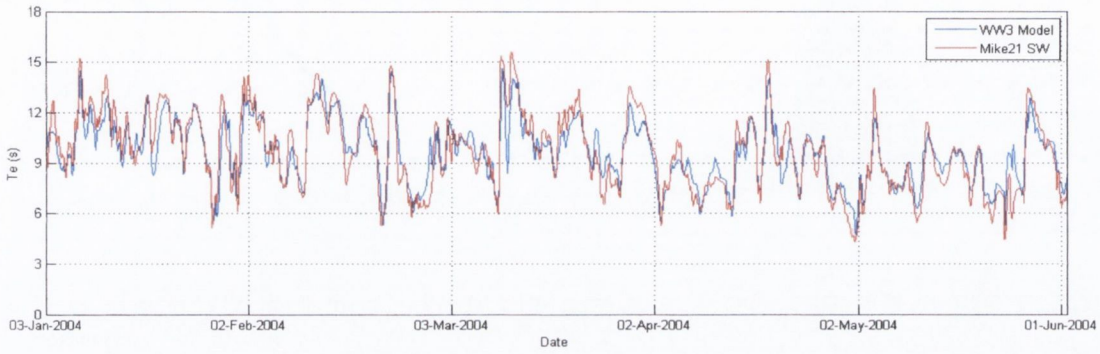

Figure 4.46 Time Series Comparison: T_e (s) from MIKE 21SW against T_e (s) from WWIII. Location: 52.766°N, 9.579°W. Time span: January - June 2004.

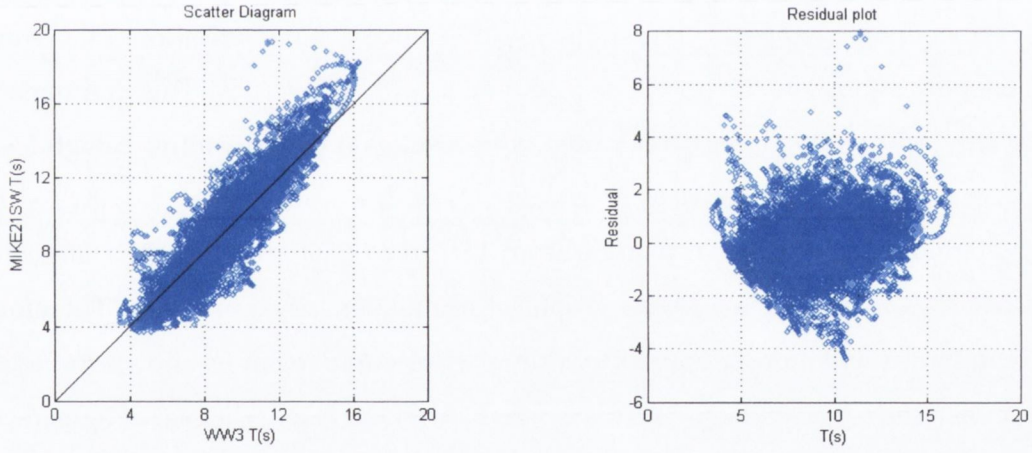

(a) (b)

Figure 4.47 Evaluation plots: T_e (s) from MIKE21SW vs. T_e (m) from WW3 model. Location: 52.766°N, 9.579°W. Time span: Jan 2004 - Jan 2006. (a) Scatter diagram, (b) Residual plot

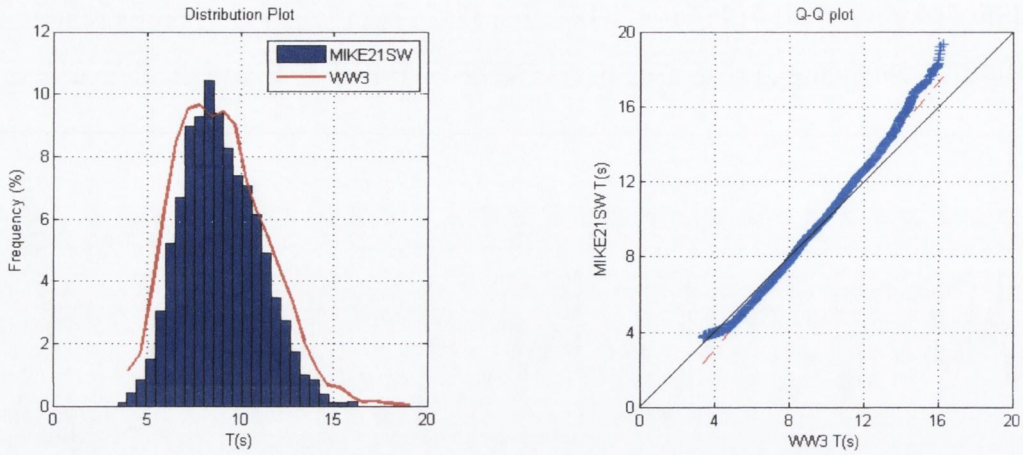

(a) (b)

Figure 4.48 Evaluation plots: T_e (m) from MIKE 21 SW vs. T_e (m) from WW3 model. Location: 52.766°N, 9.579°W. Time span: Jan 2004 - Jan 2006. (a) Frequency distribution comparison, (b) Quantile-Quantile plot.

4.7.2.3 Wave Directionality

This study also facilitated a comparison study on mean wave direction (MWD). It will be seen in Chapter 5 Wave Energy Resource Characterisation that wave directionality is presented via wave roses for a number of sites. This comparison study reduced the uncertainty associated with results on directionality. A high level of agreement was found between both data sets with a scatter index of 0.09. As the range of values for directionality jump from 1 degree to 360 degrees, this parameter does not lend itself to many of the graphical techniques for comparison. Therefore, the visual representation is limited to a time series comparison as shown in Figure 4.49 below. The units are degrees. It is evident that there is a high level of agreement between the two data sets.

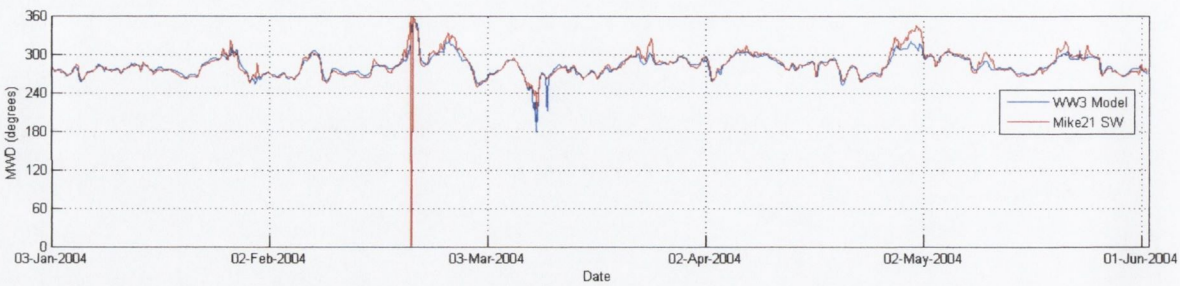

Figure 4.49 Evaluation plots: Mean wave direction (deg) from MIKE 21 SW vs. mean wave direction (deg) from WW3 model. Location 52.766°N, 9.579°W. Time span: Jan - June 2004.

4.8 Model Uncertainty

Although the aforementioned assessments of data quality and model accuracy allow a level of confidence to be placed in model outputs, there is a level of inherent uncertainty due to the number of years of wave climate simulation. This is known as aleatory uncertainty and is associated with the variability of the wave climate from year to year. It stems from the fact that the period chosen for analysis may not be fully representative of the long-term prevailing wave climate off County Clare.

It will be seen in Chapter 5 that the region is characterised using a number of graphical techniques which denote the percentage occurrence of each sea state, annual average wave power, monthly wave power, exploitable wave power and directionality. These are all based on 4 years of simulation (2004 - 2008) due to the data available to this study. This corresponds to approximately 35 000 values for each parameter. However, the IEC standards recommend a 10 year simulation for a wave energy test site. An insight to the difference between the aleotory uncertainty for 5 and 10 year is presented in Figure 2.6. This is seen as a limitation and should be acknowledged in Chapter 5 Wave Energy Resource Characterisation.

4.9 Summary

In this chapter the spectral wave modelling methodology used in this project was presented. The wave and bathymetric data sources used to develop the spectral wave model for the Loop Head region were described with reference to standards for wave energy resource assessment. The development, calibration and validation of a 3rd generation spectral wave model for the Loop Head region was described. This model was essential for achieving the first aim of the research programme which was to characterise the wave climate for a domain off the coast of County Clare adjacent to Loop Head, as this is an area of interest for ocean energy development in Ireland, as will be shown in the next chapter.

Chapter 5
WAVE ENERGY RESOURCE CHARACTERISATION

This chapter will focus on the characterisation of the wave energy resource in the Country Clare domain, with a focus on the Loop Head region. The selection of this area has been described in Chapter 3. This chapter is concerned with the first aim of the research programme which was to characterise the wave climate for a domain off the coast of County Clare adjacent to Loop Head, as this is an area of interest for ocean energy development in Ireland. The spectral wave model described in Chapter 4 is used to investigate the wave energy resource at off-shore, near-shore and shoreline locations in the Clare Domain. Potential SOWC wave energy converter sites described in Chapter 3 (Arch Point and the tip of Loop Head) are analysed in further detail. For these regions, results will be presented for a number of wave characteristics including annual mean omnidirectional power, exploitable power, annual mean significant wave height, annual mean energy period, maximum wave height, wave direction and percentage occurrence of each sea state.

Characterisation of the resource is based on hourly data generated from 4 year simulations, corresponding to 35,000 values for each parameter at each data extraction point. Results are presented using several graphical methods including bar charts, time series graphs, scatter plots and wave roses. Percentage occurrence of each sea state is presented using scatter diagrams. The scatter diagrams for potential SOWC sites are used in Chapter 7 to estimate the mean annual absorbed power and capture width ratio for a range of SOWC wave energy converter designs.

5.1 INTRODUCTION

Using the spectral wave model described in Chapter 4, this chapter aims to address the following objectives:

- To assess wave power levels off the County Clare coast from off-shore to near-shore and on-shore domains (for the purpose of this thesis, this area is referred to as the 'Clare Domain')
- To determine the wave climate characteristics in regions adjacent to Arch Point and Loop Head extending from depths of approximately 80 m to the cliff base
- To establish the percentage of occurrence of each sea state at locations in the off-shore, near-shore and on-shore areas of the Clare Domain
- To establish the percentage of occurrence of each sea state at specific SOWC sites (Arch Point and the tip of Loop Head).

Firstly the annual wave energy resource results will be presented in relation to the wider area under study i.e. for the whole Clare domain. The issue of extreme seas and the related topic of exploitable wave resource, as opposed to total wave energy resource are then discussed. Then findings will be presented for the two relevant areas of interest located off the tip of Loop Head and off Arch point. Results will include information on the wave energy resource, significant wave height, wave energy period and wave directionality. The percentage occurrence, over a year, of each possible combination of wave height and wave period (i.e. each sea state), is presented as scatter diagrams for a range of different depth contours. Additionally, wave directionality is investigated.

All results are based on the spectral wave model set-up described in Chapter 4. With the high resolution mesh circumscribing the Clare Domain, 4 year simulations took approximately 4 months of computational time running on four high performance eight core processors (3.5 GHz). Each graph is based on hourly data for the given parameter over that period.

5.2 CLARE DOMAIN

5.2.1 Wave Power Levels: Off-shore to On-shore

This section investigates the wave energy resource for off-shore, near-shore and on-shore locations. This facilitates an insight to the characteristic wave power level for each domain in the County Clare Domain.

Omnidirectional wave power values were extracted from off-shore, near-shore and on-shore locations leading from 100 m depth contour west of Arch point to the coast. (Omnidirectional wave power is defined by Equation 2.8 in Section 2.5.1). The data was extracted at locations as close to the validation point as possible. Omnidirectional wave power was output from the spectral wave model at hourly intervals over the 4 year simulation period. This corresponds to approximately 35 000 values for omnidirectional wave power at each depth contour. From this the average omnidirectional wave power was calculated for each contour. A bar chart outlining annual average wave power at specific water depth contours is presented in Figure 5.1. Figure 5.2 exhibits a polychromatic bathymetric chart detailing water depth contours corresponding to the bar chart.

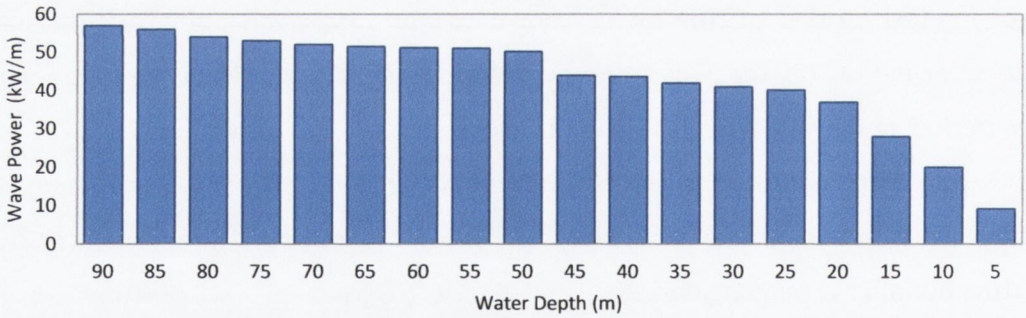

Figure 5.1 Annual average wave power (kW/m) at specific water depth contours (m) at Loop Head.

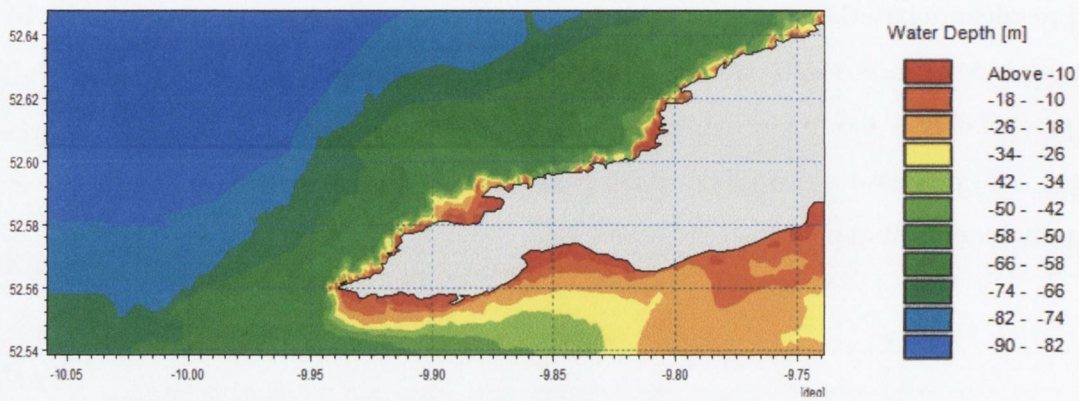

Figure 5.2 Polychromatic bathymetric chart detailing water depth contours at Loop Head.

First, considering the reduction in wave power from the 20 m depth contour to the 5 m depth contour, it is evident that the level of wave power reduces from 35 kW/m to approximately 10 kW/m. This is due to a number of processes that affect the wave field as it approaches the coast including depth induced friction, depth induced wave breaking, triad interaction and refraction.

As waves propagate from deep water to shallow water, the properties of the wave become affected by the seabed. The orbital motion of the water particles extends approximately half a wave length below the still water level. In water depths less than half a wave length, the orbital motion of water particles in contact with the seabed are subjected to friction. This decreases the wave celerity and causes wave energy dissipation. The rate of dissipation due to bottom friction is given by Equation 5.1.

$$S_{bot}(f,\theta) = -(C_f + f_c(\bar{u}\cdot\bar{k})/k)\frac{k}{sin2kd}E(f,\theta) \tag{5.1}$$

Where k is the wave number, C_f is a friction coefficient, f_c is the friction coefficient for current, u is the current velocity and d is water depth, f is the wave frequency, θ is the wave direction and $E(f,\theta)$ is the wave energy at wave direction θ. The friction coefficient, C_f, accounts for the in change in orbital velocity at the seabed, where u_b is the root mean square wave orbital velocity given by Equation 5.2.

$$u_b = \left[2\int_{f_1}^{f_{max}}\int_{\theta}\frac{\bar{\sigma}^2}{\sinh^2 kd}E(f,\theta)d\theta df\right]^{\frac{1}{2}} \tag{5.2}$$

Where σ is the orbital frequency. Both Equations 5.1 and 5.2 were employed in the 3rd generation spectral wave model used to model the wave climate off Loop Head. At a certain depth, the orbital particles affected by the seabed cause a kinematic instability within the wave. As the fluid velocity at the crest exceeds the wave speed, the crest curls and breaks, injecting fluid at the surface. The 3rd generation spectral wave model employs the established Battjes and Janssen (1978) formulation for wave breaking, described by Equation 5.3.

$$S_{surf}(f,\theta) = -\frac{2\alpha_{BJ}Q_b\bar{f}}{X}E(f,\theta) \tag{5.3}$$

Where Q_b is the fraction of breaking waves, X is the ratio of the total energy in the random wave train to the energy in a wave train with the maximum possible wave height, $\bar{f}$ is the mean frequency and $\alpha_{BJ} \approx 1$ is a calibration constant.

Due to these physical effects on the wave field, considerable levels of wave power are expelled as water depth decreases. Thus seabed friction is the major source of incident wave power reduction at near-shore and on-shore sites. This highlights the importance of installing the SOWC chamber at locations with water depths equal to or greater than 15 m. An exposure to the greater resource permits smaller chamber designs to achieve a given target power capacity.

Considering the reduction in wave power from the 50 m depth contour (55 kW/m) to the 20 m depth contour (35 kW/m) in Figure 5.1, this is due in part to the location at which data was extracted. As measurements were taken from the region of the waverider buoy on the north coast of Loop Head, locations close to shore were affected by sheltering from the headland for certain wave directions. When waves approach from 150 degrees to 225 degrees, the headland itself shelters the near-shore and coastal locations. This contributes to the decline in wave power evident in the bar chart from 50 m contour shoreward.

Between the 50 m contour and the 80 m contour, effects due to sheltering are weakened. For the region around the validation point, the wave power level remains at approximately 53 kW/m.

Extending from the 80 m contour off-shore, the wave power level remains relatively constant. The seabed does not influence the wave field and the region is exposed to waves approaching from all directions. Overall, based on wave power values extracted from a number of off shore locations in the County Clare domain, the mean annual wave power value was estimated as approximately 58 kW/m.

5.2.2 Extreme Sea States

Although locations that possess high levels of wave power are favourable for annual WEC performance, the extreme sea states associated with these regions directly affect the survivability of a given WEC. Results drawn from this work are shown in Figure 5.3 and 5.4. Figure 5.3 presents significant wave height (H_s) and maximum wave height (H_{max}) at hourly intervals for four years at a potential SOWC site with a water depth of 17 m. Figure 5.4 presents concurrent data at a deep water location (55 m depth contour) directly off-shore from the 17 m deep location to highlight the transformation of extreme sea states as they approach the coast.

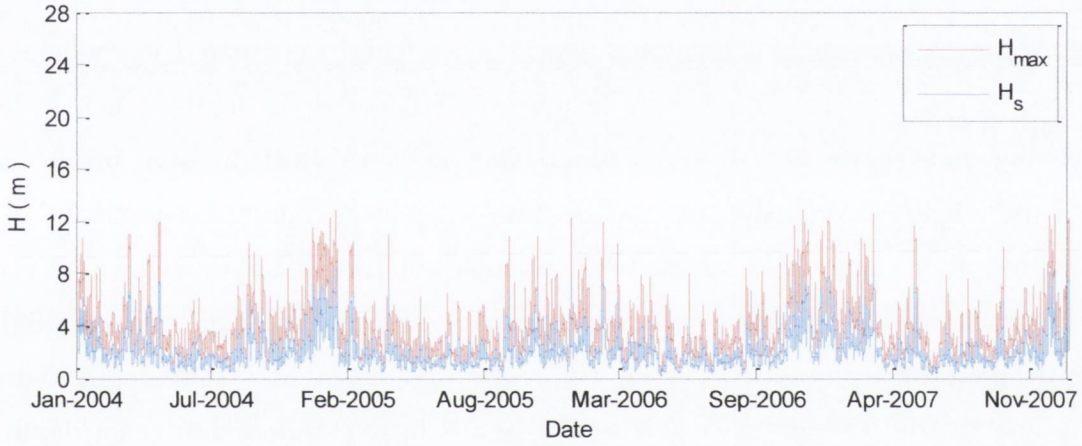

Figure 5.3. Time series data (2004-2008) for significant wave height (H_s) and maximum wave height (H_{max}) at Arch Point, Co. Clare. Water depth = 17m.

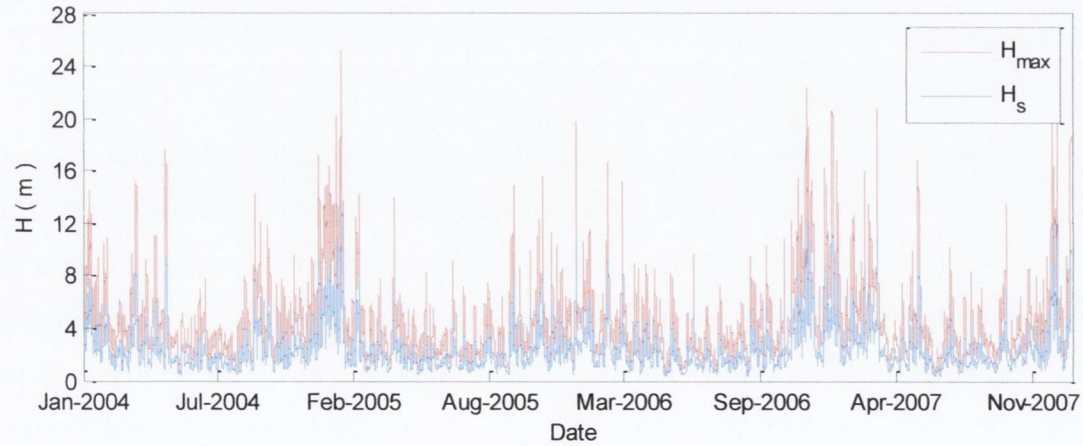

Figure 5.4. Time series data (2004-2008) for significant wave height (H_s) and maximum wave height (H_{max}) off Arch Point, Co. Clare. Water depth = 55m.

In Figure 5.3 it can be seen that over the four year duration significant wave height (blue line) reaches 8 m a number of times. However, as significant wave height is defined as the highest one third of waves, it does not represent the most extreme

loads that may have been imposed upon the cliff face. Therefore, the parameter maximum wave height is of considerable practical importance as it defines the ultimate limit state (ULS) for SOWC chamber designs to withstand. It can be seen that the maximum wave height (red line) extends above 12 m a number of times. It can also be seen that there is a direct relationship between significant wave height and maximum wave height. However, this relationship alters depending on the water depth at the potential SOWC site. For a given wave form in a given depth, there is a maximum height beyond which the wave will break, via the processes described in the previous section.

As extreme waves generally possess longer wave lengths compared to moderate waves, they experience friction from the seabed at greater water depths. Thus, wave breaking takes place at deeper contours. The point at which a wave breaks is influenced by the relationship, or ratio, between wave height and water depth. In line with this, near-shore and shoreline locations filter out exceptionally large waves via depth induced wave breaking. Formative oceanographic research dating back to 1891 has detailed the relationship between maximum wave height and water depth. With H_b denoting the trough to crest breaking wave height and d the water depth, estimates for H_b/d range between 0.78 and 0.87, with 0.78 taken as typical (Chappelear, 1959; Lenau, 1966; Longuet-Higgins, 1974; McCowan, 1891). Hence, depth induced breaking occurs when the wave height is more than circa 0.78 times the water depth.

On reviewing the results for wave height at 55 m water depth, it is apparent that large storm waves can maintain a form that facilitates exceptional wave heights. In Figure 5.4 it can be seen that maximum wave heights reach almost twice the height of corresponding waves at the site with 17 m in Figure 5.3. However, from reviewing the two figures it can be seen that as the wave regime propagates from the 55 m contour to the 17 m contour, waves above a certain size become affected by the seabed. In line with this, near-shore and shoreline locations filter out exceptionally large waves via depth induced wave breaking. To characterise the filtering of exceptionally large waves from the wave climate as the wave field approaches the coast, the H_{max}/H_s ratio was examined at a number of water depth contours leading to the 17 m deep site. The H_{max}/H_s ratio is often known as the Abnormality Index (AI).

This parameter is used in the study of rogue waves which are defined as events with AI values greater than 2 (Guedes Soares et al., 2003).

H_{max} and H_s values were extracted from the SW model at a number of depth contours ranging from 89 m deep to 17 m deep. Specifically, they were extracted from the region within the model which possesses high resolution bathymetric data. Values were recorded at hourly intervals over a four year period, 2004 - 2008.
Using this data, the H_{max}/H_s ratio was plotted against its corresponding H_s value at each water depth contour. As the wave data at each contour was sourced from the 3rd generation spectral wave model of the Loop Head region, it should be noted that certain mathematical assumptions reduce the scatter of the H_{max}/H_s ratio. Fundamentally, the 3rd generation spectral wave model used in this study defines the relationship between significant wave height and maximum wave height in deep water, as that shown in Equation 5.4.

$$H_{max} = H_s \sqrt{\frac{1}{2} lnN} \tag{5.4}$$

Where N is the number of waves estimated as $N = duration/mean\ wave\ period$. In DHI's Mike 21 spectral wave model, duration is set to 3 hours. For a typical storm with a duration of 3 hours a mean period of 10 seconds, 1000 waves occur. MIKE 21 SW calculates the maximum wave height by assuming Rayleigh distributed waves. This assumption is one that is rooted in observation. In a series of papers Longuet-Higgins (1952, 1963, 1975, 1980) has shown that the wave amplitudes in any given record will be Rayleigh distributed. The Rayleigh distribution is a continuous probability distribution for positive-valued random variables and allows estimates to made on the probability that the wave amplitude will reach a certain threshold value in a given storm (Journée and Massie, 2001). Despite these mathematical assumptions, plotting the H_{max}/H_s ratio against significant wave height still provides an important insight into the affect water depth has on extreme sea states.

Figure 5.5 presents density scatter plots of H_{max}/H_s ratio versus significant wave height at the 55 m, 28 m, 22 m and 17 m water depth contours. Bright red areas of the scatter plot denote a high density of data points. Hence, the majority of sea states

possess a significant wave height ranging from 0.5 m to 4 m. Specifically, based on the results from the SW model for each location, approximately 95% sea states possess a significant wave height between 0.5 m and 4 m. Thus, extreme seas states with a significant wave height greater than 4 m occurred circa 5% each year.

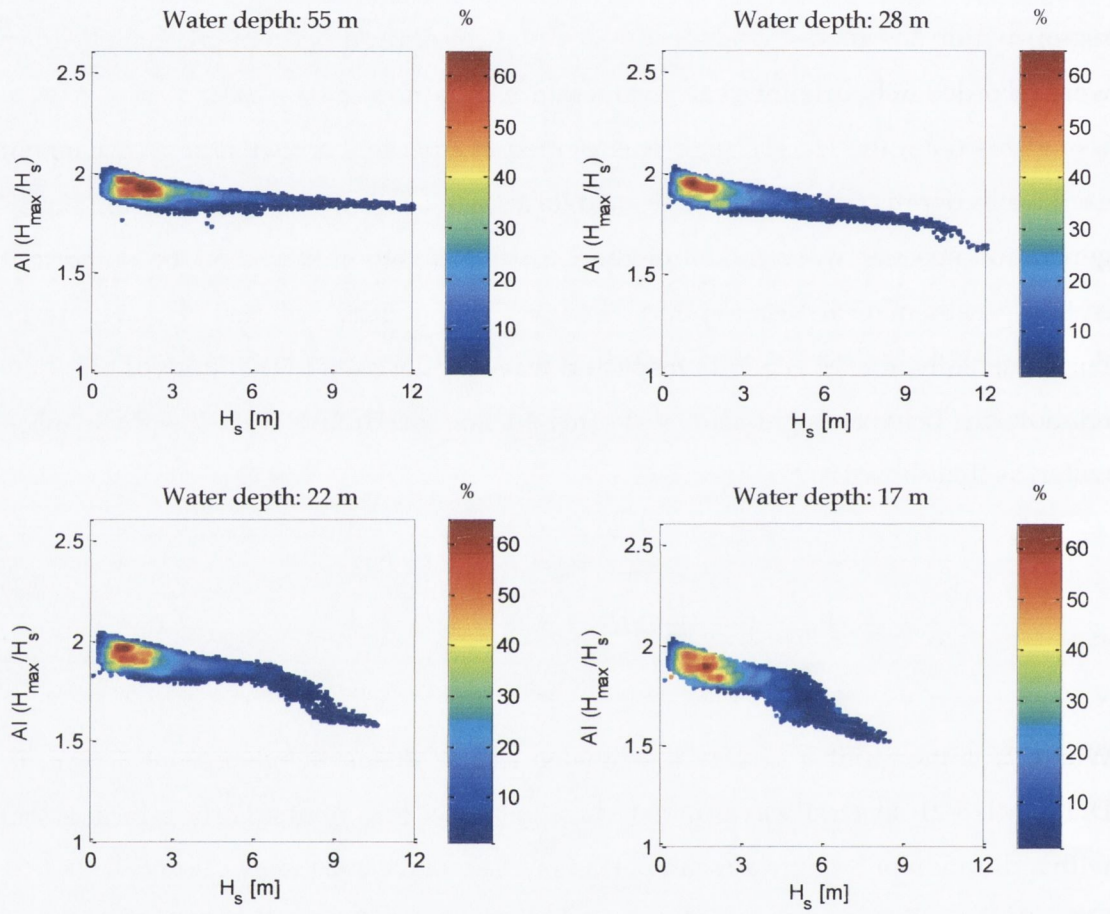

Figure 5.5. Relationship between H_{max} and H_s at 55 m, 28 m, 22 m and 17 m water depth contour. Location: Arch Point, Co. Clare. Time Period: 2004 - 2008. Colour bar denotes data density (%).

At the 55 m depth contour, it can be seen that the H_{max}/H_s ratio is relatively constant, ranging from 1.8 to 2. In this case the water depth has a minimal effect on the maximum wave height. As such, the H_{max}/H_s ratio adheres to Equation 5.4 and there is a continual relationship between significant wave height and maximum wave height for the entire range of sea states experienced at this location. At the 28 m depth contour, the H_{max}/H_s ratio decreases slightly for waves with a significant wave height greater than 10 m. Hence, when the wave field has a significant wave height beyond this value, the highest theoretical waves in that wave field begin to break due to the influence of the sea bed. Although this extreme sea state is rare, it provides evidence that filtering of extreme waves begins to take place at the 28 m depth

contour. Scatter diagrams outlining the percentage occurrence for this location reveal that 99% of sea states experienced at this water depth possess a significant wave height less than 8.5m. Thus for the most part, the seabed does not affect the wave climate. The same finding can be drawn for water depths ranging from 28 m to 55 m and onwards.

Closer to the coast, at 22 m depth contour, the H_{max}/H_s ratio begins to decrease when the wave field has a significant wave height greater than 7 m. The exact wave height may not be defined, as wave breaking is also dependent on wave period and wave length. However in Figure 5.5, the graph corresponding to the 22 m depth contour shows a noticeable decrease in H_{max}/H_s ratio at 7 m, signifying the influence of the seabed on extreme waves. The reduction in the H_{max}/H_s ratio relates directly to the reduction in maximum wave height. Thus, filtering of extreme waves is increased at the 22 m depth contour.

At the 17 m deep site, the filtering of extreme waves is extended to sea states that possess a significant wave height greater 4 m, as shown in the corresponding graph in Figure 5.5. Further evidence of this is revealed when comparing the time series graphs of maximum wave height at the 17 m depth contour (Figure 5.3) and the 55 m depth contour (Figure 5.4). It can be seen that the maximum wave height is significantly reduced at the 17 m deep site. Thus, considerable filtering of extreme waves has taken place.

5.2.3 Exploitable Wave Energy Resource

A main contributor in the decline of near-shore and shoreline wave power values is due to depth induced breaking, which curtails the wave heights of a certain height. The decline in wave power at sites with water depths less than 20 m in comparison to off-shore locations can be attributed in part to these curtailed large waves. Regarding wave energy conversion, wave heights over a certain size cannot be safely converted to electricity. Similar to cut-out speed for wind turbines, where the wind speed reaches a level that puts the turbine under risk of structural or mechanical failure, a given wave energy converter possess a cut-out wave condition. As a wind turbine design possesses a survival mode in addition to an operational mode, so does a wave energy converter. When a wave energy converter switches to survival model,

electricity generation is postponed to operational conditions. Hence, wave power levels associated with extreme seas may not be exploited for wave energy conversion. By this token, the lower power levels at 15 m water depth contours are not directly proportional to wave power levels usable for wave power conversion. This has been termed by the 'Accessible Wave Energy Resource Atlas' (McCullen, 2005) as the technical resource. The technical resource relates to sea states that can be used by a given wave energy converter for power generation. Power matrices outlining the sea states for WEC operation have been developed for the leading wave energy technologies. Depending on the type of wave energy converter, operational conditions correspond to sea states with a significant wave height ranging from 0.5 m to 10 m and beyond in some cases. As the second aim of this research programme is dedicated to a fixed SOWC type wave energy converter, its operational conditions are used to define the range of significant wave heights associated with power generation. It will be seen in Chapter 6 SOWC Wave Energy Converter Design that operational conditions in this study correspond to sea states with a significant wave height ranging from 0.5 m to 6.5 m. This range of sea states can be termed exploitable sea states and relate to usable wave power levels. It will be seen in the next section on extreme sea states, when comparing wave heights at deep water contours and the 17 m contour, there is relatively small change for exploitable sea states in comparison to extreme sea states. Regarding wave power levels, a similar trend was identified.

5.2.3.1 Exploitable Power Levels: Off-shore to On-shore

Considering average annual wave power levels at different depth contours leading to the coast, presented in Figure 5.1, an investigation was carried out on the average annual wave power levels based on operational sea states. Using the four year data set of hourly omnidirectional power for depth contours ranging from 90m to 5m, average power levels were calculated based on sea states with a significant wave height ranging from 0.5m to 6.5m. Power levels associated with significant wave heights greater than 6.5m were disregarded when calculating the average power level at a given contour. The average power level for each contour, based on sea states with a significant wave height ranging from 0.5m to 6.5m, are presented as red bars in Figure 5.6 Corresponding annual average wave power values, previously displayed in Figure 5.1 are presented as blue bars to highlight the difference in average wave power values.

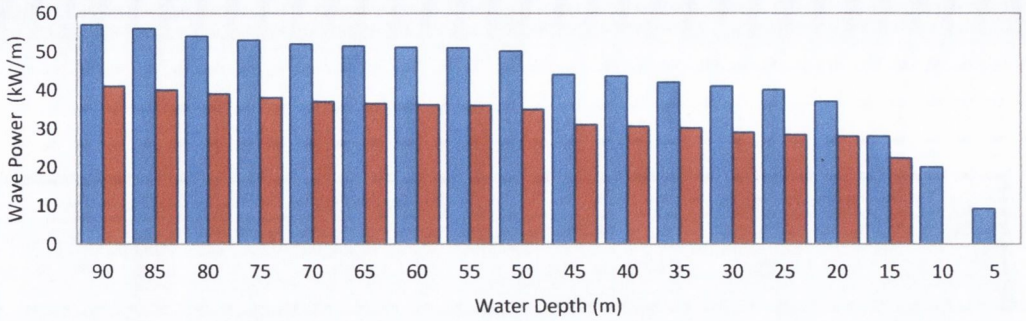

Figure 5.6. Annual average wave power (kW/m) (blue bars) and annual average wave power (kW/m) based on operational sea states (red bars) at specific water depth contours (m) at Loop Head.

The difference between the annual average wave power and annual average wave power based on operational sea states is the wave power associated with extreme sea states. Although sea states with a significant wave height greater than 6.5 m occur less than 5% of the time, their powerful nature attributes more than 15% of the annual average wave power in some cases. As depth induced breaking filters out extreme waves, the proportion of the annual average wave power related to waves greater than 6.5 m reduces at depth contours less than 20 m. For example, it can be calculated that as depth reduces from 50 m to 20 m, the reduction in average annual wave power reduces by approximately 27 % whereas the exploitable resource reduces by 16%. Hence from a wave energy conversion standpoint, the wave power levels associated with operational sea states provide a better comparison power levels at each depth contour. Additionally, it delivers a more accurate portrayal of the exploitable wave energy resource which is beneficial to project developers, investors, etc. This section on exploitable resource associated with operational sea states aimed to supplement the previous sections on overall wave energy resource for the County Clare domain. Additionally, it provides an insight to the level of wave power at depths associated with potential SOWC sites at Arch Point and the tip of Loop Head.

5.3 AREAS OF INTEREST

Results pertaining to two specific areas within the County Clare Domain are now presented. The two specific areas are Arch Point and the tip of Loop Head. Both possess potential SOWC wave energy converter sites. The areas in question, plus relevant depth contours, are shown in the Figure 5.3 below. For both regions, data was extracted from specific points in the off-shore, near-shore and on-shore domains.

The longitude and latitude co-ordinates of these points in the Arch Point region are presented in Table 5.1 and those for the tip of Loop Head in Table 5.2. Each is labelled according to its location and depth.

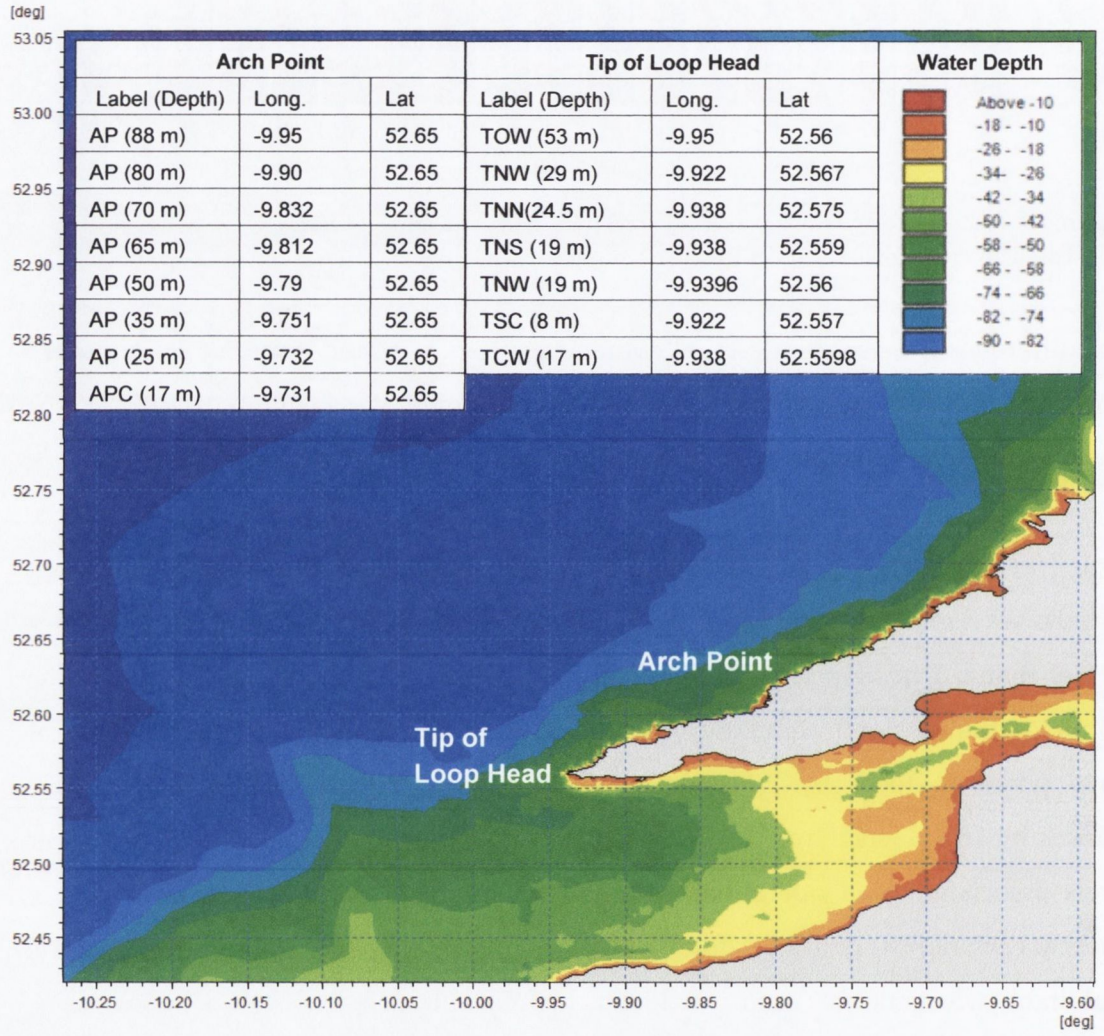

Arch Point		
Label (Depth)	Long.	Lat
AP (88 m)	-9.95	52.65
AP (80 m)	-9.90	52.65
AP (70 m)	-9.832	52.65
AP (65 m)	-9.812	52.65
AP (50 m)	-9.79	52.65
AP (35 m)	-9.751	52.65
AP (25 m)	-9.732	52.65
APC (17 m)	-9.731	52.65

Tip of Loop Head		
Label (Depth)	Long.	Lat
TOW (53 m)	-9.95	52.56
TNW (29 m)	-9.922	52.567
TNN(24.5 m)	-9.938	52.575
TNS (19 m)	-9.938	52.559
TNW (19 m)	-9.9396	52.56
TSC (8 m)	-9.922	52.557
TCW (17 m)	-9.938	52.5598

Figure 5.7. Areas of interest within Clare Domain: Arch Point and the tip of Loop Head. Each table presents the name, location and depth of each data extraction point.

Data extraction points located at depths greater than 50 m lie in the off-shore domain. Thus, the following points are in the off-shore domain: AP (88 m), AP (80 m), AP (70 m), AP (65 m), AP (50 m), TOW (53 m). Points between water depths of 50 m and 20 m lie in the near-shore domain: AP (35 m), AP (25 m), TNW (29 m), TNN (24.5 m), TNS (19 m) and TNW (19 m). The two potential SOWC sites are located at on-shore locations: APC (17 m) and TCW (17 m). It should be noted that the range of depths associated with the each domain are based on the prevailing wave conditions for the North Atlantic.

5.3.1 Arch Point

For each off-shore, near-shore and on-shore location, key parameters recommended by the IEC standards (Folley et al., 2013) were calculated. These were mean annual values for wave power, significant wave height and energy period. Also, maximum significant wave height and maximum measured wave height were retrieved from each 4 year data set. These values were directly output from MIKE 21 SW. Additionally, mean annual exploitable wave power was determined. This was based on previously mentioned range of sea states corresponding to SOWC operational conditions for power generation. These are presented in Table 5.3. Data extracted from AP (88 m) to APC (17 m) lead from off-shore to on-shore along a straight line with Latitude of 52.65 degrees.

Table 5.3 Arch Point: Summary parameters for off-shore, near-shore and on-shore locations

Location (Depth)	AP (88 m)	AP (80m)	AP (70 m)	AP (65 m)	AP (50 m)	AP (35 m)	AP (25 m)	APC (17 m)
Longitude (deg)	-9.95	-9.90	-9.832	-9.812	-9.79	-9.751	-9.732	-9.731
Latitude (deg)	52.65	52.65	52.65	52.65	52.65	52.65	52.65	52.65
Depth (m)	88	80	70	65	50	35	25	17
Annual mean P_{wave} (kW/m)	57	56	54	52	47	43	36	30
Annual mean exploitable P_{wave} (kW/m)	41	40	39	37	34	30	25	25
Annual mean H_s (m)	2.67	2.65	2.60	2.52	2.37	2.34	2.23	1.995
Annual mean T_e (s)	8.79	8.82	8.85	8.89	8.92	8.93	9.02	9.59
Maximum H_s (m)	14.86	14.87	14.67	14.27	14.09	13.87	11.81	8.45
Max Wave Height H_{max} (m)	27.03	27.02	26.68	25.96	25.60	25.21	24.24	12.9

Regarding wave power levels for off-shore, near-shore and on-shore locations, a similar trend to that previously described can be seen. The wave power levels reduce in the near-shore and on-shore domains. This is due to the filtering of high waves which is supported by values for annual mean significant wave height.

5.3.1.1 Percentage Occurrence of Each Sea-state

The percentage occurrence per year of each possible combination of wave height and energy period was computed for locations corresponding to Table 5.3. These are presented as scatter diagrams in Figure 5.8 below.

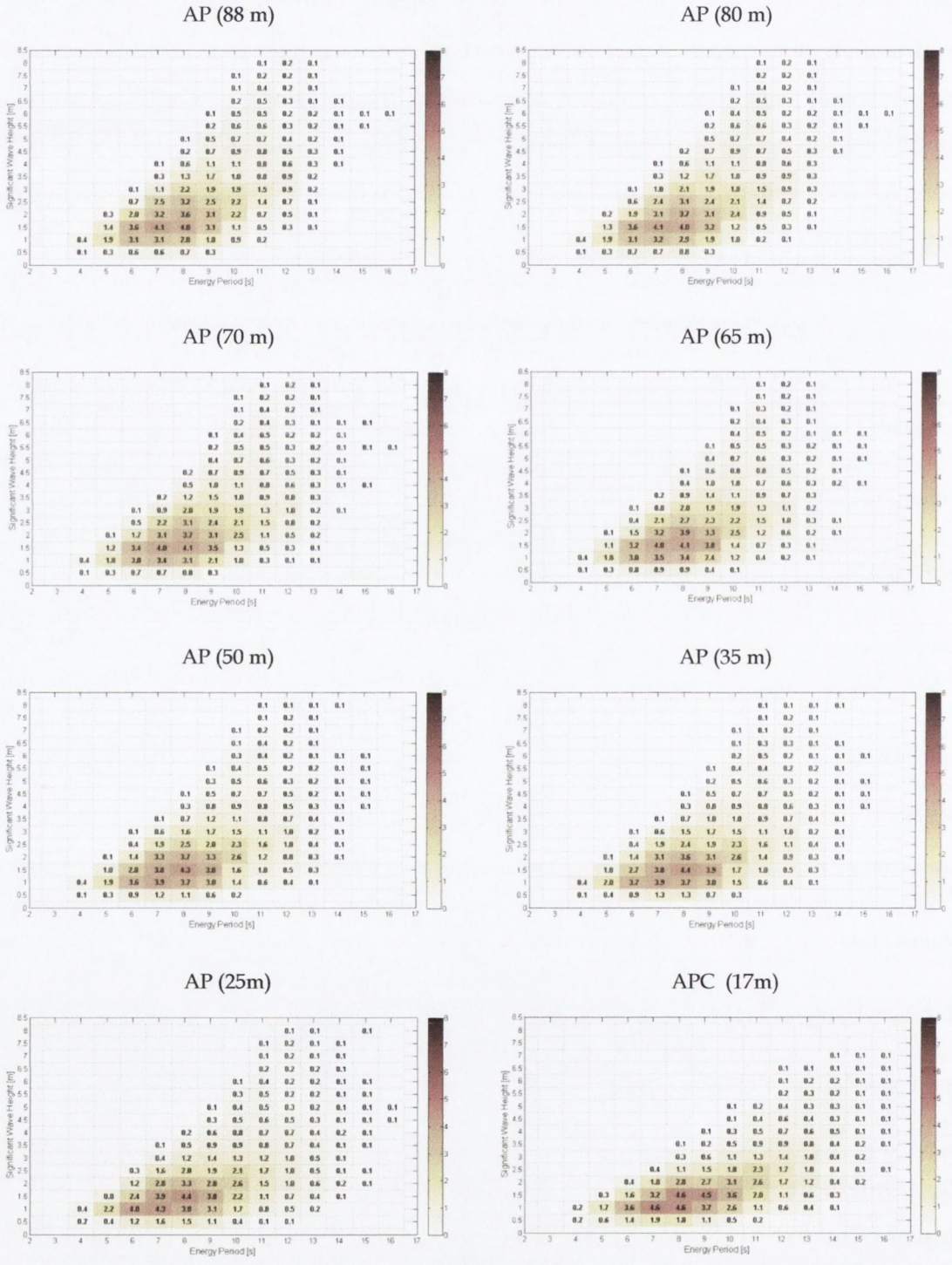

Figure 5.8 Scatter diagrams (Hs, Te) different depth contours at Arch Point, leading to the coast.

The effect of extreme wave filtering appears in the scatter diagrams as a reduction in the occurrence of large waves coupled with an increase in less extreme waves. Additionally, for the on-shore site, APC (17 m), an increase in the percentage occurrence of moderate sea states is evident. This denotes wave regimes with significant wave heights less than 3 m. Regarding the application of these scatter diagrams to wave energy converter designs, it can be seen that the most commonly occurring energy period ranges between 6 s and 9 s. However, depending on the resonant nature of the wave energy converter under design, it is important to consider the high levels of power associated beyond 9 s.

5.3.1.2 Directionality

The following wave rose diagrams portray information regarding wave directionality at the points in question. The overall percentage occurrence of each wave direction may be inferred from the length of the segment in the given diagram with the percentage bar.

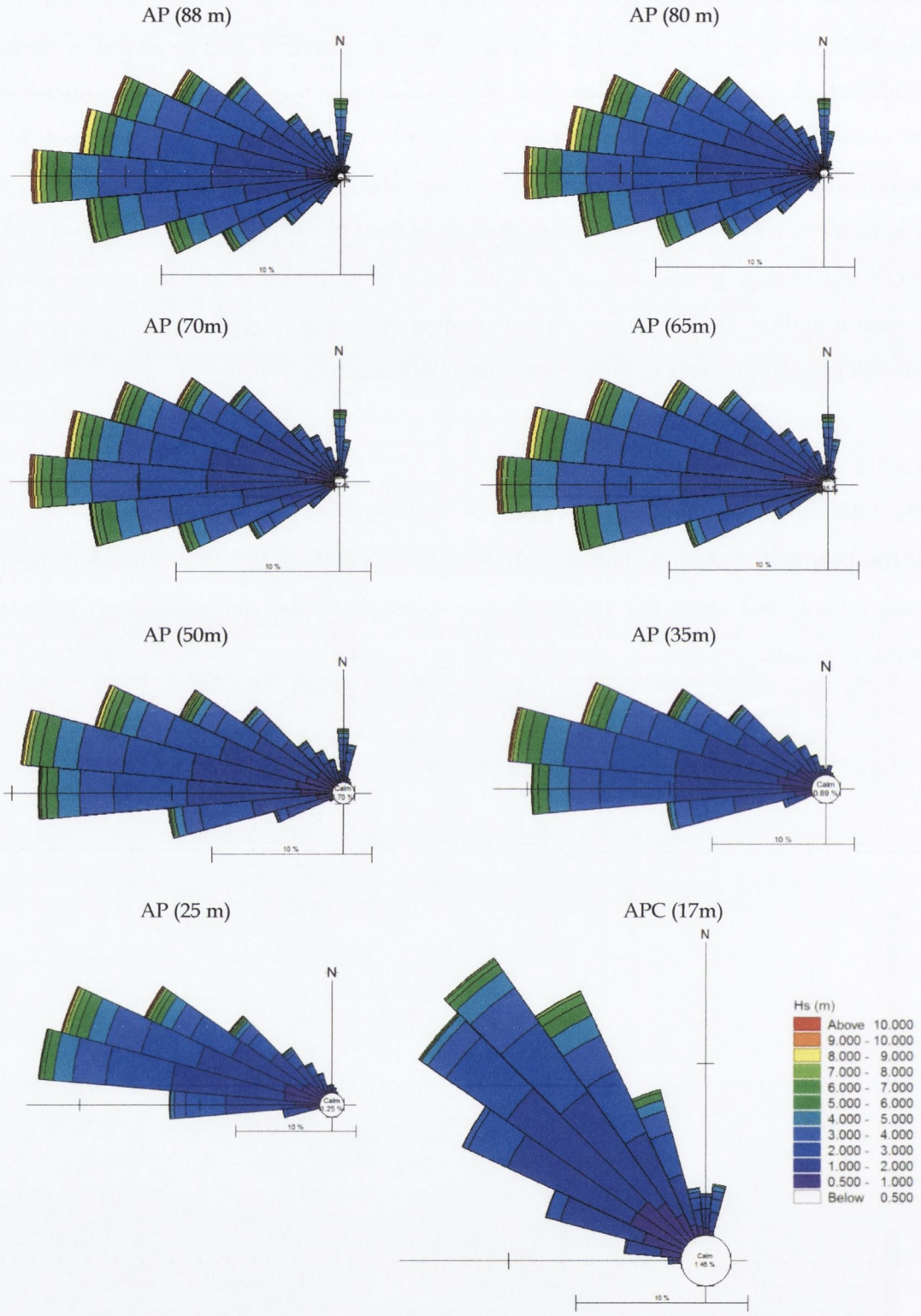

Figure 5.9 Wave roses (H_s, MWD) different depth contours at Arch Point, leading to the coast.

The effect of wave refraction is highlighted in the above wave roses. As the wave field propagates to shallower waters, the influence of the sea bed causes the wave to refract and align parallel with the depth contours. Thus, the directional spread of the

wave field at near-shore and on-shore locations is narrowed. This is shown by the wider range of direction portrayed in wave roses for deep water locations compared with the narrow range at APC (17 m). The predominant wave direction at APC (17 m) is north westerly as the waves align with the depth contours leading to the coast at Arch Point.

5.3.2 Tip of Loop Head

Tables and graphs presented for the Arch Point area are now presented for off-shore, near-shore and on-shore locations at the tip of Loop Head.

Table 5.4 Loop Head: Summary parameters for off-shore, near-shore and on-shore locations

Location (Depth)	TOW (53 m)	TNW (29 m)	TNN (24.5 m)	TNS (19 m)	TNW (19 m)	TCS (8 m)	TCW (17 m)
Longitude (deg)	-9.95	-9.922	-9.938	-9.938	-9.9396	-9.922	-9.938
Latitude (deg)	52.56	52.567	52.575	52.559	52.56	52.557	52.5598
Depth (m)	53	29	24.5	19	19	8	17
Annual mean P_{wave} (kW/m)	51	38	42	37	50	18	47
Annual mean exploitable P_{wave} (kW/m)	37	27	31	28	44	16	34
Annual mean H_s (m)	2.51	2.1	2.28	2.12	2.69	1.76	2.76
Annual mean T_e (s)	8.77	**9.08**	9.13	9.18	9.35	9.72	9.43
Maximum H_s (m)	14.30	11.27	11.83	10.01	12.33	5.33	10.07
Max Wave Height H_{max} (m)	25.98	20.68	18.49	15.13	13.27	7.2	12.07

Unlike the data extracted from the Arch Point area where locations AP (88 m) to APC (17 m) lead from off-shore to on-shore along a straight line, the data extraction points at the tip of Loop Head were position around the Headland. Therefore wave direction affects locations on the north, south and west coasts of the headland

differently. In line with this, the results above are very site specific and do not necessarily reflect a simple relationship related to extreme wave filtering.

5.3.2.1 Percentage Occurrence of Each Sea-state

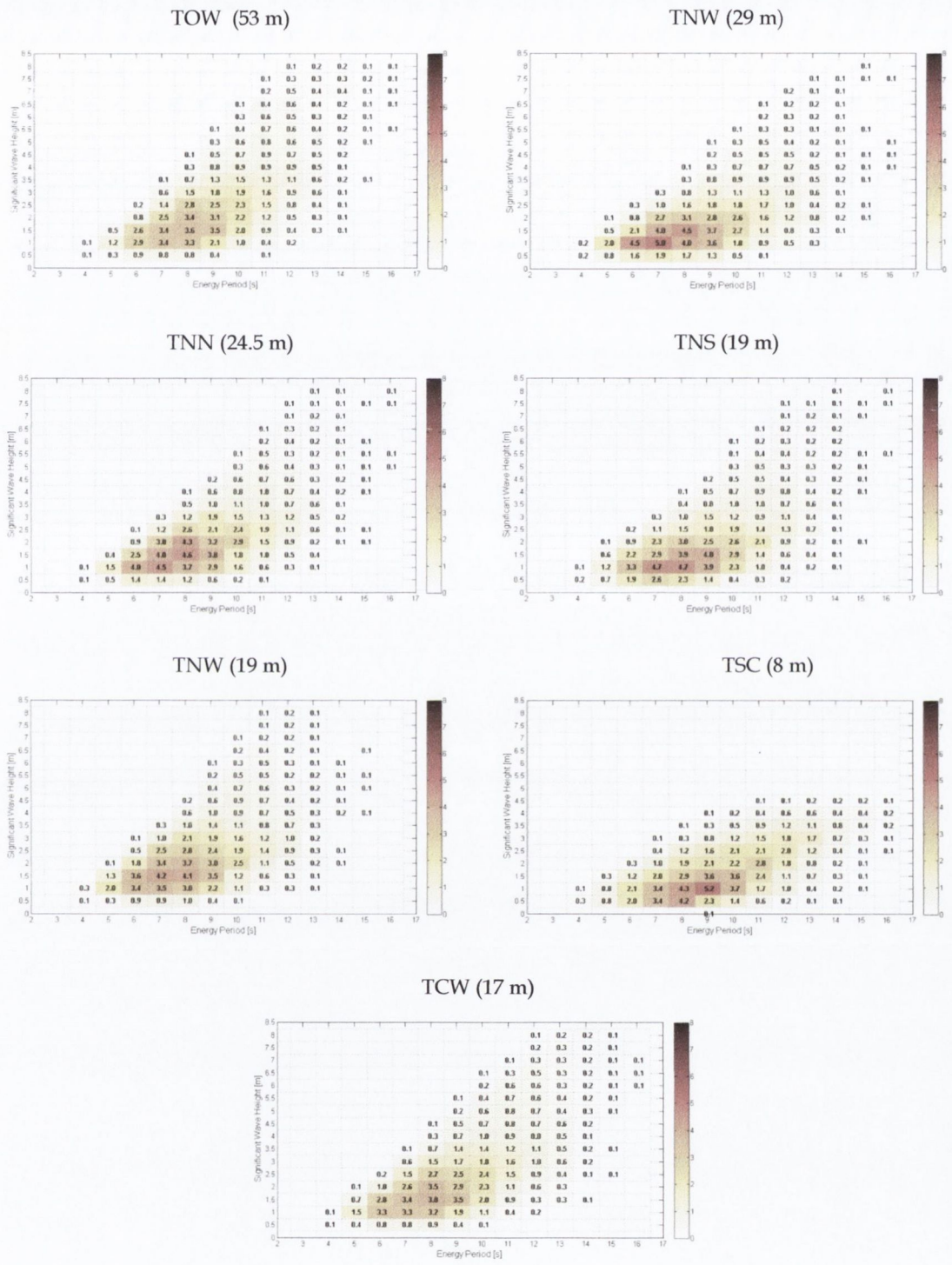

Figure 5.10 Scatter diagrams (H_s, T_e) different depth contours at Tip of Loop Head, leading to the coast.

Overall, the scatter diagrams in Figure 5.10 appear relatively similar apart from TSC (8 m). This location is within the 16 m depth contour which is considered extremely non-linear and the boundary for accurate wave climate modelling using a 3rd generation spectral wave model (Folley et al., 2013). Results from TSC (8 m)

should not be used for wave energy converter design as they are accompanied by a high level of uncertainty. However, all other scatter diagrams clearly identify that the most commonly occurring energy period in this region ranges between 7 s and 8 s. This is valuable information for the design of a resonant wave energy converter.

5.3.2.2 Directionality

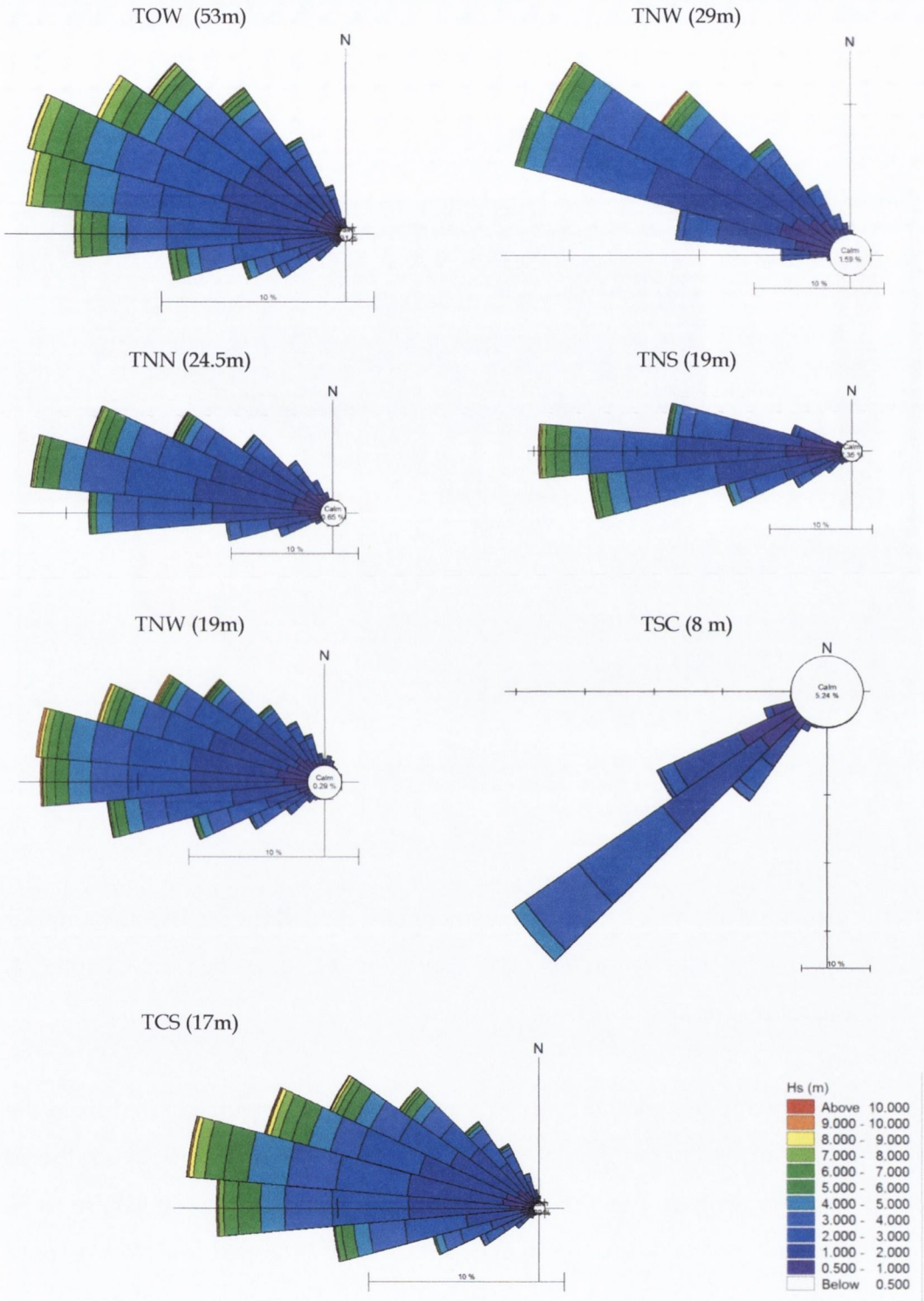

Figure 5.11 Wave Roses (H_s, T_e) different depth contours at the Tip of Loop Head

The characteristic of each of the above wave roses directly corresponds to the orientation of the data extraction point with respect to the tip of the headland. Near-

shore and on-shore locations north of Loop Head are sheltered from southerly waves while locations south of Loop Head are sheltered from northerly waves. This is highlighted when superimposing a selection of wave roses on to a map of the area. This is presented in Figure 5.12 accompanied by characteristics of wave directionality at Arch Point.

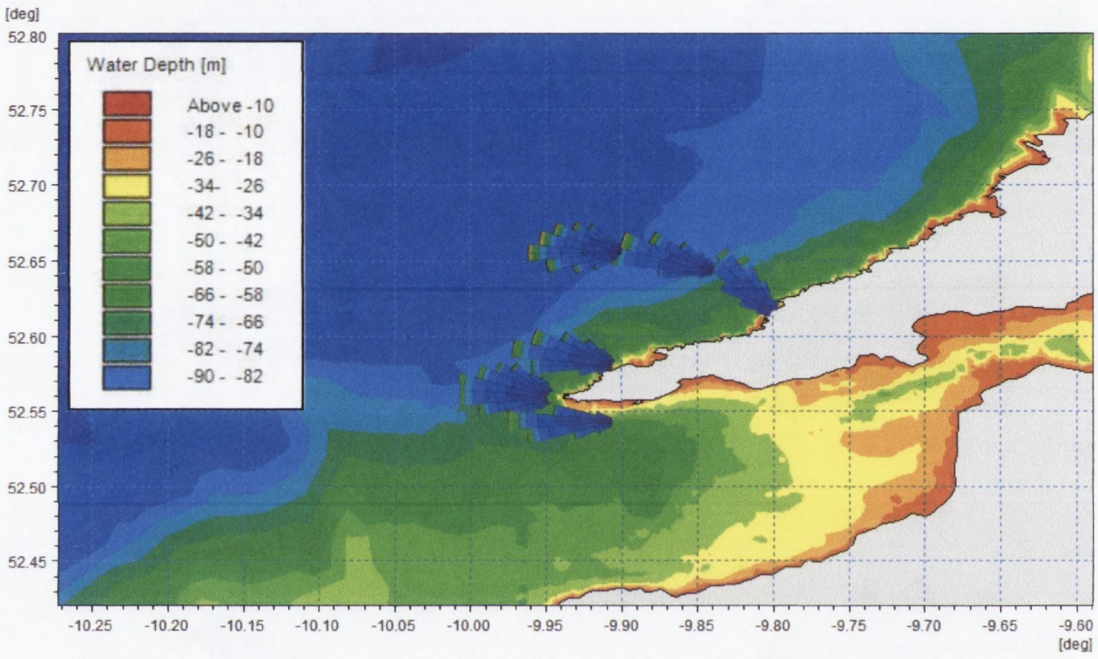

Figure 5.12 Characteristics of wave directionality at Arch Point and the tip of Loop Head.

5.4 SUMMARY

Chapter 5 presented the results of the wave climate modelling for the areas under study. Using the 3rd generation spectral wave model, described in Chapter 4, Chapter 5 addressed specific objectives.

For the Clare Domain, the annual average wave power levels were charted from the 90 m depth contour to 5 m depth contour in decrements of 5 metres. Between the 90 m and 50 m depth contour, the annual average power ranged from 60 kW/m to 50 kW/m. From the 45 m contour to the 20 m depth contour, it ranged from 45 kW/m to 40 kW/m. For the 15 m, 10 m and 5 m contour, average values were 28 kW/m, 20 kW/m and 9 kW/m respectively. (As mentioned in Section 5.3.2.1, it should be noted that the level of uncertainty increases within the 16 m depth contour since it is considered extremely non-linear and thus, is difficult to accurately model).

To put these values in context, the annual average wave power values for the 4 main wave energy test sites in Europe are as follows: 21.8 kW/m at EMEC (Scotland), 14.8 kW/m at SEM-REV (France), 26.9 kW/m at Yeu (France) and 37.5 kW/m at Lisbon (Portugal) (Babarit et al., 2012). Ireland's proposed Atlantic Marine Energy Test Site (AMETS) at Belmullet has an estimated annual average wave power of 80.6 kW/m (Babarit and Hals, 2011). Each of the aforementioned values are based on data sets covering more than 10 years. Although this study was limited to 4 year simulations, a level of confidence may be placed in its results as they approximate wave power values published in the Accessible Wave Energy Resource Atlas for Ireland (2005). In contrast to the broad scope of the Atlas for Ireland, the 3rd generation spectral wave model validated for the Clare Domain facilitated detailed analysis of numerous parameters at locations of interest.

Analysis of maximum wave heights at off-shore and near-shore locations in the Clare Domain highlighted the phenomenon of extreme wave filtering at depths less than 25 m. Extreme wave heights may not be exploited for power generation as they surpass the operational mode of most WECs. In line with this, a distinction was made between annual wave power levels and wave power levels that corresponded to operational conditions for a SOWC wave energy converter. This was termed the exploitable resource. Plotting the annual average exploitable power levels leading from the 90 m depth contour to the 5 m depth contour highlighted that the reduction in usable wave power is much less than the decrease in equivalent annual average wave power levels. This finding may cause developers to further consider WEC development at these shallower locations particularly as they are afforded relative protection by the filtering out of the most extreme sea states.

For the specific areas of interest, Arch Point and the tip of Loop Head, detailed analysis of the wave climate highlighted the differences between the locations. Regarding the percentage occurrence of each sea state, presented in the form of scatter diagrams for each site, the wave climate around tip of Loop Head exhibits a higher range of significant wave heights over a given year, compared with Arch Point. The reason for this is that the tip of Loop Head possesses a steeper seabed slope. Hence, during energetic wave conditions, the significant wave height is less affected by near-shore processes.

In relation to directionality, the wave roses for Arch Point showed that within the 35 m depth contour, the region was sheltered from wave fields approaching from South-West to South-East Directions. Conversely, the tip of Loop Head is exposed to waves approaching from North to South. Additionally, oceanographic studies have shown that the depth contours that surround a headland, such as Loop Head, can cause a focusing of wave energy at the tip of the headland (Harold et al., 2001). As a wave field propagates towards the tip, the waves turn toward the depth contours due to refraction. This phenomenon has been identified at the tip of Loop Head and is reflected in the high wave power levels.

Although the wave power levels and directionality differ for Arch Point and the tip of Loop Head, the scatter diagrams for each location show that the most commonly occurring range of energy periods is the same. For all depth contours at each site, the most commonly occurring energy period ranges from 6 s to 9 s. It will be seen in Chapter 6 SOWC Wave Energy Converter Design that this information is central to the design and efficiency of a given SOWC wave energy converter. Chapter 6 also provides information on the implications the wave climate has on SOWC Wave Energy Converter Design along with several other factors.

This chapter concludes the first aim of the research programme which was to characterise the wave climate off the County Clare coast from off-shore to near-shore and on-shore domains using a validated spectral wave model.

Chapter 6
SOWC Wave Energy Converter Design

While Chapters 4 and 5 focused on the first aim of the research programme, which was to characterise the wave climate for a domain off the coast of County Clare adjacent to Loop Head, as this is an area of interest for ocean energy development in Ireland, this and the following chapter focus on the second aim of the overall research programme, which was to use the findings from a wave climate modelling study conducted to achieve the first aim and build upon an earlier TCD (Marine Institute, 2000) study to investigate design parameters which may influence the survivability and feasibility of potential SOWCs installed at Loop Head. Factors affecting optimal SOWC chamber design will be considered in this chapter. These include wave climate, structural integrity, geology, hydrodynamic effects, construction method and turbine selection. In line with this, the SOWC design developed within the current research programme aimed to negotiate a balance between these elements. This design was based on the wave climate at a given SOWC site, the structural integrity of the SOWC chamber in a given rock type, and hydrodynamic and aerodynamic effects within the SOWC chamber that affect performance. Details on the wave climate at locations of interest were taken from the results section of Chapter 5 on wave energy resource characterisation. Information on the geological composition of Loop Head was sourced from the School of Geological Sciences at University College Dublin, which is presently carrying out a drilling initiative on Loop Head. All of these issues will be considered in this chapter, along with hydrodynamic and aerodynamic characteristics that affect performance and hence, chamber design. The design challenge lay in the development of a chamber geometry that could survive extreme sea states and induce favourable hydrodynamic

behaviour for generative motion to take place within the SOWC chamber as conditions demand. The assessment of hydrodynamic behaviour of chamber designs within these bounds will be given in chapter 7.

6.1 INTRODUCTION

A key focus is placed on SOWC chamber design. Falcão (2004) terms the wave to pneumatic energy conversion stage as a critical element in the energy conversion chain, from wave to wire. This is because inappropriate chamber design is known as a source for major losses, directly affecting short-term and long-term electricity production. SOWC wave energy converters are highly resonant systems. A SOWC wave energy converter configuration inherently possesses a natural frequency at which resonance occurs. If the frequency of the incident wave conditions coincides with the natural frequency of the SOWC wave energy converter, the device efficiency is maximised. Fundamentally, adjustments to the chamber design can tune the natural frequency of the device to a target resonant period. The target resonant period for a SOWC chamber design is the period at which optimal annual power conversion efficiency is experienced at the site of interest (Delaure, 2001). This target resonant period is site specific. Thus, an understanding of the local site wave energy resource is essential to achieve optimal matching of the device's natural response characteristics to the incident power distribution. Ultimately, tailoring chamber design according to location is important. However, there are design limitations unique to the SOWC's site specific nature. The influence of these site specific constraints on device design and their implications for device performance and feasibility will be explored throughout this chapter. The factors affecting SOWC design include (i) wave climate at the deployment site; (ii) structural integrity of the chamber, (iii) geology (iv) hydrodynamic complexities associated with chamber design, (iv) construction method, and (v) turbine selection. All of these factors will be discussed in this chapter. All were considered when selecting specific design variables for investigation. The effects of a set of particularly important factors on SOWC performance will be described in Chapter 7.

6.2 Factors Affecting SOWC Chamber Design

To achieve reasonable annual efficiencies, an understanding of the wave climate at the deployment site is essential in the chamber design process. A strategically designed chamber induces a favourable hydrodynamic response when exposed to the deployment site's prevailing wave conditions. Thus, identification of a target resonant period at which optimal annual power conversion efficiency is experienced at the site of interest is central to SOWC design.

Tuning the oscillating water column to induce a natural hydrodynamic response at a target resonant period may be achieved by altering the chamber's geometrical parameters. Considering the cross sectional view of the SOWC in Figure 6.1 design parameters that facilitate adequate tuning capabilities include front wall thickness, depth of SOWC entrance, chamber incline, chamber length and water plane area. In Figure 6.1, thickness of the front wall and depth of SOWC entrance are denoted by T and D respectively. D is based on the water level at mean low water springs.

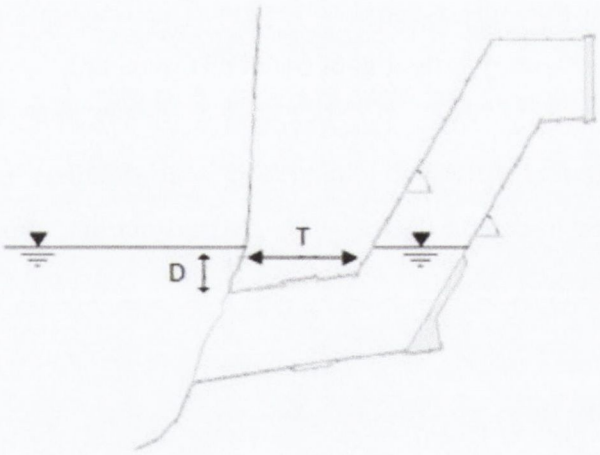

Figure 6.1 Cross sectional view of SOWC chamber design

Correspondingly, alterations in design parameters which affect the mass of fluid within the chamber, or water plane stiffness, intrinsically affect the natural frequency of the water column. In addition to tuning the OWC to a target resonant period, increasing bandwidth at, and around the target period is advantageous with respect to increasing overall annual power conversion efficiency. A balance exists between water column amplification at resonance and its related bandwidth, which is explored in this chapter.

In light of the above, a benefit of this study in relation to SOWC design pertains to the high resolution bathymetric data incorporated in the Loop Head region of the spectral domain model, described in Chapter 4. The high resolution seabed model that extends to the coast, coupled with nearby spectral wave model validation points at the 55 m and 20 m depth contour allows a level of confidence to be placed in the wave climate conditions at locations of interest. The locations of interest relating to potential SOWC installation sites are at points where the depths range from 15 m to 25 m. In line with this, the results outlined in Chapter 4 facilitated the identification of target periods at which optimal annual power conversion efficiency is experienced at the site of interest.

Theoretically, the target resonant period associated with the deployment site combined with an understanding of hydrodynamic tuning methods provide an opportunity to develop an idealised chamber design. However, due to the site-specific nature of SOWC chamber construction, realistic and practical limitations may impede the installation of idealised chamber designs. This is a significant point which affects the feasibility and energy potential of the SOWC concept.

The principle influences on SOWC chamber design are detailed below under four headings; wave climate, structural integrity, hydrodynamic affects and turbine selection.

6.3 WAVE CLIMATE

Regarding the prevailing wave conditions at potential deployment sites, the following wave climate characteristics influence the design and location of SOWC wave energy converters: (i) percentage occurrence of each sea state, (ii) spectral shape of the sea conditions, (iii) annual wave power level (kW/m), (iv) relationship between wave energy density and water depth, (v) water depth at SOWC site, and (vi) extreme sea states.

Primarily, the percentage occurrence of each sea state at the site is required to identify the target resonant period for the SOWC system. Inducing this optimal resonant period augments yearly efficiencies in the wave to pneumatic energy

conversion stage, when compared to a chamber with its natural frequency outside the range of prevailing sea states. The spectral shape of sea conditions is a standard approach for characterising the wave energy resource and estimating wave power levels. The annual wave power level is required to appropriately design the chamber width and water plane area in order to achieve a target power generation capacity. The depth of water at a SOWC location i.e. at a cliff base, affects the maximum height of waves and hence, average wave power level available to the chamber. The relationship between wave energy density through the water column and water depth influences the depth of inlet orifice and chamber width. In relation to structural integrity of the SOWC chamber design, an investigation of extreme sea states is required to assess the maximum loads that a SOWC wave energy converter must withstand. This has implications for the SOWCs front wall, which needs to be sufficiently thick to protect the integrity of the structure in the face of such loads.

6.3.1 Percentage Occurrence of Each Sea-state

The percentage occurrence for each sea state over an average year at a potential deployment site is valuable information. This information is generally presented using scatter diagrams, like those displayed for Arch Point (Figure 5.8) and the tip of Loop Head (Figure 5.10) in Chapter 5 Wave Energy Resource Characterisation. These statistics on each sea state for a given site allow the target operational period for the SOWC chamber design to be estimated. This period denotes a balance between high percentage occurrence and high power level. In general, SOWC wave energy converters possess a relatively narrow bandwidth, with high efficiency levels centred around its resonant period. Therefore, the identification of the target period is more important to the design of an SOWC in comparison to a wave energy converter with a relatively broad bandwidth. Favourable performance consists of maximised efficiency during commonly occurring moderate sea states. Although the efficiency is reduced for less frequent energetic sea states, these conditions possess considerable wave energy which allows the WEC generation capacity to be reached. Thus, the high power levels available to the wave energy converter compensate for decreased wave to pneumatic efficiencies. With this chamber design, electricity generation theoretically maintains at a more constant level for different sea conditions compared with a chamber tuned to energetic sea states. This scenario theoretically induces maximum electricity generation during heavy sea states and suboptimal electricity

generation during moderate and low sea states, when favourable efficiency is required to approach generation capacity. In this case, variability in electricity generation for different sea states is increased. As with wind turbines, variable electricity generation is seen as a challenging issue with respect to the integration of wave energy converters into the electrical grid.

It will be seen in Chapter 7 that factors associated with the structural integrity of the SOWC can shift its natural period. Depending on the deployment site, this shift can move its natural period away from the target period for the site. This can significantly affect its performance in the ways described above.

6.3.2 Spectral Shape of Incident Wave Field

Unlike the percentage occurrence of each sea state, the spectral shape of the incident wave field does not directly affect chamber design. However, it is central to estimating the wave energy associated with each sea state which does affect chamber design. As described in Section 2.5.2, the concept of the wave spectrum is a standard approach for characterising the wave energy resource and estimating wave power levels. Additionally, it lends itself to estimating the power absorbed by a wave energy converter. Both of these uses were exploited in this study to aid the design and analysis of the SOWC wave energy converter.

The selection of an appropriate standard spectrum to characterise the site is important as it directly influences estimates of wave energy available to the wave energy converter and predictions of wave power absorption. Estimates for wave energy available to the SOWC wave energy converter and its influence on chamber design is outlined in Section 6.3.3 Wave Power Level.

The response of the SOWC wave energy converter to the incident wave field governs its operational performance. As standard wave spectra characterise the incident wave field based on a limited number of parameters, there can be discrepancies between measured and standard spectra. Therefore it is important to establish that the spectrum chosen to characterise the wave conditions is appropriate for the site in question.

Figure 6.2 provides a key example of how a standard wave spectrum affects predictions of wave power absorption by a resonant wave energy converter. This example is taken, not from Loop Head, but from a nearby location on the west coast of Ireland: Galway Bay.

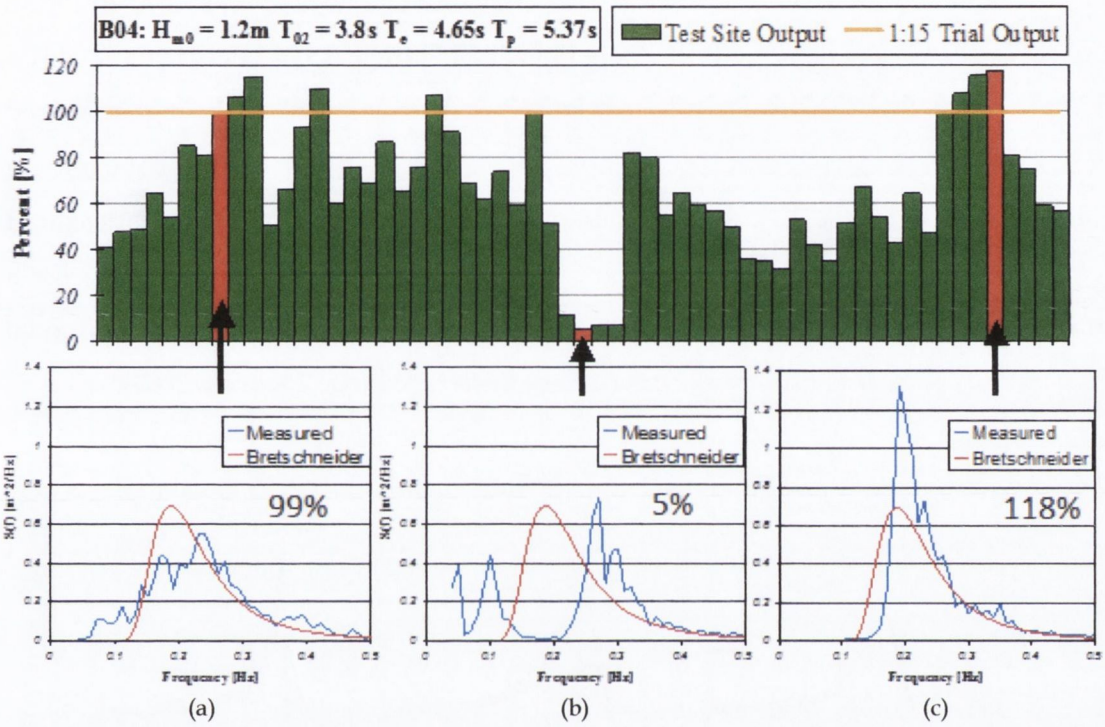

(a) (b) (c)

Figure 6.2 Lower section: Measured spectrum at three separate times (a),(b),(c) overlaid with standard Bretschneider spectrum. Upper section: Power output by WEC deployed at test site relative to predicted power output from tank testing trials. Source: (Nielsen and Holmes, 2010)

The three graphs in the lower section of Figure 6.2 present the measured wave spectrum at three separate times at the Galway Bay ¼ scale wave energy converter test site. Although the plots of the measured wave spectra are considerably different from one another, calculating the integral of each measured spectrum shows that the areas under these curves are equal. Hence, their significant wave height and period values are equal. These wave parameter values are shown in the upper left hand corner of Figure 6.2 Thus, plotting the standard Bretschneider spectrum based on these wave parameter values for each case shows the discrepancy that can occur between the measured spectrum and a standard spectrum. The largest discrepancy can be seen in the central spectral plot, (b). In this case, the measured wave spectrum exhibits twin peaks which indicates that the wave field possess bimodal properties. The 5% associated with spectral plot (b) denotes the level of agreement between power output for the target Bretschneider sea state as opposed to the output from the

device when exposed to the bimodal sea state for the same wave statistics. Although detailed analysis of bimodal sea states is outside the scope of the present research programme, this example lends itself to the subject of appropriate selection of standard spectra with respect to accurate WEC power absorption estimates.

Regarding wave conditions at Loop Head, Co. Clare, analysis of wave records from the waverider buoy deployed off Arch Point has shown wave conditions to differ from those at the Galway ¼ scale test site. Based on a study analysing measured wave spectra at Arch Point (Venugopal et al., 2011), the spectral shape of sea conditions off Loop Head are predominantly single peaked. Examples of measured wave spectra (blue line) overlaid with fitted Bretschneider spectra (red line) for a number of cases are presented in Figure 6.3. There are anecdotal reports of bimodal seas but no estimates of their occurrence have been recorded (Holmes, 2009).

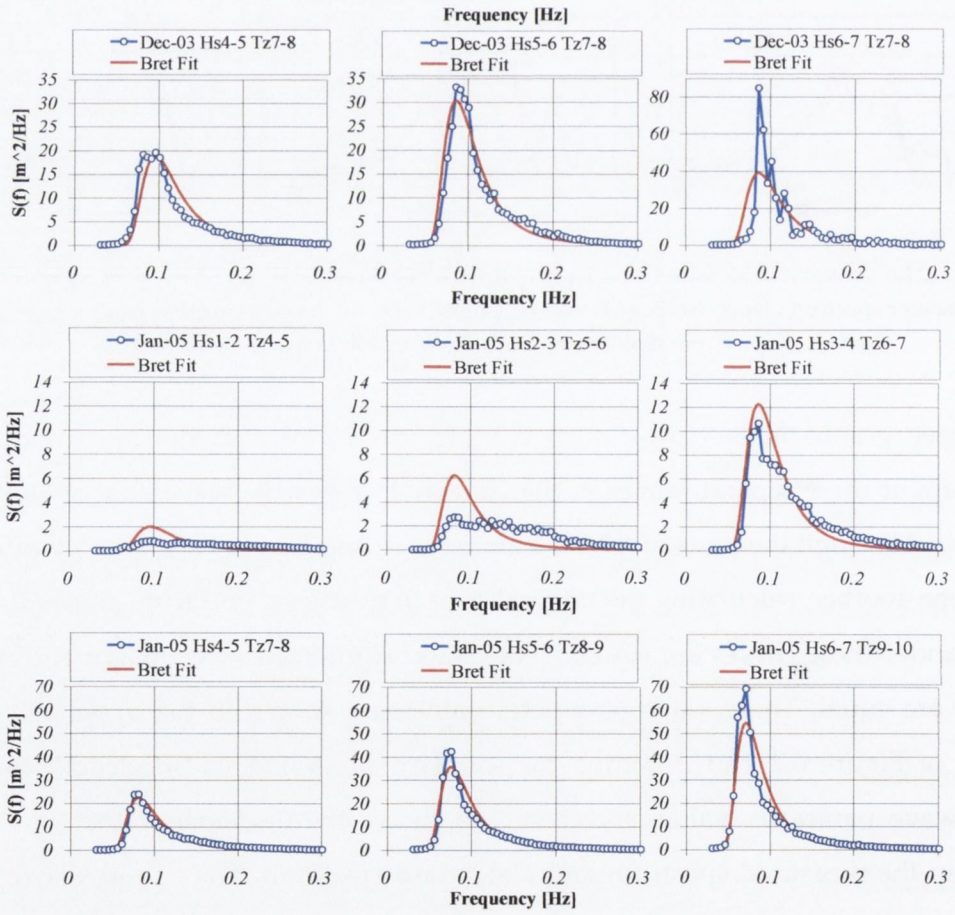

Figure 6.3 Measured wave spectra at Arch Point., Co. Clare overlaid with fitted Bretschneider spectra. Source: (Holmes, 2009).

The above spectral analysis is based on data measured by a wave rider buoy located at the 55 m water depth contour. As the wave field propagates towards the coast, slight changes in the wave spectrum occur due to reduction in water depth. With respect to potential SOWC deployment sites, it is acknowledged that non-linear effects taking place at the cliff base may affect the wave spectrum. However, regarding the near-shore domain where depth is greater than 10 m, the change in spectrum is relatively minor and is unlikely to significantly change the WEC's optimum tuning condition for the particular sea state (Folley and Whittaker, 2009). The water depths at locations of interest in this study range from 15 to 25 m. Therefore, this research adopts the aforementioned finding that a relatively minor change in wave spectrum occurs in the region between the waverider buoy location and coastal sites with water depth greater than 10 m, which includes this areas investigated in this study.

In summary, in light of the predominantly single peaked nature of the sea climate off Loop Head and the nature of the water depth at locations of interest in this study, it is established that there is sufficient level of agreement displayed between measured spectra at Arch Point, Loop Head and fitted Bretschneider spectra. Therefore the Bretschneider spectrum was employed to assess SOWC design performance at locations of interest around Loop Head.

6.3.3 Wave Power Level

The level of wave power at a potential SOWC site affects the size of the chamber required to achieve the target power generation capacity set for the project in question. Given that the target power capacity is set, an optimal chamber design induces favourable turbine operation conditions for the most commonly occurring sea states at the deployment site. Matching the chamber to the turbine is a complex design task as a number of factors must be accounted for including optimal operational damping, phase of water column motion and sufficient pneumatic power. This section details the relationship between wave power, pneumatic power and chamber design parameters that can be tailored to create sufficient levels of pneumatic power. Theoretically a SOWC chamber with a wide chamber inlet and large water plane area allows a greater intake of wave power than a narrow chamber with a small water plane area. For a fixed OWC wave energy converter, the wave

power subjected to it is dependent on the width of its chamber entrance. Consider the two chamber widths shown in Figure 6.4.

(a) (b)

Figure 6.4 Inclined OWC chambers: (a) 5 m wide (b) 12.5 m wide

For this type of fixed shoreline terminator type WEC, the approximate level of wave power available to the OWC can be estimated by multiplying the incident wave power by the chamber width. Hence, with an incident wave power level of 30 kW per metre wave front, the 5 m wide chamber is subjected to (5 m x 30 kW/m) 150 kW and the 12.5 m wide chamber to (12.5 m x 30 kW/m) 375 kW. The same method may be applied to the SOWC wave energy converter. However, it should be noted that this simple calculation for estimating the incident wave power available to a WEC cannot be applied to the majority of wave energy technologies designed for the near-shore and off-shore domain which accept wave power in a number of planes. Also, the interaction between the incident wave energy resource and the SOWC chamber is considerably more complex, see Section 6.6 Hydrodynamic Effects.

Regarding the wave energy resource, a given target power generation may be achieved by a relatively wide chamber and large water plane area in a location with moderate wave power levels or by a narrower chamber and smaller water plane area in a location possessing high wave power levels. Thus, when planning an SOWC installation, the level of the wave energy resource must be measured in order to determine the width and water plane area that will be required to deliver the target power production level.

To introduce the importance of this issue, it is convenient to briefly describe the design of the Islay LIMPET OWC wave power plant (Whittaker et al., 2002). Estimates on the annual average incident wave energy in conjunction with a target installed capacity provided the basis for determining the chamber size within

structural limits. The wave data used to estimate wave energy levels was measured at a location 300 m from the designated LIMPET site, which was located in the side of a headland. At this point an annual average incident wave energy resource of 15.9 kW/m was estimated. Due to LIMPET site's orientation to the prevailing waves in comparison to the wave measurement location, it was predicted that the OWC chamber would experience a slightly higher level of wave energy than 15.9 kW/m. In line with this, an installed capacity of 500 kW and a utilisation of 40% to provide an output of 200 kW was set as the target capacity for the project. Accounting for a correctly tuned OWC chamber subjected to the annual average incident wave energy and a turbine rated at 500 kW, a chamber width of 21 m was selected to achieve the set power output objectives. Considering the predicted annual average wave energy resource at the site (15.9 kW/m), the 21 m wide chamber captures wave power levels circa (21 m x 15.9 kW/m) 333.9 kW on average. Theoretically this induces appropriate power levels to match the turbine generation capacity. However these simplistic calculations are based on annual average wave conditions. When considering the seasonal variability of the wave energy resource at a given location and hydrodynamic affects, determining the optimal chamber design becomes more difficult. Hypothetically, there is an optimal chamber design for each sea state which induces ideal operating conditions for the turbine. In line with this, Whittaker et al. (2002) outlined that determining the optimal chamber width for LIMPET was a complex process.

On completion of the project, it was found that the OWC chamber was not achieving its target power output. This was predominantly due to a significant difference in the actual wave power entering the OWC chamber. Research has suggested that the wave energy actually impinging the LIMPET chamber was 66% of that predicted by the pre-construction study (Wavegen, 2002). This was caused by a difference between the pre-construction estimate of the sea bed profile and the actual bathymetry leading to the OWC chamber. Before construction, a survey indicated a depth of 7 m at the coastline with an immediate 1:25 slope seawards. However, it has been found that the actual bathymetry exhibits a depth of 5 m close to shore which remains level for approximately 80 m prior to deepening. Hence, the near-shore and coastal processes affecting the wave climate diminish the wave energy resource.

With respect to the influence of wave energy resource on chamber design, LIMPET provided evidence at full scale that a chamber designed for a more energetic wave climate to that which it is exposed to, has a significant effect on performance. With lower wave energy levels impinging the chamber, sub-optimal pneumatic power levels are experienced by the turbine. These sub-optimal operational conditions result in a reduction in performance. Furthermore, the above case study addressed a number of important issues that affect SOWC design: (i) chamber size based on wave energy resource levels, (ii) the importance of accurate wave energy resource predictions, and (iii) the effect of bathymetry on wave energy resource.

Considering the wave climate at Loop Head, Chapter 5 showed that the wave energy resource varies around the headland due to a number of factors including water depth and the position of the site relative to the prevailing wave direction. Considering the target capacity of 500 kW for LIMPET, designed with respect to an annual average incident wave energy resource of 15.9 kW/m, the higher wave energy resource at sites at Loop Head suggests that the same target capacity could be achieved with a narrow chamber design. This assumes that the narrower chamber possesses an overall design that induces a natural response circa the target period for the site.

A narrower design is favourable for the SOWC concept as there are structural limitations for the chamber width which are dependent on the geology of the cliff. This is discussed in Section 6.4 Structural Integrity and presents the maximum width that can be constructed at Loop Head.

6.3.3.1 Chamber Width

Regarding the minimum chamber width, the target capacity must be considered which directly relates to turbine selection and cost-effective power output. Initial attention was given to the idea of a large number of relatively narrow (< 5 m) chambers designs which require minimal reinforcement. Considering the annual average wave power at two potential SOWC sites outlined in Chapter 5 - Arch Point (25 kW/m) and the tip of Loop Head (34 kW/m) – the annual average wave power values available to a 5 m wide chamber are 125 kW and 170 kW for Arch Point and Loop Head respectively. Even with the relatively high wave power levels at these

locations, the estimated pneumatic power generated via these chamber designs was deemed insufficient to promote cost effective power generation.

It will be seen in Section 6.8 Turbine Selection that the Wells turbine, typical to OWC power generation, was selected as the power take off for the SOWC wave energy converter. Capital costs for Wells turbines rated from 200 kW to 1 MW have highlighted that, given an appropriate chamber design, turbines with a higher rating are more cost effective. To quantify this point, costs for manufactured Wells turbines with increasing power ratings were sought. Unit costs for four different turbines manufactured by Wavegen (2005) are present in Table 6.1

Table 6.1 Turbine rating and associated cost for four separate Wells turbines

Turbine Rating	Cost
200 kW	€ 321 k
500 kW	€ 402 k
800 kW	€ 429 k
1 000 kW	€ 562 k

A cost benefit analysis of each turbine in Table 6.1 shows that turbines with a higher rating are more cost effective than turbines with a lower rating. Although this finding does not account for all power take off options for SOWCs, it agrees with the general consensus outlined by The Carbon Trust's OWC wave energy converter evaluation report (2005) on appropriate turbine sizing. Based on this and the wave power levels experienced at potential SOWC sites at Loop Head, attention was shifted away from small chamber designs (< 5 m wide) as cost effective power generation is more likely for larger chamber designs. Hence, large chamber designs that can induce sufficient pneumatic power to necessitate turbines with power ratings equal to or greater than 500 kW possess greater potential for cost effective power generation. Based on this, increasingly wide chambers benefit larger turbines. However, in Section 6.6 Hydrodynamic Effects, it will be seen that limitations do exist for the width of an OWC chamber. To a greater extent, it will be seen in Section 6.5 that the width of the SOWC chamber is dictated by the structural integrity of the chamber within the cliff site.

6.3.4 Wave Energy Density and Water Depth

To maximise the wave power captured by the SOWC chamber, it is recommended that the inlet orifice is positioned as close to the water surface as possible, without exposing the chamber to atmospheric conditions. The motions of the water particles, which transmit wave energy, reduce with water depth. Thus, the wave energy density decreases with water depth (Battjes and Janssen, 1978). Therefore, a chamber inlet positioned closer to the water surface captures more wave energy than a chamber inlet positioned closer to the seabed.

The limitation with respect to this chamber design recommendation pertains to the risk of inlet broaching. This occurs when a deep wave trough temporarily causes the water level to fall below the level of the SOWC entry lip, causing a direct air passage between the pressurised air chamber and the outer atmosphere. The effects this has on hydrodynamic performance are described in Section 6.6 Hydrodynamic Effects. In terms of chamber design, previous research has shown that the risk of inlet broaching can be significantly reduced by positioning the inlet orifice a minimum of 25% water depth below the mean low water spring tide (MLW) at the installation site (Carbon Trust, 2005). Therefore, based on the tidal range at Loop Head, presented in Chapter 4, the depth of the SOWC lip has been set at 4 m. Figure 6.5 shows the depth of SOWC lip relative to MLW. Additionally, it depicts the decrease in orbital motion of the water particles with depth. This is the basis for the reduced wave power levels at greater depths.

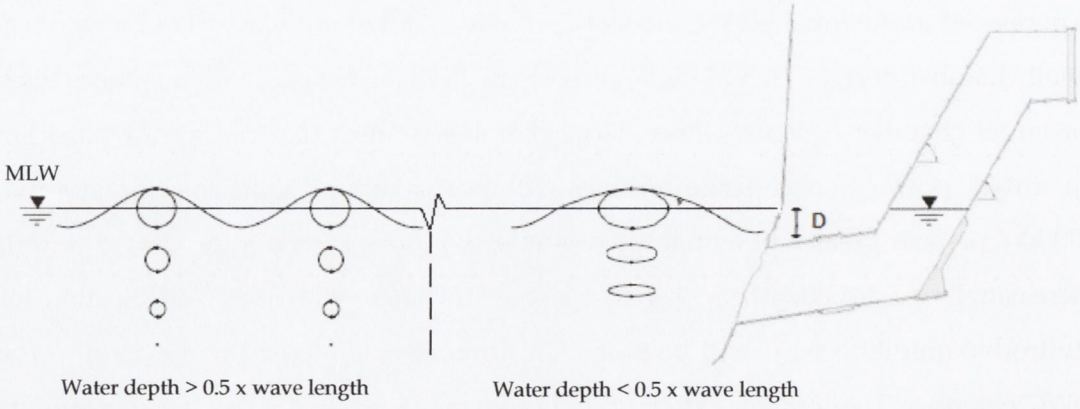

Figure 6.5 Depth of SOWC chamber lip, *D*, relative to mean low water spring tide (MLW). Circles and ellipses denote orbital motion of water particle which transmit wave energy.

6.3.5 Water Depth at SOWC Location

Water depth at sites being considered for SOWC is important for a number of reasons. Firstly, water depths greater than 15 m benefit SOWC performance, which is addressed later in this section. Secondly, the accuracy of wave climate predictions using a 3rd generation spectral wave model decrease significantly in shallower regions beyond the 15 m depth contour when sufficient bathymetric data is not available (Bouws et al., 1998). The accuracy of a 3rd generation spectral wave model decreases beyond the 16 m depth contour due to the increased levels of interaction between the seabed and the propagating waves (Folley et al., 2013). This is relevant to the 3rd generation spectral wave model developed for this research programme. In line with this, SOWC sites considered were restricted to locations that possess a water depth equal to or greater than 16 m. As tidal data is incorporated to the spectral wave model, this denotes 16 m water depth at mean low tide.

Regarding SOWC performance, Section 5.2.1 Wave Power Levels: Off-shore to On-shore and Section 5.2.3 Exploitable Wave Energy Resource, highlighted that annual wave power levels reduce significantly in water depths less than 15 m. Exposure to a greater wave energy resource permits chamber designs to achieve higher target capacities which promote cost effective power generation. Hence, the chief sites investigated in this study, Arch Point and Tip of Loop Head, possessed a water depth greater than 16 m.

6.3.6 Extreme Sea States

Although locations that possess high levels of annual average incident wave energy are favourable for annual performance, extreme sea states directly affect the survivability of a given SOWC chamber design. Survivability is central to the feasibility of the SOWC concept. Up to this point, the focus has been placed on aspects of the wave climate that facilitate chamber optimisation to induce favourable hydrodynamic behaviour. The objective of this section on extreme sea states is to highlight the extreme loads that a SOWC wave energy converter must withstand. This has implications for the SOWC's front wall, which needs to be thick enough and hence strong enough, to protect the integrity of the structure in the face of such loads.

For off-shore, near-shore and shoreline wave energy converters, the cost of over-engineering designs to survive exceptional storms can lead to excessive capital costs. This aspect of wave energy converter design significantly impacts the economic viability of a given technology. Additionally, uncertainties related to the survivability of wave energy conversion technologies reduce investor confidence. This directly affects the financial support available to confidently progress the technology through a structured development plan which outputs a marketable wave energy converter (Nielsen and Holmes, 2010).

The primary guidelines addressed in this study on extreme sea states were: 'Guidelines on design and operation of wave energy converters: A guide to assessment and application of engineering standards and recommended practices for wave energy conversion devices' (Carbon Trust, 2005); 'Off-shore Service Specification DNV-OSS-312: Certification of Tidal and Wave Energy Converters' (Det Norske Veritas, 2008); 'Annex II Task 2.1 Guidelines for the Development & Testing of Wave Energy Systems' (Nielsen and Holmes, 2010); 'Equimar's Protocol for wave and tidal resource assessment' (Davey et al., 2010) and 'Extremes and long term extrapolation' (Prevosto, 2011).

The Carbon Trust (2005) guidelines outline that promising wave energy converter technologies aim to negotiate a balance between survivability, performance, maintenance and capital costs which apply to the SOWC wave energy converter. The design challenge lies in the development of chamber geometry than can survive extreme sea states and induce favourable hydrodynamic behaviour for generative motion to take place within the OWC chamber as conditions demand.

Centring on survivability, the protocol for analysis of wave loading on near-shore and shoreline wave energy devices (Davey et al., 2010) states the wave environment at the site of a shoreline wave energy converter is very much site specific depending on the following variables: coastline profile, water depth at the device, bathymetry, incident wave spectra and directional spreading. The annual wave climate at the site of the device should be derived from measurements. If wave data from a wave rider buoy further out to is to be used, the data should be transformed to the site using a derived transfer function (CarbonTrust, 2005).

For this study, the 3rd generation spectral wave model described in Chapter 4 and 5 facilitated this requirement. Recalling Section 5.2.2 Extreme Sea States, the maximum waves heights experienced at potential SOWC sites ranged from 10 m to 13 m. It was also observed that extreme sea states are filtered out to an extent as they propagate towards the coast. This was highlighted via a comparison with off-shore locations which experienced maximum wave heights ranging from 20 m to 24 m. This means that the global loads experienced at potential SOWC sites may be smaller than those experienced in the near-shore and off-shore domain. The exact loads associated with extreme waves at a SOWC site are dependent on their form.

The load experienced by the cliff face, and hence SOWC front wall, depends on whether the impinging wave is an unbroken wave, slightly breaking, broken wave or a plunging breaker. Graphs plotting the characteristic horizontal wave force, F_h, on a vertical face for these four types of wave are presented in Figure 6.6.

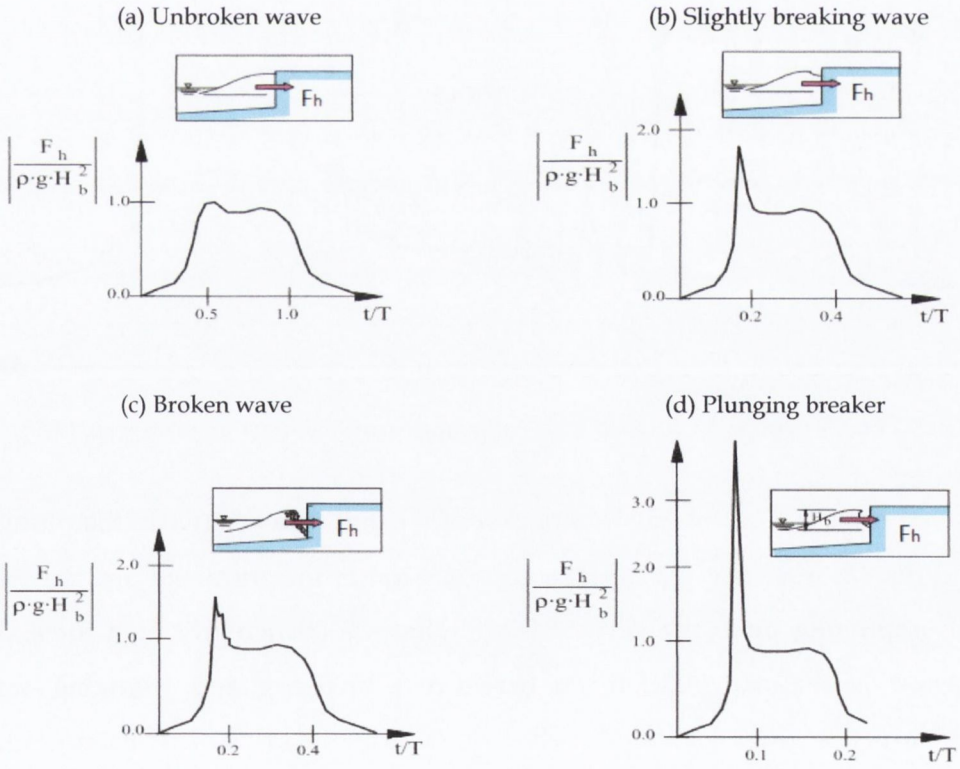

Figure 6.6 Characteristic loads associated with (a) Unbroken wave, (b) Slightly breaking wave, (c) Broken wave (d) Plunging breaker. Source: (H. Oumeraci et al., 1999).

Where ρ is sea water density (kg/m^3), g is acceleration due to gravity ($9.81\ m/s^2$) and H_b is the wave height at breaking. The horizontal axis denotes the time t in terms of the wave period T. Thus, the characteristic horizontal wave force for an unbroken

wave is relatively constant as it impinges upon a vertical face. For slightly breaking and broken waves, the force upon the vertical face peaks at impact; the force rises to approximately 1.5 times the force associated with an unbroken wave (Figure 6.6). The most extreme wave loads occur as a plunging wave impacts a vertical face. It can be seen in Figure 6.6 that the characteristic force is more than twice that associated with slightly breaking and broken waves. The reason behind this exceptionally large horizontal wave force, F_h, is outlined in Figure 6.7.

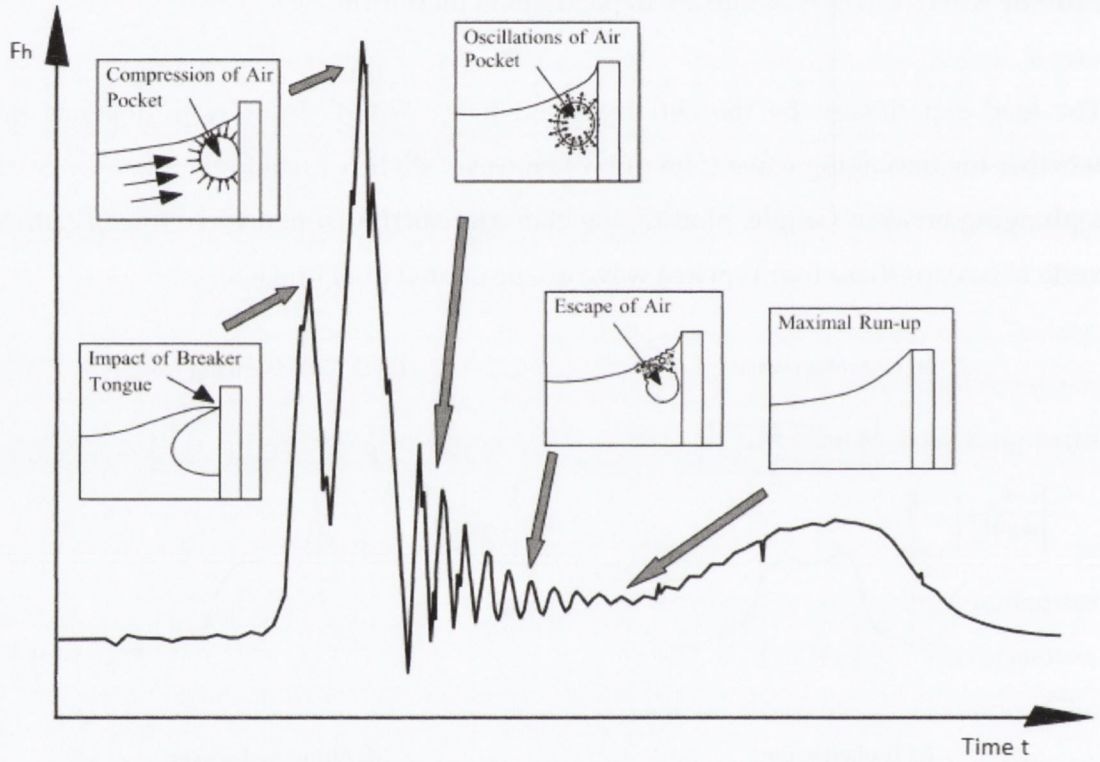

Figure 6.7 Stages of impact associated with a plunging wave. Source: (Oumeraci et al., 1999)

The extreme peak in force is due to a pocket of air that forms between the plunging wave and the vertical face. The sudden compression of the entrained air, caused by the wave impinging upon the vertical face, induces a particularly high force. This phenomenon is the main difference between a breaking and plunging wave. Plunging waves occur at locations with a steep gradient slope. The steep gradient induces a fast transition stage from deep water to shallow water which causes a rapid reduction in wave celerity. The reduction in wave celerity coupled with the high particle velocity under the wave crest causes a kinematic instability which produces the plunging wave motion.

To inspect whether a potential SOWC site possesses characteristics that may induce a plunging type wave, the Irribaren number can be calculated for the range of extreme sea states associated with that site. The Irribaren number, ξ, also known as the surf similarity parameter, accounts for sea bed slope α, wave height in deep water H_0 and wave length in deep water λ_0 as shown in equation (6.1).

$$\xi = \frac{tan\alpha}{\sqrt{H_0/\lambda_0}} \tag{6.1}$$

The type of wave breaking associated with the extreme sea states may be investigated by using the following established guide, developed by the Spanish engineer, Ramón Iribarren Cavanillas (Iribarren and Norales, 1949):

	$\xi < 0.5$	Spilling wave
$0.5 <$	$\xi < 3.3$	Plunging wave
	$\xi > 3.3$	Surging Wave

Using the extreme sea state information presented in Chapter 5, the Iribarren number was calculated for maximum wave heights that occurred at the 17 m deep location at Arch Point and the 17 m location at the Tip of Loop Head. In line with this, the seabed slope at both locations was examined.

Based on the bathymetric model developed as part of the SW wave model, the water depth at Arch Point remains relatively constant for approximately 40 m off-shore, followed by a slope of circa 1 : 25 ($\alpha = 2.3°$). In contrast, the seabed slope at the Tip of Loop Head is approximately 1 : 9 ($\alpha = 6.3°$). The bathymetric data for these locations were sourced from the UK hydrographic office and digitised admiralty charts. Using the maximum wave heights and corresponding wave lengths for each site, described in Chapter 5, coupled with information on the seabed slope, the range of Irribaren numbers may be calculated. These are presented in Table 6.2.

Table 6.2 Irribaren number for maximum wave heights

Parameter	Arch Point APC (17 m)	Tip of Loop Head TCS (17 m)
Seabed Slope	Plateau, then 1:25	1:9
Maximum Wave Height	12.9m	12.48 m
Irribaren number	$\xi < 0.5$	$0.5 < \xi < 3.3$

The 1:25 seabed gradient and level section of seabed leading to Arch Point results in Irribarren values less than 0.5 for the range of maximum wave height scenarios. This suggests that the influence of the seabed causes these maximum wave heights to spill, rather than plunge against the cliff face. Conversely, the steeper seabed gradient leading to the Tip of Loop Head causes the Irribaren number to fall within the range of values associated with plunging breakers. Regarding SOWC survivability, a seabed profile that reduces the likelihood of large plunging waves at the cliff face is favourable.

6.3.6.1 Long Term Extrapolation

For a wave energy converter to be granted certification for insurance by Det Norske Veritas (DNV), it must provide evidence that it can survive a 1 in 100 year wave (DetNorskeVeritas, 2008). DNV are an international organisation for managing risk in maritime industry. Thus, for a SOWC wave energy converter to become certified it must meet these criteria.

Survival testing of SOWC chamber designs is outside the scope of this study. However, a brief description of the requirements follows. In survival based design of marine structures, the probability of wave heights exceeding a certain level is expressed as a return period. The return period is the time duration during which this level is exceeded once on average (e.g. 20 year return period). The level is defined as a return value (e.g. 20 year H_s value). Times series wave data are generally unavailable to directly measure a 20 year, 50 year or 100 year value for maximum wave height. To overcome this, a number of methods have been developed to predict maximum wave height values. These include block maxima, storm maxima, r-largest or total sample methods (Tawn, 1988). To appropriately extrapolate data over a specified time period to investigate the probability of extreme wave heights, suitable statistical distributions are fitted to the wave data set. It is generally recommended that the Gumbel Generalised Extreme Value (GEV) distribution be the default choice of distribution. The use of other distributions must be grounded in theoretical or physical consideration (Prevosto, 2011). The GEV distribution fitted to maximum wave heights measured at 17 m deep location at Arch Point is presented in Figure 6.8.

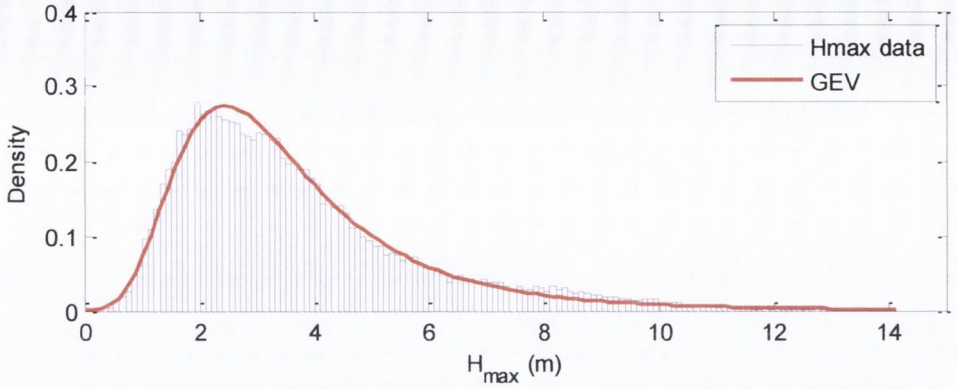

Figure 6.8 Probability Density Function (PDF) for H_{max} data set for Arch Point (17m deep location, 2004 -2008) and fitted Generalised Extreme Value (GEV) distribution.

There is a high level of agreement between the maximum wave heights recorded at the site and the GEV distribution. This establishes that the GEV distribution provides a suitable means to extrapolate data to determine a 20 year, 50 year or 100 year value for maximum wave height. Equimar's guidelines on extreme waves and long term extrapolation (Prevosto, 2011) recommend that a data base of duration of 1/5 of the return period is a minimum for a reasonable use of the return values. Therefore, the four years of wave data available to this study allows reasonable estimation of a 20 year value for maximum wave height. The confidence intervals on the return values inherently decrease with the length of the database. In relation to a 50 year and 100 year value for maximum wave height, an accurate prediction requires a data set that spans a 10 and 20 years respectively.

Extrapolating the abovementioned maximum wave height data set using the GEV distribution, gives a 20 year value maximum wave height of 13.26 m for a 17 m water depth. As described in Chapter 5, the maximum possible wave height for a given water depth is taken as 0.78 times the water depth. This limits the maximum possible wave height to 13.26 m at Arch Point, Co. Clare. For water depths which limit the maximum wave height, the return period becomes redundant once it has been established that the maximum wave height for the given depth may occur (Sarpkaya, Isaacson, 1981). Hence, 13.26 m is taken as the most extreme wave possible at Arch Point. Based on this maximum wave height, and a range of possible wave lengths, the Irribaren number may reach 0.35 with the aforementioned seabed gradient. This suggests that plunging waves are unlikely to occur even for the most extreme wave height. Regarding the tip of Loop Head, the maximum possible wave height at 17 m

water depth was recorded during the spectral wave model simulation period. Hence, no extrapolation was necessary. In contrast to Arch Point, calculations of the Irribarren for these maximum wave heights suggest that plunging waves will occur at this site due to the seabed gradient leading to the site.

The wave loads associated with the maximum wave heights at each site are investigated in Section 6.4 Structural Integrity. Regarding the survivability of a SOWC wave energy converter, it is the possible occurrence of these types of waves that impose a risk of structural failure. Hence, it affects the dimension of certain SOWC design parameters required to uphold the structural integrity of the structure.

6.4 Structural Integrity

Due to the site specific nature of shoreline SOWC chamber construction and operation, practical limitations may impede idealised chamber designs. This is a significant factor which affects the feasibility and energy potential of the SOWC concept. The SOWC design is strongly influenced by the characteristics of the cliff into which it is being built. Certain design parameters have to be tailored to uphold the structural integrity of the chamber within the given rock type. Three chief design parameters which are affected by site characteristics are thickness of the front wall, chamber width and depth of OWC entrance.

The chief design limitations associated with the SOWC are interconnected with the structural integrity of the chamber within the cliff. Where the chamber is excavated within rock, the front wall of the chamber needs be thicker than the front walls of conventionally constructed chambers. The nature of the rock also limits the width of chamber that can be sustained. It is useful to explore the performance of chamber designs which can be created within rock without reinforcement as this minimises construction costs. Hence the variables of front wall thickness and chamber width are explored in this research. The limits imposed by these constraints upon chamber design directly affect hydrodynamic performance.

6.4.1 Structural Limitations

'Guidelines on design and operation of wave energy converters' (CarbonTrust, 2005) describes the protocol for structural design: the design of a wave energy converter shall be based on the most severe environmental conditions/loads that the structure may experience in its design life. This directly corresponds to the wave loads associated with maximum wave heights described in Section 6.3.6 Extreme Sea States.

For Arch Point, Co. Clare, it was shown that the seabed profile causes extreme waves to spill rather than form in to plunging breakers. However, calculations of the Irribaren number for the tip of Loop Head suggest that steeper seabed gradient leading to the site can cause extreme waves to form in to plunging breakers.

To investigate the forces exerted on the cliff at each site, estimates of wave load were calculated for both extreme high impact breaking waves that occur only occasionally and also waves of prevailing sea states that repeatedly impact particular points in the cliff. With respect to high impacts, estimates of maximum pressures are required in relation to breaking waves, including plunging waves. With respect to prevailing sea states, as suitable SOWC locations generally possess water depths of at least 15 m, a significant proportion of sea states consist of unbroken waves. It will be seen that the distribution of pressure on the cliff face is different to breaking waves. In line with this, the coastal engineering manual published by U.S Army Corps of Engineers (2002) encourages calculation of wave loads associated with maximum unbroken waves in addition to broken waves.

The characteristic distribution of pressure on a vertical face for unbroken and breaking waves is presented in Figure 6.9. A cross sectional view of a potential SOWC chamber design is superimposed to highlight the distribution of forces acting on the front wall. The distribution of pressure on the cliff face is denoted by Euclidean vectors.

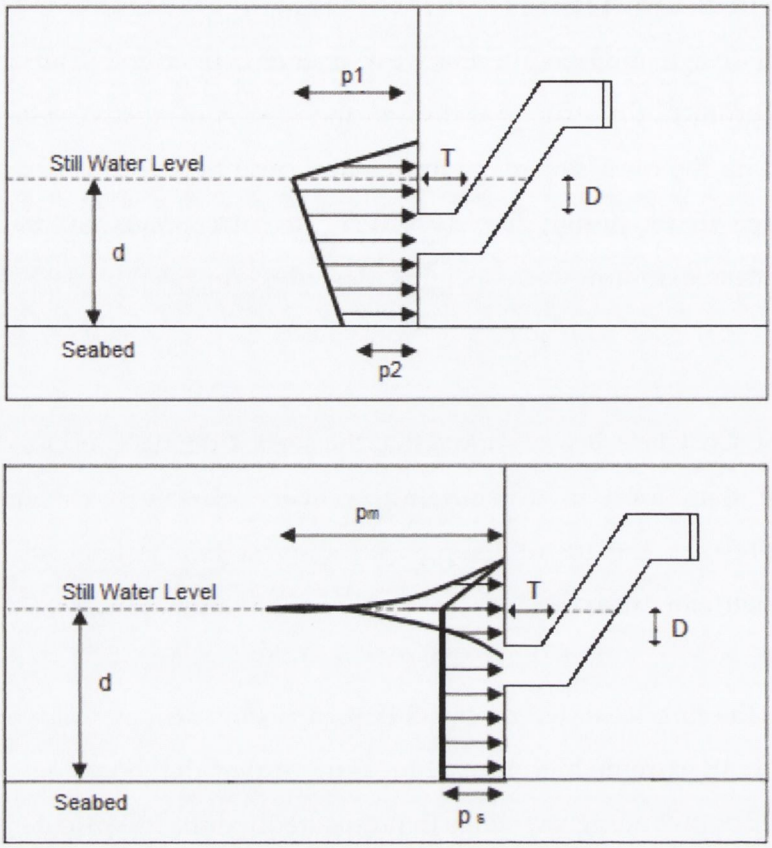

Figure 6.9 Pressures on SOWC front wall due to unbroken waves (top) and breaking waves (bottom). Adapted from Coastal Engineering Manual (U.S. Army Corpsof Engineers, 2002)

It can be seen from Figure 6.9 that although the pressure distributions for unbroken and breaking waves are different, the maximum loads for both categories occur around the still water level. As expected, the wave load associated with the breaking wave is significantly larger when compared with the unbroken wave loading. One reason for the unbroken wave's lower load is that a higher proportion of the energy is reflected from the vertical face. For breaking waves, the turbulent vortices generated at the surface of large breaking waves causes a high rate of energy dissipation as it impacts against the vertical surface. Hence, less energy is reflected. The strength and size of turbulent vortices generated at the surface of breaking waves induce high impact loads to take place around the still water level (U.S. Army Corps of Engineers, 2002).

There are a number of methods for estimating the wave loads associated with sea states. For example, those outlined by the Coastal Engineering Manual (CEM) of the US army Corps of Engineering (U.S. Army Corps of Engineers, 2002) and the

PROVERBS project (H. Oumeraci et al., 1999). The PROVERBS project was a European research effort titled PRObabilistic design tools for VERtical BreakwaterS (PROVERBS). A number of these were compared and were found to provide similar results. For the purposes of this study results are presented according to the method provided by the US army Corps of Engineering (U.S. Army Corps of Engineers, 2002) for both unbroken and broken waves.

To quantify the loads acting at the still water level for both categories, the maximum wave heights for unbroken and breaking waves at Arch Point were considered. For the case of waves that do not break at the cliff face, Equation 6.2 was used to calculate the maximum pressure, $p1$, acting on the front wall at the still water level. As the wave is unbroken, the water depth d determines what the maximum wave height, H. The equations assume that the maximum wave height is $H = 0.5d$.

$$p1 = (p2 + \rho gH)(H + \delta_0)/(d + H + \delta_0) \tag{6.2}$$

$$p2 = \rho gH/cosh(2\pi d/L) \tag{6.3}$$

$$\delta_0 = (\pi H^2/L)\coth(2\pi d/L) \tag{6.4}$$

Where $p2$ defines the pressure at the base of the cliff, L the wave length and δ_0 denotes section of wave impacting the cliff face above the still water level. Thus, considering the water depth at Arch Point and the tip of Loop Head, the maximum unbroken wave heights were taken as 8.5 m and 8 m respectively. In this case, the maximum pressure acting on the SOWC front wall is estimated as 78 kN/m² (Arch point) and 72 kN/m² (Tip of Loop Head).

For breaking waves impacting the cliff face, the maximum sea state may be considered. Although plunging waves are unlikely at Arch Point, calculations of maximum wave load at both sites assume impact via plunging wave. It must be noted that wave structure interaction for extreme waves is highly non-linear. A detailed investigation on this complex problem was outside the scope of this study. However, the following method, provides estimates that are in line with similar OWC chamber design studies, namely the Ceodouro Project: overall design of an

OWC in the new Oporto Breakwater (Martins et al., 2005). The method assumes a parabolic pressure distribution which is highlighted in the above schematic for pressures due to breaking waves (Equation 6.7). The maximum pressure on the cliff face at still water level, p_m, is given by Equation 6.5

$$p_m = p_n(1 - 2|z|/H^2) \quad \text{for H/2 > z > -H/2} \tag{6.5}$$

$$p_n = 202\rho g d/(H/L) \tag{6.6}$$

$$p_s = 0.5\rho g H(1 - 2z/H) \quad \text{for 0 < z < H/2} \tag{6.7}$$

where p_n is the pressure related to the parabolic pressure distribution and p_s is the static pressure acting on the cliff face, as shown in Figure 6.7. For Arch Point, a maximum breaking wave height was based on results presented in Section 5.2.2 Extreme Sea States. With a wave height of 13.26 m, the maximum pressure acting on the front wall is 1278 kN/m^2. For the tip of Loop Head with a maximum wave height of 12.8 m, the maximum pressure is estimated as 1202 kN/m^2. These values approximate values presented in a wave loading study carried out by Sewave Ltd. (2005). The considerable increase in wave load, compared with an unbroken wave, is due to a number of reasons. Firstly, the maximum unbroken wave height considered was 8.5 m while the maximum broken wave height was 12.8 m. Also, for the case of an unbroken wave impacting a vertical face, Equations 6.2 - 6.4 assume that the wave is almost totally reflected. These equations are known as Sainflou's formula and assume linear wave theory (Sainflou, 1928). Regarding the broken 12.8 m high wave impacting the cliff face, non-linear effects are assumed. Equations 6.5 - 6.7 were developed by Minikin (1963) and calculate the maximum pressure occurring at the still water level. As previously mentioned, it assumes a parabolic distribution and that the wave breaking varies from a height H/2 above the still water level to a maximum of p_m at the still water level and then again to a depth of H/2 below the still water level. The resulting pressure given is based on the static and dynamic force. In this case, less energy is reflected by the cliff face. Detailed analysis of the front wall thickness that is required to withstand forces of this nature based on the site's geological composition is outside the scope of this study. If this was to be

investigated, physical model tests would be recommended as they model all of the strong non-linear interactions between waves and structures.

However, work has been carried out on this aspect by Sewave Ltd. (Sewave, 2005). A wave tank model was constructed and instrumented to measure global and local loads in representative survival seas. These survival seas were analogous to extreme sea states found on the west coast of Ireland. Survival tests performed were equivalent to 2 hour storms at full scale, with a maximum significant wave height equal to 11 m. These conditions exceed maximum significant wave heights modelled at Arch Point, Co. Clare, outlined in Section 5.2.2. The report specified a minimum front wall thickness of 5 m. This design criterion was based on the geology of potential sites on the Faroe Islands. The geology of each cliff site comprised basalt rock. With this rock type, a maximum chamber width was identified as 12.5 m (Sewave, 2005). The following section compares the structural properties of basalt with other rock types feasible for SOWC construction and investigates the geological composition at Loop Head.

6.5 GEOLOGY

The geology of potential SOWC sites directly affects key design parameters including the thickness of the front wall and width of the chamber. Important geological aspects considered in SOWC chamber design were rock type, homogeneity of rock and orientation of rock layering.

6.5.1 Rock Type

To continue on from Sewave Ltd.'s finding on specifying a minimum front wall thickness of 5 m in basalt rock based on extreme wave conditions, a question was posed on how this information can be utilised with respect to other rock types.

Specific rock types suitable for the construction of SOWC chambers have been identified by the Geology Department at Trinity College Dublin (Holland, 1997), the Department of Geotechnical Engineering at Chalmers University of Technology, Gothenburg (Lindblom, 1997), Trenchless Technology Centre at Louisiana Tech. University (Sterling, 1997), Sewave Ltd. (Sewave, 2005), Tara Mines Ltd. (McConnell,

2012) and Priority Drilling Ltd. (McCarthy, 2012). The specified rock types were limestone, shale, sandstone, basalt, and quartzite. SOWC construction is not limited to these five rock types, but these were the rock materials considered by the above listed references.

The dimensions of the chamber that are feasible within these rock types are dependent on the construction technique. A number of construction techniques were investigated over the course of this research programme. However, to appropriately extend Sewave Ltd.'s findings on front wall thickness to other rock types, the assumed construction approach was tunnelling via the conventional drill and blast method as this was the construction method proposed by Sewave Ltd. Tunnelling is a complex process that is associated with many variables. The focus of this investigation is placed directly on comparing the physical and mechanical properties of aforementioned rock types with basalt. These are presented in Table 6.3 below. The values for each property assume that rock types are homogeneous and isotropic.

Table 6.3 Physical and mechanical properties of specified rock types

Parameter	Basalt	Limestone	Sandstone	Shale	Quartzite
Density (g/cm^3)	n/a	2700	2000	2500	n/a
Porosity (%)	0.1-1.0%	5-30%	5-30%	10-30%	0.1-0.5%
Schmidt Hardness Index	61	35-51	10-37	n/a	n/a
Coeff of Permeability	10^{-14} – 10^{-12}	10^{-13} – 10^{-10}	10^{-10} – 10^{-8}	n/a	10^{-14} – 10^{-13}
P-Wave Velocity(m/s)	5000 – 7000	3500 – 6500	1500 – 4600	2000 – 4600	n/a
Elastic Modulus (GPa)	40-90	15 -55	1-30	1-70	50 - 90
Compressive Strength (MPa)	100 – 300	30 – 250	20 – 170	5 – 100	150 – 300
Tensile Strength (MPa)	10-30	6-25	4-25	2-10	2-20
Poisson's Ratio	0.1-0.2	0.18-0.33	0.21-0.38	0.2-0.4	0.17
Strain at Failure (%)	0.35	n/a	0.20	n/a	0.20
Point Load Index (MPa)	9-15	3-7	1-8	n/a	5-15
Fracture Mode I Toughness	>0.41	0.027-0.041	0.027-0.041	0.027-0.041	>0.41

It can be seen that comparisons can be made for many parameters. To draw key implications for chamber design based on rock type, findings from the 2nd Trinity College Dublin Colloquium on Rock Engineering for Ocean Wave Energy (Holland, 1997; Lindblom, 1997; Sterling, 1997) along with consultancy from Tara Mines Ltd. (McConnell, 2012) and Priority Drilling Ltd. (McCarthy, 2012) were utilised.

Basalt and quartzite have been identified as preferred rock types for SOWC construction and operation (Holland, 1997; Sewave, 2005). These permit minimum front wall thickness of approximately 5 m and maximum wide chamber spans of 12.5 m. A reason for this is their low porosity levels and coefficients of permeability. These properties increase their ability to withstand compaction forces.

Conversely, limestone, sandstone and shale possess higher porosity values. In these rock types where the size of pores can be of the same order of magnitude as the size of grains, the ability to withstand compaction forces is reduced. The force at which compaction failure takes place, relates to local shear forces acting through the grains and grain contacts. This is known as pore collapse, which typically consists of reorientation of the grains to better fill the void. This failure mode is normally observed in high porosity rock materials (Fjar et al., 2008) In line with this, the compressive strength of limestone, sandstone and shale is less than the compressive strength of basalt and quartzite which are less porous.

In underground engineering and tunnelling excavation, rock masses are subjected to compressive forces and lateral forces. The compressive strength with lateral pressures is known as the triaxial compressive strength. Triaxial compression tests can be used to measure the stress and axial strain behaviour for a given rock type. As elastic modulus is defined as the rate of change of stress with strain, this parameter in Table 6.3 describes the behaviour of a given rock when subjected to loads in different planes (Gu et al., 2008). There is correlation between compressive strength and elastic modulus. Hence, it can be seen in Table 6.3 that elastic modulus values are higher for basalt and quartzite when compared with limestone, sandstone and shale. Poisson's ratio measures the ratio of lateral strain to axial strain. Basalt and quartzite exhibit low values which indicate a stiffer material, compared with limestone, sandstone and shale.

The above points complemented with consultancy from Tara Mines Ltd. (McConnell, 2012) and Priority Drilling Ltd. (McCarthy, 2012) provided sufficient evidence that Sewave Ltd.'s findings with respect to front wall thickness and chamber width should be appropriately altered when the rock type differs from basalt. Specifically, for limestone, sandstone and shale, it was recommended that front wall thickness is increased beyond 5 m and chamber width reduced from 12.5 m. This reduces the risk of structural failure for both construction and operation of the SOWC wave energy converter.

Regarding Loop Head, Co. Clare, the predominant rock type is sandstone. Therefore, SOWC chamber designs installed at this location require front wall thicknesses greater than 5 m and chamber width less than 12.5 m. However, as the range of sandstone's physical and mechanical properties, described in Table 6.3 are relatively broad, further investigation into the geological composition at Loop Head was required to identify its specific structural properties. This relates to the homogeneity of the geology. Additionally, the School of Geological Sciences at UCD identified that the orientation of rock layering at Loop Head affects the structural properties of a specific site. Information on these aspects identifies further structural limitations on potential SOWC chamber designs.

6.5.2 Rock Homogeneity

From a geological point of view, the most suitable sites for SOWC installation consist of predominantly homogenous or suitably layered rock (Holland, 1997). This facilitates a necessary understanding of chamber design conditions and structural properties of the cliff. In line with this, it reduces the possibility of unforeseen structural risks associated with construction techniques required to excavate the chamber.

To investigate the homogeneity of the geology at a potential SOWC site, the drilling of a borehole at the site of interest is recommended. In the case of Loop Head, a separate research programme investigating the geology at coastal locations around Loop Head has been underway since 2009. The programme was co-ordinated by University College Dublin with Griffith Geoscience funding and support from

industry partners Statoil ASA (Haughton et al., 2010). Since 2009 over eight boreholes have been cored around the headland. The locations of five of these boreholes are presented in Figure 6.10 below.

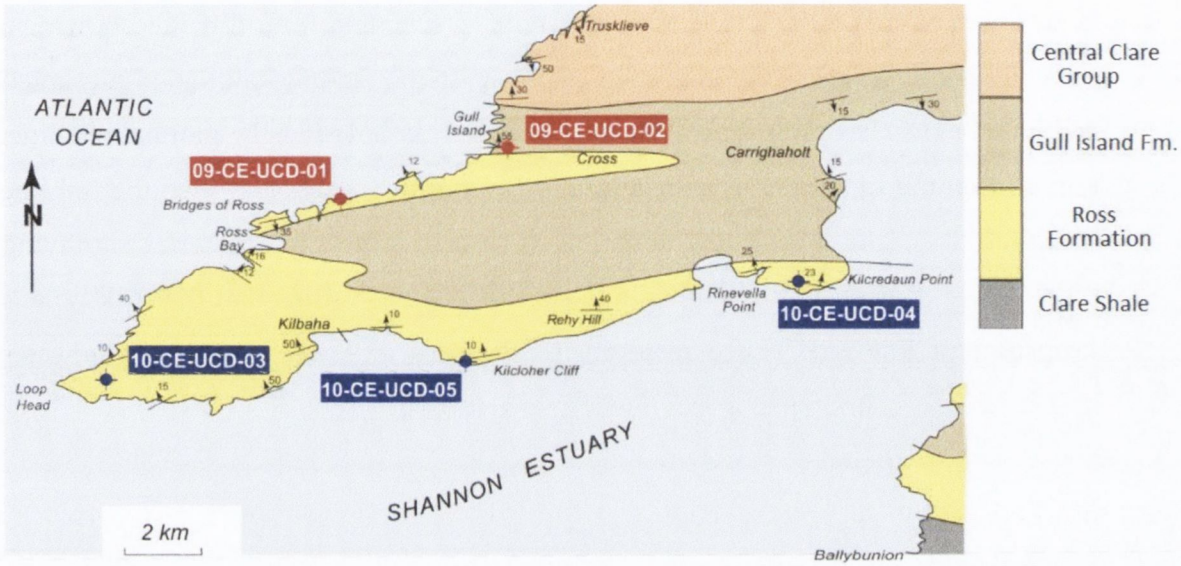

Figure 6.10 Locations of boreholes cored as part of the Co. Clare drilling and training initiative. Red: Proof of concept boreholes. Blue: Phase 2 boreholes. Source: (Haughton et al., 2010)

The geology of the most westerly section of Loop Head, from the headland's tip to Ross Bay, is comprised of the Ross sandstone formation. This formation consists of alternating, parallel bedded sandstones and dark shales. It can be seen in Figure 6.10 that the Ross formation (yellow area) predominantly covers the coastal perimeter of the headland. In line with this, the majority of potential SOWC sites are located in these areas. Additionally, the majority of boreholes were drilled at coastal locations, targeting the Ross formation.

A borehole cored vertically through the rock formation allows characterisation of the rock type at that location and provides information on the homogeneity of the geology. Regarding the boreholes cored at Loop Head, gamma ray logging was employed to analyse the geology. This method comprises lowering a gamma ray instrument into the borehole which then measures the naturally occurring gamma radiation at 0.15 m intervals. Since many rock types naturally possess levels of radioactivity, the gamma ray instrument measures the level of natural gamma rays emitted by the rock material surrounding the tool. Loop Head predominantly

comprises layers of sandstone and layers of shale and clay. Shale and clay possess higher levels of radioactivity compared with sandstone.

Therefore, analysis of results from the gamma ray logger allows the rock type to be determined, based on the levels of radioactivity. A schematic of a cliff site, showing a vertically cored borehole accompanied by its synthetic gamma ray log, is presented in Figure 6.11. The gamma ray log is presented as a vertically plotted red line, representing the radiation levels extending through the borehole. When the red line deviates to the right, it indicates an increased level of radioactive material, signifying shale or clay. When the red line deviates to the left, this means that the rock type is comprised of less radioactive material. In the case of Loop Head, this indicates sandstone. This is known as a wireline logging method.

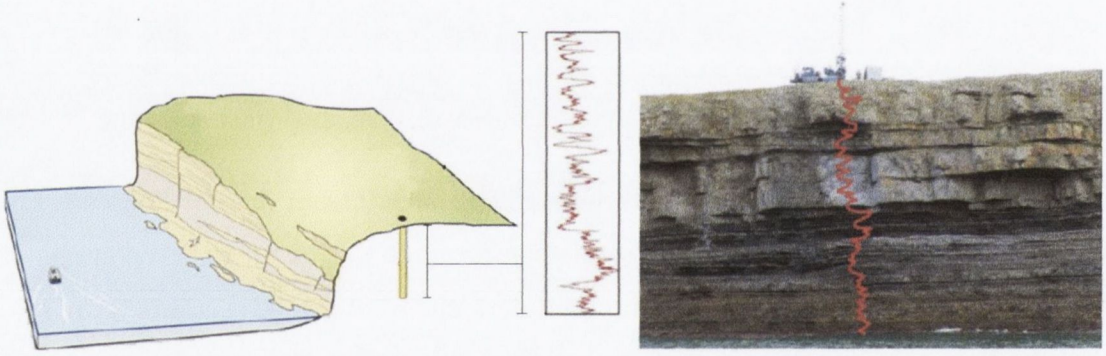

Figure 6.11 Schematic of cliff site with boreholes accompanied by a synthetic gamma ray log (left) and photograph of Loop Head Cliff with superimposed gamma ray log (right). Source: (Haughton et al., 2010)

The photograph in Figure 6.11 presents Kilcloher Cliff, located on the south side of Loop Head, as its borehole is drilled. A synthetic gamma ray log is superimposed on to the cliff face to highlight that the results from the gamma ray log may be compared with the observable geology at the cliff face. This technique facilitates an investigation in to the homogeneity of the geology extending from the cliff face inland. If the rock type indicated by the gamma ray log matches the geology at the cliff face at the same elevation, it provides evidence that the layer of rock extending inland is homogeneous. Analysis carried out by UCD on gamma ray logs for the aforementioned boreholes has suggested this to be the case for a number of sites around Loop Head. However, detailed information provided by each borehole, such as geotechnical logs, is not in the public domain. Additionally, as the boreholes are

sparsely populated, inferences on the homogeneity of rock strata between boreholes are accompanied by large levels of uncertainty. In the case of SOWC construction, further information is required to assess the homogeneity of rock strata in the horizontal plane.

Regarding the homogeneity of geology in the vertical plane at Loop Head, communications with the School of Geological Sciences at UCD has provided an insight to the geological characteristics of the Ross formation at coastal sites. Photographs of cliff faces at Loop Head, taken during the bathymetric survey described in Chapter 3, reveal considerable information with respect to the geological formation in the vertical plane. Photographs presenting a front elevation view and side view of a section of cliff located at the tip of Loop Head are presented in Figure 6.12 below. A filter was applied to each photograph to highlight geological features.

Figure 6.12 Front elevation view (left) and side view (right) of cliff section at tip of Loop Head. Height of cliff is circa 35 m above sea level.

Looking at the front elevation view, it can be seen that the cliff face consists of a number of layers of rock. The side view presents the profile associated with these layers. The rock layers depicted in the photograph on the left hand side correspond to the same layers in the photograph on the right hand side, which are portrayed at a different angle. The lower section of the cliff comprises thick layers of sandstone, as can be seen in the lower band bounded by two grey lines. Between these bands, vertical foliation layers can be observed. Foliation layers indicate that the layers of sandstone have been exposed to significant compressive loads. The thick layers distinguishable in Figure 6.12 comprise fine grained sandstone which is hard in nature and less porous than many compositions of sandstone. This finding narrows the range of the physical and mechanical properties for sandstone outlined in Table 6.3 The sandstone composition at this site possesses compressive strength between 100 MPa and 250 MPa.

With respect to homogeneity, the vertical cliff face is not solely comprised of sandstone. Between the upper band of grey lines, thin shaley layers can be identified. However, the elastic modulus, compressive strength and tensile strength values for shale lie in the same range as values for sandstone which reduce the negative aspects associated with cliffs comprising inhomogeneous rock types. The main structural concern with respect to rock homogeneity in the vertical plane is related to hollows and fissures within the cliff. Examples of hollows at the cliff face are highlighted in the grey boxes in Figure 6.12. As these are easily identifiable, they may be avoided when selecting potential SOWC sites. However, analysis of the cores and boreholes drilled at Loop Head has given evidence that fissures and hollows exist within the sandstone and shale layers extending inland from the coast. The possible existence of these irregularities located in a potential SOWC chamber construction zone increase the chance of unforeseen structural risks associated with construction techniques required to excavate the chamber.

The risk of fissures and hollows within the cliff also induce concern with respect to operation of the SOWC wave energy converter. Efficient operation of the oscillating water column concept requires a pressurised, sealed chamber. The potential presence of hollows of fissures at SOWC chamber walls could reduce efficiency levels in the pneumatic to mechanical stage of energy conversion. This reiterates the requirement

for geological surveys of potential SOWC wave energy converter sites. In the event that constructed SOWC chambers experience reduced aerodynamic efficiencies due to fissures and hollows within the cliff section, chamber linings have been identified as a potential solution.

6.5.2.1 Chamber Lining and Reinforcement

In mining, lining a shaft with concrete is frequently used to inhibit local deterioration and failure of the rock excavation. The lining may be used to support broken rock and to improve strength of rock mass by increasing lateral stress (Fjar et al., 2008). In the case of SOWC chambers at Loop Head, it may be required to provide a robust seal within the excavation. Additionally, rock support by means of rock bolts as well as sprayed concrete provide chamber reinforcement if required. These are discussed in Section 6.9 Construction and Design.

6.5.3 Orientation of Rock Layering

Regarding the orientation of rock layering, the most suitable sites for SOWC installation possess horizontal rock layering. The previously described section of cliff located at the tip of Loop Head (Figure 6.12) exhibits horizontal layering. This orientation provides favourable geotechnical conditions compared with tilted and vertical layering. At a number of locations around Loop Head, the cliffs possess tilted and vertical layering. The cliffs around Loop Head were once horizontally layered but due to compressive forces that have taken place over geological time, the rock formation has altered (Geological Survey of Ireland, 2005). At certain locations, the rock layering has been tilted or folded. In some cases geological folds have caused the layering to be rotated from horizontal to vertical laying. Examples of tilted layering and vertical layering on the northern coast of Loop Head were photographed during the bathymetric survey of the area (Figure 6.13).

Figure 6.13 Orientation of rock layering. Tilted rock layering (left) and vertical rock layering (right)

Regarding SOWC chamber construction and structural integrity, tilted and vertical layering induces increased structural instability compared with horizontal layering (Haughton et al., 2010). As a result, horizontal rock layering is favoured over tilted or vertical rock layering.

6.6 HYDRODYNAMIC EFFECTS

OWC wave energy converters have received considerable attention since the 1970s. From seminal papers authored by Evans (1978, 1982) to commercial companies involved in the development of full scale projects, much information exists on the hydrodynamic behaviour of OWCs. Evans outlines that the design of an OWC chamber requires knowledge of their hydrodynamic characteristics, which are quantified by the dynamic response of the inner fluid volume to the excitation from the outer flow (diffraction) and the generation of waves outside by the pressure variation above the fluid column (radiation flow).

Although substantial research has been carried out on OWCs, few studies have been conducted on the hydrodynamic effects associated with SOWC chamber designs, which possess inherently different geometries due to their structural limitations. The

chief structural limitations which dictate SOWC chamber design are front wall thickness, chamber width, depth of SOWC entrance and chamber incline. Each of these directly affects hydrodynamic behaviour of the water column. Prior to investigating these design parameters in the context of the SOWC wave energy converter via numerical analysis, findings from previous studies on conventional OWC chamber types are summarised. These summaries are presented under headings relating to the chamber design parameter: front wall thickness, chamber width, depth of OWC entrance and chamber incline.

6.6.1 Front Wall Thickness

Previous research has suggested the effect that an increase in front wall thickness has on performance (Delaure, Y, Lewis, 2003; Morris-Thomas et al., 2007; Wavegen, 2003; Weber, 2006). These studies relate to hydrodynamic analysis of the Pico OWC design, Oceanlinx's 2007 prototype OWC wave energy converter and the LIMPET OWC design. However, the maximum front wall thickness analysed in these major studies was 6.7 m at full scale for the Pico Design. Based on research carried out in Section 6.4 Structural Integrity, the SOWC front wall thickness is generally required to be greater than 6.7 m to uphold the chamber's structural integrity within the cliff. Therefore, in the present research a priority was placed on the effect of alterations in front wall thickness beyond 6.7 m. Additionally, the Pico design does not possess an incline and chamber inclines are inherent to SOWC construction techniques.

Regarding findings from the aforementioned studies, resonant period and bandwidth were shown to increase with increased wall thickness. This was found in both physical and numerical modelling tests. In general, an incremental increase greater than 0.5 m is necessary to induce an influential difference in resonant period at full scale. The most relevant finding relates to Delaure and Lewis (2003) which considered two front wall thicknesses that corresponded to full scale dimensions of 1.8 m and 6.7 m. The study was carried out at 1:36 scale. Thus, the actual front wall thicknesses were 51 mm and 187 mm. The fundamental chamber design was the Pico plant. When extending the front wall thickness from 51 mm to 187 mm, it was found that the resonant period increased by 0.2s. The study inferred that, at full scale, this corresponds to an increase of 1.2s.

This finding is important as it shows that the thickness of the front wall influences the frequency at which the water column resonates. The reason the natural frequency altered was due, in part, to the increase in chamber volume which induced a greater mass of water within the chamber. If the greater front wall thickness which the SOWC requires, in comparison to other OWC designs, moves the resonant frequency towards the target resonant frequency associated with the prevailing wave climate, annual power production may be increased. Therefore, an objective of this study was to determine trends associated with altering frontwall thickness, predominantly relating to alterations in resonant frequency and annual average power absorption at potential SOWC sites. This was achieved via analysis of isolated chambers exposed to a range of appropriate wave frequencies and in conjunction with wave conditions associated with Arch Point and the tip of Loop Head. Specifically, this facilitated SOWC chamber design optimisation for specific locations of interest, within the bounds of structural limitations. (These studies can be seen in Section 7.9 and 7.10).

As inferred above, these effects related to efficiency associated with the prevailing wave climate and thus, these effects accrue over time and would be reflected in annual power production. However, the effects of increasing wall thickness on the efficiency of power production per water column oscillation are more complex.

The aforementioned study by Delaure and Lewis (2003) also showed that the response of the water column was amplified to an extent at resonance. This would suggest a greater efficiency of power production with increasing front wall thickness. However, in contrast, Morris-Thomas et al. (2007) analysed Oceanlinx's 2007 precommercial prototype OWC at 1:12.5 scale. Two front wall thicknesses were considered, relating to 0.5 m and 1 m at full scale. When extending the front wall to 1m, a decrease in efficiency was found which was explained by an increase in flow seperation in the vicinity of the chamber orifice. Furthermore, at full scale it is expected that hydrodynamic losses will increase with increased front wall thickness (Whittaker, 2013).

6.6.2 Chamber Width

As mentioned in Section 6.3.3 Wave Power Levels, a wide chamber and large water plane area induces a greater intake of wave power than a narrow chamber with a small water plane area. This detail is important when designing a SOWC chamber for a site specific wave climate, based on a target power production capacity. In addition to this, there are hydrodynamic affects to take into consideration when specifying chamber width. As the width of the column increases there is an increasing risk of transverse excitation within the water column. This phenomenon can reduce the energy capture performance of the water column (Wavegen, 2002). Research on the inclined LIMPET design has suggested that a noticeable decline in performance takes place when chamber widths extend beyond 12 m. However, for chamber widths up to 12 m, Figure 6.14 implies that transverse excitation effects do not greatly affect performance.

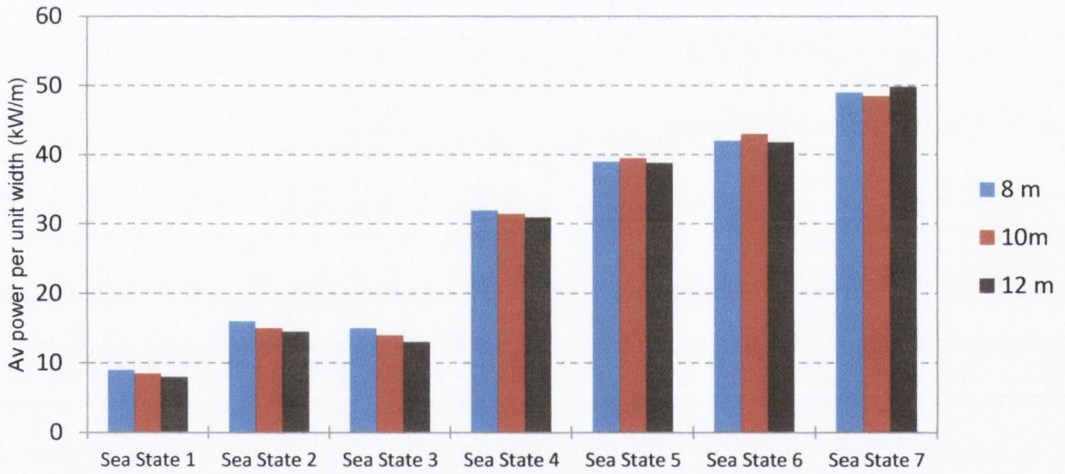

Figure 6.14 Influence of device width on pneumatic power capture per unit width. Source: (Wavegen, 2003) Chamber design: LIMPET. Device widths: 8 m, 10 m and 12 m.

Figure 6.14 presents results from a set of tests carried out by Wavegen on the LIMPET design (Wavegen, 2003). The effects of chamber width on performance were investigated while keeping all other design parameters constant. The conclusion from this study stated that transverse waves in the chamber did not develop for widths up to 12 m as the device width was only a small portion of a typical wave length. Hence, average power per unit width (kW/m) did not decrease significantly up to a chamber width of 12 m.

This finding is extremely relevant to SOWC chambers constructed within geological conditions outlined in Section 6.5, as the maximum permitted width was 12.5 m. Thus, effects due to transverse wave excitations may be demoted when designing a SOWC chamber at the proposed locations. This finding extends to SOWC chamber designed for Loop Head which possesses a geological composition of predominantly sandstone and shale.

Regarding hydrodynamic performance it is recommended that the chamber width account for expected wave directionality. If waves commonly approach the SOWC wave energy converter at an angle, there is potential for a crest and a trough to inhabit the chamber at the same time. This occurrence negatively impacts hydrodynamic performance. However, findings from The Carbon Trust's report evaluating OWC chamber designs suggested a limiting chamber width of 40 m for shoreline and near-shore OWCs (The Carbon Trust, 2005). Thus, for SOWC chambers which are less than 12.5 m wide, this phenomenon should not be an issue.

6.6.3 Depth of OWC Inlet

The predominant design criterion for this parameter relates to reducing the risk of inlet broaching. This takes place when a deep wave trough temporarily causes the water level to fall below the level of the SOWC entry lip, causing a direct air passage between the pressurised air chamber and the outer atmosphere. This has a detrimental effect on hydrodynamic performance. The sudden change in pressure within the plenum significantly reduces power production. In contrast to this, an OWC inlet close to the mean water level intakes higher wave power levels due to the increased levels of wave energy in the proximity of the free surface. OWC inlets positioned deep below the mean water level cause the portion of incoming wave energy above the inlet to be reflected. Therefore the optimal OWC inlet depth lies as close to the surface as possible, without inducing risk of inlet broaching. Previous full scale OWC projects have shown that the risk of inlet broaching can be significantly reduced by positioning the inlet orifice a minimum of 25% water depth below the mean low water spring tide at the installation site (Carbon Trust, 2005). Based on tidal data for Loop Head presented in Chapter 4, it is recommended that the minimum depth of inlet should be 4.0 m below mean water level.

The Depth of OWC inlet also affects the natural period of the device (Delaure and Lewis, 2003). To investigate whether this design parameter may lend itself as a means to tune the SOWC to the target period for a given site, hydrodynamic analysis was carried out on three inlet depths: 3m, 4m and 5m below mean water level. To quantify the effect inlet depth had on the natural period of an established OWC chamber design, the Pico design was employed. The overall chamber design and inlet area was maintained. Using the BEM code WAMIT, each chamber design was analysed with the hydrodynamic model set-up described in Chapter 7. The natural period for each inlet depth (3m, 4m, 5m) can be identified in Figure 6.15 below.

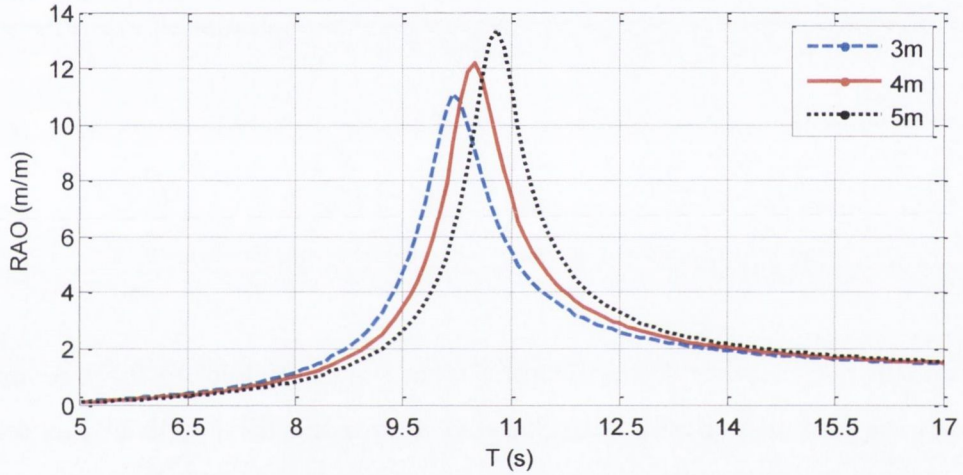

Figure 6.15 Response amplitude operator (RAO) for three SOWC chamber designs. Depth of inlet equal to 3m, 4m and 5m below mean water level.

The peak response of each plot signals the natural period of the OWC. It can be seen that deepening the OWC inlet by 1 m increases the natural period by approximately 0.4 s. An equivalent investigation was carried out for SOWC chamber designs presented in Chapter 7. It will be seen in Chapter 7 that SOWC chamber geometries within required design bounds possess high natural periods greater than the target period at Loop Head. In terms of tuning the SOWC to the prevailing wave climate, no benefit may be gained by increasing the depth of the inlet. Therefore, the inlet depth was based on the tidal range at Loop Head. For SOWC chamber designs analysed in Chapter 7, the inlet depth is set at 4 m below water level.

6.6.4 Chamber Length

The length of the chamber can be divided into two sections; (1) the section leading from the OWC inlet to the free surface of the oscillating water column and (2) the section comprising the air plenum, which denotes the pressurised volume of air between the free surface and the turbine inlet.

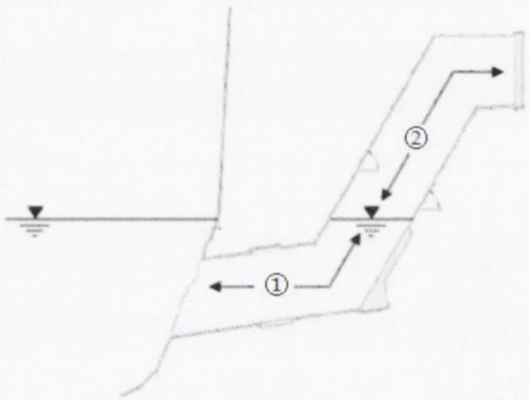

1. Section leading from the OWC Inlet to the free surface
2. Section comprising the air plenum

Figure 6.16 Sections of the SOWC chamber (cross sectional view)

The length of the chamber section leading from the OWC inlet to the free surface influences the natural period of the chamber. Increasing the length of this section increases the period at which resonance takes place. Figure 6.17 illustrates this by comparing the response of three chamber lengths 410 mm, 325 mm and 260 mm.

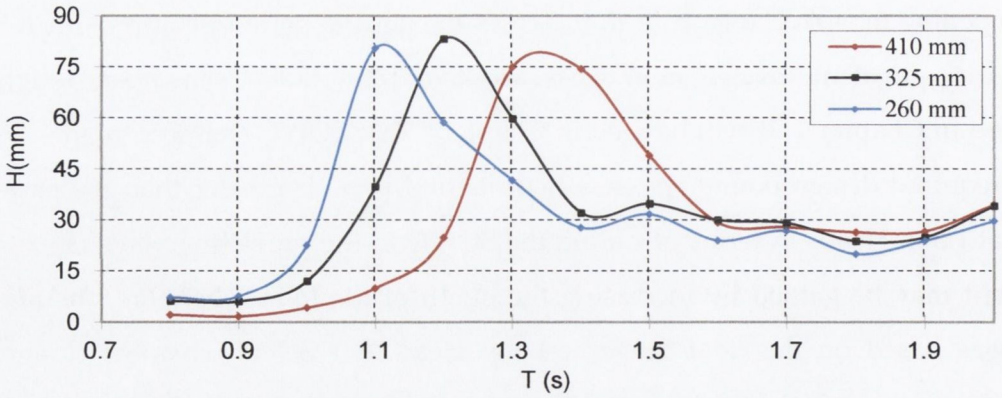

Figure 6.17 Effect of chamber length on resonance. Amplitude within chamber, H (mm), vs. wave period, T (s).

These chamber designs were tested in a wave flume at the HMRC during a recent training course on 'Experimental Testing in Wave Tanks and Flumes', run as part of

the MARINET programme (2012). The wave flume was 25 m long by 3 m wide and 1 m deep. Each chamber was fixed to a metallic frame. The wave flap and generator were located at the upstream end of the flume approximately 12.8 m in front of the OWC models. The rectangular flap wave maker was hinged at its base and driven by a D.C. motor. Wave regimes applied to the models were controlled via a wave generation computer programme. Active power absorption was built in the wave generation system to minimise interference associated with reflected waves. The passive absorption materials placed at the downstream end of the gently sloping beach further minimised reflected waves affecting accurate hydrodynamic analysis of the OWC chambers. The power take off was represented by an applied damping induced by an orifice plate at the top of the chamber. An orifice to water plane area ratio of 1:16 was applied to each of the three chambers. The scale of the OWC models was 1:50.

To determine the natural period for each of the three chamber lengths, 11 monochromatic tests were run with different wave periods. Wave probes were employed to measure the incident wave field and the surface elevation within the OWC chamber. Each probe was aligned on the centreline of the flume with a spacing defined according to Mansard and Funke calibration method specifications (Mansard and Funke, 1980). Within the chamber under investigation, a wave probe was positioned at its centroid. Using this apparatus, the surface elevation of the oscillating water column was recorded for wave periods ranging from 0.8 s to 2.0 s with 0.1 s increments. It can be seen in Figure 6.17 that increasing chamber length, increases the natural period of the water column. Although the differences in natural period are small at the 1:50, the principle is magnified for larger designs. This topic will be revisited in Chapter 7 in the context of full scale chamber performance when exposed to wave climates associated with Loop Head, Co. Clare. This design parameter is a predominant means of tuning the SOWC wave energy converter to the wave climate.

Regarding the section of chamber comprising the air plenum, previous research has shown that air compressibility increases with plenum chamber volume and for the majority of OWC operating conditions, air compressibility reduces power capture (Folley, 2005). Chamber length also affects pneumatic efficiency via frictional affects caused by the chamber wall. Frictional resistance varies in proportion to airway

length (Munson et al., 1990). Hence, airway losses increase with chamber length due to frictional resistance. However, shorter chamber lengths with a smaller air plenum induce higher pressure and greater air flow, to which conventional OWC turbines have been designed. These points relate to conventional OWC structures comprising of concrete or steel. Although, these points are valid for SOWC chamber design it is speculated that frictional effects may be increased due to tunnelling construction as opposed to conventional methods.

With respect to the frictional effects of chamber walls associated with SOWC chamber construction, few studies address this aspect. To the author's knowledge, the most relevant work on this was carried out during a study which explored the potential for using disused coastal mineshafts to exploit wave energy via the OWC concept (Scholes et al., 2004). The mineshafts analysed revealed rough walls and sudden changes in cross sectional area which induced detrimental effects on air flow and pressure in the context of turbine operation. Crudely, longer shafts were expected to possess more cross sectional changes than shorter sections of chamber. Conclusions recommended the shortest airway to the turbine possible.

Two limitations with respect to reducing chamber length relate to excessive pressure levels and exposing the turbine to sea water. As higher pressures are induced in smaller air plenums, there is an increased risk of approaching pressure levels that may affect the turbine operation and to a greater extent, the structural integrity of the chamber. This issue may be overcome by increasing the chamber length or implementing relief valves as described in Section 6.7.1. A dominant factor countering short chamber design pertains to the risk of exposing the turbine to high levels of sea water. To combat the risk of exposing the turbine to seawater during energetic sea states and facilitate short chamber lengths, fast operating valves in front of the turbine have been proposed in a prominent report published as part of a European effort to disseminate ocean energy (WaveNet, 2003).

However, in this study which aims to define the bounds of SOWC chamber design at Loop Head, Co. Clare, the minimum chamber length was set in accordance with The Carbon Trust's Oscillating Water Column Wave Energy Converter Evaluation Report (2005). This considers maximum wave amplitude within the chamber at mean high

water level (MHWL) at Loop Head. As seen in Chapter 4, MHWL is +2.1 m with respect to local datum at Carrigaholt on the south side of Loop Head. At MHWL, the maximum amplitude was estimated as +8.5 m. This was based on design, operation and results from previous full scale OWC projects, namely Pico (Falcão, 2009) and LIMPET (Wavegen, 2002). This accounted for chamber incline, back pressure caused by the turbine and more extreme wave climate compared with LIMPET's site location. LIMPET predicted a maximum amplitude of +3.3m, which at MHWL, equates to +5.9m with respect to local datum. The turbine is positioned at +8.54 m. Hence, a distance of approximately 2.64 m gap exists between maximum water level within chamber and turbine position (The Carbon Trust, 2005). A conservative 5 m gap was taken for the SOWC design due to extreme sea states associated with Loop Head, giving a turbine position of 13.54 m above local datum. This reduces the risk of seawater ingestion by the turbine. Pico has suffered this consequence during extreme sea states with a turbine position of +8.02 m above local datum (Falcão, 2009).

6.6.5 Chamber Incline

An inclined chamber is favourable for performance and SOWC construction. Regarding hydrodynamic performance, an incline stimulates water ingress and egress resulting in less turbulence and lower energy loss (The Carbon Trust, 2005). Additionally, an angled chamber increases the water plane area which in turn, exerts force on a larger area of air compared with a vertical chamber. For all inclines, columns with parallel front and rear walls below the water line induce the best performance. Tank testing carried on the SOWC concept in the HMRC investigated the effect chamber incline had on performance using a 1:40 scale model. Overall results recommended a chamber incline of 60° (Holmes, 1997). It will be seen that a 60° incline is also favourable in relation to construction.

6.7 Construction and Design

Prior to describing a proposed construction process for the SOWC wave energy converter designed for Loop Head, it is acknowledged that there are a number of important factors that affect planning permission for a project of this nature. Loop Head possesses designated Special Areas of Conservation (SACs), National Heritage Areas (NHAs) and Special Protection Areas (SPAs) which oppose new constructions.

Outside these areas, the following consenting is required prior to construction: foreshore license for site investigation, foreshore lease, environmental impact statement, natural impact statement, planning permission statement and a grid connection offer (Slevin et al., 2011). However, this section simply aims to present a potential construction method for a chamber design based on bounds identified in the previous section.

Having identified the bounds of chamber design at Loop Head, further investigative work on the required construction technique was carried out. Due to details presented in Section 6.6.4 Chamber Length, a SOWC design has been adopted which places the power take off approximately 13 m above local datum. In short, this induces favourable turbine operating conditions and performance as energy losses due to frictional resistance and air compressibility are minimised.

To position the turbine circa 13 m above local datum, an access tunnel is required to lead from ground level to the specified location of the turbine. The necessary length of this tunnel, and hence cost, is dependent on the cliff height and topography. Access tunnels may be constructed via conventional drill and blast methods, providing a passageway at an appropriate gradient to the designated level above local datum.

With respect to this, identification of exact sites that favour access tunnels was outside the scope of this study. The objective of this section was to identify the stages of construction subsequent to the construction of an access tunnel. The stages of construction described are those proposed by Sewave (2005) and Tara Mines (2013). Each stage is accompanied by a simplified cross sectional view of the cliff site, presented in Figure 6.18 (i) - (viii).

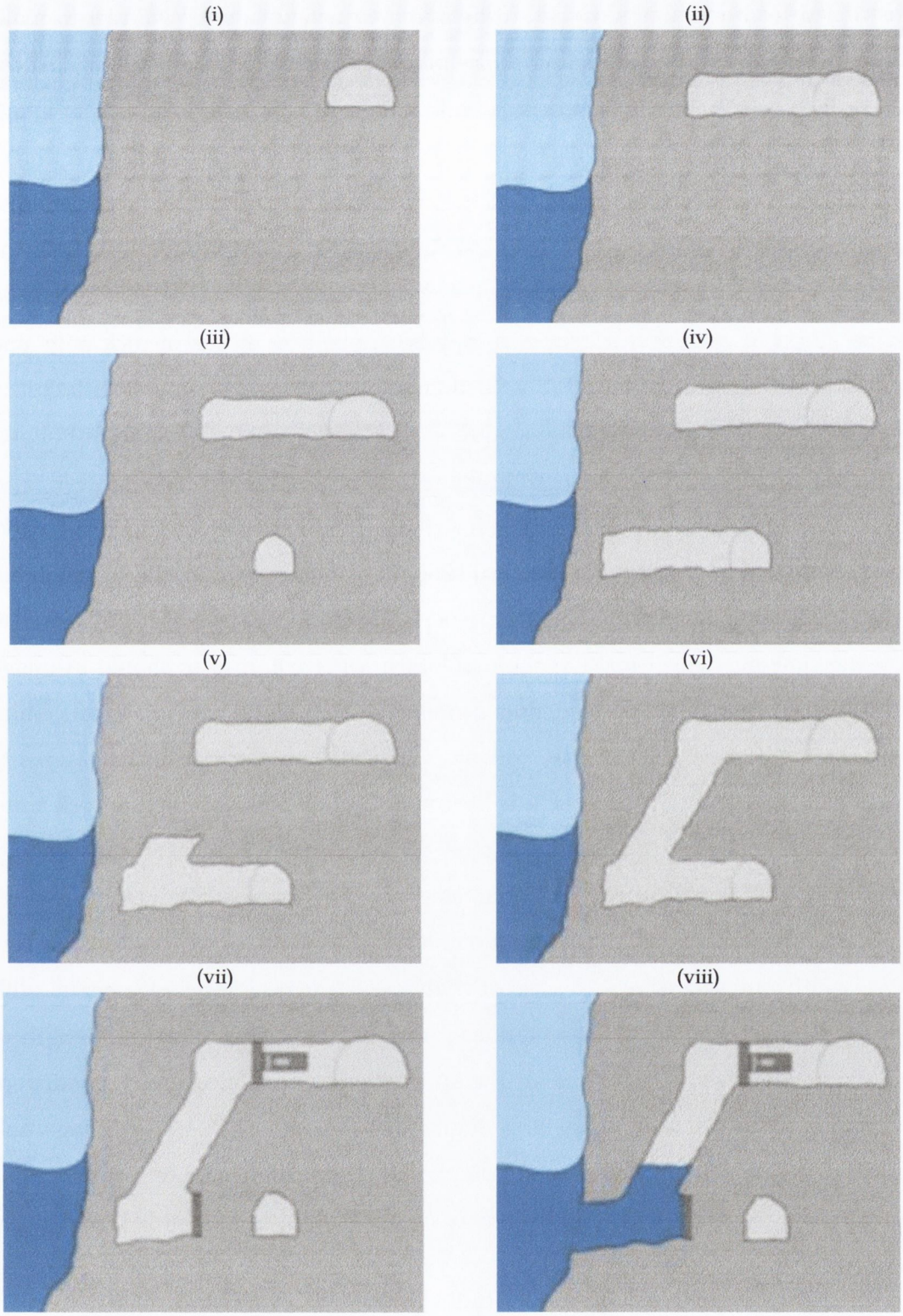

Figure 6.18 Construction option proposed by Sewave (2005): Stages (i) – (viii) of construction plan

Following the construction of the access tunnel, presented in the upper left corner of image (i), a tunnel is excavated to house the turbine and power take off. This will be referred to as the upper cross tunnel, shown in image (ii). Subsequently a tunnel is

constructed from the access tunnel to the specified level of the OWC inlet to make preparations for the tunnel leading to the ocean, as displayed in image (iii). At the level of the OWC inlet, the tunnel is extended towards cliff face, as shown in image (iv). This will be referred to as the lower cross tunnel. The inclined vertical section of the OWC is then drilled and blasted, joining the lower cross tunnel to the upper cross tunnel, as shown in image (vi). Prior to the final excavation, which exposes the chamber to ocean waves, inspections of the vertical inclined chamber may be carried out. Based on inspection, rock support may be applied by means of rock bolts and sprayed concrete. This stage of construction also facilitates the implementation of concrete lining, if chamber sealing is required due the presence of fissures or hollows within the construction. Subsequently, the chamber is sealed from the lower cross tunnel and upper cross tunnel, except for the turbine inlet orifice and relief valve orifice, as shown in image (vii). The final tunnel excavation, connecting the chamber to the ocean, completes the chamber construction process. This allows ocean waves to enter the chamber which initiates the oscillating water column, as shown in image (viii). Regarding the full construction process, the final drill and blast procedure possesses the highest level of risk (Sewave, 2005). Potential precaution measures to reduce risk of structural failure include the application of rock support via rock bolts, grouting and concrete spraying. Details on these measures have been provided by Tara Mines (2013). Rock bolts of 33 mm steel rebar at approximately 1.5 m centres and 6.0 m long cable bolts into the roof increase the structural integrity of chambers where widths are excessive. The use of shotcrete (70 mm of sprayed concrete with steel fibre mixed similar to metro tunnels) may be applied to improve strength of rock mass by increasing lateral stress. The application of these measures is contingent on chamber inspection by tunnelling engineers. The use of chamber linings and additional reinforcements directly affects capital costs and hence, techno-economic viability. The inclusion and implications of chamber linings is outside the scope of this study.

In relation to chamber incline, a 60° angle was applied throughout this study for the following reasons: (i) it is favourable for hydrodynamic performance, as established in the initial study on the SOWC concept (Holmes, 1997), (ii) it induces a sufficient level of overall structural integrity (Sewave, 2005), and (iii) it allows cut or blasted rock to overcome friction and slide out of the chamber (Tara Mines, 2013).

6.7.1 Relief Valves

In addition to designing the SOWC wave energy converter to withstand wave loads, a strategy is required to handle high pressure levels within the chamber. The solution adopted by the majority of OWC wave energy converters to date is relief or 'blow-off' valves. During energetic sea states, high levels of pneumatic power within the chamber can induce pressure levels that may affect the structural integrity of the chamber and operation of the turbine. The inclusion of relief values, allow excess pressure to flow to the atmosphere. Both Pico and LIMPET have protection valves (a vertical sluice-gate in Pico and a butterfly valve in LIMPET) (Falcão, 2004). Further information on these is presented in Results from the work of the European Thematic Network on Wave Energy (WaveNet, 2003) and a summary report on LIMPET (Whittaker et al., 2002). The consequence of not installing a relief valve in a full scale OWC chamber was realised in the early 1990s off the south west coast of Ireland, during a project aimed at extracting energy from a natural blowhole. The Commissioners of Irish Lights explored the opportunity to harness wave energy for a Lighthouse located on Bull Rock, an island off West County Cork. Concrete was used to seal the cavern leading to the natural blowhole. Without a means to dissipate excess pressure within the chamber, structural failure occurred when exposed to high pneumatic power during a storm (McCormick, 2012).

Installation of relief valves in a SOWC chamber design differs to that for a conventional OWC chamber. To relieve excess pressure, detouring airflow past the turbine directly to atmospheric pressure, a venting shaft is required. This comprises a direct shaft from the chamber to an environment at atmospheric pressure, which allows the airflow to bypass the turbine. The design and installation of a relief valve is site specific (The Carbon Trust, 2005) and dependent on the wave climate. Based on valve diameters for Pico and LIMPET, coupled with their chamber size and wave climates, a maximum relief valve diameter of 3.5 m is estimated. These can be opening from 0% to 100% according to the sea state (Crom et al., 2009). Although the modelling of relief valves is outside the scope of this study, it is an important design feature specific to the SOWC concept and must be included in costing estimates for SOWC wave energy converter construction.

6.8 TURBINE SELECTION

In SOWC design turbines are used to convert pneumatic power into electrical power. To optimise power take-off, a turbine must be designed to fit with the characteristics of a specific SOWC. The design of an appropriate turbine or power-take off unit is dependent on the wave power level (Section 6.3.3), which is related to the significant wave height of the impinging waves (Sarmento et al., 2001). Fundamentally, the pneumatic power generated by the chamber design at the selected deployment site should induce appropriate operating conditions for the selected turbine. Reciprocally, an appropriate turbine design should apply a damping to the system that induces satisfactory annual performance. As stated in Section 6.3.3, the level of wave power at a potential SOWC site affects the size of the chamber required to achieve the target power generation capacity (kW) set for the project in question. Additionally, costs of turbines presented in Table 6.1 show that higher power capacities are more cost effective.

Turbines with higher power ratings differ in terms of their size, design and damping, which should be matched appropriately to the operating conditions induced by the chamber. The characteristics of the damping depend on the type of turbine, its spoke dimensions and operational rotational speed. Several self-rectifying turbines have been developed for the application of alternating airflow in OWCs, each with their own characteristic curves for mechanical power vs. pressure difference. In this study, a number of Wells turbines are considered. The Wells has an almost linear relationship between pressure drop and volume flow, and may be modelled as a simple linear damping. More specifically, the turbine damping is related to turbine radius, r, hub to tip ratio, h, and running speed, ω (rad/s) by the proportional relationship shown below (Equation 6.8).

$$Turbine\ Damping = \frac{k\omega}{r(1-h^2)} \tag{6.8}$$

where k is a constant dependent on the solidity, S, of the turbine. Solidity is defined as blade plan form blockage area divided by the annular duct area where the rotor rotates. Since there is a limitation on tip velocity (Mach 0.55 with $v = r\omega$), the damping is effectively related to (Equation 6.9):

$$Turbine\ Damping \propto \frac{k}{r^2(1-h^2)} \tag{6.9}$$

This assumes that at times of maximum generation, the turbine is running at maximum speed. Therefore, the primary design factors that can be used to induce an optimal damping and hence, conversion efficiency, are turbine radius, solidity and hub to tip ratio. More specifically, the damping of a particular turbine can be calculated using the Equation 6.10.

$$B_A = 0.2625\omega D_t^3 A_R^2 N_p (1-h^2)\left[tan(\frac{\pi}{2}S)\right] \tag{6.10}$$

Where D_t is tip diameter (m), ω running speed (rad/s) ; $A_R = A_c/A_A$; Column to duct area ratio; A_c Water column cross sectional area (m2); $A_A = 1/4\pi D_t^2(1-h^2)$; Turbine duct area (m2); N_p number of rotor planes; h hub to tip ratio and S Solidity.

Matching the turbine to the chamber can be achieved by comparing the turbine's characteristic damping values at operational running speeds with the theoretical optimal turbine applied damping for a given chamber design. To calculate the optimal turbine applied damping which maximises power output for the OWC, the Equation 6.11 is employed:

$$B_{A\,opt} = \left[B_2^2 + \left[\frac{K - M_E\omega_i^2}{\omega_i}\right]^2\right]^{1/2} \tag{6.11}$$

Where $B_{A\,opt}$ is optimal level of turbine applied damping; ω_i Angular frequency (rad/sec) of ith frequency; k water plane stiffness; given by $K = A_c\rho_w g$; A_c Surface area of OWC; ρ_w Density of water; M_E Effective mass of water column (entrained mass + added mass); B_A Applied damping which extracts energy from the system (representing the turbine); B_2 Secondary damping (radiation damping) + damping losses. As part of this research programme, Equation 6.11 was employed in Chapter 7 to match a standard manufactured Wells turbine to specific SOWC chamber designs.

6.9 SUMMARY

While Chapters 4 and 5 focused on the first aim of the research programme, which was to characterise the wave climate for a domain off the coast of County Clare adjacent to Loop Head, this chapter and Chapter 7 focus on the second aim of the overall research programme, which was to use the findings from a wave climate modelling study conducted to achieve the first aim and build upon an earlier TCD (Marine Institute, 2000) study to investigate design parameters which may influence the survivability and feasibility of potential SOWCs installed at Loop Head. Factors affecting optimal SOWC chamber design were considered in this chapter. These included wave climate, target capacity (kW), structural integrity, geology, hydrodynamic effects, construction method and turbine selection.

The percentage occurrence of each sea state at potential SOWC sites allows the target resonant period to be identified. The level of the wave energy resource affects the size of the SOWC chamber required to achieve a given target power generation capacity. Regarding favourable characteristics of potential SOWC sites, water depths greater than 15 m induce sufficient wave power levels to promote cost effective power generation. Additionally, the 15 m depth contour is seen as the outer limit of the wave breaking zone for the majority of sea states experienced at Loop Head. This benefits the average annual wave energy resource, the level of accuracy associated with wave climate modelling of the site and the cyclical wave loads applied to the front wall of the SOWC. In terms of extreme sea states, sites that promote spilling waves rather than plunging waves are preferred as the increase in force associated with a plunging wave is significant. These aspects of the wave climate allow the idealised chamber design to be hypothesised.

An idealised chamber design comprises tailored geometrical parameters that induce a natural hydrodynamic response at the target resonant period which gives optimal annual power conversion efficiency at the SOWC installation site. The idealised design is then compromised by structural considerations. Section 6.4 Structural Integrity and Section 6.5 Geology highlighted that the maximum chamber width and minimum front wall thickness for SOWC designs installed at Loop Head are 12.5 m and 5 m respectively.

Section 6.6 detailed hydrodynamic effects that influence the performance of the SOWC wave energy converter. Based on this, the SOWC inlet at Loop Head should be set 4 m below mean water level and the turbine positioned approximately 13.5 m above local datum. A chamber incline of 60° is favourable for performance and SOWC construction.

The construction method assumed during this design process was that described in Section 6.7. Considering the aforementioned design bounds imposed on SOWC design, there is an incentive to optimise performance within a chamber width of 12.5 m. With many aspects of OWC design well documented, a knowledge gap remains concerning extending the front wall thickness to dimensions required to uphold the structural integrity of an SOWC wave energy converter. Work carried out on this aspect is presented in Chapter 7 on hydrodynamic analysis in parallel with an assessment of the performance of different SOWC chamber designs at locations of interest at Loop Head.

Chapter 7
HYDRODYNAMIC ANALYSIS

Factors affecting optimal SOWC chamber design were considered in Chapter 6. Clément (2003) has outlined that numerical hydrodynamic modelling is a particularly useful method for optimising WEC design and so this approach was taken in this research programme. In the current chapter, results of a series of hydrodynamic analyses will be presented which validate a numerical model of a SOWC and throw light on how the design of this WEC may be optimised. Together these two chapters (6 and 7) focus on the second aim of the overall research programme, which was to use the findings from a wave climate modelling study conducted to achieve the first aim and build upon an earlier TCD (Marine Institute, 2000) study to investigate design parameters which may influence the survivability and feasibility of potential SOWCs installed at Loop Head. In the preceding two chapters (4 and 5) the focus was on the first aim of the research programme which was to characterise the wave climate for a domain off the coast of County Clare adjacent to Loop Head, as this is an area of interest for ocean energy development in Ireland. Output from the spectral wave model, the development of which was described in Chapters 4 and 5, served as input for the hydrodynamic analyses which will be presented in this chapter.

Chapter 6 identified the values of parameters of SOWC designs which lead to optimal performance at two locations on Loop Head. It also indicated that design parameters which need to be altered from values associated with optimal performance in order to optimise SOWC survivability are (i) front wall thickness and (ii) chamber width. In this chapter numerical hydrodynamic analyses will be described which were used to compare the performance of different chamber designs. In these analyses variations in two performance indicators associated with

variations in relevant SOWC design parameters were examined: (i) the upper limit for mean annual power absorption and (ii) the capture width ratio. Trends identified in efficiency levels for designs favoring survivability versus performance provided preliminary information regarding the feasibility of installing SOWC as constructed by the technique in question at Loop Head. To establish the validity of the hydrodynamic model set up, benchmarking comparisons were made with corresponding physical models and relevant studies.

Research objectives addressed in this chapter, relevant to the second aim of the overall research programme (which was to use the findings from a wave climate modelling study conducted to achieve the first aim and build upon an earlier TCD (Marine Institute, 2000) study to investigate design parameters which may influence the survivability and feasibility of potential SOWCs installed at Loop Head) include the following:

- To develop a numerical hydrodynamic model of a SOWC wave energy converter
- To validate the set-up of this hydrodynamic model by benchmarking it against tank testing data
- To validate this model by benchmarking it against a model of the full scale Pico OWC (Brito-Melo et al., 1999)
- To use a hydrodynamic model to identify trends in efficiency associated with changes in SOWC design parameters which may be necessary to promote the survivability of these WECs in their potential locations at Arch Point and the tip of Loop Head.

7.1 METHODOLOGY

The methodology for hydrodynamic numerical modelling was developed to achieve the research objectives listed above. This methodology permitted alterations in SOWC chamber design; assessment of hydrodynamic performance when chamber design is altered; inclusion of power take off characteristics; inclusion of site specific wave conditions at locations of interest; assessment of SOWC chamber design performance at locations of interest; and identification of trends in performance when chamber design and location were altered. What follows is a description of aspects of

the methodology including model formulation, selection of performance indicators, numerical modelling software, the benchmarking process, and assessments of performance of SOWCs with different chamber designs at two sites on Loop Head.

Model Formulation

A hydrodynamic model was adopted to assess the hydrodynamic properties of wave and wave-structure interaction associated with three dimensional SOWC chamber configurations when certain design parameters were altered. Central to this was selection of the equation of motion for a fixed SOWC that lent itself to answering the aforementioned research questions. Additionally, a suitable type of power take off (PTO) system was incorporated to allow determination of the performance indicators for a given SOWC wave energy converter configuration. This process facilitated calculation of the power function for given chamber designs and PTOs.

Performance Indicators

To assess the hydrodynamic behaviour of a given SOWC design, the following hydrodynamic properties were calculated: added mass M_a, radiation damping B, excitation force F_{ex}, response amplitude operator (RAO) and the upper limit for power absorption $p(\omega)$, for a range of designated wave frequencies. In order to answer the research questions regarding the effect different chamber designs have on performance at locations of interest, suitable performance indicators were required. The performance indicators employed were the upper limit for mean annual power absorbed, $\overline{P_{max}}$, and capture width ratio η. These are detailed in Section 7.3 Performance Indicators. The RAO identifies the frequency of the incident wave climate to which a given chamber design is best tuned. The upper limit for mean annual power gives a measure of the performance of a given design in a given location over a year. It can be used to compare levels of performance for different designs in the same location. Capture width ratio is denoted as absorbed power divided by incident power and is a measure of efficiency. It can be used to compare different designs in different locations.

Numerical Modelling Tools

SOWC chamber configurations were constructed using a geometric modelling program, Multisurf version 8.0 (Aerohydro, 2011). The Boundary Element Method

(BEM) code, WAMIT (WAMIT, 2011) was then employed to calculate the frequency dependent hydrodynamic coefficients for given SOWC designs in the presence of surface waves. These hydrodynamic coefficients were required to solve the equation of motion and hence, assess the hydrodynamic characteristics of specific chamber designs. Input files for WAMIT were developed to appropriately model a fixed SOWC wave energy converter for a range of suitable wave periods. Outputs from WAMIT were post-processed using Matlab® (Mathworks, 2013). Post processing involved the extraction of hydrodynamic coefficients corresponding to the free surface of the SOWC at each designated wave frequency. Specific outputs required to solve the equation of motion were added mass, radiation damping and excitation force.

The methodology components required to analyse a single chamber design in the absence of a site specific wave climate are depicted as a flow diagram in the dash-lined box in Figure 7.1. This set of processes comprises model formulation, chamber construction, preparation of input files to facilitate appropriate analysis using WAMIT and post-processing of output files. This holistic procedure is termed the 'hydrodynamic model set-up'.

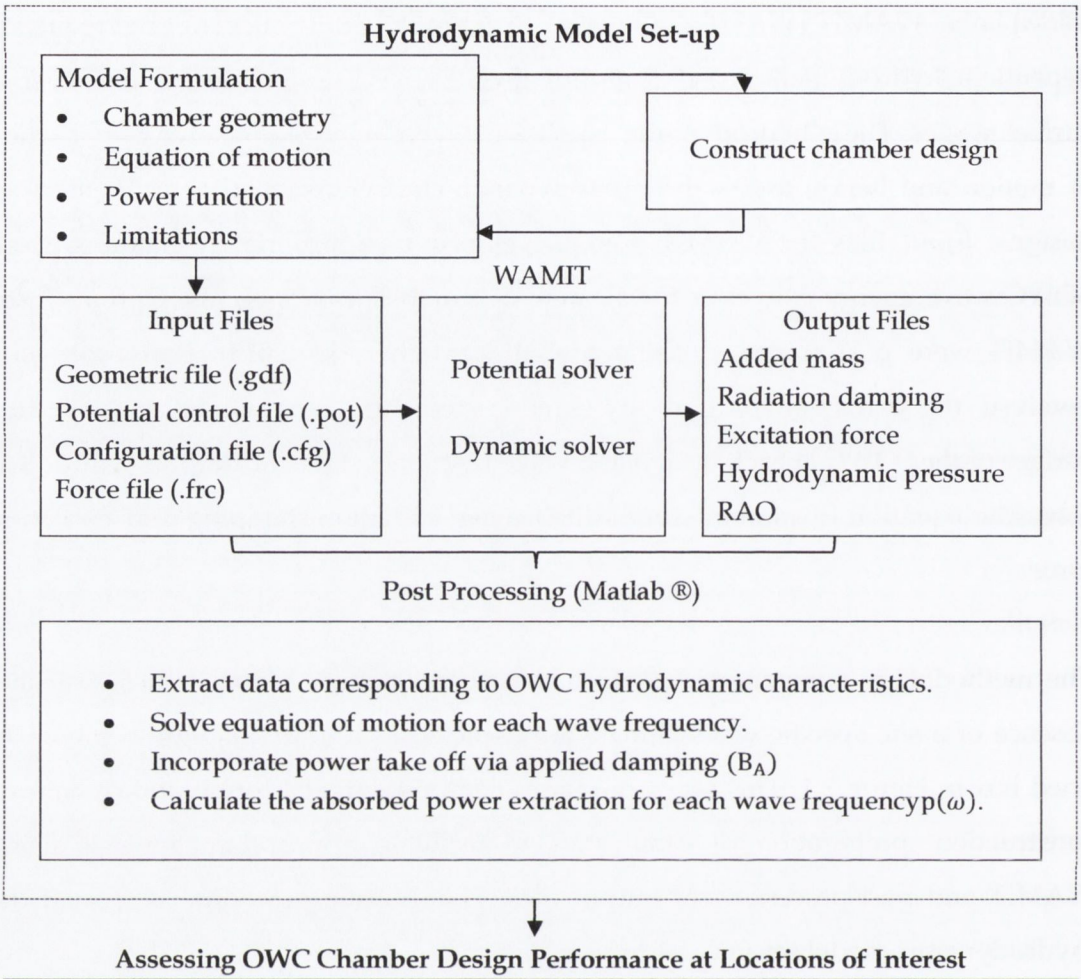

Assessing OWC Chamber Design Performance at Locations of Interest

Calculate upper limit for mean annual absorbed power, $\overline{P_{max}}$, using the following steps:

1) Extract full time series data sets for H_s & T_p values from site of interest within domain of spectral wave model outlined in Chapter 4.
2) Using this data, generate scatter diagram, $C(H_s, T_p)$, which denotes hours per year for each sea state (H_s, T_p) appropriate for SOWC operation.
3) Select suitable standard spectrum for site, S, based on spectral representation of wave climate.
4) Apply $P(H_s, T_p) = \int S(H_s, T_p, \omega)p(\omega)d\omega$ to each cell of scatter diagram, where $P(H_s, T_p)$ is the upper limit for absorbed power for a single sea state, $S(H_s, T_p, \omega)$ is the energy spectrum, based on associated H_s& $T_p$values and $p(\omega)$ is the power function representing a given chamber design with a specific applied damping signifying the turbine (B_A)
5) Calculate upper limit for mean annual absorbed power $\overline{P_{max}}$, using $\overline{P_{max}} = \sum_{H_s} \sum_{T_p} C(H_s, T_p)P(H_s, T_p)$.
6) Calculate upper limit for capture width ratio, η, using the average incident wave power (kW/m) at the site of interest, the upper limit for mean annual absorbed power and the width of the subterranean OWC chamber design.

Figure 7.1 Flow chart outlining the processes involved in the hydrodynamic model set-up and the methodology implemented to calculate performance indicators, $\overline{P_{max}}$and η for a given chamber design.

Benchmarking

Two benchmarking exercises were carried out. To assess and verify the accuracy of the hydrodynamic model set-up, a benchmarking study was carried out using experimental results from physical wave tank testing programmes. Tank testing data for a fixed OWC chamber design was sought and used as a comparison for results output from WAMIT and the hydrodynamic model. The tank tested OWC chamber was modelled at 1:36 scale. Additionally, a comparison study was carried out using data sourced from a study that analysed a full scale OWC chamber design with the boundary element code, AQUADYN (Brito-Melo et al., 1999). The design analysed was the Pico OWC chamber which is comparable in size to proposed SOWC designs.

Assessing OWC Chamber Design Performance at Locations of Interest

To establish values for performance indicators for a given SOWC design at specific locations of interest, outputs from the hydrodynamic model were used in conjunction with wave climate conditions. Specifically, the primary output used from the hydrodynamic model was the power function for the SOWC wave energy converter, which defined the power absorbed for a range of designated wave frequencies with a given PTO. The wave climate conditions for a specific site were defined by its scatter diagram detailing the typical percentage occurrence of each sea state over a year and a suitable wave spectrum, S, for the area of interest. The scatter diagram and selected wave spectrum were based on work carried out using the spectral wave model for the Loop Head region, described in Chapter 4. Thus using the power function, scatter diagram and suitable wave spectrum, the performance indicators for a specified OWC design were determined.

To address the research objectives of this chapter, this procedure was carried out for a number of different SOWC chamber designs. The results for these investigations are given later in this chapter.

7.2 Model Formulation

This section describes the model formulation implemented to analyse SOWC chamber designs and address the research objectives presented at the start of this chapter. Considering the breadth of this research programme, a limit was placed on the level of detail incorporated into the model but the model still had to incorporate

sufficient detail to be able to reliably detect effects of altering specified SOWC design parameters on performance at locations of interest.

As mentioned previously, in order to facilitate the analysis of a relatively large number of different chamber designs, a numerical modelling approach was adopted. Additionally, this methodology lent itself to efficient analysis of SOWCs in conjunction with turbine variation along with alterations in scatter diagrams, which characterised the different locations of interest. SOWC chamber configurations were constructed using a geometric modelling program, Multisurf version 8.0 (Aerohydro, 2011a). The Boundary Element Method (BEM) code, WAMIT (WAMIT, 2011) was then employed to calculate the frequency dependent hydrodynamic coefficients for given SOWC designs in the presence of surface waves. These hydrodynamic coefficients were required to solve the equation of motion and hence, assess the hydrodynamic characteristics of specific chamber designs.

WAMIT is based on linear potential theory. Linear wave theory is assumed which allows the system dynamics to be represented in the frequency domain, with the accompanying tools of linear superposition and Fourier analysis. As described in the literature review in Chapter 2, linear wave theory has been utilised extensively in the analysis of wave energy converters, including shoreline OWCs (Brito-Melo et al., 1999; Wavegen, 2002). With respect to this project, international guidelines propose that model formulation in the frequency domain is appropriate for the early stages of WEC design (Holmes, 2003). In terms of chamber geometry optimisation, modelling in the frequency domain lends itself to principal system investigation more so than the time domain. The associated linear equation of motion limits the number of variables affecting hydrodynamic performance, which allows direct relationships to be inferred between chamber design and hydrodynamic behaviour. These points comparing the applications of the frequency domain and time domain to OWC design are reiterated in Table 7.1, which was sourced from Weber (2006).

Table 7.1 Evaluation of applicability of mathematical model domain to develop task. Range of markings: (- - -, - -, -, 0, +, + +, + + +). Source: (Weber, 2006).

Applicability of Domain to development task	Domain	
	Frequency	Time
Principle system investigation and selection	+ +	-
Design Optimisation	+ + +	- -
Operational Optimisation	+	+ +
System Control	- - -	+ + +

Weber (2006) notes that the statements made on the evaluation of the applicability of the modelling approach are not absolute and rather dependent on many factors particular to the development stage. However, it gives an indication to the strengths of each model domain. In the overall development on an OWC system, both modelling techniques are valuable and complementary.

In the research programme for this thesis, mathematical formulations assuming linear wave theory were employed to examine trends in chamber performance at Loop Head cliff base locations where water depth was 17 m.

To examine trends in chamber performance at locations of interest, four dominant components were required. These were (i) the equation of motion associated with chamber design, (ii) the power function incorporating the power take off unit, (iii) the wave spectrum characterising wave conditions at site of interest and (iv) a scatter diagram detailing the typical percentage occurrence of each sea state over a year.

7.2.1 Equation of Motion

The force and displacement approach was adopted to model the hydrodynamics of the SOWC. More specifically, the massless piston model was used to simulate the free surface within the chamber. As the SOWC structure is fixed, the system can be described as the damped motion of an oscillating mass with a single degree of freedom. The oscillating mass corresponds to the mass of water within the SOWC chamber exposed to the time varying force of the incident waves. Then Newton's second law ($Force = mass \times acceleration$) gives the following linear differential equation (Equation 7.1).

$$m\ddot{X} = F_e + F_R + F_S \tag{7.1}$$

Where m is the mass of the oscillating system, F_e is the wave excitation force (N) acting on the lower end of the OWC, X is the heave amplitude of the water column, F_R is the force associated with the damped motion and F_S is the spring force. Assuming linear wave theory, ω_i is the angular frequency of ith frequency (rad/s) of the incident wave field. Considering $F_R = -B\dot{X}(\omega_i)$ and $F_S = -kX(\omega_i)$, Equation 7.1 may be expanded to Equation 7.2

$$F_e(\omega_i) = \left[\{k - m(\omega_i)\omega_i^2\} + jB(\omega_i)\omega_i\right]X(\omega_i) \tag{7.2}$$

Where $X(\omega_i)$ is the complex heave amplitude of water column at frequency ω_i, $B(\omega_i)$ is the added (radiation) damping (Ns/m) at frequency ω_i and k the heave stiffness which is given by $k = A_c\rho_w g$ (N/m). A_c is the surface area of OWC (m^2) and ρ_w the density of water (kg/m^3). m, the mass of the oscillating system, is considered the effective mass which is the sum of the entrained mass and the added mass $M_a(\omega_i)$ (kg).

The frequency dependent hydrodynamic parameters M_a, B and F_e were obtained from the BEM software WAMIT while k and A_c were calculated based on the chamber geometry under analysis. The theory behind WAMIT's calculation of M_a, B and F_e is presented in Section 2.6.1.1. Using WAMIT's output of M_a, B and F_e for a given range of wave periods, it was possible to calculate the complex heave amplitude of the water column $X(\omega_i)$ for each period using a routine developed in MATLAB. Equation 7.2 was coded and applied for each wave period subjected to the SOWC chamber design. It will be seen in Section 7.3.1 that $X(\omega_i)$ corresponds to the RAO of the water column. Plotting RAO vs. angular frequency allows the natural frequency of a given chamber design to be identified. This method is employed in Sections 7.6, 7.9 and 7.10.

7.2.2 Power Function

Regarding the addition of the power take off (PTO) to the SOWC system, different options and levels of detail were considered. A number of self-rectifying turbines have been developed for the application of alternating airflow in OWCs, each with their own characteristic curves for mechanical power vs. pressure difference. Leading technologies include the Wells turbine, impulse turbine, Dennis Auld turbine and Oceanlinx's 3rd generation turbine. As this study focuses primarily on the effect of chamber design on performance at different locations around Loop Head, a simple fixed blade Wells turbine was employed to minimise the number of variables. The Wells turbine has an almost linear relationship between pressure drop and volume flow, and may be modelled as a linear damping B_A. Using WAMIT's output for F_e, M_a, B and appropriate values for B_A, the power function $p(\omega)$ for the OWC may be calculated for a given range of wave frequencies using Mei's solution for sinusoidal excitation (Mei, 1976) (Equation 7.3).

$$p(\omega) = \frac{\frac{1}{2} B_A \omega_i^2 |F_e|^2}{\left(k - m\omega_i^2\right)^2 + (B_A + B_2)^2 \omega_i^2} \tag{7.3}$$

where $p(\omega)$ is the average power output (kW) at frequency ω_i, B_A is the applied damping which extracts energy from the system (representing the turbine) (Ns/m) and B_2 is the secondary damping (Ns/m). The secondary damping should comprise the radiation damping and the loss damping due to energy losses that increase significantly with incoming wave power. However, in the present research programme where the upper limit for power extraction was used as a performance indicator to compare chamber designs, the secondary term was based on the radiation damping B (Ns/m).

7.2.3 Limitations

It is acknowledged that there are inherent limitations associated with the use of a frequency domain model, which adopts the force and displacement approach, due to its linear nature. As it relies on mathematical assumptions and approximations which simplify the wave structure interaction, it is understood that the behaviour of an actual SOWC system deviates from the numerical model in non-linear conditions. In

the case of energetic sea conditions particularly, there can be discrepancy between performance results for a full scale SOWC device and those of a corresponding frequency domain model. This is due to the exclusion of effects including, but not restricted to: hydrodynamic loss effects; air compressibility or losses at the power take off which may affect the pneumatic damping characteristic and non-linear wave effects. However, it should be noted that a key function of the model was to compare the natural response of separate SOWC chamber designs and assess its impact on performance over a year. Although discrepancies between this linearised model and realistic conditions are inevitable, the model fulfils its key function. Also as the performance indicator parameters values are averaged over a year, the errors are averaged. Additionally, as indicated by international guideline TRL 1 to 3 for WEC development, a frequency domain model is suited to the purposes of this study (See Section 2.2 Standards and Best Codes of Practice).

7.3 PERFORMANCE INDICATORS

To obtain an objective and quantitative indication of the difference in performance between specific chamber designs at different sites of interest, two performance indicators were chosen that accounted for wave conditions at potential SOWC installation sites. The two parameters employed as performance indicators in recent distinguished studies (Babarit et al. 2012; Babarit & Hals 2011) were the upper limit for mean annual power absorption, $\overline{P_{max}}$, and capture width ratio η.

The upper limit for mean annual power absorption for the SOWC is heavily influenced by the wave climate at the deployment site and is a useful index for comparing the performance of different SOWC configurations at the same site (see Section 7.3.2 Upper Limit for Mean Annual Absorbed Power). Capture width ratio is a generic performance indicator defined as the ratio between mean annual absorbed power and the incoming wave power available to the wave energy converter. Therefore, it allows SOWC designs to be compared against other designs at different sites of interest (see Section 7.3.3 Annual Average Capture Width Ratio)

The upper limit for mean annual absorbed power and capture width ratio are the overarching performance indicators required to fulfil the principal aims of the current research programme addressed in this chapter. However, to calculate them,

the response amplitude operator (RAO) must first be computed. It demonstrates the wave frequencies to which a given device best responds. (The RAO was used in the benchmarking process to verify the hydrodynamic model set up and WAMIT computations in Section 7.5.) . Therefore, the RAO is described first to provide a context within which to conceptualise the other two performance indicators.

7.3.1 The Response Amplitude Operator (RAO)

In the context of SOWCs, the RAO can be defined as the displacement of the water column within the chamber in relation to the incident wave field. It is representative of the relative degree to which the water in the chamber rises in response to an incoming wave. Mathematically, it can be described by Equation 7.4 which is an extension of Equation 7.2 that accounts for ς_a wave amplitude. Each term is related to the heave motion of the water column.

$$RAO = \frac{X(\omega_i)}{\varsigma_a} = \frac{F_{ex}(\omega_i)}{\{k - M_E(\omega_i))\omega_i^2\} + j(B(\omega_i) + B_A)\omega_i} \tag{7.4}$$

The RAO varies depending on the frequency of the impinging waves. For a given device there is a particular frequency, or band of frequencies, which coincide with an increased RAO. If the waves impinge at a lower or higher frequency the RAO response is less. If the design of the device is altered, the wave frequency associated with the maximum RAO may also alter. This is important because the maximal power output of the device occurrs in response to wave frequencies associated with maximal RAO response. Therefore to maximise device performance, its design should be tailored to produce maximal response to the wave frequencies which are most prevalent throughout the year. The point at which the highest RAO occurrs is known as resonance. The RAOs for three separate example chamber designs analysed in are presented in Figure 7.2.

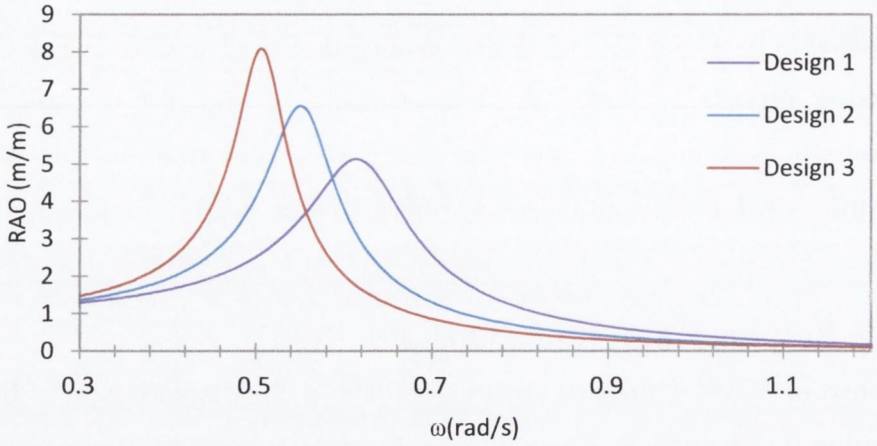

Figure 7.2 RAO vs. vs. angular frequency (ω rad/s) for three separate SOWC chamber designs.

It can be seen that resonance occurs at a different frequency (otherwise known as wave period) for each chamber design. As mentioned above, this is valuable information with respect to selecting a chamber design for a site's prevailing wave climate and optimising annual power conversion efficiency.

The damping effect provided by the power take off (PTO) i.e. the turbine, has an effect on the amplitude of the RAO, although it does not substantially affect the frequency point at which it occurs. A common power take-off for OWCs is a Wells turbine, which acts as a linear damper. If there is no damping provided by a PTO, the water column in the OWC chamber can rise readily and the RAO at resonance becomes very high. This effect appears particularly marked when using a linear numerical model. However, without a PTO and its associated damping, no power can be extracted. When a PTO is applied, the damping offers some resistance, hence the rise of the water column and correspondingly, the RAO, become more moderate. Excess damping greatly reduces the RAO and is associated with low power extraction. However, between the extremes of no damping and excessive damping there is an optimal damping value which is associated with maximum power extraction. The diagram below demonstrates RAO values varying according to wave frequency and the level of damping provided by the PTO. It shows the motional behaviour of the water column in three stages relating to the incident wave frequency, ω as follows: (i) low frequency, prior to resonance, (ii) resonance, and (iii) high frequencies, after resonance.

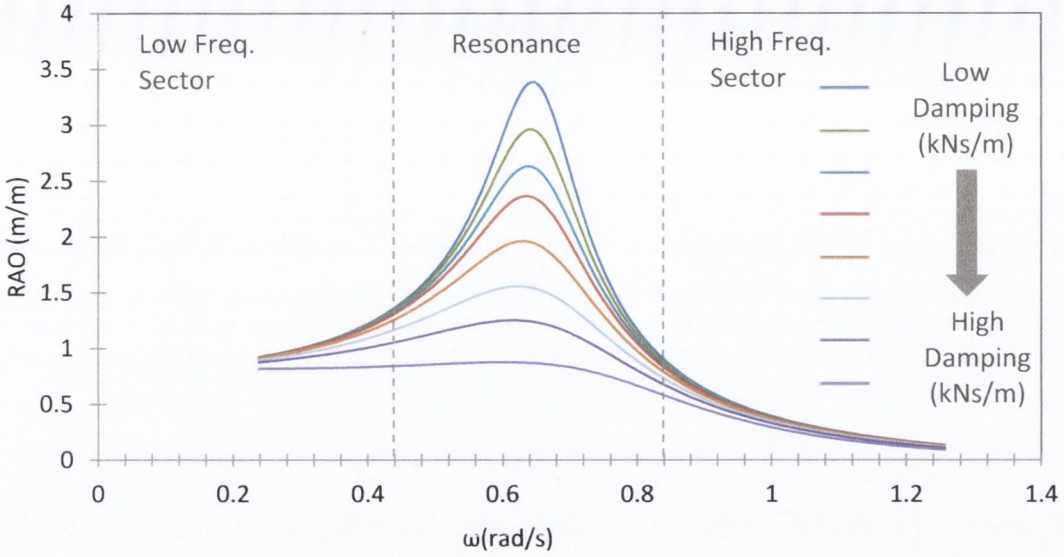

Figure 7.3 RAO vs. angular frequency (ω rad/s) for one SOWC chamber design with varying levels of applied damping B_A.

In Figure 7.3 the different lines represent the response of the water column within the chamber when different dampings are applied. To understand the motional behaviour of the water column, it is convenient to split the above figure in to three sections: (i) low frequency, prior to resonance, (ii) high frequencies, after resonance, and (iii) resonance.

At low frequencies (high periods), where the wave length is large compared to the horizontal length of the SOWC chamber, the RAO for the water column tends towards 1 and the phases lag tends to zero. This is due to the dominance of the restoring term, k, when $\omega^2 \ll k/(M + M_a)$, which influences the vertical motion of the SOWC.

At higher frequencies (low periods), where the wave length is small compared to the horizontal length of the SOWC chamber, the RAO is dominated by the mass of the water column and associated added mass. High frequencies may be defined as frequencies where $\omega^2 \gg k/(M + M_a)$. In this case, the preponderant mass of the system induces negligible values for the response amplitude operator.

At resonance, where $\omega^2 \approx k/(M + M_a)$, the RAO of the water column is controlled by the damping applied to the SOWC system. Without damping, the RAO may

extend to unrealistic values exceeding ten times the incident wave height. In this case the incident waves are amplified within the chamber but not converted into a useable form of energy. In order to extract energy from the motion of the water column, an external power take-off mechanism is required. The most common power take-off is a Wells' turbine, which acts as a linear damper. The effect of altering the damping associated with Wells' turbine can be seen in Figure 7.3 above. The hydrodynamic response of the water column reduces as the damping is increased. Conversely, it can be seen that damping has a minimal effect on the frequency at which resonance occurs.

The RAO obtained with different levels of damping converges towards one for low frequencies and towards zero for high frequencies, consistent with the behaviour experienced for an undamped system. Around the natural frequency, increased damping reduces the RAO to the point where the resonance peak disappears. This can be observed where the lowest line shows no discernible increase in response at the system's natural frequency.

7.3.2 Upper Limit for Mean Annual Absorbed Power

The upper limit for mean annual power absorption $\overline{P_{max}}$ is influenced by the wave climate at the deployment site and was used to compare the performance of different SOWC configurations at the same site. A brief description of its derivation follows. Considering the power function for a given SOWC design $p(\omega)$ (Equation 7.3), the maximum power that the SOWC system can absorb from a specific sea state (H_s, T_p) is given by Equation 7.5.

$$P(H_s, T_p) = \int S(H_s, T_p, \omega) p(\omega) d\omega \tag{7.5}$$

Where $S(H_s, T_p, \omega)$ signifies a suitable standard spectrum (Bretschneider, JONSWAP, TMA) that characterises the wave conditions at the location of interest. To calculate the upper limit for mean annual power absorption for a given SOWC wave energy converter at a specific site, let $C(H_s, T_p)$ represent the scatter diagram of sea state probabilities for the location of interest (Equation 7.6).

$$\overline{P_{max}} = \sum_{H_s} \sum_{T_p} C(H_s, T_p) P(H_s, T_p) \tag{7.6}$$

This performance indicator is termed upper limit as calculations are based on linear wave theory, carried out in the frequency domain and power is calculated based on an optimal damping coefficient applied by the turbine. Thus, hydrodynamic loss effects, air compressibility, losses at the power take off and non-linear wave effects are not included. Also, studies have shown that frequency domain models overestimate the dynamic response of the water column (Babarit et al., 2012). Hence, the prefix upper limit is required.

In line with this, it is realised that the maximum power absorption level will never be reached in real-world applications. However, it is still an informative result since it gives an upper limit to the amount of wave energy that could be absorbed by a SOWC wave energy converter. Furthermore, the calculation of this parameter when altering a specific chamber dimension allows a quantitative measure of the effect that alteration has on performance. Fundamentally, it provides a quantitative method to directly compare chamber designs at the same potential site location.

7.3.3 Annual Average Capture Width Ratio

Capture width ratio η, is a generic performance indicator defined by the ratio between absorbed power P_{abs} (kW) and the incoming wave power P_{wave} (kW/m), available to the wave energy converter. The capture width ratio can be calculated using Equation 7.7 below.

$$\eta = \frac{P_{abs}}{P_{wave} B} \tag{7.7}$$

where B is the width of the SOWC chamber. It should be noted that the dimension of B depends on the working principle of the wave energy converter. The capture width ratio may be employed to investigate the performance.

In this study, the capture width ratio is based on annual average values for power absorption and incident wave power. To account for yearly wave conditions at the site of interest, P_{abs}, is taken as $\overline{P_{max}}$ and P_{wave} denotes the annual average wave power (kW/m) associated with the site. Therefore, it allows annual performance for different SOWC designs to be compared against other designs at different locations of interest.

The annual average wave power at the site of interest was determined using results from the spectral wave climate model for the Loop Head region, described in Chapter 4. Specifically, it was computed using Equation 7.8 at hourly intervals and averaged over the finite time span.

$$P_{wave} = \rho g \int_0^{2\pi} \int_0^{\infty} c_g(f,\theta) E(f,\theta) df d\theta \tag{7.8}$$

where c_g is the group velocity and E is the energy density. When calculating annual average wave power for a location, the hourly intervals and time span correspond to those used to generate the scatter diagram $C(H_s, T_p)$. This is important to note since $C(H_s, T_p)$ is fundamental to the calculation of $\overline{P_{max}}$. Hence, $\overline{P_{max}}$ and P_{wave} are based on the same wave climate statistics. This eliminates discrepancies that may occur if the scatter diagram and average wave power were based on wave climate statistics for different time intervals and time spans.

7.4 WAMIT

The BEM code, WAMIT, was used to calculate the frequency dependent hydrodynamic coefficients for given SOWC designs in the presence of surface waves. It is a powerful numerical tool for modelling waves and wave structure interaction. Specifically, it was employed to calculate added mass, radiation damping and excitation force which are central to Equations 7.2, 7.3 and 7.4.

WAMIT is based on linear potential theory. The benefit of this method is that its computational efficiency facilitates the analysis of a number of chamber designs at several locations, which comprise an extremely large number of scenarios for wave structure interaction. For wave energy application, the agreement between linear

theory and experiments is reasonable in small to moderate sea states. However, there can be characteristic discrepancies in wave conditions that excite resonances within the chamber due to non-linear and viscous effects. The aim of this study was to provide upper estimates for wave energy absorption to examine trends in device performance when altering certain design parameters.

WAMIT was originally developed for the analysis of various types of floating and submerged structures. For these cases, the hydrodynamic response of the structure in waves can be seen as a superposition of the motion of the body in still water and the forces on the restrained body in waves. The motion of the body in still water is known as the radiation problem and the forces on the restrained body in waves is known as the diffraction problem. However, there is a difference in relation to wave interactions with an SOWC compared to floating and submerged structures, and that is the interior free surface within the chamber. In contrast to the conventional case where the structure is rigid and moving with six modes of rigid motion, WAMIT permits the addition of further modes of motion to represent the free surface of the SOWC. In line with this, the radiation and diffraction problem alter accordingly. In the analysis of a fixed SOWC, the radiation problem relates to an oscillatory pressure applied to the free surface in otherwise calm waters. The diffraction problem relates to the spatially averaged amplitude of the water column displacement to the amplitude of the incident waves when there is no pressure acting on the free surface. Solving the radiation and diffraction problem for the SOWC structure approximates the velocity potentials on the interior surface which satisfies several boundary conditions, as described in Chapter 2. Using the calculated velocity potentials on the interior surface, the hydrodynamic coefficients are determined for a range of wave frequencies defined by the user.

WAMIT is a multifaceted numerical package with numerous input settings and parameters as well as a wide range of output quantities. The inputs and outputs associated with the analysis of an SOWC chamber design are outlined in Figure 7.4 below.

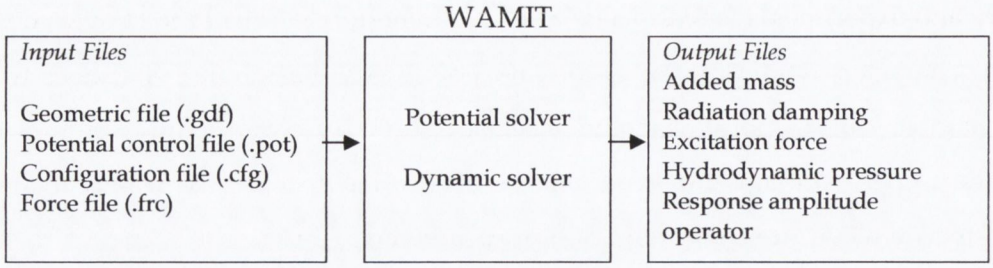

Figure 7.4 Flow chart detailing WAMIT's inputs and outputs

7.4.1 Inputs

Four input files were required to analyse a given SOWC chamber design. The four files are the geometric data file, configuration file, force file and the potential file. The geometric data file specifies the SOWC chamber geometry. This was constructed using a geometric modelling program which exports the geometry to a format accepted by WAMIT. The potential, configuration and force file facilitate set-up to appropriately analyse the geometry. Full descriptions of these files are detailed in the user manual (WAMIT, 2012). The following sections present aspects of these files that are central to the model set-up.

7.4.1.1 Geometry Definition

When constructing the SOWC chamber designs, a right-handed Cartesian co-ordinate system was employed, with the x-axis pointing toward the submerged opening of the SOWC and the z-axis pointing upward. To import the geometry to WAMIT, the geometry was discretised. There are two different approaches to discretise the body surface; the low order method (panel method) or the high order method.

The low order method approximates the body surface with flat quadrilateral panels. It is assumed that the velocity potential is constant in each panel. The velocity potential is represented in terms of surface distributions of sources and normal dipoles. This is used to determine hydrodynamic quantities such as pressure and force coefficients. The quadrilateral panels are described by the co-ordinates of each vertex in the design.

The high order method describes the geometry's body surface by smooth continuous surfaces, known as patches. Patches are required to be smooth with continuous

surface co-ordinates and slope. To achieve this higher order continuous definition, B-splines are used. B-splines can be defined as mathematical functions that provide smooth surfaces to a given degree of accuracy. The velocity potential and pressure is represented by continuous B-splines on each patch. Fundamentally, B-splines represent the body surface, velocity potential and pressure on the body surface. In general, the high order method induces more accurate results than the low-order method for the equivalent computational time (Aerohydro, 2011). For this reason, the higher order method was adopted in the present research programme to characterise the OWC chamber geometry.

7.4.1.2 Hydrodynamic Model Set-up

In the potential file, the range and number of wave frequencies applied to the SOWC chamber geometry were set. The range of wave frequencies were selected to correspond to all possible wave periods experienced off the West coast of Ireland. This denotes periods from 4 s to 20 s corresponding to 0.25 Hz to 0.05 Hz respectively. The water depth was set to 17 m, based on the water depth at the potential SOWC sites. In the configuration file, the technique to model the OWC free surface was specified. In the force file, the modes of motion associated with the water column within the SOWC chamber were set. These were the piston mode and first sloshing mode relating to the heave and pitch motion of the water column. Additionally, the stiffness and damping matrices were set in the force file. The stiffness associated with the water plane area was input to cell (7, 7) in the stiffness matrix. The damping corresponding to the turbine was input to cell (7, 7) of the damping matrix. Instruction was input to the file to evaluate the following hydrodynamic parameters: added mass coefficient, damping coefficient, hydrodynamic pressure, excitation force and response amplitude operator.

7.5 Benchmarking Using Experimental Results

To verify the hydrodynamic numerical model set-up, comparisons were made between data from physical experiments and corresponding designs modelled numerically. Key aspects investigated were the OWC free surface and the effect of water depth on the hydrodynamic characteristics of the OWC. Small wave response tests were used as they best emulated potential flow conditions. This benchmarking

process was conducted prior to investigating the effect of different full scale chamber designs on performance at certain deployment sites.

Experimental data for these tests were available for the Pico OWC design (Delaure, 2001). This is a shoreline OWC wave energy converter located on the Island of Pico, which is in the Azores archipelago. It is one of a limited number of fixed OWC wave energy projects which has data available from experimental tank testing carried out at an appropriately small scale to simulate potential flow conditions. Furthermore, information on its hydrodynamic characteristics at full scale was available. This facilitated a further comparison study which is also presented in this section. This benchmarking process was conducted prior to investigating the effect of different full scale chamber designs on performance at certain deployment sites.

The small scale tank tests carried out using the Pico OWC design that were used in the present research programme were performed at 1:36 scale. The 1:36 physical model of the Pico OWC design was tested in the wave tank at the Hydraulic Maritime Research Centre (HMRC) in Cork. A cross sectional view of the Pico OWC design is presented Figure 7.5 along with its scaled dimensions.

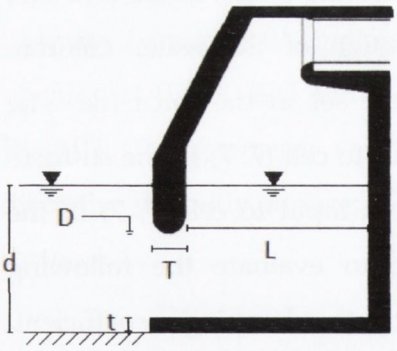

Design Parameter	Value
Front wall draft, *D*	0.048 m
Front wall thickness, *T*	0.051 m
Water column length, *L*	0.250 m
Water column width, *W*	0.305 m
Water depth, *d*	0.240 m
Water step thickness,*t*	0.020 m
Water plane area, *WPA*	0.07625m^2
Inlet area	0.052460m^2

Figure 7.5 Pico OWC design (left); 1:36 Scale dimensions (right)

The dimensions of the wave tank in which the model was deployed were 28 m long by 18 m wide by 1 m deep. The wave generation system consisted of a series of 40 adjacent paddles each 0.425 m wide, 0.94 m high with a freeboard 0.24 m high. The wave makers were capable of active absorption designed to cancel reflected and radiated waves. Efficiencies of absorption were between 90% and 95% of the incident waves for the range of sea states applied to the scaled OWC. The scale tests covered

periods ranging from 0.8 s to 2.3 s. The wave tank was calibrated to ensure that these conditions were accurately applied and that the incident wave field, which defined the system excitation force, was precisely known.

The analysis of wave interaction with the OWC model was measured using twin wire resistance probes at a number of locations outside and within the structure. These measured surface elevation which allowed the response amplitude operator (RAO) to be determined. It is these data on the response amplitude of the OWC which was used to benchmark the numerical model utilised in the present research programme.

7.5.1 Numerical Model

To assess the agreement between results computed using WAMIT and those from the small scale tank testing, a replica of the 1:36 Pico design was constructed a geometric modelling programme. For reasons outlined in Section 7.4.1.1 Geometry Definition, the high order method was adopted to characterise the chamber geometry. The most noteworthy aspect of hydrodynamic model set up relates to the modelling of the OWC free surface. Two approaches were considered during this research programme. The first applies a weightless lid to the OWC free surface. The second employs a recent addition to the hydrodynamic code in WAMIT version 7, which allows an oscillatory pressure to be applied to the OWC free surface.

7.5.1.1 Weightless Lid

The weightless lid approach was developed by Lee et al., (1996) as a method for simulating the motion of an OWC. It allows the approximation of viscous damping through the addition of linear damping to the modes of oscillation associated with the free surface of an OWC. The lid is assigned to the free surface of the water column using a function known as generalised modes. It is considered as an extension to the body surface and represented as an additional patch. This approach specifies the normal velocity on the free surface and modifies the boundary condition at the free surface. When the lid is applied, the free surface boundary condition for the solution of the diffraction problem is altered to that of a surface with the boundary condition of no flow. This boundary condition is outlined in Chapter 2,

Section 2.6.1 Hydrodynamic Theory. This approximates the non-atmospheric conditions within an OWC chamber.

7.5.1.2 Free Surface Pressure Patch

This recent addition to hydrodynamic code for WAMIT version 7, was developed specifically with the simulation of oscillating water columns in mind. Prior to this development, the OWC free surface was modelled using the weightless lid approach. The new modelling approach specifies the pressure distribution on the free surface. This feature is known as a free surface pressure (FSP) patch. The pressure distribution is described by Equation 7.9 below.

$$p_0(x,y) = -\rho g \sum_{j=7}^{6+M_p} \xi_j n_j(x.y) \tag{7.9}$$

Where M_p is the number of pressure modes associated with its application, ξ_j is the complex amplitude of the free surface and the spatial distribution of each mode is described by $n_j(x.y)$. When analysing OWCs using a BEM code such as this, the predominant pressure mode associated with the oscillation of the water column is heave. Although the free surface pressure patch is a relatively recent feature in WAMIT, the concept of the surface pressure distribution has been applied to a three dimensional OWC design in a study Brito-Melo et al. (1999) using the radiation-diffraction code, AQUADYN. This used in the following section to compare results for a full scale OWC wave energy converter. Regarding the comparison with experimental results from small scale testing carried out by Delaure (2003) the RAO was used to compare results.

7.5.1.3 Comparison

Figure 7.6 presents the RAO for the heave motion of the water column within the 1 : 36 Pico chamber design. This graph, plotted against wave period, displays the RAO calculated using the weightless lid and free surface pressure patch (FSP) method.

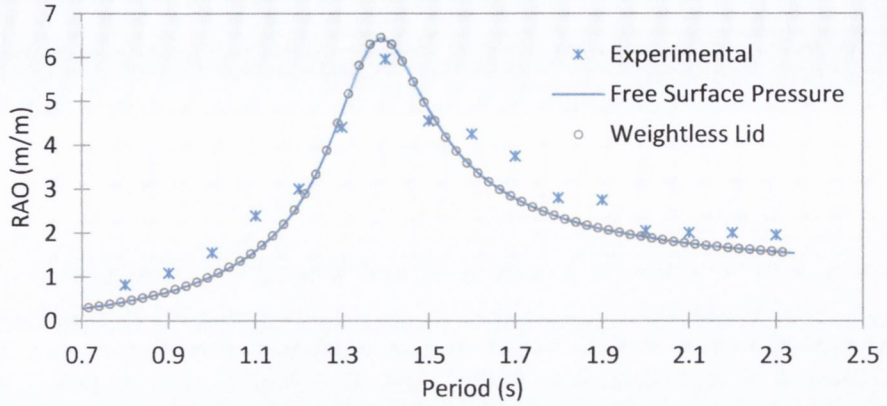

Figure 7.6 RAO (m/m) vs. Period (s) for Pico OWC Design at 1:36 Scale. Experimental results compared against BEM prediction using free surface pressure patch (FSP) and BEM prediction using IGENMDS.

It can be seen that there is a discrepancy between numerical and experimental results. This is expected due to the idealised context of linear potential flow theory on which the numerical results are based, as well as experimental errors and accuracy associated with the physical testing. However, this graph provides evidence that the natural period for the 1:36 scale Pico design established during tank testing corresponds to results generated using the weightless lid and free surface pressure patch. No damping was applied in the experimental set up which induces the relatively large amplification for experimental results. Considering the hydrodynamic model set-up, a finite water depth was set which corresponded to the experimental set-up. This reduced the RAO compared with results for infinite water depth. The hydrodynamic model set-up (WAMIT input) was the same for the weightless lid and free surface pressure patch approach. It can be seen that there is a high level of agreement between both methods. Both approaches were set with the same degrees of freedom corresponding to the heave mode and first sloshing mode. The high level of agreement between both methods with this set-up was confirmed by the founder of WAMIT Inc. (Newman, 2013). Through this communication, it was also theorised that the level of agreement between both methods would reduce when analysing more complex chamber geometries.

7.5.2 Power Take Off

Both the weightless lid and free surface pressure patch facilitate the application of a Wells Turbine, suitable for the extraction of power from an OWC system. This power take off mechanism interacts with the reciprocating air flow which results from the

OWC motion. This generates air pressure oscillations, causing a pneumatic pressure to act directly on the water column interior surface. This force associated with this pressure is proportional to the column surface area. This force can be related to the column surface velocity through the turbine damping constant. Regarding the force and displacement approach used in this study to model the OWC, the damping may be represented as a real applied damping coefficient B_a with the units Ns/m. This is not to be confused with the damping coefficient associated with the pressure and volume method for modelling the OWC system which uses the units Ns/m^5. Considering the units, the damping coefficients associated with the force and displacement method is generally orders of magnitude greater than those for the pressure and volume approach.

In relation to the implementation of a linear damping using the weightless lid and free surface pressure patch, the same approach is possible for both methods. Using the force file in WAMIT, the applied damping is supplemented to the damping matrix for the water column. From this, the FORTRAN routine associated with each method, applies the damping to the heave mode of the free surface. As the damping applied by the Wells turbine is dependent on its rotational speed, a constant operational speed must be assumed using this method.

7.6 Benchmarking using Potential Flow Models

To authenticate the numerical model set-up at full scale, the Pico design was utilised again as suitable data was available for comparison. Additionally, the full scale Pico OWC design is comparable in size to proposed SOWC designs. Specific data that lent itself to a model comparison assessment was sought from a study which analysed the full scale Pico chamber using the boundary element code, AQUADYN. This data is presented in a paper titled 'A 3D boundary element code for the analysis of OWC wave power plants' by Brito-Melo et al. (1999)'. The full scale geometry of Pico OWC design analysed in this benchmarking study is presented in Figure 7.7.

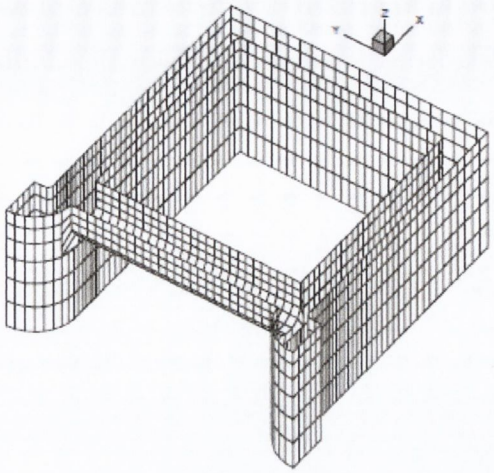

Design Parameter	Value
Front wall draft, D	1.8 m
Front wall thickness, T	1.8 m
Water column length, L	12 m
Water column width, W	12 m
Water depth, d	8.64 m
Water step thickness,t	0.72 m
Water plane area, WPA	144 m^2

Figure 7.7 Pico OWC design (left); Full Scale dimensions (right)

Similar to model formulation employed in this study, the analysis carried out by Brito-Melo et al. (1999) was formulated in the frequency domain. Additionally, AQUADYN is a radiation-diffraction code based on the same fundamental theories as WAMIT. To appropriately model the free surface of the oscillating water column, AQUADYN required a modification in the dynamic boundary condition on the internal water free surface to account for the imposed oscillatory pressure distribution within the chamber. This is similar to the free surface pressure patch developed for WAMIT. However Brito-Melo et al. (1999) had agreed access to the source code in AQUADYN allowing details to be specified for the Pico design. User access to the commercial code is not typical and means that results from WAMIT may be more approximate compared with the aforementioned specialised case. The hydrodynamic parameters available for comparison from this study are the non-dimensionalised forms of added mass and radiation damping associated with the heave mode of the water column. These are defined by Equations 7.10 and 7.11 below.

$$\overline{M_a} = \frac{M_a}{\rho L^k} \tag{7.10}$$

$$\bar{B} = \frac{B}{\rho L^k \omega} \tag{7.11}$$

As Brito-Melo employed a pressure distribution approach, the free surface pressure patch method was used in this study. Comparisons for non-dimensionalised added mass and damping are presented in Figure 7.8 and 7.9 respectively.

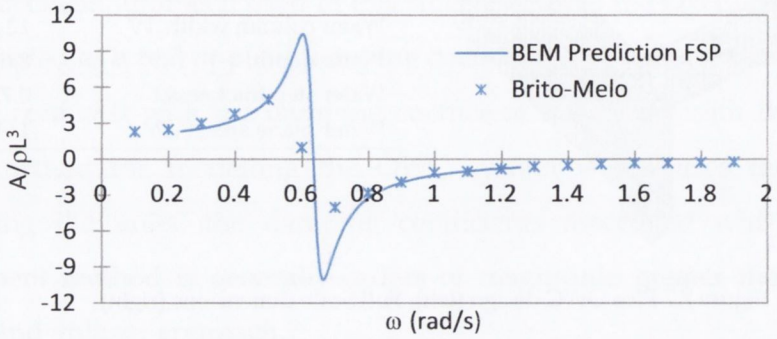

Figure 7.8 Non-dimensional added mass coefficient for full scale Pico OWC design. Numerical results from Brito-Melo et al., (1999) compared against BEM prediction using free surface pressure patch (FSP).

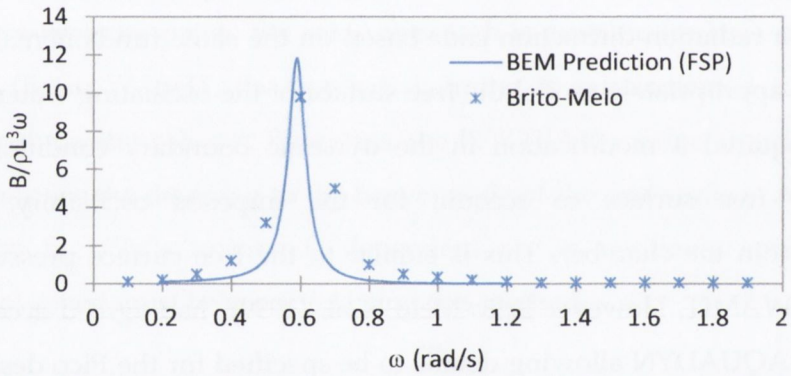

Figure 7.9 Non-dimensional radiation damping coefficient for full scale Pico OWC design. Numerical results from Brito-Melo et al., (1999) compared against BEM prediction using free surface pressure patch (FSP).

It can be seen that the maximal values for both parameter occur at an approximately similar wave frequency. However, there is a discrepancy. This has been attributed to a combination of two factors. Firstly, as Brito-Melo et al. (1999) were key researchers in the development and operation of the Pico plant and had special access to AQUADYN's source code to appropriately model the Pico design, there may be a higher level of detail incorporated in their model, pertaining to pressure distributions within the chamber. Secondly, the Pico design analysed with WAMIT was directly scaled up from the 1:36 scale design presented in Figure 7.5. This design did not possess the curved sections at either side of the OWC inlet, shown in Figure 7.7. In light of this, results were considered to display an appropriately level of agreement to progress to analysis of SOWC chamber designs.

From carrying out above benchmarking process, the appropriate hydrodynamic model set-up was refined.

7.7 Assessing SOWC Design Performance at Locations of Interest

This section describes the process used to calculate the performance indicators, upper limit for mean annual power absorption, and capture width ratio for SOWC chamber designs at Arch point and the tip of Loop Head. These performance indicators were used to compare the relative efficiency of different SOWC chamber designs.

As SOWCs are strongly resonant systems, the performance of a specific design can vary significantly depending on the prevailing wave climate at the deployment site. To establish values for performance indicators for a given SOWC design at specific site, outputs from the hydrodynamic model of the SOWC wave energy converter were used in conjunction with corresponding wave climate conditions extracted from the spectral wave model described in Chapter 4. Specifically, the primary output used from a hydrodynamic model was the power function for the SOWC wave energy converter, which defines the power absorbed for a range of designated wave frequencies with a given PTO. The wave climate conditions for specific sites were defined by their scatter diagrams detailing the typical percentage occurrence of each sea state over a year and a suitable wave spectrum for areas of interest. Thus using the power function, scatter diagram and suitable wave spectrum, the performance indicators for specified SOWC designs were determined.

A summary of the process implemented to calculate the performance indicators $\overline{P_{max}}$ and η for a given chamber design is outlined as follows:

1) Extract full time series data sets for H_s & T_p values from site of interest within domain of spectral wave model outlined in Chapter 4.
2) Using these data, generate scatter diagram $C(H_s, T_p)$ which denotes hours per year for each sea state appropriate for SOWC operation.
3) Select suitable standard spectrum for site, S, based on measured wave spectrum.

4) Compute frequency dependent hydrodynamic properties for each design and determine power function $p(\omega)$.
5) Apply Equation 7.5 to each cell of scatter diagram,
6) Calculate upper limit for mean annual absorbed power $\overline{P_{max}}$, using Equation 7.6.
7) Calculate upper limit for capture width ratio η using Equation 7.7.

The sites considered in the following sections are Arch Point and the tip of Loop Head. Ten chamber designs are investigated. This facilitates an investigation of front wall thickness and chamber width.

7.8 SITES

As outlined in Chapter 3 Site Viability and Chapter 5 Wave Energy Resource Characterisation, the sites selected for investigation were Arch Point and the tip of Loop Head. In Chapter 5, the percentage occurrence for each sea state was presented as recommended by resource assessment guidelines (Folley et al., 2013; Venugopal, Davey, Helen Smith, et al., 2011). In this chapter, it was appropriate to present the occurrence for each sea state in hours per year. This was achieved by multiplying percentage occurrence of each sea state by the number of hours in a year. 'Wave energy: A guide for investors and policy makers (Waveplam, 2009)' recommends this format as it allows the power generation by the wave energy converter to be conveniently converted to kilowatt hours. This provides clear information on the potential for electricity generation from a given site. This format also lends itself to assessing the power absorbed by the SOWC wave energy converter and calculation of overall capture width ratio. As outlined at the start of this section, the methodology employed to calculate power absorbed requires the sea state to be described in terms of significant wave height and peak period. This follows the methodology outlined in 'Numerical benchmarking study of wave energy converters (Babarit et al., 2012)'. Annual average hours per year of significant wave height and peak period are presented for Arch Point and the tip of Loop Head in Figure 7.10 below.

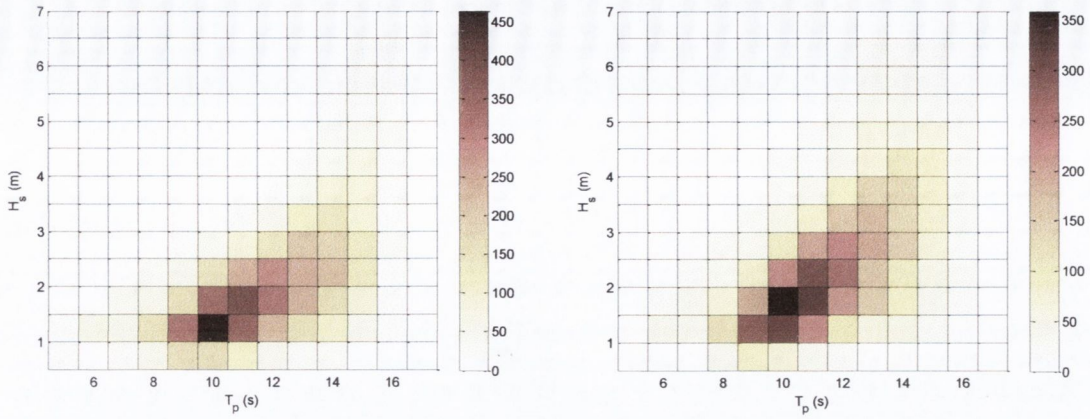

Figure 7.10 Annual average hours per year (H_s, T_p) for Arch Point (Left) and the tip of Loop Head (Right).

Comparing the scatter diagrams for both locations, it can be seen that the highest number of hours are focused around the same peak periods, between 9 - 11 seconds. However, there is a larger spread of significant wave heights at the tip of Loop Head. As the tip of Loop Head is more exposed and possesses a steeper seabed slope, during energetic sea states the significant wave height is less affected by near-shore processes. Therefore, the tip of Loop Head experiences higher significant wave heights over a given year. Due to this, the tip of Loop Head has higher values for annual average wave power and watt hours per year, as shown in Table 7.2.

Table 7.2 Wave power parameters for Arch Point and the tip of Loop Head

Parameter	**Arch Point**	**Tip of Loop Head**
Depth	17 m	17 m
Average wave power	25 kW/m	34 kW/m
Total Watt hours per year	220 MWh/m	299 MWh/m

Oceanographic studies have also shown that the depth contours that surround a headland, as with Loop Head, can cause focusing of wave energy at the tip of the headland (Harold et al., 2001). As a wave field propagates towards the tip, the waves turn toward the depth contours due to refraction. This causes concentration of wave energy at the tip of the headland. It has been found that this phenomenon contributes to the high annual wave power level at the tip of Loop Head. To put the annual average wave power resource in context with other areas in Europe, information on the resource for a number of wave energy test sites was sourced. The annual average wave power values for each site are presented in Table 7.3.

Table 7.3 Average annual wave power at European wave energy test sites.
Source: (Babarit et al., 2012)

SEM-REV	Yeu	EMEC	Lisbon	AMETS
14.8 kW/m	26.8 kW/m	21.8 kW/m	37.5 kW/m	80.6 kW/m

SEM-REV and Yeu are located off the west coast of France. The European Marine Energy Centre (EMEC) is based off the island of Orkney, north of Scotland. The Lisbon site is situated off the west coast of Portugal. The Atlantic Marine Energy Test Site (AMETS) is located off the North West coast of Ireland. Each of these sites is located in deep water. Further information on these test sites is presented in Babarit et al. (2012). It can be seen that the resource at Arch Point and the tip of Loop Head is favourable in the context of other sites explored for wave energy converter installation. Additionally, each of the European wave energy sites is located in deep water. Hence, it is important to note that the resource at Arch Point and the tip of Loop Head, located in 17m water depth, is comparable with the resource at off-shore European test sites. This finding was reinforced by a recent study which investigated the wave energy resource between AMETS and the coast (Curé, 2011). It showed that the annual wave energy value at the 20m depth contour is 28.6 kW/m. This is in keeping with the average wave power values computed for Arch Point and Loop Head.

7.8.1 Wave Spectrum

To calculate the wave power absorbed by the SOWC wave energy converter using Equation 7.5, a suitable wave spectrum is required. Based on details presented in Chapter 6, Section 6.3.2 Spectral Shape of Incident Wave Field, which investigated measured wave spectra at Loop Head, the Bretschneider spectrum was selected. The Bretschneider spectrum is given by Equation 7.12.

$$S(f) = \frac{5}{16}\frac{H_s^2}{T_p^4} f^{-5} \cdot \exp\left\{-\frac{5}{4}\frac{1}{T_p^4} \cdot f^{-4}\right\} \tag{7.12}$$

where $S(f)$ (m^2/Hz) is spectral density, f (Hz) wave frequency, H_s(m) significant wave height and T_p is peak period. In line with this equation, scatter diagrams and all

performance matrices presented in this chapter are plotted in terms of significant wave height and peak period.

7.9 Altering Front Wall Thickness: 11 m Wide Chamber

As mentioned earlier, the aim of this section is to calculate the performance indicators for different SOWC designs in order to compare their relative performance and efficiency. In Chapter 6 the chamber design parameters likely to produce optimal performance were identified. It will be recalled however, that the proposed construction technique of excavating the chamber within rock, conferred some constraints upon design parameters. In particular, to maintain the structural integrity of the rock, the thickness of the front wall of the chamber may need to be greater than for other OWC designs. Therefore the effect of increasing front wall thickness is investigated, as follows. This section presents results outlining the influence front wall thickness has on the hydrodynamic behaviour of the OWC. Five front wall thicknesses were assessed: 1.8 m, 4.8 m, 8.8 m, 12.8 m and 16.8 m. The fundamental design was based on findings presented in Chapter 6. Although front wall thickness is varied in the analyses described below, the following design parameters remain constant: front wall draft, chamber incline, water column width, incline, water depth, water plane area and inlet area. The fixed values for each of these parameters are presented in Figure 7.11 below.

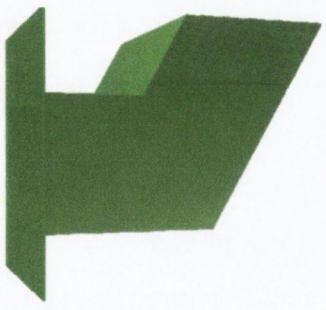

Design Parameter	Value
Front wall draft	4.0 m
Chamber Incline	60 deg
Water column width	11.0 m
Water depth	17.0 m
Water plane area	86.0 m^2
Inlet area	71.5 m^2

Figure 7.11 Left: Cross sectional view of SOWC chamber design. Right: Full Scale dimensions

A front wall thickness of 1.8 m was selected as the initial design as it provided an insight to the hydrodynamic performance in comparison to a conventional OWC chamber. The Pico OWC chamber design modelled in Section 7.6 possesses a front wall thickness of 1.8 m. Hence, this front wall thickness facilitated initial comparisons

between the Pico design and the fundamental SOWC chamber design, which is comparable with respect to width and water plane area. Front wall thickness of 4.8 m is considered the very minimum front wall thickness permitted for a SOWC chamber design. However, given the construction technique in question, the required front wall would likely need to be thicker than this. Increasing front wall thickness increases the structural integrity of the chamber.

As front wall thickness increases, the volume of the chamber enlarges which augments the associated water mass. This, coupled with the lengthening of the chamber, directly affects the hydrodynamic behaviour of the oscillating water column. For each chamber design, the hydrodynamic parameters relating to the heave mode of the oscillating water column were computed using WAMIT for angular wave frequencies 1.25 rad/s to 0.25 rad/s. These correspond to the range of wave periods experienced off the West coast of Ireland. This denotes wave periods from 4 s to 20 s corresponding to the full range of wave periods on the x-axis of scatter diagrams for Arch Point and the tip of Loop Head.

The first investigation on front wall thickness and its effect on hydrodynamic behaviour aimed to identify the natural frequency for each design. Resonance, being the condition with maximum amplification of the water column with respect to the incident amplitude, is considered the most favourable condition for the extraction of wave energy. As outlined in Section 7.4.1 The Response Amplitude Operator, plotting the RAO against frequency provides a convenient method for identifying the natural frequency. To clearly identify the frequency at which resonance takes place, the five chamber designs were modelled without an external damping representing the power take off. A caveat associated with this approach is that the values for RAO at resonance are exceptionally high, as occurs with linear numerical modelling where damping is not incorporated. However, the method is suited to identifying the frequency point where resonance occurs. To provide an overall insight to the hydrodynamic behaviour associated with each chamber design, added mass (M_a), radiation damping (B) and RAO were plotted against angular frequency (ω). It should be noted that WAMIT outputs the non-dimensionalised form of each hydrodynamic parameter, M_a, (B) and RAO. Therefore, each hydrodynamic parameter corresponding to the heave motion of the water column was

dimensionalised using a routine developed in MATLAB. Specifically, Equations 2.31 and 2.32 were coded and applied for each angular frequency. These frequency dependent hydrodynamic parameters are presented for each front wall thickness in Figure 7.12 and Figure 7.13, accompanied by a side view schematic of the submerged section of the chamber. Each graph corresponds to the heave motion of the water column.

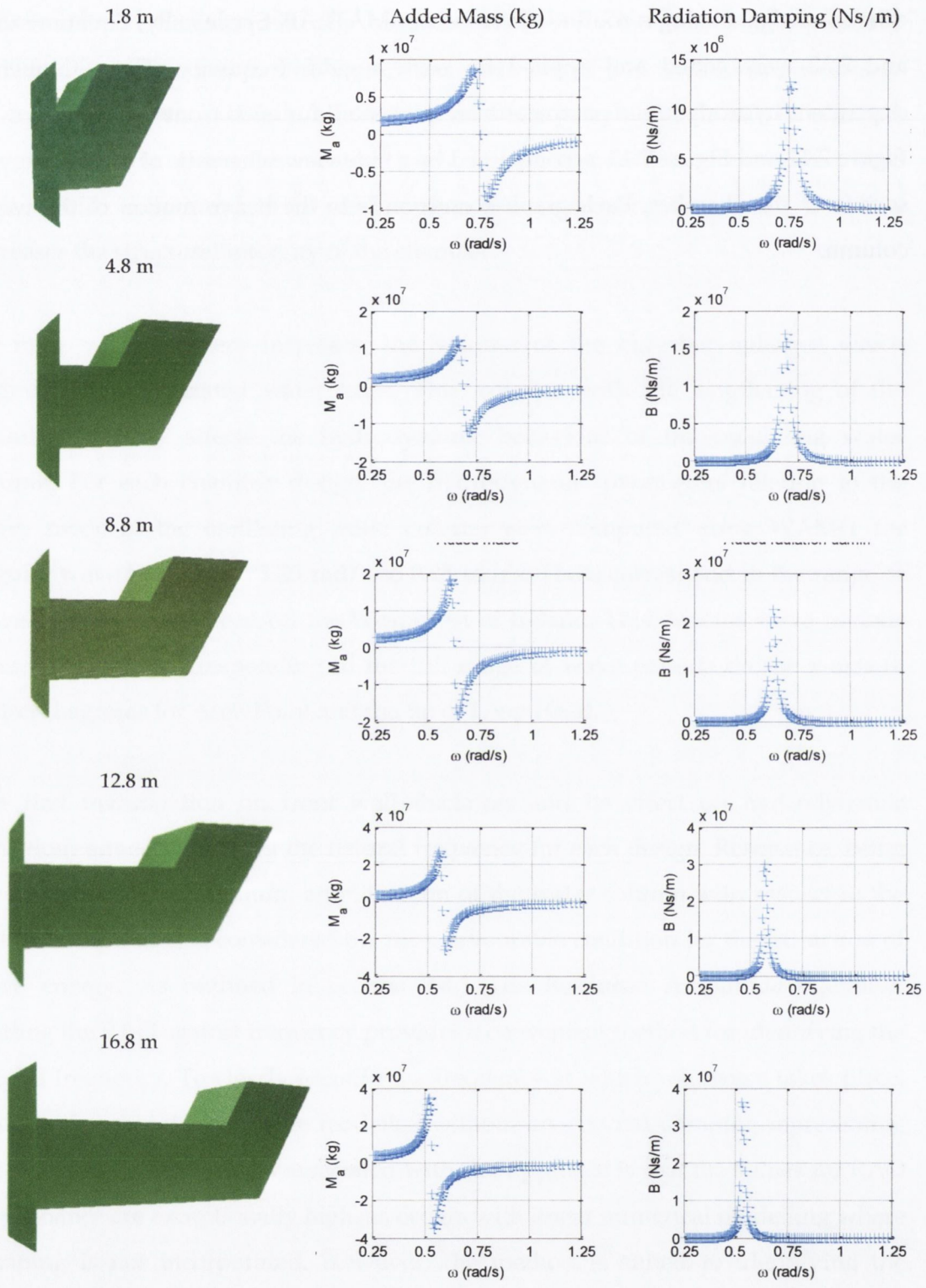

Figure 7.12 Added mass (kg) vs. angular frequency (rad/s) and radiation damping (Ns/m) vs. angular frequency (rad/s) for SOWC chamber designs with varying front wall thickness: 1.8 m, 4.8 m, 8.8 m, 12.8 m and 16.8 m. Chamber width = 11 m. Depth of inlet = 4 m. Incline = 60 degrees.

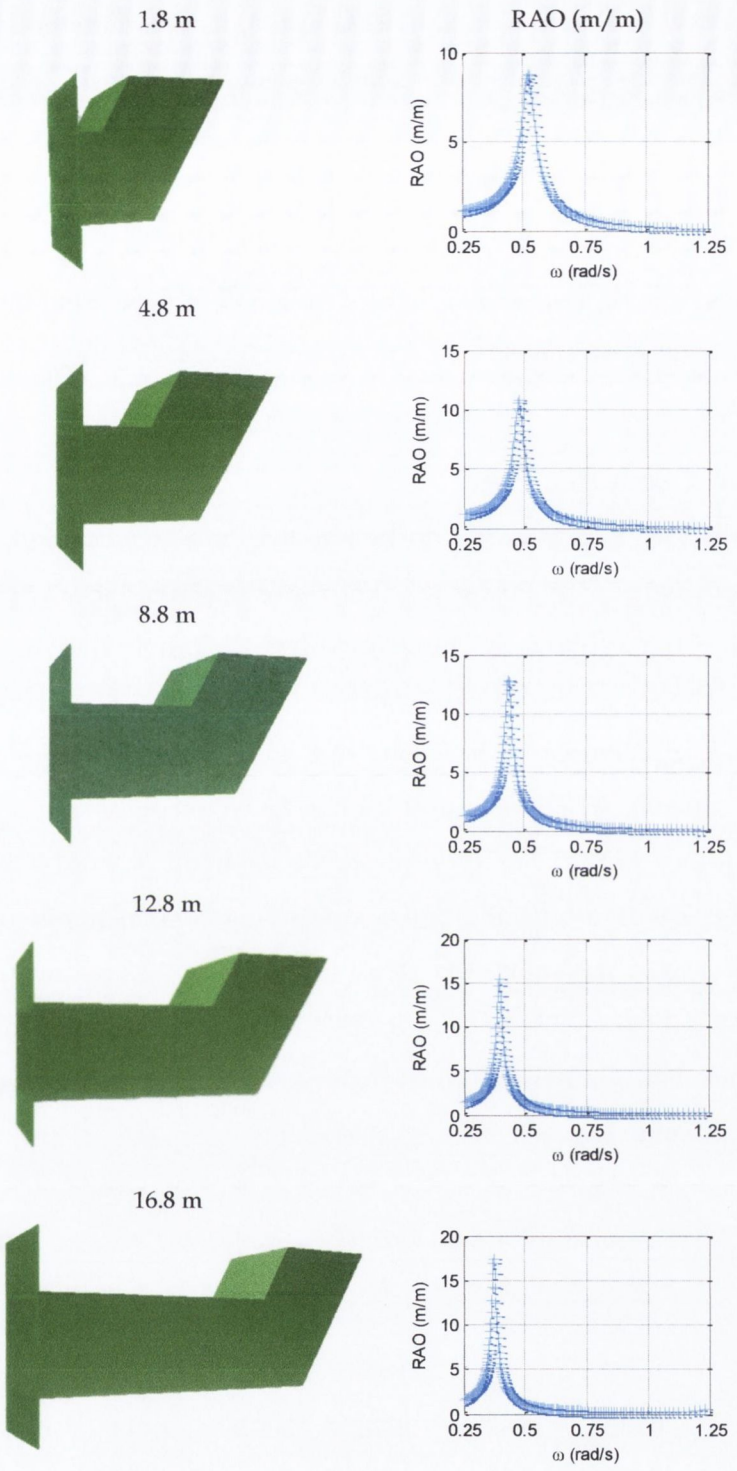

Figure 7.13 RAO (m/m) vs. angular frequency (rad/s) for SOWC chamber designs with varying front wall thickness: 1.8 m, 4.8 m, 8.8 m, 12.8 m and 16.8 m. Chamber width = 11 m. Depth of inlet = 4 m. Incline = 60 degrees.

It can be seen that extending the front wall thickness induces two consistent trends for each of the above parameters. These trends are best described by considering the RAO for each design, presented in Figure 7.13. Also, as the RAO is dependent on the

mass of the water column and radiation damping, it considers the effects presented in Figure 7.12. The first trend to note is the consistent shift in the frequency at which resonance occurs. As the front wall is extended, resonance takes place at a lower frequency. The second trend relates to the relative rise in amplitude of the RAO. This is predominantly due to the larger volume of water within the chamber and hence, increased mass. The implications of these trends will be seen when the power matrix for absorbed power is presented for each design.

7.9.1 Power Take Off

To generate the power matrix for absorbed power for a given design, the power take off must be considered. The power take off was represented as an applied damping. The selection of the applied damping considered a number of factors, previously outlined in Chapter 6, Section 6.7 Turbine Selection. The theoretical optimal damping was calculated for each design and used to select an appropriate turbine. Standard Wells turbines manufactured for OWCs were considered in this study as it facilitated an assessment of the upper range of absorbed power by a realistic power take off. Using Equation 6.10, the optimal damping coefficients were calculated for each chamber design. The values for 1.8 m, 4.8 m, 8.8 m, 12.8 m and 16.8 m front wall thicknesses ranged from 2398 kNs/m to 2974 kNs/m. Considering this information, details for a number of potential Wells turbines options were sourced. These details are presented in Table 7.4.

Table 7.4 Summary of Wells turbine designs. Source: (Wavegen, 2004)

Turbine		*1*	*2*	*3*	*4*	*5*	*6*	*7*
D_t	m	2.5	2	2.5	2.1	3.536	2.836	3.536
R_{tip}	m	1.25	1	1.25	1.05	1.768	1.418	1.768
R_{hub}	m	0.813	0.62	0.775	0.336	1.149	0.454	1.149
R_{mid}	m	1.031	0.81	1.013	0.693	1.459	0.936	1.459
A_c	m^2	99	99	99	99	99	99	99
A_A	m^2	2.833	1.933	3.02	3.107	5.668	5.667	5.668
A_R	m^2	34.94	51.22	32.78	31.86	17.47	17.47	17.47
h	1	0.65	0.62	0.62	0.32	0.65	0.32	0.65
S	1	0.6	0.6	0.62	0.6	0.6	0.65	0.6
Capacity	kW	500	200	515	300	1000	800	400

Based on the design bounds for the SOWC chamber established in Chapter 6, coupled with the wave power level at Arch Point and Loop Head, the target capacity was set at approximately 500 kW. This narrowed the choice of turbines to option 1 and 3 which possess a capacity of 500 kW and 515 kW respectively. The damping applied by the Wells turbine is dependent on its rotational speed. Using Equation 6.9 from Section 6.8 Turbine Selection, the range of dampings for turbine options 1 and 3 were calculated. These are presented in Figure 7.14.

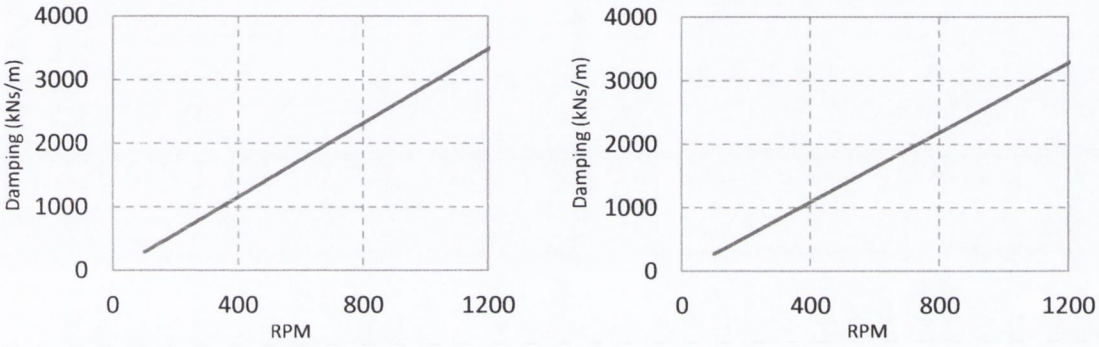

Figure 7.14 Effect of rpm on damping.
Left: Turbine option 1 (500 kW). Right: Turbine option 3 (515 kW)

The dampings for each turbine are presented for a broad range of rotational speeds. The operational speed for a turbine of approximately this size ranges between 700 rpm and 1200 rpm (Whittaker et al., 2002). Therefore, the applied dampings that can be induced by turbine option 1 range from 2032 kNs/m to 3484 kNs/m. For turbine option 2, applied dampings can range from 1913 kNs/m to 3280 kNs/m. In light of this and the range of theoretical optimal dampings for each chamber design, both turbines provide an appropriate range of dampings for this study. However, as the focus of this section is on chamber design, a single turbine option was selected to reduce the number of variables. The turbine chosen was option 1 with a capacity of 500 kW. Within the range of dampings associated with this turbine, optimal damping coefficient values were applied to each chamber design when calculating absorbed power.

7.9.2 Power Matrices

In this study, the power matrix format provides an indicator for the absorbed power at each sea state. Section 7.4.2 Upper Limit for Mean Annual Absorbed Power provides the basis for this stage of analysis. To generate the power matrix for

absorbed power for a given design, the power function was computed using Equation 7.3 with the corresponding optimal damping. Using this in conjunction with the wave spectrum for the site, the power absorbed at each sea state was calculated using Equation 7.5. The resulting power matrices for SOWC chamber design are presented in Figure 7.15 below.

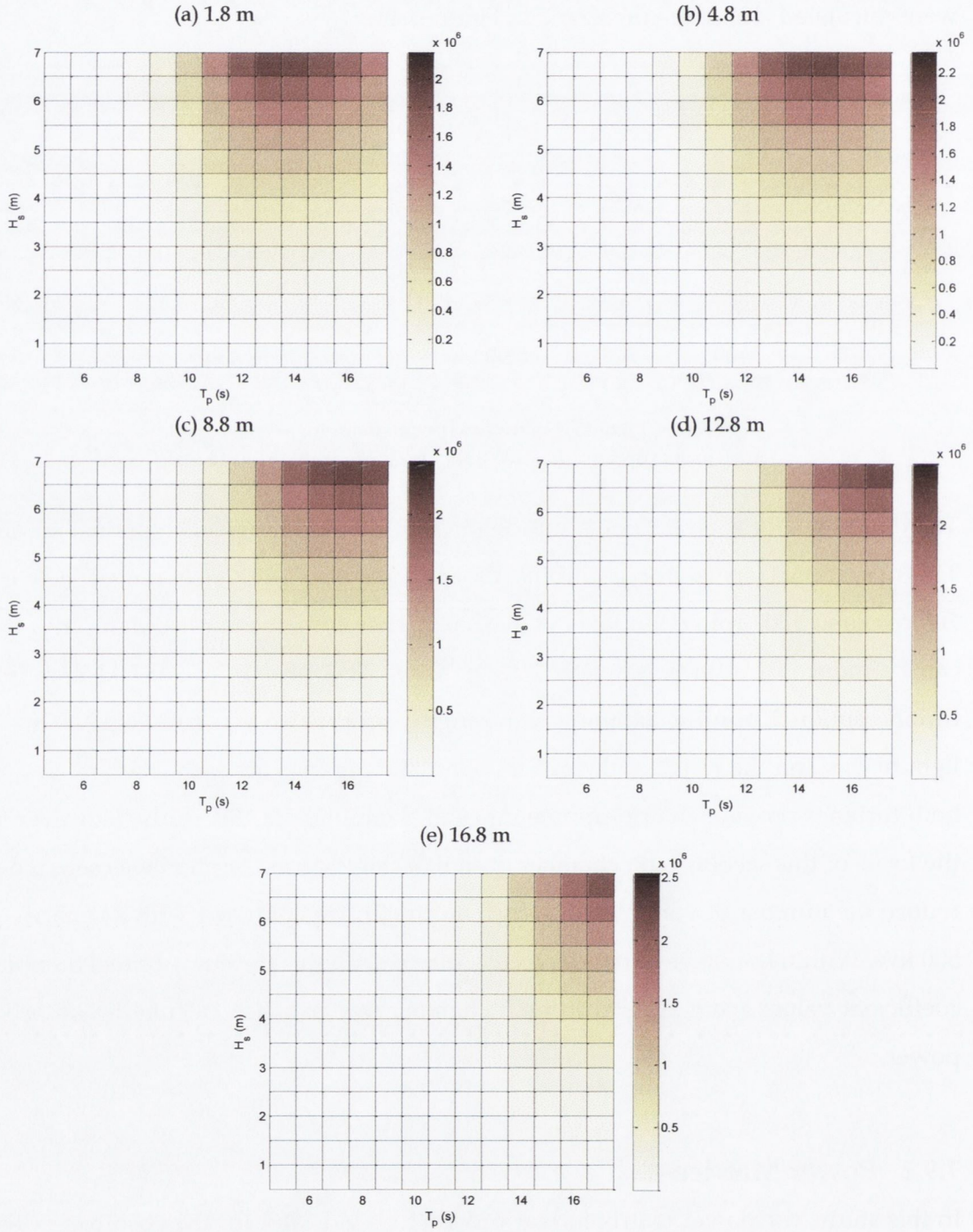

Figure 7.15 Power matrices denoting upper limit for power absorption for each sea state. Units: Watts. Front wall thickness: (a) 1.8 m, (b) 4.8 m, (c) 8.8 m, (d) 12.8 m and (e) 16.8 m. Chamber width = 11 m. Depth of inlet = 4 m. Incline = 60 degrees.

Considering matrix (a) corresponding to a front wall thickness of 1.8 m, it can be seen that high levels of power absorption are occur when exposed to sea states with a peak period ranging between 12 s and 15 s. This is due to the Eigen frequency of the water column which occurs within this range of wave periods. Considering matrices (b) to (e), it can be seen that as front wall thickness is increased, the periods at which maximum power absorption takes place shifts to higher values. This is due to the shift in natural frequency for each design, as previously highlighted by the corresponding graphs for RAO Figure 7.13. Fundamentally, as front wall thickness increases, the volume of the chamber is enlarged, which increases mass of the water column. As a result, the period at which resonance takes place increases. How this affects performance over the span of a year at a particular location depends on the prevailing wave conditions.

7.9.2.1 Performance at Arch Point

Multiplying each cell of the power matrix by its corresponding cell in the scatter diagram for Arch Point (Figure 7.10) facilitates an investigation into the level of power absorbed by the SOWC for each sea state. As the scatter diagram is represented as hours occurrence per year, the resulting matrix is in terms of Watt hours. The matrix for each SOWC design is presented in Figure 7.16. These were limited to sea states suitable for SOWC wave energy converter operation, as defined in Chapter 5 as sea states possessing a significant wave height equal to or less than 6.5 m.

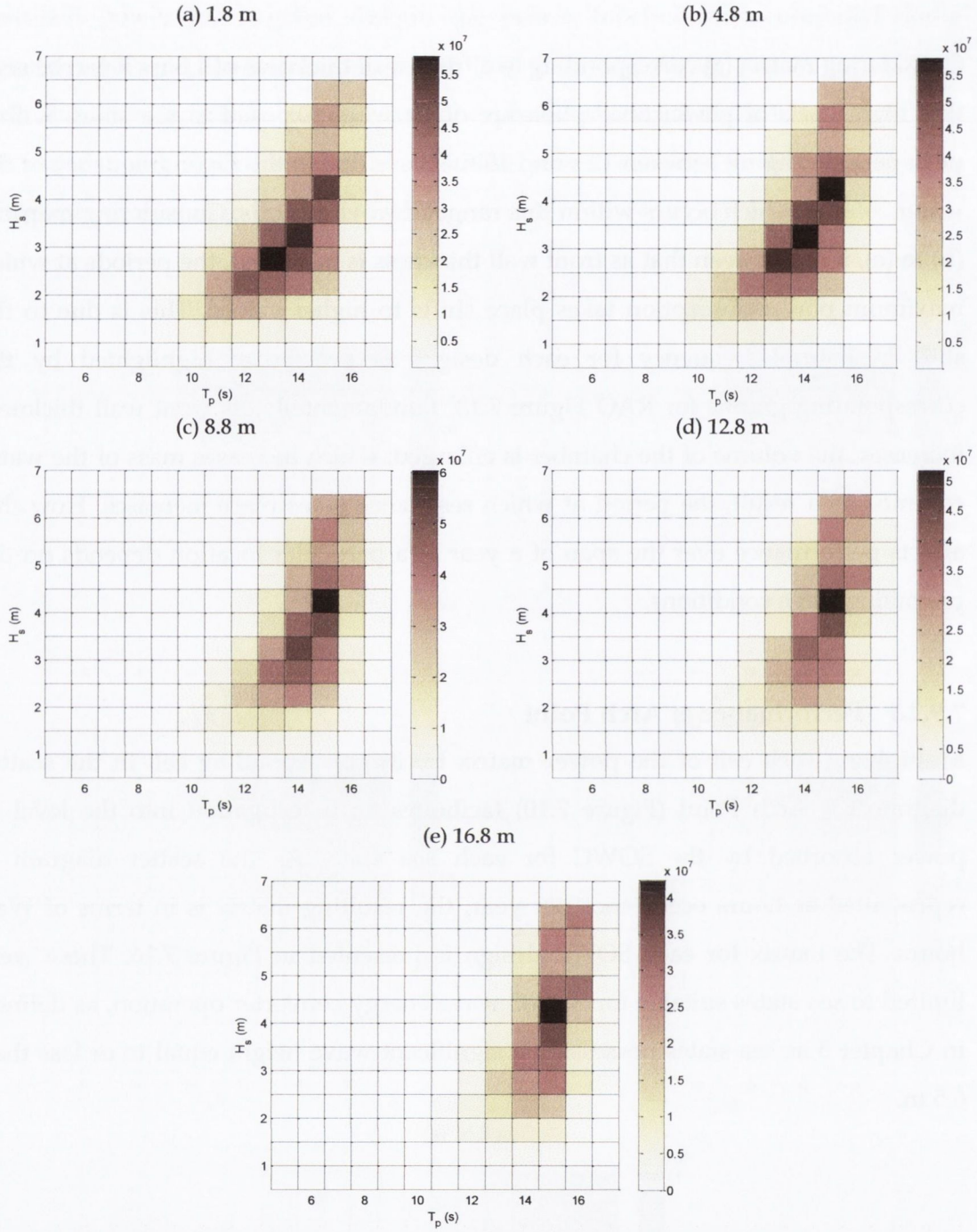

Figure 7.16 Matrices highlighting the sea states where the most power absorption takes place at Arch Point. Hours occurrence multiplied by power matrix. Units: Watt hours.
Front wall thicknesses: (a) 1.8 m, (b) 4.8 m, (c) 8.8 m, (d) 12.8 m and (e) 6.8 m.

Considering the power matrices for each design (Figure 7.15) and the scatter diagram for Arch Point (Figure 7.10), it is evident that increasing the front wall thickness is associated with maximum power absorption occurring at higher wave periods. This detunes the SOWC wave energy converter from the most commonly occurring sea states. The above matrices presented in Figure 7.16 reveal the resulting effects. Regarding (a) 1.8 m and (b) 4.8 m, it can be seen that high levels of power are

absorbed from a wider range of sea states in comparison to (d) 12.8 m and (e) 16.8 m. As the front wall thickness is increased, the periods at which maximum power absorption takes place is shifted away from commonly occurring sea states. This is detrimental to overall power absorption over a year as efficiency is reduced for sea states with low levels of power, when maximised performance is favourable. Conversely, efficiency is increased for energetic sea states, when optimal performance is not necessary due to the high level of incident wave power. To quantify the effect of front wall thickness on annual performance at Arch Point, the performance indicators described in Section 7.4 were employed. The upper limit for mean annual absorbed power was calculated for each design using Equation 7.6. This was supplemented with capture width ratio as defined by Equation 7.7. These are presented in Table 7.5 below.

Table 7.5 Performance indicators for SOWC chamber designs with varying front wall thickness at Arch Point, Co. Clare.

Front Wall Thickness	Mean Annual Absorbed Power	Capture Width Ratio
1.8 m	156 kW	56 %
4.8 m	151 kW	54 %
8.8 m	123 kW	44 %
12.8 m	86 kW	31 %
16.8 m	61 kW	22 %

The above results show that as front wall thickness increases, the annual performance decreases. This is predominantly due to the previously described detuning effect. It is acknowledged that the values for each performance indicator are higher than those associated with non-linear conditions. However, it is predicted that the overall trend, influenced by detuning, will remain in non-linear conditions.

7.9.2.2 Performance at Loop Head

As described in Section 7.8 Sites, there is a larger spread of significant wave heights at the tip of Loop Head due to the exposed location. Considering the scatter diagram for the tip of Loop Head (Figure 7.10) it can be seen that energetic sea states possessing a significant wave height greater than 3 m and a period greater than 13 s constitute a larger proportion of the wave climate over a given year in comparison to Arch Point. Therefore, it is interesting to investigate the affect this has on power

absorption for each chamber design. Matrices equivalent to those presented for Arch Point are presented for the tip of Loop Head in Figure 7.17 below.

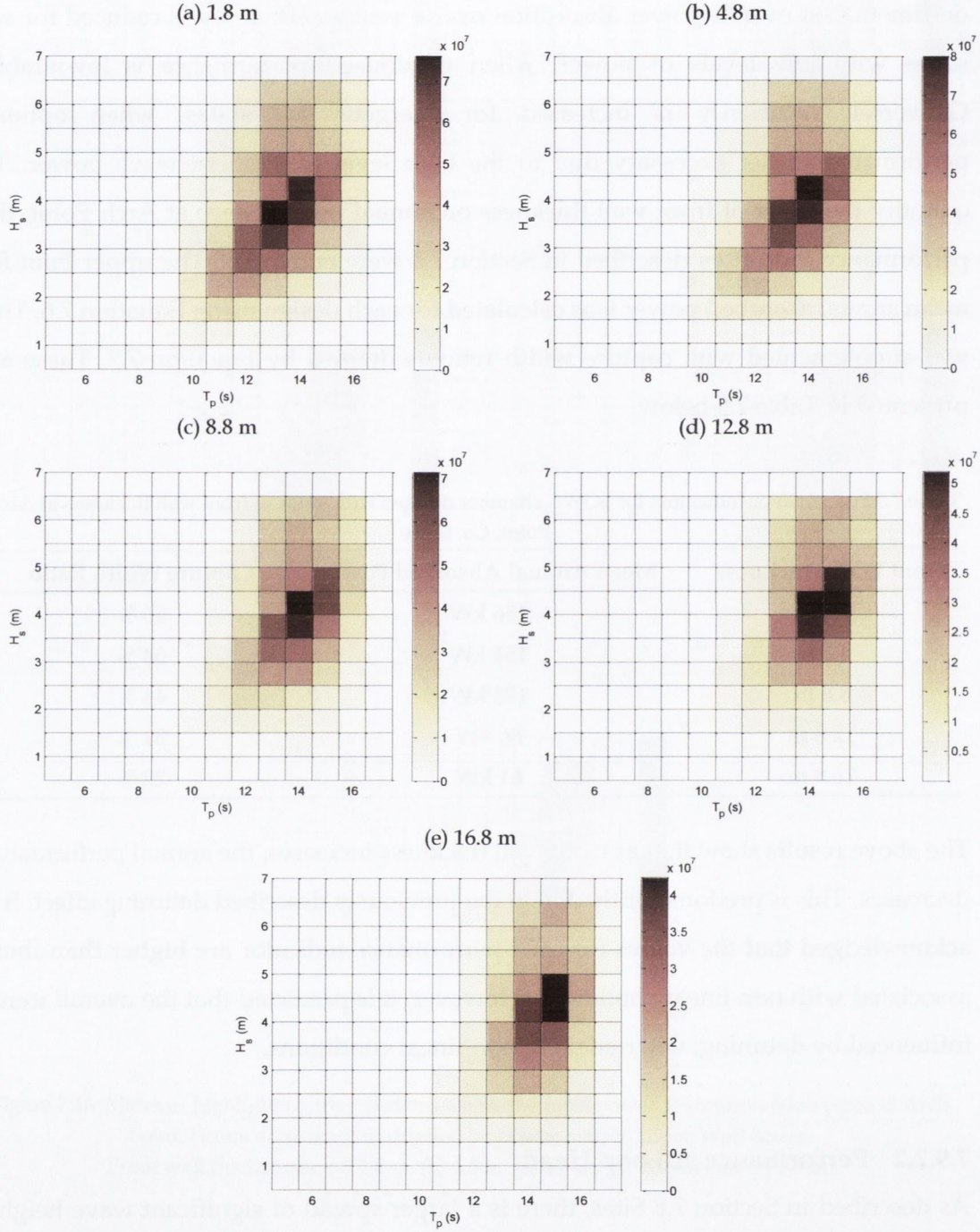

Figure 7.17 Matrices highlighting the sea states where the most power absorption takes place at the tip of Loop Head. Hours occurrence multiplied by power matrix. Units: Watt hours.
Front wall thicknesses: (a) 1.8 m, (b) 4.8 m, (c) 8.8m, (d) 12.8m and (e) 6.8m.

Comparing the overall trend of power absorption with that for Arch Point, it is evident high levels of power are absorbed from a wider range of sea states. This can be attributed to the larger spread of energetic sea states in comparison with Arch

Point. Focussing on the pattern of power absorption in Figure 7.17, as front wall thickness increases, a similar effect to that experienced for Arch Point is apparent. SOWC chamber designs with a front wall thickness of 1.8 m and 4.8 m absorb high levels of power from a wider range of sea states than chamber designs with a front wall thickness of 12.8 m and 16.8 m. However, a larger proportion of the annual resource is made up of the higher range of wave periods (above 13 s). Considering the power matrices for front wall thicknesses of 8.8 m and 12.8 m, this characteristic of the wave climate at the tip of Loop Head favours the performance of these designs in comparison to Arch Point. This suggests that as front wall thickness increases, the decline in annual performance is less marked than is the case for Arch Point. To investigate this supposition, the upper limit for mean annual absorbed power and capture width ratio are presented for each chamber design in Table 7.6.

Table 7.6 Performance indicators for SOWC chamber designs with varying front wall thickness at the tip of Loop Head, Co. Clare.

Front Wall Thickness	Mean Annual Absorbed Power	Capture Width Ratio
1.8 m	203 kW	54 %
4.8 m	199 kW	53 %
8.8 m	176 kW	47 %
12.8 m	135 kW	36 %
16.8 m	105 kW	28 %

Considering capture width ratio, increased front wall thickness is slightly less detrimental to overall performance in comparison to Arch Point. Additionally, the greater annual average wave power for Loop Head induces high values for mean annual absorbed power for each design. In light of this analysis, the tip of Loop Head appears a more favourable location for SOWC wave energy converter installation.

7.10 Altering Front Wall Thickness: 8 m wide chamber

The 11 m wide chamber design was identified as the maximum permitted width for the SOWC chamber design using the tunnelled construction technique. This limitation was based on the structural integrity of the chamber declining significantly for widths greater than 11 m. Conversely, consultancy from Tara Mines (McConnell, 2012) highlighted that reducing the chamber width reduces structural risks associated with wide tunnel spans. Based on this, an 8 m span was considered more

favourable than an 11 m span in terms of structural integrity. In terms of power generation, reducing the width reduces the incident wave power available to the SOWC wave energy converter. These opposing influences on chamber design directly affect the feasibility of the SOWC concept. This section aims to quantify the reduction in power associated with the 8m wide design.

To investigate these issues, the five previously analysed chamber designs were altered from 11 m wide to 8 m wide. This reduced the volume of the chamber and water plane area of the free surface. Hence, the mass of the water column was affected along with the water plane stiffness. However, the fundamental design constituting a 4m front wall draft and 60 degree incline remained constant. Similarly to the study on 11m wide chamber designs, front wall thicknesses analysed were 1.8m, 4.8m, 8.8m, 12.8m and 16.8m. The fixed values for each design parameter are presented in Figure 7.18.

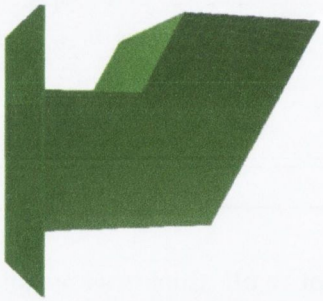

Design Parameter	Value
Front wall draft	4.0 m
Chamber Incline	60 deg
Water column width	11.0 m
Water depth	17.0 m
Water plane area	62.5 m^2
Inlet area	52.5 m^2

Figure 7.18 Left: Cross sectional view of SOWC chamber design. Right: Full Scale dimensions

Similarly to Section 7.10, a front wall thickness of 1.8 m provides an insight to the hydrodynamic performance associated with a conventional OWC design that is not bound by the same structural limitations as a SOWC wave energy converter. 4.8 m is considered the minimum front wall thickness permitted for SOWC chamber design. Based on results from the 11 m wide design, a front wall thickness of 16.8 m was again taken as the maximum front wall thickness.

To identify the natural frequency for each design the RAO was employed. As the RAO is the only parameter required to achieve this, the presentation of other

hydrodynamic properties is not necessary. The RAO for each design with no applied damping is presented in Figure 7.19.

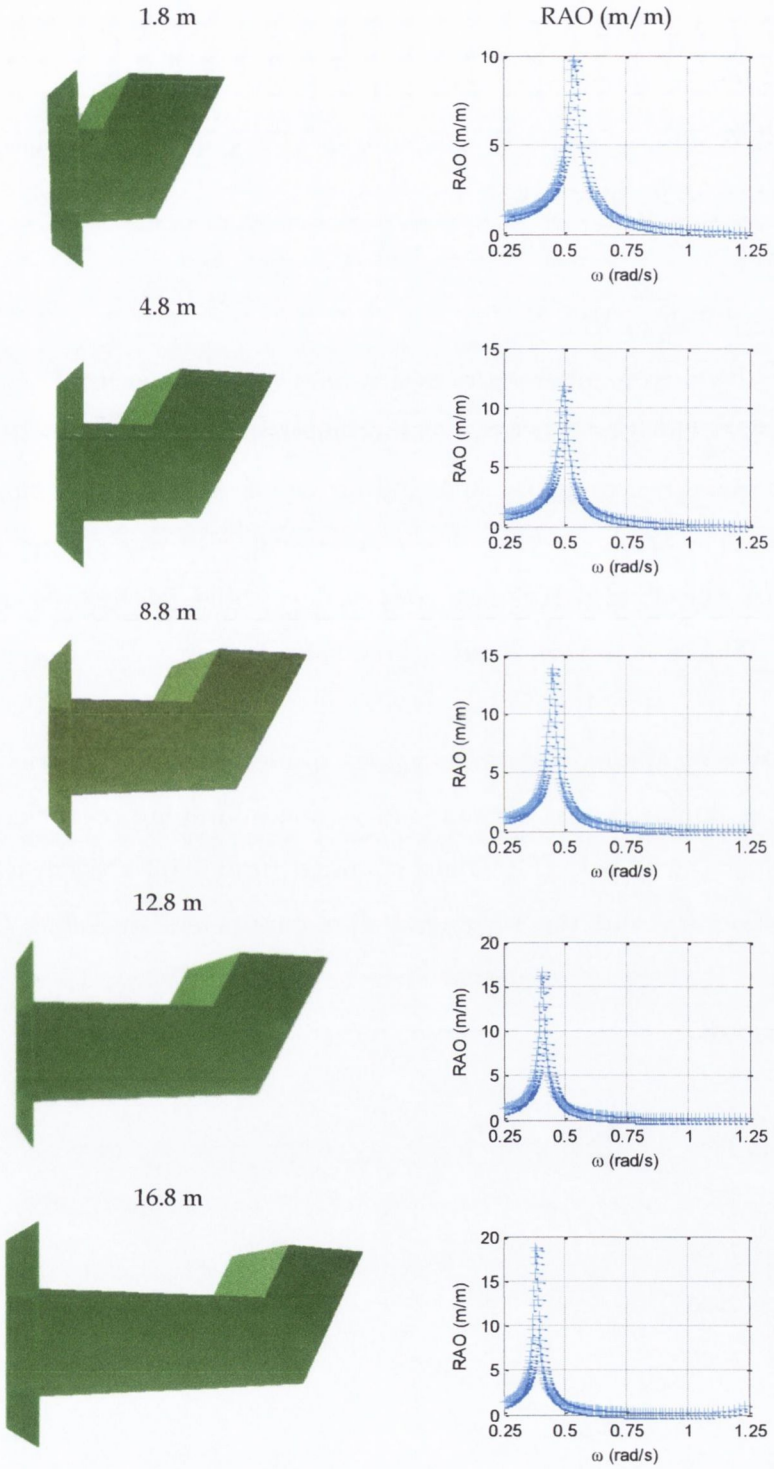

Figure 7.19 RAO (m/m) vs. angular frequency (rad/s) for SOWC chamber designs with varying front wall thickness: 1.8 m, 4.8 m, 8.8 m, 12.8 m and 16.8 m. Chamber width = 8 m. Depth of inlet = 4 m. Incline = 60 degrees.

As with the 11 m wide chamber designs, the frequency at which resonance takes place reduces as front wall thickness is increased. Hence the overall trend, regarding the increase in natural period with increased front wall thickness, remains. In relation to the relative amplitude of the water column, there is a slight increase in RAO at resonance for each design in comparison to 11 m wide chambers. Apart from this aspect, the overall hydrodynamic behaviour of the 8 m wide is relatively similar to that for its 11 m wide counterpart.

7.10.1 Power Take Off

Considering the 8 m chamber width and annual wave power level at Arch Point and the tip of Loop Head, a 500 kW turbine was not suitable for this design. As the overall pneumatic power available to the turbine is reduced in comparison to 11 m wide chambers, a turbine with a lower power capacity was sought for this study. Regarding the selection of turbines presented in Table 7.4, turbine option 4 with a capacity of 300 kW was considered appropriate. This was based on power capacity and the range of optimal damping coefficients for each chamber design compared with the range of applied damping values induced by the turbine at operational speeds. Using Equation 6.10 the range of optimal damping coefficients for the five chambers were calculated. The values spanned from 1902 kNs/m to 2401 kNs/m. Using Equation 6.9 and the turbine design parameters in Table 7.4 the turbine dampings for a range of rotational speeds were calculated. These are plotted in Figure 7.20 below.

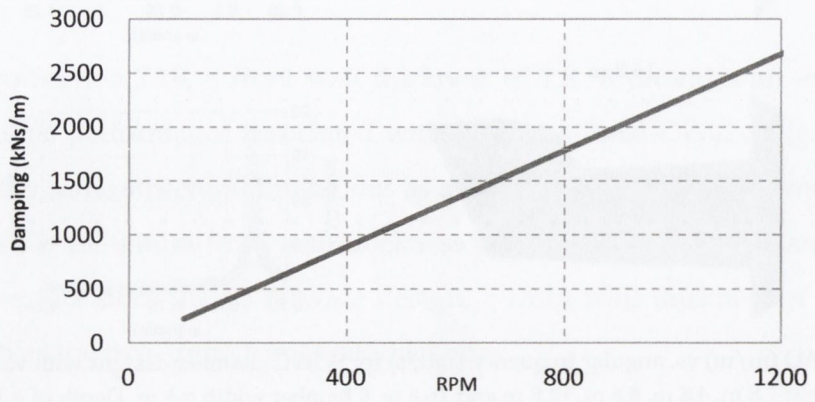

Figure 7.20 Effect of rpm on damping. Turbine option 4 (300 kW)

Assuming an equivalent range of operational speeds (700 rpm -1200 rpm) associated with the 500 kW turbine (Whittaker et al., 2002), the applied dampings induced by this design extend from 1562 kNs/m to 2678 kNs/m. As this range of dampings covers the range of optimal damping coefficients, it was suitable for this study. When calculating absorbed power, optimal damping coefficients within this range were applied to each chamber design.

7.10.2 Power Matrices

Power matrices denoting absorbed power are presented for each of the 8 m wide chamber designs in Figure 7.21 below.

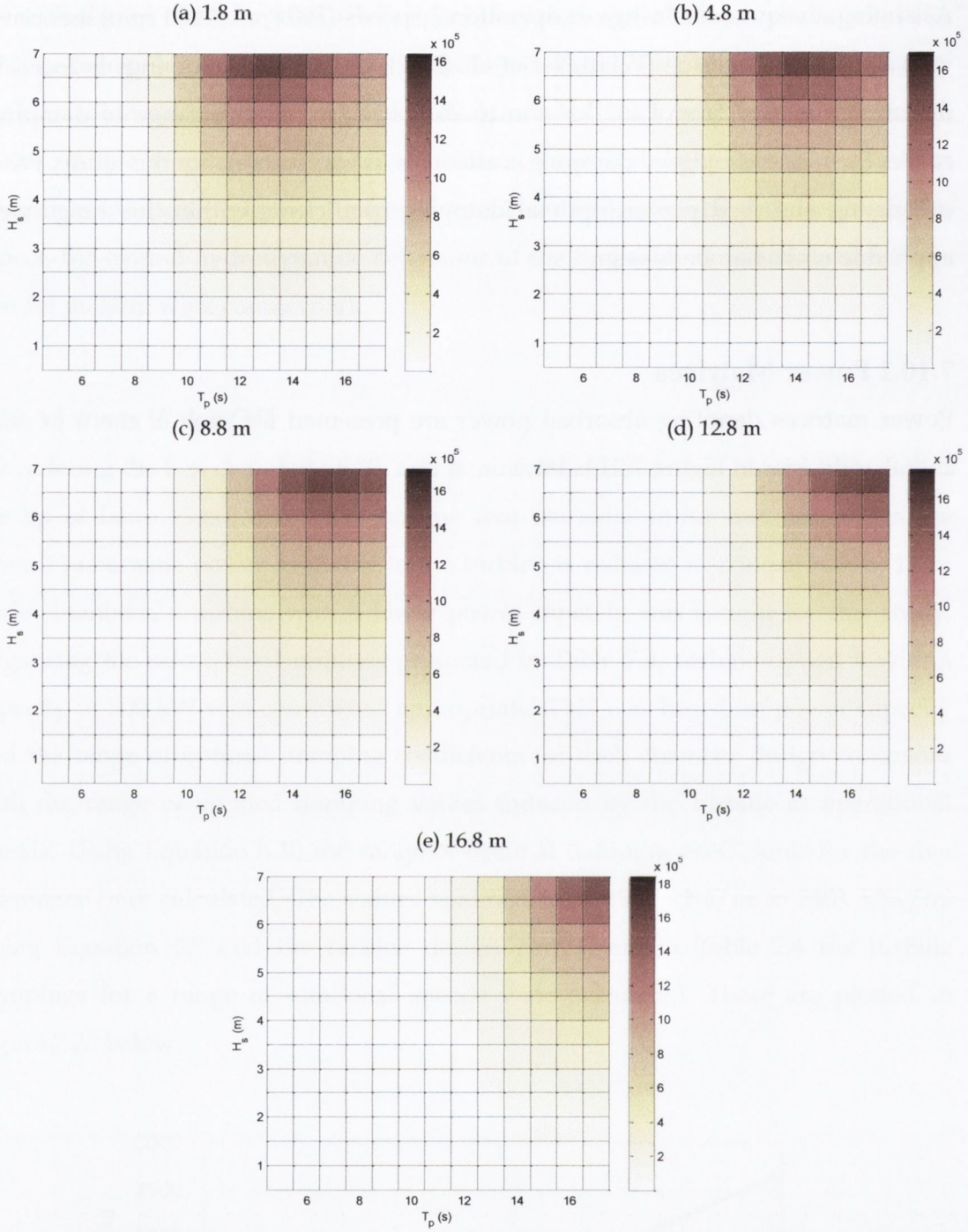

Figure 7.21 Power matrices denoting upper limit for power absorption for each sea state. Units: Watts. Front wall thickness: (a) 1.8 m, (b) 4.8 m, (c) 8.8 m, (d) 12.8 m and (e) 16.8 m. Chamber width = 8 m. Depth of inlet = 4 m. Incline = 60 degrees.

It is evident that the trend in power absorption is equivalent to that for an 11 m wide design. However, the power absorption is reduced due to the smaller chamber design coupled with a lower applied damping representing the power take off. Also, comparing the matrix for each front wall thickness with its 11 m wide counterpart, there is very slight shift in the range of periods at which maximum power absorption

takes place. For each design, the change in period at which maximum power absorption takes place is approximately 0.5 s less than that for the equivalent 11 m design. This is predominantly due to the reduction in chamber volume compared with the 11 m wide design. This reduces the mass of the water column within the chamber which reduces the period at which resonance takes place within the chamber. Hence, it is interesting to quantify this affect and investigate how this influences the capture width ratio for a given chamber design when exposed to the annual average wave conditions for Arch Point and the tip of Loop Head.

7.10.2.1 Performance at Arch Point

Matrices denoting watt hours absorbed power per year are presented for each of the 8 m wide chamber designs in Figure 7.22 below.

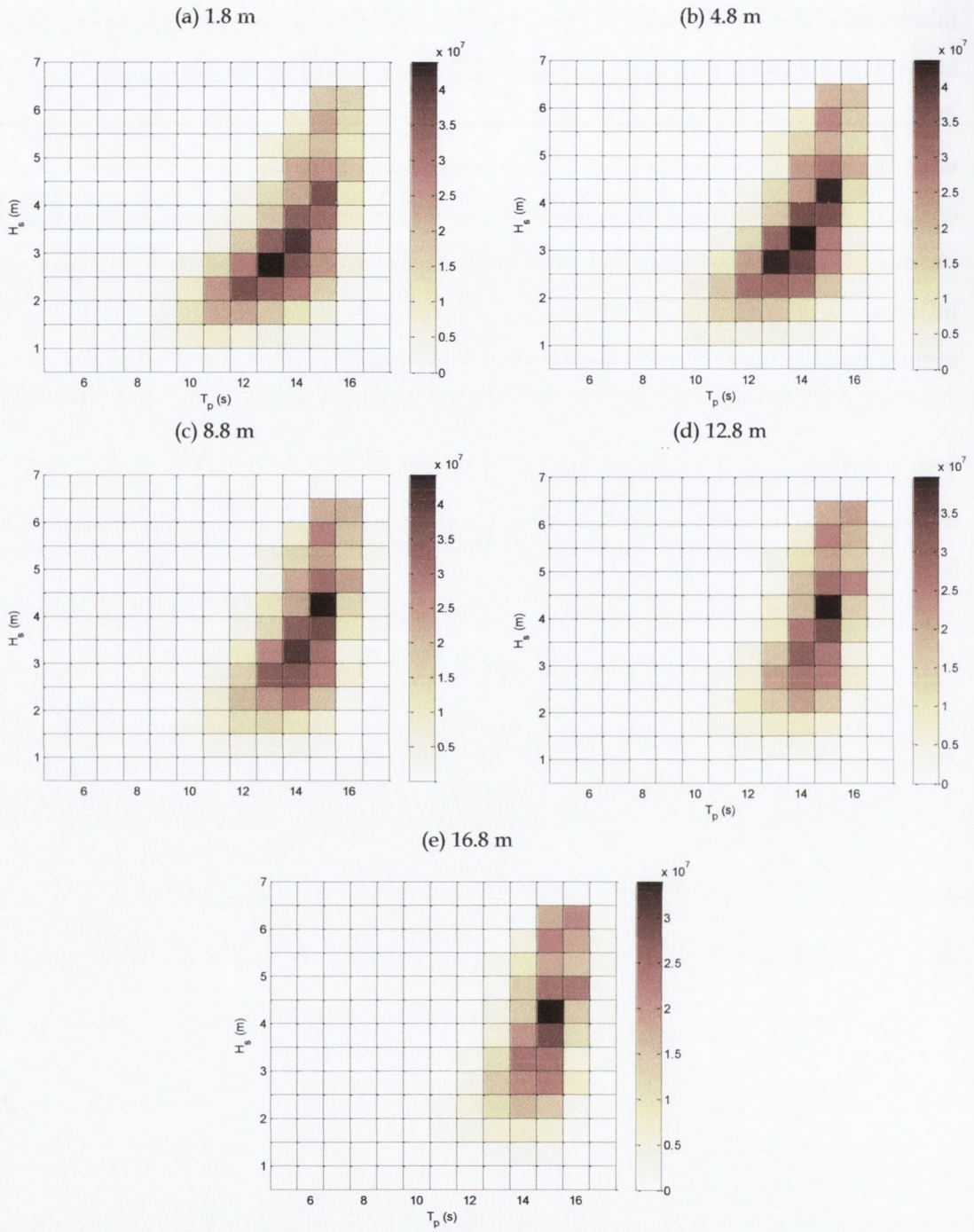

Figure 7.22 Matrices highlighting the sea states where the most power absorption takes place at Arch Point. Hours occurrence multiplied by power matrix. Units: Watt hours.
Front wall thicknesses: (a) 1.8 m, (b) 4.8 m, (c) 8.8 m, (d) 12.8 m and (e) 6.8 m.

There is a noticeable reduction in the scale denoting watt hours for each matrix in comparison to 11 m wide designs. This is attributed to the reduced incident wave power available to each SOWC wave energy converter. In terms of wave power per metre wave front, kW/m, the reduced width of the chamber reduces the incident wave power by approximately 75 kW/m. This is based on the average annual wave

power at Arch Point. Apart from this, the overall trend in power absorption is equivalent to those presented for the 11 m designs performance at Arch Point. To reveal the influence of the slight shift in natural frequency it is necessary to calculate the performance indicators. These are presented in Table 7.7.

Table 7.7 Performance indicators for SOWC chamber designs with varying front wall thickness at Arch Point, Co. Clare. Chamber width = 8 m.

Front Wall Thickness	Mean Annual Absorbed Power	Capture Width Ratio
1.8 m	112 kW	56 %
4.8 m	110 kW	55 %
8.8 m	92 kW	46 %
12.8 m	64 kW	33 %
16.8 m	52 kW	26 %

Regarding capture width ratio, the reduction in performance with increased front wall thickness is less than for the 11m wide design. This is influenced by the slight shift in natural frequency. The extent to which the 8.8m and 12.8m are detuned from the prevailing wave climate is lessened.

7.10.2.2 Performance at Loop Head

Matrices denoting watt hours absorbed power per year are presented for each of the 8 m wide chamber designs in Figure 7.23 below.

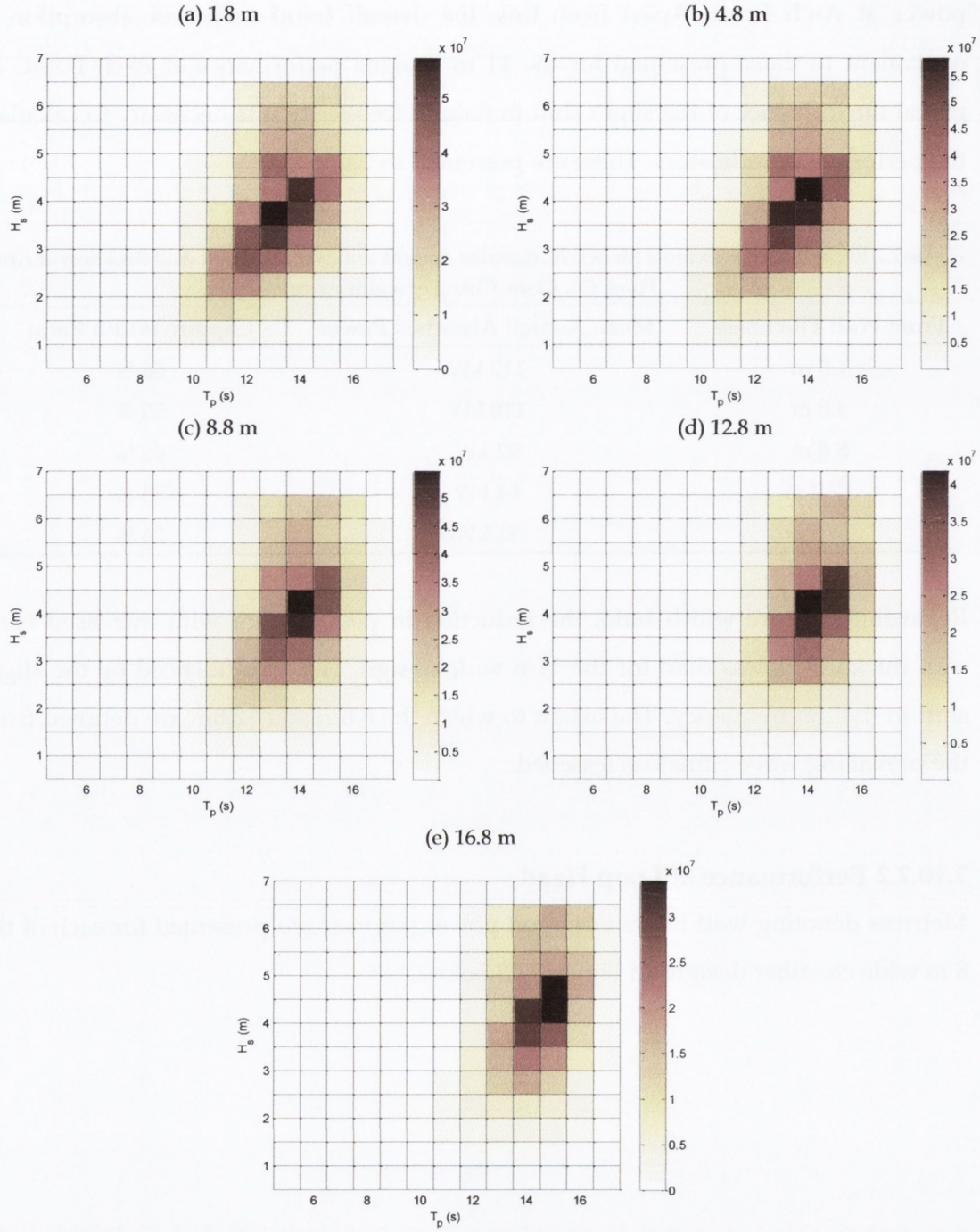

Figure 7.23 Matrices highlighting the sea states where the most power absorption takes place at the tip of Loop Head. Hours occurrence multiplied by power matrix. Units: Watt hours.
Front wall thicknesses: (a) 1.8 m, (b) 4.8 m, (c) 8.8m, (d) 12.8 m and (e) 6.8 m.

The above graphs display previously described trends for reduction in chamber width, increased front wall thickness and performance at the tip of Loop Head. The watt hours absorbed for each sea state are less compared with the 11 m wide design due to the reduction in incident wave power available to the chamber. Increased front wall thickness detunes the SOWC wave energy converter from prevailing sea states. As with Arch Point, this detuning effect is slightly reduced due to the

reduction in natural period. The above points are confirmed by the performance indicators outlined in Table 7.8 below.

Table 7.8 Performance indicators for SOWC chamber designs with varying front wall thickness at the tip of Loop Head, Co. Clare. Chamber width = 8 m.

Front Wall Thickness	Mean Annual Absorbed Power	Capture Width Ratio
1.8 m	150 kW	55 %
4.8 m	147 kW	54 %
8.8 m	133 kW	49 %
12.8 m	106 kW	39 %
16.8 m	81 kW	30 %

7.11 SOWC DESIGN

Following analysis of different SOWC chamber geometries within established design bounds, findings associated with their performance at Arch Point and Loop Head are summarised in Figure 7.24 and Figure 7.25 below.

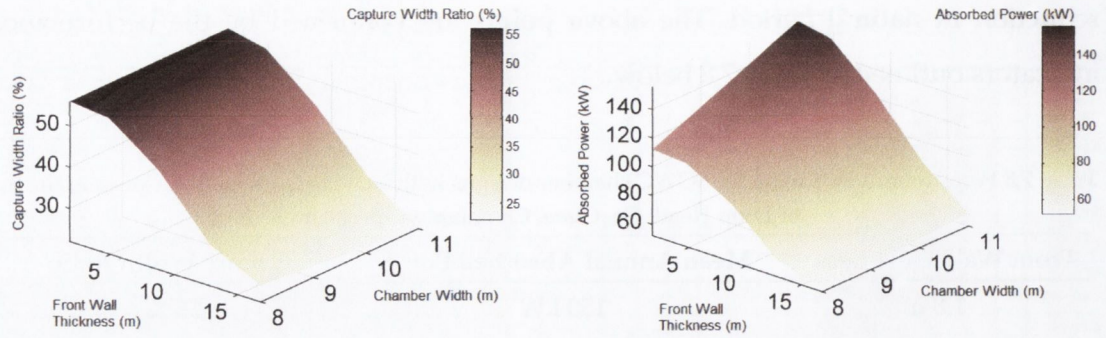

Figure 7.24 Location: Arch Point. Effect of front wall thickness and chamber width on annual average capture width ratio (left) and mean annual absorbed power (right)

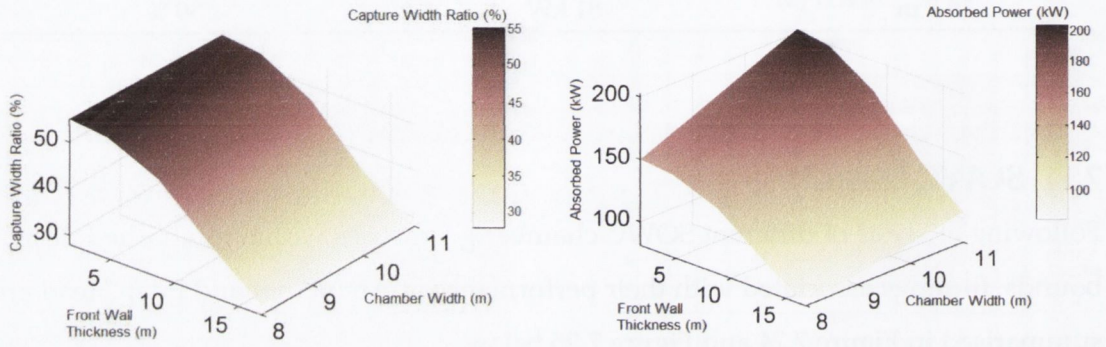

Figure 7.25 Location: Tip of Loop Head. Effect of front wall thickness and chamber width on annual average capture width ratio (left) and mean annual absorbed power (right)

These graphs plot the values presented in Tables 7.5, 7.6, 7.7 and 7.8 corresponding to the annual average capture width ratio and mean annual absorbed power for each chamber design assessed at each location. Each graph is predominantly described by affects associated with the tuning of the SOWC chamber design relative to the wave climate at Arch Point and the tip of Loop Head. The bounds of chamber design, established in Chapter 6, are based on the structural limitations associated tunnelling construction technique. As previously mentioned, 4.8 m is the very minimum value for front wall thickness. Based on the fundamental SOWC design with a 60 degree incline and front wall draft of 4 m, the performance of the 4.8 m front wall thickness is shown to perform the best at both locations. As front wall thickness is increased, the performance reduces as the SOWC wave energy converter becomes detuned from the prevailing wave climate. The extent to which the design is detuned is dependent on the extent to which the front wall is increased. This conflicts with design based on structural integrity. Thus a balance must be met in terms of the design of the front wall. Figure 7.24 and Figure 7.25 provide an insight to where this balance can be achieved. The same applies to chamber width. Reducing the width increases the

structural integrity of the chamber however it reduces the incident wave power available to the SOWC wave energy converter. The decisions made on these issues are dependent on the site. Considering the wave power level at the tip of Loop Head is greater than Arch Point, increasing the front wall thickness or reducing chamber width in light of structural considerations may be achieved without reducing power absorption to an unfeasible level. Cost benefit analysis of Wells Turbines (Section 6.3.3) has shown that economics favour high capacity turbines. Thus, to reach a given power generation target, a small number of large chambers coupled with high capacity turbines is favoured over a large number of small chambers coupled with lower capacity turbines. This accentuates the need for both capture width ratio and absorbed power when assessing the suitability of a chamber design for a given location. Although capture width ratio overall shows the relative performance for the 8 m wide design to be slightly better in comparison with the 11 m wide design, it is the mean annual absorbed power which is central to its feasibility for a potential site.

As mentioned previously, the method used in this study is suitable for comparison of alterations in specific design parameters, rather than for accurately identifying exact annual power production. It is a method compatible with preliminary enquiry TRL stages 1-3. It provides upper limit of mean annual power values with a given turbine and does not model non-linear effects. In summary, the figures given provide an initial guide and overall show the direction of any change created by alterations of the parameters under study at Arch Point and the tip of Loop Head. This can in turn guide further investigation. In terms of mean annual absorbed power, increased accuracy for a selected SOWC chamber design may be achieved via a tank testing programme and/or the development of a spectral or time domain model in which non-linearities such as vortex shedding may be incorporated.

7.12 Summary

In this chapter results of a series of hydrodynamic analyses were presented and they threw light on how the design of an SOWC may be optimised. These results were relevant to second aim of the overall research programme, which was to use the findings from a wave climate modelling study conducted to achieve the first aim and build upon an earlier TCD (Marine Institute, 2000) study to investigate design

parameters which may influence the survivability and feasibility of potential SOWCs installed at Loop Head.

The findings from Chapter 7 may be summarised as follows. Initially, benchmarking exercises were carried out. One exercise assessed agreement between results computed using WAMIT, as set up for this study, and small scale (1:36) tank testing, which operates predominantly in line with linear wave theory. Central to the hydrodynamic model set-up is the modelling of the OWC free surface. Two approaches were carried out. One was the traditional approach, known as the weightless lid method and the other was a newly available WAMIT option called the free surface pressure patch. In the course of this exercise it was not only found that WAMIT results compared adequately with tank test results, but also that the new method for OWC surface modelling showed good agreement with the traditional method. In a second benchmarking exercise, the WAMIT model, as set up for this study, was used to analyse the operation of a full scale OWC and to compare the results of this with experimental data available on that device. A satisfactory level of agreement was found.

Following the above validation of the numerical model, performance indicators were calculated for a number of different SOWC designs. The parameters for these designs which best produced optimal performance, were identified in Chapter 6. In the course of this investigation they were kept constant, with the exception of the variables under investigation. These variables were front wall thickness and chamber width. As already discussed, increased front wall thickness and reduced chamber width may be required to support structural integrity and SOWC survivability. Thus the effect of altering such variables was sought.

These analyses were conducted for SOWCs in two potential sites, namely Arch point and the Tip of Loop Head. These sites are associated with different wave climate scatter diagrams. At the tip of Loop Head sea states possessing a significant wave height greater than 3 m and a wave period greater than 13 s constitute a larger proportion of the wave climate over a year than is the case at Arch Point.

For each site, initially five SOWC designs were analysed with progressively increasing front wall thicknesses while other parameters were kept constant. The chamber width for this series was 11m. Results showed the SOWC with a front wall thickness of 1.8 m was adequately tuned to the wave period of the prevailing sea state and gave optimal performance. The results were similar to those of the Pico OWC, which uses this front wall thickness. However, as the front wall increased, the tuning changed and became associated with a different and higher wave period. Correspondingly, the upper limit of annual power and capture width ratio reduced as front wall increased. This pattern was evident for both sites. However, as noted above, the tip of Loop Head experiences more energetic seas than Arch Point. This is reflected in higher values for annual power and capture width ratio found for the tip of Loop Head.

The same basic chamber design was then used to examine the effect of altering chamber width. Reducing the chamber width necessitates reducing the incident wave front and therefore the amount of wave power available to the device. Also the change in tuning associated with increased front wall thickness allowed the power of those higher period waves to become more available for extraction.

Further chamber designs, now with a width of 8 m, were investigated with the same series of front wall thickness increases. The same pattern of change in tuning associated with increasing front wall thickness was seen. Correspondingly annual power values and capture width ratio reduced in relation to increasing front wall thickness. However, capture width ratio overall was not quite as reduced as it was for the 11 m chamber. This is because the reduced width in turn reduced the volume of water in the chamber. It is the increases in chamber water volume, associated with the increased front wall thickness, that change the point of resonance to higher wave frequencies. Therefore for any given front wall thickness, the 8 m chamber with its slightly smaller water volumes, would be tuned to a slightly lower wave frequency than its 11 m counterpart. Hence for any given increment in front wall thickness, the change in tuning away from the frequency of the prevailing wave climate was very slightly less than for the 11 m chamber. However this effect was not sufficient to overcome the effect of the reduced wave energy available to the narrower chamber. Thus the narrower chamber still produced less annual power. The effect of this

reduced performance is further compounded by the fact that the lower power output would require use of a lower capacity turbine. As described in Section 6.3.3, low capacity turbines are less cost effective compared with higher capacity turbines. This indicates that to achieve a given target capacity, it is more cost-effective to install a small number of devices with higher levels of power absorption than a large number of smaller chambers with lower levels of power absorption. Further details on costs associated with SOWC wave energy converter design are discussed in Chapter 8.

Chapter 8
DISCUSSION AND CONCLUSIONS

In this chapter, the way in which the aims and objectives of the research programme described in this thesis were achieved and key findings relevant to them will be summarised and discussed. The limitations of the methodology used will be considered. The implications of key findings will be outlined and future research priorities will be identified. This will be achieved by initially summarising key issues addressed in each chapter.

8.1 DISCUSSION

8.1.1 Chapter 1: Introduction

Chapter 1 introduced the rationale for the research programme described in this thesis and set out two main aims. The first aim was to characterise the wave climate for a domain off the coast of County Clare adjacent to Loop Head, as this is an area of interest for ocean energy development in Ireland. The second aim was to use the findings from a wave climate modelling study conducted to achieve the first aim, and build upon an earlier TCD (Marine Institute, 2000) study to investigate design parameters which may influence the survivability and feasibility of potential SOWCs installed at Loop Head.

The first aim of characterising the wave climate for a domain off the coast of County Clare adjacent to Loop Head entailed the following specific objectives.

- To develop and calibrate a 3rd generation spectral wave model for on-shore, near-shore and off-shore domains off Loop Head

- To assess wave power levels off the County Clare coast from off-shore to near-shore and on-shore domains (for the purpose of this thesis, this area is referred to as the 'Clare Domain')
- To determine the wave climate characteristics in regions adjacent to Arch Point and Loop Head extending from depths of approximately 80 m to the cliff base
- To establish the percentage occurrence of each sea state at locations in the off-shore, near-shore and on-shore areas of the Clare Domain
- To establish the percentage occurrence of each sea state at specific SOWC sites (Arch Point and the tip of Loop Head).

The second aim was to use the findings from a wave climate modelling study conducted to achieve the first aim and build upon an earlier TCD (Marine Institute, 2000) study to investigate design parameters which may influence the survivability and feasibility of potential SOWCs installed at Loop Head.

The potential efficiencies of accessing all opportunities for wave energy extraction adjacent to areas designated for other wave energy projects provided a rationale for both aims of the research programme. Such efficiencies might include shared infrastructure. In addition the second aim prompted preliminary study of whether SOWCs would constitute a feasible technology for utilising the on-shore resource in the above area. SOWCs were chosen for study to see whether they might address challenges of survivability and/or high construction cost encountered by a range of other WECs (Holmes and Nielsen, 2010).

In line with this, the project set out to discover if SOWC design parameters which optimise survivability would impair performance, and to see if the resulting findings have implications for feasibility. The second aim was achieved by pursuing the following objectives:

- To investigate factors affecting subterranean oscillating water column (SOWC) wave energy converter to determine bounds for chamber design.
- To develop a numerical hydrodynamic model of a SOWC wave energy converter
- To validate this model by benchmarking it against tank testing data

- To validate this model by benchmarking it against a hydrodynamic model of the full scale Pico OWC (Brito-Melo et al., 1999)
- To use a hydrodynamic model to identify trends in efficiency associated with changes in SOWC design parameters which may be necessary to promote the survivability of these WECs in their potential locations at Arch Point and the tip of Loop Head.

8.1.2 Chapter 2: Literature Review

Chapter 2 provided a literature review. It described supports for wave energy, including accepted standards for project development. It indicated that, as an experimental study exploring the validity of WEC concept and design in relation to the intended environment, this research programme was in line with the ESB Technology Readiness Levels 1 to 3. Methodology designated as appropriate to these stages was used. In particular it was noted that international guidelines propose that hydrodynamic model formulation in the frequency domain is appropriate for the early stages of WEC design. Theory was then described which underpinned this methodology. This included linear potential flow theory and suitable methods for numerically modelling wave-structure interaction with a fixed OWC wave energy converter. Regarding resource characterisation, the theory behind 3rd generation spectral wave modelling was described.

8.1.3 Chapter 3: Site Viability Study and Survey

Chapter 3 described a preliminary investigation that was carried out prior to wave climate modelling and hydrodynamic analysis associated with the two aims of the research programme. Although the previous TCD study (Marine Institute, 2000) on which this thesis was based had identified the coast off County Clare as potentially suitable for WEC deployment, a review was carried out to check if this area remained appropriate for further investigation. First, this review showed that the areas in question were adjacent to other areas being considered for wave energy. This related to the rationale of exploring opportunities for shared infrastructure. Secondly, accepted site selection criteria formulated by Waveplam (2009) and the Carbon Trust (2005) were used to assess the suitability of the study locations for WECs and SOWCs. In addition, site suitability criteria specifically related to SOWCs were

explored. The process required information that was accessed from previous studies, publically available data and a site survey conducted by the author at Loop Head.

From the review it was concluded that the area possessed acceptable levels of wave energy and a cliff shoreline structure appropriate for potential installation of SOWCs. That is, Loop Head had some areas of steep cliff descending into water that was sufficiently deep, unobstructed by rocks and debris making it a suitable SOWC shoreline site. Information at that time indicated that the geology of Loop Head was suitable for SOWC installation. With respect to planning and human activity, conservation areas at the tip of Loop Head but not Arch Point were identified. This was not held to be a barrier to the project as a whole. Infrastructure with the potential for further development appeared to be available.

Also crucial for the viability of the study was the availability of bathymetric, metocean and off-shore boundary data required for the generation of a 3rd generation spectral wave model. In addition, local wave measurements were necessary for calibration and validation of the wave model. Such information was available for the area in question.

In view of all of these considerations, the Clare Domain and Loop Head site were considered suitable for further investigation.

8.1.4 Chapter 4: Spectral Wave Model

Chapter 4 described the process of developing, validating and calibrating a 3rd generation spectral wave model. The model was set up initially to cover an area extending from the Clare coast to a border approximately 100 km for the coast. An area named the 'Clare Domain' extending from the Clare coast to a border approximately 20 km from the coast was then modelled with a greater level of detail and accuracy.

The process of setting up and validating the model involved a number of stages. Initially creation of the model required two dimensional spectral wave data set at model boundaries. Various sources were reviewed to identify the most appropriate model to provide these data. The UKNS model (Beg, 2013) was chosen. Physical

measurements from the M1 buoy were used to assess the accuracy of data provided by the UKNS model. The M1 Buoy data were obtained from the Irish Marine Institute. Comparisons were also made for metocean data: wind and surface elevation due to tide. For validation of the surface elevation data related to tides, corroborating data were obtained from a tidal measuring gauge situated at Carrigaholt on the coast of County Clare.

Bathymetric data were also incorporated into the 3rd generation spectral wave model. Bathymetric data with different levels of resolution and accuracy were used for different areas of the region under study. Digitised admiralty chart data were used for the wider area extending from the Clare coast to a border approximately 100 km from the coast. Admiralty chart data with higher resolution were used for the Clare Domain, a smaller region extending about 20 km from the coast and to a depth of 150 m. For a more circumscribed sea area off the tip of Loop Head and Arch Point, finer resolution bathymetric data were used with data points set approximately 5 m apart. Finally, fair sheet data were used to provide bathymetric data for regions close to the cliffs.

MIKE 21 SW model calibration and validation was performed against wave measurements recorded by a wave rider buoy located off Arch Point, Co. Clare. Additionally, data output from MIKE 21 SW was compared with output from a Wave Watch 3 spectral wave model at the 20 m depth contour off Killard Point. In both cases the level of agreement between model outputs and comparison data was high, possessing a scatter index less than 0.2 and correlation factor greater than 0.85.

The 3rd generation spectral wave model was used to generate information for the Clare Domain regarding wave resource characteristics, including wave height, period, power and directionality. Samples of these results were given in Chapter 5. Available data sets facilitated 4 year simulations. High performance computing allowed models to be run using high resolution flexible mesh circumscribing the Clare Domain.

In summary a 3rd generation spectral wave model with corroborated accuracy was developed. A possible limitation in terms of accuracy relates to the fact that data

obtained over a 4 year span may not *fully* reflect conditions likely to occur over longer time periods. This is known as aleatory uncertainty.

8.1.5 Chapter 5: Wave Energy Resource Characterisation

Chapter 5 presented the results of the wave climate modelling study for the areas under investigation. The results presented in Chapter 5 achieved the first aim of the research programme by characterising the wave climate for a domain adjacent to Loop Head. The more detailed objectives entailed by the first aim of the research programme (listed above under summary of Chapter 1) were also met by the results presented in Chapter 5. A 3rd generation spectral wave model for on-shore, near-shore and off-shore domains off Loop Head was developed and calibrated. The annual average wave power levels where a SOWC wave energy converter could potentially be located were determined. Two locations investigated in detail were the tip of Loop Head and Arch Point. Scatter matrices for these two SOWC sites were also generated which showed the percentage occurrence of selected sea states.

The annual wave energy resource results were presented in relation to the wider area under study i.e., for the whole Clare Domain. These showed that between depths of 90 m and 50 m annual average wave power ranged between 60 and 50 kW/m. Between depths of 45 m and 20 m they ranged between 45 and 40 kW/m. For depths shallower than 15 m the wave resource rapidly reduced. Findings were then presented for the two relevant areas of interest located off the tip of Loop Head and off Arch point. Results included information on the wave energy resource, significant wave height, energy period, annual mean power, annual mean exploitable power, maximum wave height and wave directionality.

The percentage occurrence, over a year, of each possible combination of wave height and wave period (i.e. of each sea state), was presented as scatter diagrams for a range of different depth contours. These showed that in shallower waters wave heights were lower than at greater depths, and also that greater wave heights were associated with longer wave periods. The directionality of waves for the different sites was illustrated using rose diagrams. This showed that Arch Point was sheltered by the headland from waves from some directions, thus reducing the annual average wave power. The issue of extreme seas and the related topic of exploitable wave resource,

as opposed to total wave energy resource, were then discussed. In shallower waters where the sea bed rises it causes waves to break and lose power. Thus extreme sea states are filtered out as they approach shore. The exploitable resource was defined as the wave resource related to the operational conditions of a SOWC wave energy converter. This corresponded to significant wave heights between 0.5 m and 6.5 m in height. More extreme wave heights are not exploitable as most WECs are designed to shift into survival mode in response to such waves and thus cease operation. A comparison was presented between total average annual power and the exploitable resource for depths ranging from 90 m to 5 m. In deep water the non-exploitable component can be approximately 15 % of the total. For example, it can be calculated that as depth reduces from 50 m to 20 m, the reduction in average annual wave power reduces by approximately 27 % whereas the exploitable resource reduces by 16 %. Hence, in real terms, the difference in useable energy between deep water and sites nearer shore, is not as great as first appears.

8.1.6 Chapter 6: SOWC Wave Energy Converter Design

Chapter 6 presented information on a range of factors which influence the design and operation of SOWC wave energy converters in relation to the sites under study. These factors fall into categories including geology, wave climate, chamber design parameters, turbine characteristics and construction costs. The main findings are listed below.

8.1.6.1 Geology

The geological make-up of Loop Head cliffs had been investigated in the course of a UCD study (Haughton et al., 2010). Bore holes were used to take samples. The cliffs were found to consist of fine grained sandstone. This type of sandstone is harder and less porous than other softer types of sandstone but ideally quartzite or basalt are preferred for SOWC installation because of their compressive strength. The sandstone was interspersed with horizontal layers of shale. This did not of necessity present a challenge in relation to the suitability of the cliff for SOWC installation because its compressive strength is similar to that of sandstone. However there were some areas where the rock layering had become tilted or vertical which are potentially unsuitable for SOWC chamber construction. Chamber construction within

tilted or vertically layered rock may induce unsafe structural instability compared with horizontal layering. In addition there were some areas where fissures and hollows were visible in the cliff surface. The existence of such features in a SOWC site would be detrimental as they may impair the air tightness of the chamber.

In summary, the rock had moderate as opposed to high compressive strength and may prove to have some intermittent hollows and fissures. Any consequent vulnerability in terms of rock integrity would need to be taken account of when designing an SOWC chamber. Information from other sources (McConnell, 2012; Sewave, 2005) suggest that a potential SOWC at a site where the rock had high compressive strength would need to have a front wall thickness of at least 4.8 m plus reinforcements to survive extreme sea states. Therefore a SOWC wave energy converter constructed within Loop Head is likely to require front wall thickness that is greater than this. Information received on rock integrity also indicated that the maximum chamber width that could be sustained with reinforcements is likely to be 8 m with 11 m as an outside limit (McConnell, 2012; McCarthy, 2012; Holland, 1997).

8.1.6.2 Wave Climate

The greatest threat to rock integrity comes in the form of extreme waves. The likely frequency and force of breaking waves and plunging waves at Arch Point and Loop Head was investigated. The highest and most dangerous forces are associated with plunging waves. It was found that plunging waves were unlikely to form at Arch Point but could occur at the tip of Loop Head. The study data, which spanned 4 years, were used to predict the maximum height of waves that may occur over 20 years. This maximum height was estimated to be 13.26 m. The forces exerted on the cliff face were estimated to be 78 kN for non-breaking waves and in the order of 1200 kN for breaking waves. It was noted that the figure of 4.8 m front wall thickness mentioned above (in the section on geology) as the requirement for SOWCs to survive extreme sea states, was estimated in relation to seas in a range similar to the most extreme projected to occur over 20 years at Loop Head.

Another characteristic which effects chamber design is tidal range. The inlet of the SOWC chamber must be set at a minimum of 25% below spring tide range to reduce the risk of inlet broaching (Carbon Trust, 2005). The depth of the inlet effects SOWC

performance. Increasing depth of the inlet reduces the level of energy available and increases the energy period to which the device is best tuned. In relation to the spring tide data, the basic SOWC design modelled in these studies had an inlet depth of 4 m. Water depth at the entrance to the chamber must be at least 16 m. As was seen above, water depths shallower than this have lower energy levels.

8.1.6.3 Chamber Design Parameters

A range of chamber design parameters affect SOWC performance including front wall thickness, chamber width, incline of the chamber, length of air plenum, and type of turbine used. Two of these SOWC chamber design parameters, front wall thickness and chamber width, affect the survivability of SOWCs. Some design parameters also affect construction costs, which determine the feasibility of SOWC installation. What follows is a summary of key findings concerning SOWC chamber design parameters.

Front Wall Thickness

Previous studies have shown that increase in front wall thickness, and correspondingly, the length of the chamber increase the wave period at which resonance takes place. This phenomenon occurs due to the increased volume of water in the chamber that is associated with the increased chamber length. In addition it has already been shown that a SOWC is likely to need a front wall thickness of at least 4.8 m in order to preserve rock integrity and at Loop Head this value is likely to be higher than 4.8 m.

Chamber Width

Previous studies have shown that, on the one hand, OWC chamber width is best set at no more than 12 m in order to prevent internal sloshing inside the chamber, which reduces performance. Conversely, a reduced chamber width reduces the incident wave power available to the device.

Incline

Previous studies have confirmed that the incline of the SOWC chamber affords maximum performance if set at an angle of 60 degrees. Therefore this parameter was held at this setting in the basic chamber design under study.

Length of Air Plenum

The larger the air plenum between the water surface and the turbine, the greater the energy losses due to friction and air compressibility. However if a turbine is set too low, it can be damaged by exceptionally high seas rising within the chamber. Also small plenums are prone to high pressures which may cause turbine damage. Relief valves should be installed to avoid pressure build up. A Carbon Trust (2005) report advises that the turbine should be set at least 2.64 m above the highest anticipated level of the water column, but some devices with this setting have had turbines damaged by water ingress. Therefore the basic SOWC design modelled in this study had the turbine placed 5 m above the anticipated top level of the water column, which equated to 13 m above sea level.

8.1.6.4 Turbine Selection

Different turbines have different maximum capacities for power production and provide different levels of damping. To optimise performance, the turbine with a capacity matching the power potential of the SOWC, and which is able to provide damping in the optimal range should be chosen. The pricing of turbines is such that it is more cost-effective to install a small number of devices with high power output and high capacity turbines, than it is to install a larger number of devices with lower power output and lower turbine capacities.

8.1.6.5 Construction Costs

A target, as yet aspirational, which has been set for the wave industry is the aim of limiting costs to approximately €4 million per MW installed (The Carbon Trust, 2005). Despite initial hopes that SOWCs would entail a method of construction that would be relatively inexpensive compared to that of other WECs, very early indications are that this may not be the case. Developers wishing to contain construction costs may be faced with the choice of favouring SOWCs with either high survivability and poorer performance, or low survivability and higher performance. In summary the parameters for a basic SOWC design that were likely to favour performance were as shown in Table 8.1.

Table 8.1 SOWC Design Parameters

Parameter	Value or Setting
Front wall thickness	Value tailored to suit prevailing wave climate. The parameter value applicable to SOWC design which afforded best tuning was 4.8m
Chamber width	11 m
Chamber incline	60 degrees
Depth of inlet	4 m
Height of air plenum	13 m above sea level
Turbine capacity and damping	Matched to SOWC chamber characteristics
Water depth at cliff base	At least 17 m

The possible constraints on SOWC design that may result from the need to ensure device survivability are listed in Table 8.2.

Table 8.2 Constraints on SOWC Design

Parameter	Constraint
Front wall thickness	The front wall thickness that best suits performance may not suit survivability. Indications are that at Loop Head this is likely to exceed 4.8m
Chamber width	The chamber width that best suits performance is 11m whereas the width that best suits survivability is 8m

8.1.7 Chapter 7: Hydrodynamic Analysis

Chapter 7 presented the methodology used for numerical hydrodynamic analysis. The theoretical model formulation underpinning the hydrodynamic modelling, based on the massless piston and linear theory, was described. The equation of motion entailed by this theory and the equation relating to the power take off system were presented. Limitations of the model formulation were discussed. That is, that as a linear model, it could not model energy losses related to non-linear effects. Therefore results for annual power generation would be obtained as upper limits for power, rather than the somewhat lower values likely to occur. This also corresponded to an optimal damping representing the power take off. However as a study within TRL 1 to 3, final and definitive power production values were not required for the present project, and the performance indications used were sufficient for facilitating comparisons between SOWCs with different chamber designs.

The performance indicators used in the course of the study were the Response Amplitude Operator (RAO), the Upper Limit of Average Annual Power, and the

Capture Width Ratio. The RAO can be defined as the displacement, or amplitude, of the oscillating water column within the SOWC chamber, in relation to the incident wave field. The RAO varies depending on the frequency of the impinging waves. For a given device there is a particular frequency, or band of frequencies, which coincide with an increased RAO. If the waves impinge at a lower or higher frequency the RAO response is less. If the design of the device is altered, the wave frequency associated with the maximum RAO may also alter. For example, increasing front wall thickness increases the volume of water in the tunnel leading to the incline. This in turn decreases the wave frequency at which the RAO response is maximal. The maximal power output of the device occurs in response to wave frequencies associated with maximal RAO response. Therefore to maximise device performance, its design should be tailored to produce maximal response to the wave frequencies which are most prevalent throughout the year. The point at which the highest RAO occurs is known as resonance. Calculation of the RAO is a necessary step en route to the calculation of the two other performance indicators described below: the Upper Limit of Average Annual Power, and the Capture Width Ratio.

The upper limit for mean annual power gave a measure of the performance of a given SOWC design in a given location over a year. It can be used to compare levels of performance for different designs in the same location. Capture width ratio is denoted as absorbed power divided by incident wave power and is a measure of efficiency. It can be used to compare different designs in different locations.

SOWC chamber configurations were constructed with Multisurf version 8.0 (Aerohydro, 2011a); the frequency dependent hydrodynamic coefficients for SOWC designs in the presence of surface waves were calculated with WAMIT (WAMIT, 2011); and outputs from WAMIT were post-processed using Matlab® (Mathworks, 2013).

Benchmarking exercises were then described. One exercise assessed agreement between results obtained in the current project using WAMIT and those from a small scale tank testing. A central element of WAMIT is the modelling of the OWC free surface. WAMIT now has two ways of doing this. One is the traditional approach, known as the Weightless Lid and the other is a newly available option in WAMIT

called the Free Surface Pressure Patch. In the course of this exercise it was found that WAMIT results compared adequately with tank test results. Also the new method for OWC surface modelling showed a good agreement with the traditional method. In a second benchmarking exercise, the results from the WAMIT model, as set up for the present project, were compared with those from a model based on data from the full scale Pico OWC. A satisfactory level of agreement was found.

Following the validation of the numerical hydrodynamic model, performance indicators were calculated for a number of different SOWC designs. The parameters for these SOWC designs associated with optimal performance, identified in Chapter 6, are listed in Table 8.1 above. In the course of this investigation they were kept constant, with the exception of two paramaters under study. These were front wall thickness and chamber width. As already discussed, increased front wall thickness and reduced chamber width may be required to support rock integrity and SOWC survivabilty. Thus the effect of altering such SOWC model parameters on performance indicators was sought.

These analyses were conducted for SOWC models at two potential sites, namely Arch point and the Tip of Loop Head. Different wave climate scatter diagrams were found for these two sites. At the tip of Loop Head energetic sea states constituted a larger proportion of the annual wave climate compared with Arch Point. This was due to both its exposed location and convergence of wave power at the tip of a headland due to refraction. For each site, initially five SOWC designs were analysed with progressively increasing front wall thicknesses while other parameters were kept constant. The chamber width for this series of analyes was 11 m. Results showed the SOWC with a front wall thickness of 1.8 m was adequately tuned to the wave period of the prevailing sea state and gave optimal performance. (The results were similar to those of the model of the full scale Pico OWC, which uses this front wall thickness.) However, as the front wall thickness increased, the tuning changed and became associated with a different and higher wave period. Correspondingly, the upper limit of annual power and capture width ratio reduced as front wall increased. This pattern was evident for both Arch Point and the tip of Loop Head. However, as noted above, the tip of Loop Head had more energertic seas than Arch Point. This

was reflected in higher values for annual power and capture width ratio found for the site at the tip of Loop Head.

The same basic chamber design was then used to examine the effect of altering chamber width. Reducing the chamber width necesitated reducing the incident wave front and therefore the amount of wave power available to the SOWC. Chamber designs, now with a width of 8 m, were investigated with the same series of front wall thickness increases. The same pattern of change in tuning associated with increasing front wall thickness was seen. Correspondingly annual power values and capture width ratio reduced in relation to increasing front wall thickness. The capture width ratio overall was not quite as reduced as it was for the 11 m chamber. However, the narrower chamber still produced less annual power than the 11 m chamber. The effect of this reduced performance was further compounded by the fact that the lower power output would require use of a lower capacity turbine. Low capacity turbines are not as cost efficient as higher capacity turbines. This indicates it would be more efficient to install a small number of devices with high performance than a large number of low performance devices.

In conclusion, purely in terms of the interaction between the non-extreme prevailing wave climate and SOWC parameters, it was found that

- Increasing front wall thickness and reducing chamber width were associated with comparative losses in SOWC annual power production
- The tip of Loop Head site was more favourable for wave energy extraction than Arch Point.

8.2 CONCLUSIONS

8.2.1 Aim: Characterisation of County Clare's Wave Energy Resource

The findings related to the first aim and its accompanying objectives are outlined below.

- **To develop and calibrate a 3rd generation spectral wave model for on-shore, near-shore and off-shore domains off Loop Head**

The rationale for the first aim which was discussed in Chapter 1 included the possibility of achieving efficiencies by using all opportunities for wave energy extraction adjacent to areas designated for other wave energy projects. For example, proximal locations of WEC systems would facilitate shared infrastructure. As an area off the Clare coast, north of Loop Head had been designated as an area of interest for marine energy there was reason to add to the pool of wave climate data in areas nearby.

A 3rd generation spectral wave model was developed for a region extending from the Clare coast to a boundary area 150 km off-shore. Its level of resolution for an area extending from the coast to 20 km off-shore produced particularly useful accurate data for this region. This area is referred to in this thesis as the 'Clare Domain'. The model also provided more detail again on areas adjacent to Arch Point and Loop Head extending form depths of approximately 80 m to the coast.

Validation of input data was included throughout development of the model. The operation of the model was validated against physical wave measurements recorded by a waverider buoy. Sufficient statistical correlation (scatter index < 0.25 and correlation coefficient > 0.85) between modelled and measured results was achieved. This was also achieved when comparing data from this study's spectral wave model data with another wave climate study for an overlapping region at Killard Point.

Wave climate data for the Clare Domain and specific areas covered in this study will now be available to potential wave energy developers interested in this area. In addition in Chapter 1, it was noted that some of the difficulties in installing previous shoreline WEC devices had been the lack of accurate wave climate and bathymetric data for shoreline locations. Potential wave energy developers interested in developing deep water shoreline WEC devices in this region now have accurate data available. The first objective entailed by the first aim of the research programme was achieved.

- **To assess wave power levels off the County Clare coast from off-shore to near-shore and on-shore domains**

The 3rd generation spectral wave model developed in this project provided information on wave power levels for the Clare Domain. Results have been given in Chapter 5 and in the summary of Chapter 5 included above in this chapter. As can be seen, the level of wave energy compares well with other locations designated for marine energy. Of note is the manner in which wave energy levels drop as water depth reduces. However, also of note is the degree to which extreme wave heights diminish towards the coast. A distinction is made between average annual wave energy resource and the exploitable energy resource. Exploitable resource is defined as the wave resource associated with significant wave heights between 0.5 m and 6.5 m. As seen from the results, the drops in actual exploitable resource as depths reduce from off-shore towards near-shore positions is much less than the drop in equivalent average annual power ratings. This means that the difference in wave power between off-shore sites and depths of approximately 20 m are not as great as would be suggested by review of average annual power alone. This finding may cause developers to further consider WEC development at these shallower locations particularly as they are afforded relative protection by the filtering out of the most extreme sea states. The second objective entailed by the first aim of the research programme was achieved.

For the regions referred to in the following objectives, results were presented for wave characteristics including information on annual mean power, exploitable power, annual mean H_s, annual mean T_e, maximum H_s, maximum wave height H_{max}, the percentage occurrence of each sea state and wave directionality.

- **To determine the wave climate characteristics in regions adjacent to Arch Point and Loop Head extending form depths of approximately 80 m to the cliff base**

- **To establish the percentage of occurrence of each sea state at locations in the off-shore, near-shore and on-shore areas of the Clare Domain**

- **To establish the percentage of occurrence of each sea state at specific SOWC sites (Arch Point and the tip of Loop Head).**

Therefore, the three objectives listed above and entailed by the first aim of the research programme were achieved. The scatter diagrams provided essential data for the numerical hydrodynamic analysis of potential SOWCs at Arch Point and the tip of Loop Head as described in Chapter 7.

8.2.1.1 Limitations

Limitations include the following: 1) IEC standards recommend that wave climate models are based on 10 years of data, whereas this study had access to data spanning 4 years. Thus it may be subject to aleatory uncertainty. However, the accuracy of the model was corroborated by comparison to other research. 2) The wave rider buoy used in validating the wave climate was at some distance from the sites of particular interest at Loop Head. 3) Further validation points in the area of interest allow confidence to be placed in results extracted from a larger area within the model domain.

8.2.1.2 Further research

1) Accuracy would be increased by accessing 10 years of data for model development. A difficulty with respect to this is the non-availability of appropriate data.
2) The data produced by this model could be made available to wave energy developers in order to access information for further purposes. This could include information regarding the wave energy resource in particular locations, weather windows and extreme value analysis.

8.2.2 Aim: Factors affecting SOWC Design

The objectives related to the second aim will be addressed in the order in which they are listed in Chapter 1 Introduction.

- **To investigate factors affecting subterranean oscillating water column (SOWC) wave energy converter to determine bounds for chamber design**

The ranges of factors affecting SOWC design were identified in Chapter 6. This allowed the design bounds presented in Table 8.1 to be identified. Subsequent hydrodynamic analyses of potential SOWC designs were maintained within these bounds.

- **To develop a numerical hydrodynamic model of a SOWC wave energy converter**

A numerical hydrodynamic model of a SOWC wave energy converter was developed using the BEM code, WAMIT, as discussed in Chapter 7. It was based on the massless piston approach which employed linear wave theory.

- **To validate the set-up of the hydrodynamic model by benchmarking it against tank testing data**

To verify the accuracy of the hydrodynamic model, a benchmarking study was conducted using experimental tank testing data for a fixed OWC chamber design modelled at 1:36 scale. This study showed that the hydrodynamic model developed in the current research programme produced results comparable to those from tank testing data. This validated the hydrodynamic model developed in the current research programme.

There was another interesting finding from this benchmarking study. WAMIT, the software used for hydrodynamic analysis, models the OWC free surface. A central element of WAMIT is the modelling of the OWC free surface. This has traditionally been carried out using a procedure referred to as the weightless lid approach. Recenlty, a new procedure referred to as the free surface pressure patch approach has been developed and is an option in WAMIT version 7. The validation exercise provided an opportunity to trial the newer approach. It was found that its results matched those of the traditonal method.

- **To validate the hydrodynamic model by benchmarking it against a hydrodynamic model of the full scale Pico OWC**

To further verify the accuracy of the hydrodynamic model, a benchmarking study was carried out using data from a study that analysed a full scale OWC chamber design with the boundary element code, AQUADYN (Brito-Melo et al., 1999). The

design analysed was the Pico OWC chamber which was comparable in size to SOWC designs modelled in the current research programme. This study showed that the hydrodynamic model developed in the current research programme produced results comparable to those from the model based on data from the full sized Pico OWC chamber. This further validated the hydrodynamic model developed in the current research programme.

- **To use a hydrodynamic model to identify trends in efficiency associated with changes in SOWC design parameters which may be necessary to promote the survivability of these WECs in their potential locations at Arch Point and the tip of Loop Head**

This objective constitutes a significant component of the work involved in this research programme. A number of steps were taken to achieve it. The first step was to identify and quantify the SOWC design parameters, in the context of each location, which were likely to optimise performance. The results of this process are outlined earlier in this chapter in Table 8.1. The next step was to identify which parameters, if any, would need to be adapted to support the survivability of the device. These are listed above in Table 8.2.

A range of information in this thesis has relevance for the survivability of the SOWC chamber. First, it has been established that there are some factors that favour survivability. For example, it has been shown that the most extreme sea states tend to be filtered out from the wave climate at the 17 m depth contour where the SOWCs in question are potentially situated. Second, the wave climate modelling allows sites to be identified where plunging waves are unlikely to form. However, even if there is some protection from the most extreme forces of the sea, it was established nevertheless that the integrity of the rock forming the SOWC chamber would be vulnerable to forces impacting upon it. As shown in Chapter 7, this had implications for the thickness of the front wall and the width of the chamber.

Although full geological data were not available directly to establish the particular ability of rock at Loop Head to withstand the forces of its local sea, estimates were obtained. These indicated that a minimum value for front wall thickness was 4.8 m and a maximum value for chamber width of 8 - 11 m was required for survivability

provided the chamber walls were reinforced. These estimates took account of the fact that the cliffs at Loop Head are made of fine-grained sandstone, which has less compressive strength than quartzite or basalt.

Therefore, as already described the performance related to designs with different widths and front wall thicknesses were investigated. Increasing the front wall thickness away from the optimal performance value of 1.8 m past the threshold of 4.8 m reduced the upper limit of average annual power and capture width ratio because the chamber then ceased to be tuned to the prevailing wave period. Reducing the width of the chamber from 11 m to 8 m also reduced performance as the incident wave front, and hence the wave energy captured by the device, was reduced. Overall, the performance of the potential SOWC at the tip of Loop Head was greater than that of the potential SOWC at Arch Point, due to the higher level of wave resource at the former site. However, at the tip of Loop Head, the risks to the survivability of the device would be greater due to the greater exposure to extreme sea states. This may necessitate a thicker front wall than that required at Arch Point. This in turn would reduce performance. The performance of potential SOWCs at both sites was significantly affected by changes in parameters adjusted to suit survivability.

Losses associated with friction, which may increase as the front wall lengthens and which have not been incorporated into the linear model, could exacerbate this effect further.

8.2.2.1 Limitations

The limitations associated with this method have been discussed in Chapter 2. To recap, in this research programme the performance indicator results (upper limit of average annual power and capture width ratio) were obtained using a linear model which does not factor in energy losses due to non-linear effects such as turbulence and friction. This must be born in mind if comparing them with performance indicator results for other WECs achieved by non-linear methods. If the SOWC designs modelled in this study were modelled in full scale, their performance indicator values may be somewhat lower than the values obtained in the current project. Furthermore, other types of effects with potential to reduce performance

were outside the scope of this study, for example aerodynamic and thermodynamic effects.

However, it also must be acknowledged that there are other potential design modifications, such as refinement of the SOWC power take-off system, that were not included in this research programme. If they had been, this might have elevated performance indicator values for the same SOWC chamber designs in question. Despite the level of uncertainty regarding definitive levels of power production, the performance indicator values obtained in this project were wholly suitable for identifying trends in performance related to changes in the design parameters under study, and are in keeping with methodology appropriate to TRL stages 1 to 3. Therefore the first objective entailed by the second aim, of developing a hydrodynamic model appropriate to the aims and objectives of the research programme, was achieved.

Another limitation of the current research programme concerns the benchmarking study menitoned above. There was a small degree of discrepancy between the results of the original numerical modelling of the full scale OWC described in Brito-Melo et al. (1999) and the replication carried out by the numerical model developed for this study. This may be accounted for by the fact that the authors of that study had special access to the numerical model source code and so a higher level of detail may have been incorporated into their model, than was available with the standard WAMIT programme. There were also slight variations in the chosen designs compared.

As there was satisfactory agreement between the numerical model used in this study and the tank testing data from the first validation study, and as the discrepancy with the model of the full scale OWC was relativley small, there were reasons likely to account for this discrepancy. Overall it was concluded that the objectives corresponding to the second aim of the research programe were met.

8.2.2.2 Further Research

The results of the current research programme have implications for future research priorities in this field. A number of important questions need to be addressed.

- Do SOWC wave energy converters with optimal design parameters produce sufficient energy for their deployment to be feasible?
- Do adjustments in optimal SOWC design parameters to optimise survivability, reduce performance sufficiently to render the SOWC non-viable?

These are difficult questions to answer definitively, with the modelling procedures used in the current research programme, because the power values they yield are upper limit estimates rather than realistic predictions.

Decisions about the feasibility of potential WECs are made on the basis of the cost per unit of power and definitive information regarding costings was not available. Estimates were obtained suggesting that SOWC construction costs would not be low enough to reach the aspirational target of €4 million per MW given earlier. However, the performance indicators could throw light on the possible feasibility of SOWCs in some circumstances. If upper limit estimate performance indicator values obtained in this study were already substantially lower than values for equivalent devices, but had comparable costs, this would definitely indicate that considerable technological improvement beyond the designs modelled here would be needed for the devices to approach feasibility. However, this is not the case. Therefore possibly more investigation is warranted. More accurate modelling of the SOWCs studied in this project may reduce their performance values on the one hand, and yet refinement of the technology could potentially enhance them on the other. Therefore at this stage, it is not possible to confirm the feasibility of SOWCs at Loop Head as modelled, and yet it may be premature to rule this out.

The findings provided by this research programme may justify funding further investigations aiming to clarify this question. Examples of further investigation include the following:

Direct geological and engineering information could be obtained to clarify the minimal front wall thickness and width values that could be sustained at Loop Head, plus more accurate costings for construction and reinforcements. The influence of wave directionality on device performance could be examined. Refinements in the power take off system and other chamber adjustments could be explored to see if performance could be enhanced. Non-linear, aerodynamic and thermodynamic

modelling could be carried out to provide predictions of power production that are as accurate as possible. With respect to non-linear hydrodynamic modelling, spectral or time domain modelling could be carried out. Such investigations would then allow a more accurate prediction of costs per unit power, which would offer guidance on the feasibility of SOWC installation at Loop Head. With respect to non-technical issues, it would be advisable to explore further whether there are likely to be any out-right barriers to project development, for example, in relation to conservation areas.

Alternative approaches would include: 1) Investigation of other sites on the Irish coast. Learning from this study would prompt particular attention to the compressive and triaxial strength of the rock at a proposed site. 2) Investigation of other WEC technologies which may be able to take advantage of the near-shore, on-shore sites with water depths in the region of 17 m, which have comparatively high wave energy levels, in combination with relatively low exposure to extreme seas, as confirmed by this study.

8.2.3 Closing Comments

The results of the research programme described in this thesis have clear implications for its two major aims. With respect to the first aim, the results indicate that the domain off County Clare possesses an exploitable resource with promising levels of energy for potential wave energy projects. They also show that the near-shore and on-shore environment in this domain maintains good levels of power with relative filtering of extreme waves.

With respect to the second aim, the results do not provide unequivocal confirmation that SOWC installations are cost-effective technologies to tap the wave energy resource at Loop Head, County Clare. However, they do provide useful information on SOWC design features that may help to guide prospective developers toward possible solutions to the inherent challenges of SOWC refinement and installation highlighted in this thesis.

As with any renewable energy technology, the viability of the SOWC wave energy converter concept is dependent on a number of issues. Primary issues include its

cost-competiveness, governmental support and public approval.

The current cost of power generation via fossil fuels is relatively low compared with costs of power generation via emerging wave energy conversion technologies. Therefore commercial companies are not inclined to invest in developing the technology further. Therefore government financial support and incentives are required to encourage researchers and commercial enterprises to carry out the developmental work required to bring the technology toward economic viability.

From all of the literature reviewed as part of this research programme, the most comprehensive account of the economic viability of the OWC wave energy conversion concept is given in The Carbon Trust's (2005) report 'Oscillating Water Column Wave Energy Converter Evaluation Report', which was published as part of the Marine Energy Challenge. As stated in Section 2.3.2, this report argued that the fixed shoreline OWC wave energy converter concept required a 50% reduction in capital costs and increased power generation to reach commercial viability in the UK. It pointed towards the concept of the SOWC wave energy converter, as a potential solution to these challenges. However, unlike this thesis, the report did not offer an assessment of the SOWC

The potential reduction in capital costs and possible increase in power generation associated with the SOWC concept is highly dependent on site characteristics. The Site Viability Study and Survey presented in Chapter 3 outlined the key factors to take into account in assessing potential SOWC sites. These include the wave energy resource, seabed bathymetry, tidal range, grid accessibility and infrastructure, environmental and planning issues, interaction with other human activities, geology, cliff height and water depth at cliff base.

The following site characteristics are associated with reduced costs: close proximity to suitable electrical grid and infrastructure, homogeneous horizontally layered rock possessing high triaxial and compressive strength (preferably basalt or quartzite), and cliff height ranging from 16 m to 40 m above sea level. Site characteristics that favour increased power generation include annual average wave power values greater than 25 kW/m, tidal range less than 5 m, and water depth at cliff base greater than 15 m, which reduces wave power losses due to near-shore processes.

In the research programme described in this thesis, two potential SOWC wave energy converter sites were investigated: Arch Point and the tip of Loop Head. Both possessed favourable annual wave power levels greater than 25 kW/m and water depths greater than 15 m at the cliff based. However, there is cause for caution with respect to the geological composition at each site. Based on information presented in Section 6.5 Geology, the presence of hollows and fissures within Loop Head's geology increase the risk of geological irregularities in a potential SOWC construction zone. This may impose unforeseen structural risks during construction.

If a further geological study found an area of cliff in this location which did have suitable rock composition, then strategic environmental assessment, environmental impact assessment, foreshore licence for site investigation, foreshore lease, planning permission statement and grid connection offer would be required.

Regarding construction, Section 6.7 outlined the construction method proposed by Sewave Ltd. Although definitive costs for this method are not available for the Loop Head region, estimates imply that the capital costs for a single SOWC wave energy converter outweigh the estimated financial returns associated with the upper limit of mean annual power absorbed, presented in Chapter 7. The most economically viable path for SOWC wave energy converters will involve large scale arrays of SOWCs coupled with high capacity turbines (> 500 kW). This is because of the economies of scale associated with the construction of arrays, and the fact that high capacity turbines are more cost-effective that those with a low capacity, as noted in Section 7.3. In line with this, further site investigations and surveys are required to verify the length of coastline possessing cliff sites with an appropriate profile for arrays of chambers.

Prior to implementation of full scale SOWC wave energy converter arrays, the concept must first be successfully progressed from its present technology readiness level to technology readiness level 9, as outlined in Section 2.2. As previous wave energy projects have proved, developing a wave energy converter that can economically and safely convert the energy flux in ocean waves into a usable form of power is a technically demanding undertaking.

This research programme has identified locations with suitable wave power levels

(Chapter 5), defined the bounds of SOWC chamber design (Chapter 6) and provided estimates for the upper limit of annual mean absorbed power at specific sites (Chapter 7). However, further structured development plans are required to reach each successive Technology Readiness Level. Assuming sufficient financial investment, attention would be required regarding a range of issues, including those identified in this thesis. As cited in Chapter 6 and 7, the dimensions of SOWC chamber width and front wall thickness needed to promote survivability may adversely affect the device's optimal tuning and could thus possibly reduce its potential power production. Therefore, when progressing the SOWC concept further through the Technology Readiness Levels, these findings would need clarification by refined power generation predictions. If confirmed, measures to improve the relationship between project cost and the financial return of power production would be required. These may involve the pursuit of reduced construction expenses, refinement of pneumatic effects within the OWC chamber and tunnel system, enhanced turbine design and as mentioned previously, exploration of SOWC arrays, including specific spacing of chambers. In addition, assessment of potential construction risks and precautionary measures would be required.

Pending successful progression through each Technology Readiness level, it should be noted that non-technical barriers (planning permissions, environmental issues etc.) potentially affect full scale development of this concept at present. However, as Dr. Eddie O'Connor outlined at the International Conference on Ocean Energy (ICOE) 2012 in Dublin, 'Wave energy is Ireland's greatest carbon free renewable energy resource, which could deliver a sizeable enterprise sector in the process of achieving a low-carbon economy. Although commercialisation of wave energy technologies is a challenge, we must envisage our ambition for many years in the future as well as taking the preparatory steps now to achieve this ambition'.

Making further preparatory steps regarding the SOWC wave energy converter will help to establish whether or not it is an appropriate means to contribute to Ireland's future energy needs. The concept will not provide a universal solution to extracting energy at Ireland's coastline and meeting national energy targets as other near-shore and off-shore technologies offer their own advantages (see Section 1.2.1). The SOWC concept offers solutions to the main disadvantages associated with on-shore

technologies. At appropriate cliff sites, this wave energy converter design offers an accessible, invisible shoreline technology which can complement power generation in areas designated for renewable energy projects. The results of the research programme presented in this thesis may guide prospective developers interested in this device, toward possible solutions to challenges highlighted by this research.

REFERENCES

ABB. (2012), 'Energy Storage Keeping smart grids in balance', Zurich.

Aerohydro. (2011a), 'MultiSurf Version 8.0 Manual, Southwest Harbor', Maine

Aerohydro. (2011b), 'MultiSurf for WAMIT Version 8.1', Maine.

Babarit, A., Hals, J., Muliawan, M.J., Kurniawan, A., Moan, T. and Krokstad, J. (2012), 'Numerical benchmarking study of a selection of wave energy converters', *Renewable Energy*, Elsevier Ltd, Vol. 41, pp. 44–63.

Babarit, A. and Hals, J. (2011), 'On the maximum and actual capture width ratio of wave energy converters', *Procedings of 9th European Wave and Tidal Energy Conference*, Southampton.

Battjes, J.A. and Janssen, J.P.F.M. (1978), 'Energy loss and set-up due to breaking of random waves', *Procedings of 16th International Conference for Coastal Engineering. ASCE*, pp. 569–587.

Beg, M.N.A. (2013),'Implementation of a 3D Model for the North Sea and UK Surrounding Area', Brandenburg University of Technology.

Bouws, E., Draper, L., Laing, A.K., Carter, T.D.J., Eide, L. and Battjes, J.. (1998),' Guide to Wave Analysis and Forecasting'.

Bouws, E., Günther, H., Rosenthal, W. and Vincent, C.L. (1985), 'Similarity of the wind-wave spectrum in finite depth water, Spectral form'. *Journal of Geophysics*, Vol. 90, pp. 975–986.

BP. (2010), 'BP Statistical Review of World Energy', London.

Brito-Melo, A., Sarmento, A.J.N.A., Clement, A.H. and Delhommeau, G. (1999), 'A 3D Boundary Element Code for Analysis of OWC Wave-Power Plants', *Procedings of the 9th International Offshore and Polar Engineering Conference*. pp. 1–8.

Brooke, J. (2003), 'Wave Energy Conversion', Elsevier: Oxford.

Carbon Trust. (2005),' Guidelines on design and operation of wave energy converters: A guide to assessment and application of engineering standards and recommended practices for waave energy conversion devices', DNV.

Chappelear, J.B. (1959), 'On the theory of the highest waves', Corps of Engineers, Washington DC Beach Erosion Board.

Chawla, A., Tolman, H.L., Hanson, J.L., Devaliere, E. and Gerald, V.M. (2008), 'Validation of a Multi-Grid WAVEWATCH III TM Modeling System', MMAB Contribution no. 281, No. 281, pp. 1–15.

Chozas, J.F., Kramer, M.M., Sørensen, H.C. and Kofoed, J.P. (2012), 'Combined Production of a full-scale Wave Converter and a full-scale Wind Turbine – a Real Case Study', *Procedings of 4th International Conference on Ocean Energy 2012*, pp. 1–7.

Clare County Council. (2012), 'Clare Renewable Energy Strategy'.

Clément, A. (2003), 'Modelling and Standardised Design Methods. Results from the work of the European Thematic Network on Wave Energy'.

Cooley, J.W. and Tukey, J.W. (1965), 'An algorithm for machine calculation of complex Fourier series', *Mathematics and Computers.*, Vol. 19, pp. 297–301.

Coyle. (2012), 'A review of research and development in ocean energy in the Republic of Ireland'.

Cradden, L., Duperray, O., Mouslim, H. and Ingram, D. (2011), 'Joint Exploitation of Wave and Offshore Wind Power', *Procedings of 9th European Wave and Tidal Energy Conference*, Southampton.

Crom, I. Le, Neumann, F. and Sarmento, A. (2009), 'Numerical Estimation of Incident Wave Parameters Based on the Air Pressure Measurements in Pico OWC Plant', *Procedings of 8th European Wave and Tidal Energy Conference*, pp. 130–139.

Cruz, J. (2008), 'Ocean Wave Energy. Current Status and Future Perspectives', Springer, 1st.ed.

Davey, T., Venugopal, V., Smith, H., Smith, G., Lawrence, J., Cavaleri, L., Bertotti, L., et al. (2010), 'Equitable Testing and Evaluation of Marine Energy Extraction Devices in terms of Performance, Cost and Environmental Impact D2.7', *Protocols for wave and tidal resource assessment.*

Delaure. (2001), 'A hydrodynamic investigation of oscillating water column wave energy converters', Ph.D. Thesis Hydraulics and Maritime Research Centre, National University Ireland, Cork, Ireland.

Delaure, Y, Lewis, A. (2003), '3D hydrodynamic modelling of fixed oscillating water column wave power plant by a boundary element methods', Ocean Engineering, Vol. 30, pp. 309–330.

Department of Communications Energy and Natural Resources. (2014), 'Offshore Renewable Energy Development Plan', Dublin.

Department of Communications Marine and Natural Resources. (2007), 'Delivering a Sustainable Energy Future for Ireland - Government White Paper'.

Det Norske Veritas. (2008), 'Offshore Service Specification DNV-OSS-312: Certification of Tidal and Wave Energy Converters'.

DHI Software. (2011a), 'MIKE 21 Spectral Wave Module Scientific Documentation', Horsholm, Denmark.

DHI Software. (2011b), 'MIKE 21 SW Spectral Waves FM Module User Guide', Horsholm, Denmark.

DHI Software. (2011c), 'Map Projection and Datum Conversion User Guide', Horsholm, Denmark.

Dossey, L. (2013), 'Global ClimateChangeandDespair: A WayOut', *EXPLORE*, Vol. 9 No. 5.

DTI. (2004), 'The potential for using disused coastal mineshafts to exploit wave energy' Main Report. Contract Number V/06/00196/00/00. URN Number: 04/1791

Euler, L. (1755), 'Principes generaux du mouvement des fluides', *Histoire de l'Academie Royale des Sciences et des Sciences*, Vol. vol 6.

European Commission. (2008), 'Environment Policy Review-Annex', Brussels.

Evans, D. V. (1978a), 'The Oscillating Water Column wave-energy device', *Journal of Applied Mathematics*, Vol. 22, pp. 423–433.

Evans, D. V. (1982), 'Wave-power absorption by systems of oscillating surface pressure distributions', *Journal of Fluid Mechanics*, Vol. 114, pp. pp. 481–499.

Evans, D. V and Porter, R. (1995), 'Hydrodynamic characteristics of an oscillating water column device', *Applied Ocean Research*, Vol. 17 No. 3, pp. 155–164.

Evans and Porter. (1997), 'Efficient calculaion of hydrodynamic properties of OWC-type devices', *Journal of Oshore Mechanics and Arctic Engineering*, Vol. 119 No. 4, pp. 210–218.

Falcão, A.F.D.O. (2004), 'First-Generation Wave Power Plants: Current Status and R&D Requirements', Journal of Offshore Mechanics and Arctic Engineering, Vol. 126 No. 4, p. 384.

Falcão, A.F.O. (2009), 'Oscillating Water Column Technology and the Pico Plant Project', *Procedings of 9th European Wave and Tidal Energy Conference*, Uppsala, Sweden.

Falcão and Sarmento. (1980), 'Wave generation by a periodic surface pressure and its application to wave-energy extraction', *Procedings of 15th Int. Conference on Theoretical Applied Mechanics*, Toronto.

Falnes, J. (2000), 'Teaching on ocean wave energy conversion'. *Procedings of 4th European Wave and Tidal Energy Conference*, Aalborg, Denmark, pp.153-160.

Falnes J. (2002) 'Ocean waves and oscillating systems'. Cambridge University Press UK .

Fievez and Brien. (2011), 'Worlswide Deployment of the Ceto Wave Energy Technology', *Procedings of the 4th International Conference on Ocean Energy*, Dublin, Ireland.

Fitzgerald, J. and Bolund, B. (2012), 'Technology Readiness for Wave Energy Projects ; ESB and Vattenfall classification system', *Procedings of the 4th International Conference on Ocean Energy* , Dublin, Ireland.

Fjar, Erling, Holt, Horsrud, Raaen and Risnes. (2008), 'Petroleum Related Rock Mechanics' (2nd Edition), Elsevier.

Folley, M. (2005), 'The effect of plenum chamber volume and air turbine hysteresis on the optimal performance of oscillating water columns', *Procendings of the 24th International Conference on Offshore Mechanics and Arctic Engineering*, pp. 1–6.

Folley, M., Cornett, A., Holmes, B., Lenee-Bluhm, P. and Liria, P. (2013), 'IEC 62600-101 TS Ed. 1 Marine energy - Wave, tidal and other water current converters - Part 101: Wave energy resource assessment and characterisation'.

Folley, M., Cornett, A., Holmes, B. and Liria, P. (2012), 'Standardising resource assessment for wave energy converters', *Procedings of the 4th International Conference on Ocean Energy* , Dublin, Ireland.

Folley, M. and Whittaker, T.J.T. (2009), 'Analysis of the nearshore wave energy resource', *Renewable Energy*, Vol. 34 No. 7, pp. 1709–1715.

Fusco, F., Nolan, G. and Ringwood, J.V. (2010), 'Variability reduction through optimal combination of wind/wave resources - An Irish case study', *Energy*, pp. 314–325.

Gallagher, S., Dias, F. and Tiron, R. (2013), 'A Detailed Investigation of the Nearshore Wave Climate and the Nearshore Wave Energy Resource on the West Coast of Ireland', *Proceedings of the ASME 2013 32nd International Conference on Ocean, Offshore and Arctic Engineering*, pp. 1–12.

Geological Survey of Ireland. (2005), 'Co. Clare Geological Site Report'.

Government of Ireland (2004), 'All Ireland Energy Framework', Department of Environment, Heritage and Local Government.

Government of Ireland (2006), 'Ireland: National Climate Change Strategy 2007-2012', Department of Environment, Heritage and Local Government, Dublin.

Government of Ireland (2004), 'All Ireland Energy Framework', Department of Environment, Heritage and Local Government, Dublin.

Government of Ireland (2007), 'The National Development Plan 2007-2013':,Department of Environment, Heritage and Local Government, Dublin.

Gu, D.X., Tamblyn, W., Lamb, I. and Ramsey, N. (2008),'Effect of Weathering on Strength and Modulus of Basalt and Siltstone', *Procedings of the 42nd US Rock Mechanics Symposium*, San Francisco, USA.

Guedes Soares, C., Cherneva, Z. and Antão, E.M. (2003), 'Characteristics of abnormal waves in North Sea storm sea states', *Applied Ocean Research*, Vol. 25 No. 6, pp. 337–344.

Oumeraci, N.W.., Allsop, M., Crouch, M.B. de G.R.S. and Vrijling, J.K. (1999), 'Probabilitic Design Tools for Vertical Breakwaters'.

Harold, Trujillo and Thurman. (2001), 'Essentials of oceanography', 7th edition.

Harris, E.L., Orelup, E.A., Cox, A.T. and Cob, C. (2006), 'The MSC50 Wind and Wave Reanalysis'.

Hasselmann, K., Ross, D.B., Müller, P. and Sell, W. (1976), 'A parametric wave prediction model', *Journal of Physical Oceanography*, Vol. 6(2), pp. 200–228.

Haughton, P., Shannon, P., Pierce, C., Matinsen, O., Hadler-Jacobsen, F., Pulham, A. and Elliot, T. (2010a), 'Clare Drilling and Training Initiative', *Procedings of the Geoscience symposium 2010*, Dublin, Ireland.

Healy. (2012), 'MARINET Facility Types: Enabling Complete Structured Testing'.

Heath, T. (2003), 'The Construction , Commissioning and Operation of the LIMPET Wave Energy Collector', *Applied Research and Technology*, pp. 1–14.

Hewitt. (2012), 'The fracking debate – a local viewpoint', *International Journal of Ambient Energy*, Vol. 33 No. 3.

HMRC. (1997), 'Results of wave tank Rock OWC model tests', Hydrauilic Maritime Research Centre, Cork.

Holland, C. (1996),' Meeting minutes', *1st colloquium for Ocean Wave Energy at Trinity College Dublin*, Dublin, Ireland.

Holland, C. (1997),' Meeting minutes', *2nd colloquium for Ocean Wave Energy at Trinity College Dublin*, Dublin, Ireland.

Holmes. (2003), 'Ocean Energy: Development and Evaluation Protocol'. Hydrauilic Maritime Research Centre, Cork.

Holmes, B. (1997), 'Rock OWC Wave Energy Converter'. Hydrauilic Maritime Research Centre, Cork.

Holmes, B. (2009),' Sea and Swell Spectra, Strategic Programme', Hydrauilic Maritime Research Centre, Cork.

Holmes, B. and Barrett, S. (2007), 'Sea & Swell Spectra', *Procedings of 7th European Wave and Tidal Energy Conference*, Porto, Portugal.

Holmes, B. and Nielsen, K. (2010), 'Guidelines for the development and testing of wave energy systems', OES IA Annex II Task 2.1, Energy.

IEA. (2009), 'World Energy Outlook'. International Energy Agency.

Ingram, D., Smith, G., Bittencourt-Ferreira, C. and Smith, H. (2011),'Protocols for the Equitable Assessment of Marine Energy'.

IPCC. (2013), 'IPCC 5th Assessment Report: Climate Change 2013: The Physical Science Basis', International Panel for Climate Change.

Iribarren, C.R. and Norales, C. (1949), 'Protection des ports', *XVIIth International Navigation Congress*, Section II, Lisbon, pp. 31–80.

Jones, Hillier and Comfort. (2013), 'Fracking and public relations: rehearsing the arguments and making the case', *Journal of Public Affairs*, Vol. 10, p. 1490.

Journée, J.M.J. and Massie, W.W. (2001), 'Offshore Hydromechanics'. Delft University of Technology.

Kållberg, P., Berrisford, P., Hoskins, B., Simmmons, A., Uppala, S., Lamy-Thépaut, S. and Hine:, R. (2005),' ERA-40 Atlas', Shinfield Park, Reading, p. 191.

Keigher, C. (2012), Personal Communication, Irish Industrial Explosives Ltd.

Kofoed-Hansen. (2011), Personal Communication, Danish Hydraulics Institute.

Komen, G., Cavaleri, L., Donelan, M., Hasselmann, K., Hasselmann, S. and Janssen, P. (1994), 'Dynamics and Modelling of Ocean Waves', University Press, Cambridge.

Laplace, P.S. (1782), 'Theorie de l'attraction des spheroids et de la figure des planets', *Memoires de l'Acadamuue Royale des Sciences*.

Lawrence, J., Kofoed-Hansen, H. and Chevalier, C. (2009), 'High-resolution metocean modelling at EMEC ' s (UK) marine energy test sites', *Procedings of 8th European Wave and Tidal Energy Conference*, Uppsala, Sweden.

Lane, (2009), Personal Communication, Sewave Ltd.

Lane, (2011), Personal Communication, Sewave Ltd.

Lee, C.., Newman, J.N. and Nielsen, F.G. (1996), 'Wave Interactions with an Oscillating Water Column', *International Society of Offshore and Polar Engineers.*

Lenau. (1966), 'The solitary wave of maximum amplitude', *Journal of Fluid Mechanics*, Vol. 26 No. 02.

Lindblom, U. (1997), 'Meeting minutes', *Procedings for 2nd colloquium for Ocean Wave Energy at Trinity College Dublin*, Dublin, Ireland.

Longuet-Higgins. (1952), 'On the statistical distribution of the heights of sea waves', *Journal of Geophysical Research*, Vol. 11, pp. 215–266.

Longuet-Higgins. (1963), 'The effect on non-linearities on statistical distributions in the theory of sea waves', *Journal of Fluid Mechanics*, Vol. 17, pp. 459–480.

Longuet-Higgins. (1975), 'On the joint distribution of the periods and amplitudes of sea waves', *Journal of Geophysical Research*. Vol. 80 No. 19, pp. 2688–2694.

Longuet-Higgins. (1980), 'On the distribution of the heights of sea waves: Some effects of non-linearity and finite bandwidth', *Journal of Geophysical Research*, Vol. 85 No. 3, pp. 1519–1523.

Longuet-Higgins, M.S. (1974), 'On the Mass, Momentum, Energy and Circulation of a Solitary Wave', *Proceedings of the Royal Society of Applied Mathematical, Physical and Engineering Sciences*, Vol. 337.

M. Curé. (2011), 'A Fifteen Year Model Based Wave Climatology of Belmullet, Ireland', Report prepared on behalf of the Sustainable Energy Authority of Ireland (SEAI).

Mansard, E.P.D. and Funke, E.R. (1980), 'The measurement of incident and reflected wave spectra using a least squares method', *Proceedings of the 17th International Conference on Coastal Engineering*, Sydney, Australia, pp. 154–172.

Marine Institute (2000), 'Exploiting the Irish ocean wave energy resource', Infrastructure and R&D projects supported under Measure 8. (Marine Research Measure) of the operational programme for Fisheries (1994-99).

Marine Institute. (2013), Heave Sensor information available at: http://www.marine.ie/home/publicationsdata/data/buoys/HeaveSensor.htm (accessed 11 November 2012).

Marine Institute (2013), Wind Vane information available at 'https://www.marine.ie/home/publicationsdata/data/buoys/WindVane.htm'(accessed 11 November 2012).

Marine Institute and ESB. (2008), 'Wave energy network connection project, site evaluation and selection report'.

Martins, E., Ramos, F.S., Carrilho, L., Justino, P., Gato, L., Trigo, L. and Neumann, F. (2005), 'Ceo Douro Project: Overall Design of an OWC in the new Oporto Breakwater', *Procedings of 6th European Wave and Tidal Energy Conference*, Glasgow, UK.

Mathworks. (2013), 'Matlab Function Reference, R2013a', Natick, MA.

MayoToday. (2012), 'Ocean energy sector can create 70,000 jobs, Taoiseach tells Ballina conference.'

McCarthy, M. (2012), Personal Communication, Priority Drilling Ltd.

McConnell, P. (2012), Personal Communication, Tara Mines Ltd.

McCormick, M. (2012), Personal Communication.

McCowan, J. (1891), 'On the solitary wave', *Philosophical Magazine*, Vol. 32, pp. 45–58.

McCullen, P. (2005), 'Accessible Wave Energy Resource Atlas : Ireland : 2005'.

Mei, C. (1976), 'Power Extraction from Water Waves', *Journal of Ship Research*, Vol. 20 No. 2, pp. 63–66.

Milne-Thomson, L. (1968), 'Theoretical hydrodynamics', The Macmillan Press, 5th ed.

Minikin, R. (1963), 'Studies in Harbour Making and in the Protection of Coasts', *Wind, Waves and Maritime Structures*, Vol. 2.

Morris-Thomas, M.T., Irvin, R.J. and Thiagarajan, K.P. (2007), 'An Investigation into the Hydrodynamic Efficiency of an Oscillating Water Column', *Journal of Offshore Mechanics and Arctic Engineering*, Vol. 129 No. 4, p. 273.

MRIA. (2010), 'Initial Development Zones', Marine Renewable Industry Association.

Munson, B., Young, D. and Okiishi, T. (1990),'Fundamentals of fluid mechanics', New York.

Murphy, J. (2012), 'Similitude and Scaling'.The Marine Renewables Infrastructure Network programme, Hydraulics and Maritime Research Centre, National University of Ireland, Cork, Ireland

Myers, L.E., Bahaj, A.S., Retzler, C., Pizer, D., Gardner, F., Bittencourt, C. and Flinn, J. (2010), 'Equitable Testing and Evaluation of Marine Energy Extraction. Deliverable D5.2 Device classification template'.

Neumann, F., Didier, E. and Sarmento, A. (2007), 'Pico OWC Recovery Project : Recent Activities and Performance Data', *Proceedings of the 7th European Wave and Tidal Energy Conference*, Porto, Portugal, 2007.

Newman. (2013), Personal communication, WAMIT Inc.

Newman, J.N. (1974), 'Interaction of water waves with two closely spaced vertical obstacles', *Journal of Fluid Mechanics*, Vol. 66 No. 01, pp.97–106.

Nielsen, K. and Holmes, B. (2010), 'Annex II Task 2.1 Guidelines for the Development & Testing of Wave Energy Systems'.

Payne, G. (2008), 'Guidance for the experimental tank testing of wave energy converters'.

Persson, A. and Grazzini, F. (2011), 'User guide to ECMWF products'.

Pitt. (2009), 'Assessment of Performance of Wave Energy Conversion Systems'.

Pontes, M.T., Aguiar, R. and Pires, H.O. (2005), 'A Nearshore Wave Energy Atlas for Portugal', *Journal of Offshore Mechanics and Engineering*, Vol. 127, pp. 249–255.

Prevosto, M. (2011), 'The Equitable Testing and Evaluation of Marine Energy Extraction Devices in terms of Perfomance, Cost and Environmental Impact. D2.6 Extremes and Long Term Extrapolation'.

Reguero, B.G. (2012), 'Numerical modeling of the global wave climate variability and associated environmental and technological risks', UNIVERSIDAD DE CANTABRIA.

Reitan, A. (1991), 'Wave-power absorption by an oscillating water column', *Physica Scripta*, Vol. 1, p. 60.

Rice, S.O. (1944), 'Mathematical analysis of random noise', *Bell System Technical Journal*, Vol. 23, pp. 282–332.

Ris, R.C., Holthuijsen, L.H. and Booij, N. (1999), 'A third generation wave model for coastal regions. Verification.', *Journal of Geophysical Research*. Vol. 104, pp. 7667–7681.

Rourke, F.O., Boyle, F. and Reynolds, A. (2009), 'Renewable energy resources and technologies applicable to Ireland', *Renewable and Sustainable Energy Reviews*, Vol. 13 No. 8, pp. 1975–1984.

Sainflou, G. (1928), 'Essai sur les diques maritimes vertica;es.', *Annales des Ponts et Chaussees*, Vol. 98 No. 1.

Sarmento, A.J.N.A., Pontes, M.T. and Brito-Melo, A. (2001), 'The influence of the wave climate on the design and annual production of electricity of OWC wave power plants', *Procedings of the 20th International Conference on Offshore Mechanics and Arctic Engineering*, Rio de Janeiro, Brazil.

Sarpkaya T, Isaacson, M. (1981), 'Mechanics of wave forces on offshore structures', Van Nostrand Reinhold.

Scholes, H., Millar, D.L., Eyre, J.M., Dibley, R., G Davey and M Haywood. (2004), 'The potential for using disused coastal mineshafts to exploit wave energy'.

SEI. (2002), 'Options for the development of wave energy in Ireland'. Sustainable Energy Ireland, Dublin.

SEAI. (2013), 'http://www.seai.ie/Grants/NER300/'. Sustainable Energy Authority of Ireland.

Sewave. (2005), 'Front End Engineering Design Report: Tunnelled Wave Energy Converter for the Faroe Islands'.

Slevin, C., Fitzgerald, J. and Burca, C. (2011), 'Supply Chain Study for WestWave'.

Smith, G.H. and Taylor, J. (2007), 'Preliminary Wave Energy Device Protocol. Department of Trade and Industry'.

Smith, H.C.M., Smith, H.G.H. and Edwards, K.A. (2012), 'Effect of water depth on the wave energy resource and extreme wave conditions', *Procedings from the 4th International Conference on Ocean Energy*, Dublin, Ireland.

Soerensen, H. (2005), 'Wave energy deployment at Horns Rev Wind Farm'. Copenhagen, Rambøll.

Steele, K.E., Teng, C.-C. and D. W-C. Wang. (1992), 'Wave direction measurements using pitch and roll buoys', *Ocean Engineering*, Vol. 19 No. 4, pp. 349–375.

Sterling, R. (1997), 'Meeting minutes', *2nd colloquium for Ocean Wave Energy. Meeting at Trinity College Dublin*, Ireland.

Stoutenburg, E.D., Jenkins, N. and Jacobson, M.Z. (2010), 'Power Output Variability of Co-located offshore wind turbines and wave energy converters in California', *Renewable Energy*.

SustainableEnergyAuthority of Ireland. (2010), 'Ocean Energy Roadmap to 2050'.

Sustainable Energy Authorityof Ireland. (2011), 'Energy Security in Ireland: A Statistical Overview'.

Swail, V.R., Ceccacci, E.A., Cox, A.T. and Cob, C. (2000), 'The ARS40 North Atlantic Wave Reanalysis: Valdation and Climate Assessment', No. 1994.

SWAN team. (2006), 'USER MANUAL SWAN Cycle III version 40.51', Delft University of Technology.

Sykes. R. (2012), 'The Hydrodynamics of an Oscillating Water Column, An investigation using numerical and physical modelling'. Ph.D. Thesis Hydraulics and Maritime Research Centre, National University Ireland, Cork, Ireland.

Taunton, S. (2010), United Kingdom Hydrographic Office (UKHO) Archive Research Guide, Vol. 100, pp.1-5.

Tawn, J. (1988), 'An extreme-value theory model for dependent observations', *Journal of Hydrology*, Vol. 101 No. 1-4, pp. 227–250.

TCD (1996), 'Meeting minutes', *1st colloquium on Rock Engineering used for Ocean Wave Energy*, Trinity College Dublin, Ireland.

TCD (1997), 'Meeting minutes', *2nd colloquium on Rock Engineering used for Ocean Wave Energy*, Trinity College Dublin, Ireland.

Thorpe, T.W. (2001). 'An overview of wave energy technologies: status, performance and costs. Wave power: moving towards commercial viability'. Professional Engineering Publishing. S713/002/99.

The Carbon Trust. (2005), 'Marine Energy Challenge Oscillating Water Column Wave Energy Converter Evaluation Report'.

The Carbon Trust. (2006), 'Results of the Marine Energy Challenge: Cost Competitiveness and growth of wave and tidal energy'.

The Journal. (2012), '€300m to be invested in research centres in unprecedented move'. http://www.thejournal.ie/finding-e300m-science-foundation-ireland-809009-Feb2013/.'(accessed 23rd Feb 2013).

Tolman, H.L. (2002a), 'User manual and system documentation of Wavewatch iii', Washington.

Tolman, H.L. (2002b),' User manual and system documentation of WAVEWATCH-III version 2.22', Washington.

Tucker, M.J. and Pitt, E.G. (2001), 'Waves in Ocean Engineering', Elsevier Science Ltd., Oxford.

U.S.Army Corps of Engineers. (2002), 'Coastal Engineering Manual. Engineer Manual 1110-2-1100', Washington, D.C.

Venugopal, V., Davey, T., Smith, H. and Smith, G. (2010), 'Equitable Testing and Evaluation of Marine Energy Extraction Devices in terms of Performance, Cost and Environmental Impact Deliverable D2.3 Application of Numerical Models'.

Venugopal, V., Davey, T., Helen Smith, Smith, G., Holmes, B., Barrett, S., Prevosto, M., et al. (2011), 'Equitable Testing and Evaluation of Marine Energy Extraction Devices in terms of Performance, Cost and Environmental Impact - Equimar - Deliverable D2.2 Wave and Tidal Resource Characterisation.'

Venugopal, V., Davey, T., Smith, H., Cavaleri, L., Bertotti, L., Sclavo, M. and Girard, F. (2011), 'The Equitable Testing and Evaluation of Marine Energy Extraction Deliverable D2 . 4. Wave Model Intercomparison.'

Walter. (2010), 'A Fracking Nuisance', *Environmental Policy and Law*, Vol. 42 No. 4-5.

WAMIT. (2011), 'WAMIT User Manual Verson 8.0', Interface, available at: www.wamit.com.

Wavegen. (2002a), 'Research into the further development of the limpet shoreline wave energy plant'.

Wavegen. (2002b), 'Islay Limpet Project Monitoring'.

Wavegen. (2003), 'Research into the further development of the LIMPET shoreline wave energy plant'.

Wavegen. (2004), 'Initial sizing of turbines for OWC project'.

WaveNet. (2003),'Results from the work of the European Thematic Network on Wave Energy'.

Waveplam. (2009), 'Wave Energy : A guide for investors and policy makers'.

Weber, J. (2006), 'Optimisation of the Hydrodynamic-Aerodynamic Coupling of an Oscillating Water Column Wave Energy Converter Wave Energy Device', Ph.D. Thesis Hydraulics and Maritime Research Centre, National University Ireland, Cork, Ireland.

Whittaker, T., Langston, D., Fletcher, N., Shaw, M. and Falcão, A.F.O. (2002), 'Islay LIMPET Wave Power Plant', Publishable Report, Belfast.

Zubiate, L., Villate, J.L., Soerensen, H.C. and Holmes, B. (2009a), 'D3.1 Methodology for Site Selection'.

Zubiate, L., Villate, J.L., Soerensen, H.C. and Holmes, B. (2009b), 'Methodology for site selection for wave energy projects', *Procedings of 7th European Wave and Tidal Energy Conference*, Porto, Portugal.